Molecular studies of *Mycobacterium tuberculosis* complex (MTBC) virulence

Sarah N. Danchuk
Laboratory of Dr. Marcel A. Behr
Department of Microbiology and Immunology
McGill University, Montreal

A thesis submitted to McGill University in partial fulfilment of the requirements of the degree of Doctor of Philosophy

ABSTRACT

The *Mycobacterium tuberculosis* complex subspecies (MTBCs) are closely related pathogens causing tuberculosis in mammalian hosts. Research has predominantly focused on *Mycobacterium tuberculosis* (*M. tb,* the causative agent of human tuberculosis) and *Mycobacterium bovis* (*M. bovis,* a causative agent of zoonotic tuberculosis). Notably, *M. tb* is a human-adapted pathogen whereas *M. bovis* is an animal-adapted member of the MTBC. Foundational work by Robert Koch and Theobald Smith established that *M. tb* and *M. bovis* have significantly different infection outcomes, with *M. bovis* infection resulting in more severe pathology in experimental infections. Globally, more than 10 million new cases of TB are reported each year; ~1% are estimated to be due to zoonotic tuberculosis (zTB), typically attributed to *M. bovis*. However, recent studies have highlighted that another organism, *Mycobacterium orygis,* may also contribute to the global TB burden. As this organism was first characterized in 2012, it has not been subject to thorough experimental investigation and as such, knowledge on its epidemiology and pathogenesis are limited. Current molecular tools have enabled researchers to translate natural observations from clinics into systematic evaluations in the laboratory, using *in vitro, ex vivo,* and *in vivo* techniques. To this end, in this thesis, I used mycobacterial engineering to develop isogenic strains of *M. bovis* Bacille Calmette-Guérin (BCG), *M. bovis,* and *M. orygis.* BCG strains were subsequently employed in clinical diagnostics whereas *M. bovis* and *M. orygis* isogenic strains were used to investigate infection outcomes using both *ex vivo* and *in vivo* models.

In chapter II, I developed a panel of 6 mono-resistant strains of the attenuated BCG vaccine using oligo-mediated recombineering for laboratory quality control studies. In chapter III, I used the ORBIT (oligo-mediated recombineering followed by Bxb-1 integrase targeting) system to develop 8 deletion strains targeting either the canonical virulence factor ESAT-6, or the non-

canonical virulence factors MPT70/MPT83 (in *M. bovis* and *M. orygis*) and characterized their effects on protein secretion and macrophage infection. In chapter IV I used a murine infection model to characterize the experimental outcome following aerosol exposure to *M. tb, M. bovis,* and for the first time, *M. orygis*, revealing that *M. bovis* and *M. orygis* are hypervirulent compared to *M. tb* following infection of the same host (based on comparative pathology, median survival, and lethal dose). Additionally, I established that MPT70/MPT83 are critical virulence factors in *M. bovis* but not *M. orygis* in this model. It was also observed that rapid mortality seen following *M. orygis* infection could be delayed, but not overcome, by vaccination with either BCG (a live, attenuated vaccine) or novel subunit vaccines. Finally, in chapter V I, in conjunction with researchers at the University of Saskatchewan, determined that *M. bovis* and *M. orygis* show significantly worse experimental outcomes compared to *M. tb* in a calf model of infection.

Ultimately, this dissertation provides novel insights into the MTBCs and utilizes *in vitro, ex vivo,* and *in vivo* techniques to experimentally characterize *M. orygis* for the first time. This thesis established two recombineering systems in animal-associated lineages of the MTBCs and the products of the tools have been used in both clinical and research laboratories. Perhaps most importantly, this thesis has provided evidence that a third species should be considered in future pathogenesis research and may be used as a new 'foundation' for the study of MTBC virulence factors.

RESUMÉ

Les sous-espèces du complexe *Mycobacterium tuberculosis* (MTBC) sont des agents pathogènes étroitement liés qui provoquent la tuberculose chez les mammifères. La recherche s'est principalement concentrée sur *Mycobacterium tuberculosis* (*M. tb*, l'agent causal de la tuberculose humaine) et *Mycobacterium bovis* (*M. bovis*, un agent causal de la tuberculose zoonotique). Notamment, *M. tb* est un pathogène adapté à l'homme, tandis que M. bovis est un membre du MTBC adapté à l'animal. Les travaux fondamentaux de Robert Koch et Theobald Smith ont établi que M. tb et M. bovis ont des résultats d'infection sensiblement différents, l'infection par M. bovis entraînant une pathologie plus grave. Dans le monde, plus de 10 millions de nouveaux cas de tuberculose sont signalés chaque année; on estime qu'environ 1 % d'entre eux sont dus à une tuberculose zoonotique (zTB), généralement attribuée à *M. bovis*. Des études récentes ont montré qu'un autre organisme, *Mycobacterium orygis*, pourrait également contribuer à la charge mondiale de la TB. Cet organisme ayant été caractérisé pour la première fois en 2012, il n'a pas fait l'objet d'études expérimentales approfondies et les connaissances sur son épidémiologie et sa pathogénie sont donc limitées. Les outils moléculaires actuels ont permis aux chercheurs de traduire les observations naturelles des cliniques en évaluations systématiques en laboratoire, en utilisant des techniques *in vitro*, *ex vivo* et *in vivo*. À cette fin, dans cette thèse, j'ai utilisé l'ingénierie mycobactérienne pour développer des souches isogéniques de *M. bovis* Bacille Calmette-Guérin (BCG), *M. bovis* et *M. orygis*. Les souches de BCG ont ensuite été utilisées pour des diagnostics cliniques, tandis que les souches isogéniques de M. bovis et de M. orygis ont été utilisées pour étudier les résultats de l'infection à l'aide de modèles ex vivo et in vivo.

Dans le chapitre II, j'ai développé un panel de 6 souches monorésistantes du BCG en utilisant la recombinaison oligo-médiée pour des études de contrôle de qualité en laboratoire. Dans

le chapitre III, j'ai utilisé le système ORBIT développer 8 souches de délétion ciblant soit le facteur de virulence canonique ESAT-6, soit les facteurs de virulence non canoniques MPT70/MPT83 (chez *M. bovis* et *M. orygis*) et j'ai caractérisé leurs effets sur la sécrétion de protéines et l'infection des macrophages. Dans le chapitre IV, j'ai utilisé un modèle d'infection murine pour caractériser les résultats expérimentaux après exposition par aérosol à M. tb, M. bovis et, pour la première fois, M. orygis, révélant que *M. bovis* et *M. orygis* sont hypervirulents par rapport à *M. tb* après infection du même hôte (sur la base d'une pathologie comparative, de la survie médiane et de la dose létale). En outre, j'ai établi que MPT70/MPT83 sont des facteurs de virulence critiques chez *M. bovis* mais pas chez *M. orygis* dans ce modèle. Il a également été observé que la mortalité rapide observée après une infection par M. orygis pouvait être retardée, mais pas surmontée, par la vaccination avec le BCG ou avec de nouveaux vaccins à sous-unités. Enfin, dans le chapitre V, j'ai déterminé, en collaboration avec des chercheurs de l'Université de Saskatchewan, que *M. bovis* et *M. orygis* présentent des résultats expérimentaux nettement moins bons que *M. tb* dans un modèle d'infection chez le veau.

Finalement, cette thèse fournit de nouvelles informations sur les MTBC et utilise des techniques *in vitro, ex vivo* et *in vivo* pour caractériser expérimentalement *M. orygis* pour la première fois. Cette thèse a établi deux systèmes de recombinaison dans des lignées de MTBC associées à l'animal et les produits de ces outils ont été utilisés dans des laboratoires cliniques et de recherche. Peut-être plus important encore, cette thèse montre qu'une troisième espèce devrait être prise en compte dans les recherches futures sur la pathogenèse et pourrait être utilisée comme nouvelle ‘base’ pour l'étude des facteurs de virulence des MTBC.

ACKNOWLEDGEMENTS:

Before thanking everyone, I would like to acknowledge the mice and calves sacrificed over the course of this dissertation. No one likes to do animal work, but without it, this thesis would not have been possible. I would also like to acknowledge and show my appreciation to the team at University of Saskatchewan for making me feel so welcome during my visit and Dr. Vivek Kapur at Penn State for his invaluable assistance, especially during the final years of this degree.

I have to say thank you to the people I have spent years alongside, supporting me every day and who have made this experience so meaningful. To the members of the Behr lab, I am forever grateful for the people I got to meet, the experiences I got to have and the stories I will always tell. To Dr. Marcel Behr, you may be expecting a sassy comment, but you'll have to settle for this instead: I applied to this program 6 days before the deadline, and you took a chance on me, not knowing how it would work out. You have always supported me, guided me and showed me what it is like when you really care about something. I will not be able to adequately convey everything I've learned these last few years under your mentorship, but please know how thankful I am. I could not have asked for a better supervisor and I hope to take your compassion and your curiosity wherever I go. To Shannon Duffy (my SD^2), I am more grateful than you'll ever know to have you in my life. Without you I wouldn't have made it through the pandemic- let alone this degree. Thank you for being my confidant, accomplice, sweetest friend, and for making so many memories in this place with me. To Jaryd Sullivan (Winterpeg), thank you for being an amazing friend, pushing me to be a better scientist, and for still cheering me on from afar. You're my favourite annoying big brother. To Ori Solomon, we got off to a rocky start, but you managed to turn it around. Thank you for helping me get through these last few months and always being around to joke around or commiserate with. I appreciate your friendship more than you know.

Finally, to Fiona McIntosh, thank you for spending 70+ aerosol infections with me and for your continuous guidance and support throughout the years.

I also need to say thank you to Andréanne Lupien; you have no idea the impact that you've had on me nor how you have shaped these last (many) years. You are the person I go to for anything involving science but also someone I turn to for advice, a laugh, or even just a walk around the hospital. You are an amazing teacher, and I cannot wait to see even more from the Lupien lab.

To my advisory committee Samantha Gruenheid and Benoit Cousineau: thank you for your guidance over the years and for your feedback every step of the way. Your assistance has helped me write a thesis I can be proud of.

Lastly, I would like to thank my family, friends, and partner for their unwavering support. To my parents Carol and Nicholas: thank you for encouraging me from a young age to ask 'why' and 'how come' and for your constant belief in me, even at the expense of many shampoos and soaps for my 'potions'. To Celine Agnes, you were one of the first people I met in this city and became one of my favourite things about it. I cannot wait to see what is next for you. To Carina Filice and Lilia Shaban, thank you for your constant support, check-ins, calls, movie nights, girls' weekends and everything in between. You have no idea how much it means to me and how excited I am for this next chapter with both of you. Finally, to my partner Jordan Francis, I will never be able to describe how much I've appreciated your love, support and steadfast assurance that I can do this. Thank you for believing in me when it all seemed impossible and for choosing a very stressed out, overwhelmed PhD student living 600 km away to be your girlfriend.

To anyone else reading, thank you too.

TABLE OF CONTENTS

LIST OF FIGURES

CHAPTER I

CHAPTER II

CHAPTER III

CHAPTER IV

LIST OF TABLES

CHAPTER II

CHAPTER III

CHAPTER IV

CHAPTER V

CHAPTER VI

ABBREVIATIONS

-/-	genetic deletion; null
ADC	Albumin, Dextrose, and Catalase
AFB	acid-fast bacilli
ARD	animal resource department
AtC	anhydrotetracycline
attB	bacterial attachment site
attP	phage attachment site
BCCM	Belgian Coordinated Collections of Microorganisms
BCG	*Mycobacterium bovis* Bacille Calmette-Guérin
BDQ	bedaquiline
BMDMs	bone marrow derived macrophages
BPaL	bedaquiline, pretomanid, linezolid
BPaLM	bedaquiline, pretomanid, linezolid, moxifloxacin
bTB	bovine tuberculosis
CC	critical concentration
CCAC	Canadian Council on Animal Care
CD	cluster of differentiation
CFP-10	10 kDa culture-filtrate protein
CFU	colony forming unit

CFZ	clofazimine
CL3	biosafety level 3
CMC	Christian Medical College
COVID	Coronavirus Disease 2019
DS-TB	drug-susceptible tuberculosis
dsDNA	double-stranded DNA
DST	drug-susceptibility test
EMB	ethambutol
ESAT-6	6 kDa early secreted antigenic target
ESX	early secretory antigen target secretion
FQ	fluoroquinolone
FRDR	fluoroquinolone resistance determining region
GOI	gene of interest
H&E	hematoxylin and eosin
HGT	horizontal gene transfer
HIV	Human-Immunodeficiency Virus
HYG	hygromycin
HygR	hygromycin-resistant
IFN	interferon
IGRA	Interferon- γ release assay
IL	interleukin
INFAR	interferon-$\propto$ receptor

INH	isoniazid
IS	insertion sequence
IV	intravenous
IVN	isovaleronitrile
KAN	kanamycin
KanR	kanamycin-R
LJ	Lowenstein-Jensen
LOD	limit of detection
LPA	line probe assay
Ly6C	lymphocyte antigen 6 complex
Ly6G	lymphocyte antigen 6 complex locus G6D
LZN	linezolid
M. bovis Δmpt70_mpt83	*M. bovis Δmpt70-dipZ-mpt83*
M. bovis	*Mycobacterium bovis*
M. orygis Δmpt70_mpt83	*M. orygis Δmpt70-dipZ-mpt83*
M. orygis	*Mycobacterium orygis*
M. tb	*Mycobacterium tuberculosis*
MCP	monocyte chemoattractant protein
MDR-TB	multidrug resistant tuberculosis
MFX	moxifloxacin
MIP	macrophage inflammatory protein
MLN	mediastinal lymph node
MOI	multiplicity of infection

MPB	major protein from *M. bovis*
MPO	myeloperoxidase
MPT	major protein from *M. tuberculosis*
MRCA	most recent common ancestor
MTBC	*Mycobacterium tuberculosis* complex
NAAT	nucleic acid amplification assays
NCBI	National Centre for Biotechnology Information
NETs	neutrophilic extracellular traps
NTMs	non-tuberculous mycobacteria
OADC	Oleic acid, Albumin, Dextrose, and Catalase
OD_{600}	optical density at 600 nm
ORBIT	Oligo-mediated recombineering followed by Bxb1 integrase targeting
PAMP	pathogen associated molecular pattern
PANTA	Polymyxin B, Amphotericin B, Nalidixic acid, Trimethoprim, Azlocillin
PCA	principal component analysis
PCR	polymerase chain reaction
PDIM	phthiocerol dimycocerosate
PE	proline-glutamic acid
PGL	phenolic glycolipids
PPD	purified protein derivative

PPE	proline-proline-glutamic acid
pre-XDR-TB	pre-extensively drug-resistant tuberculosis
PZA	pyrazinamide
qRT-PCR	quantitative real-time polymerase chain reaction
RANTES	regulated on activation, normal T-cell expressed and secreted
RD	region of difference
RD	region of difference
RI-MUHC	Research Institute of the McGill University Health Centre
RIF	rifampin
RR-TB	rifampin resistant tuberculosis
RRDR	rifampin-resistance determining region
RskA	anti-sigma factor K
SC	subcutaneous
SCID	severe compromised immunodeficiency
SC-IMC	single-cell imaging mass cytometry
Sec	general secretion system
SigK	sigma factor K
SL	sulfalipid
SLID	second-like injectable drugs
SNP	single nucleotide polymorphism

ssDNA	single-stranded DNA
STREP	streptomycin
T7SS	type VII secretion systems
Tat	twin-arginine translocation export pathway
TBLN	tracheobronchial lymph node
TCH	thiophene-2-carboxylic acid hydrazide
Th1	T-helper subtype 1 cells
Th2	T-helper subtype 2 cells
TLC	thin layer chromatography
TNF	tumor necrotic factor
TST	tuberculin skin test
Ultra	GeneXpert Ultra
VIDO	Vaccine and Infectious Disease Organization
WGS	whole genome sequencing
WHO	World Health Organization
WT	wildtype
XDR-TB	extensively drug-resistant tuberculosis
Xpert	GeneXpert
ZEO	zeocin
ZeoR	zeocin resistant
ZN	Ziehl-Neelson
zTB	zoonotic tuberculosis

CONTRIBUTIONS TO ORIGINAL KNOWLEDGE

The contributions to original knowledge described in this thesis are as follows:

1. Development of panel of mono-resistant BCG strains (n=6 strains) and distribution of strains nationally and internationally
    a. First to utilize mycobacterial recombineering system (pNIT:ET) to develop panel of mono-resistant BCG strains
    b. First to publish on the utility of these strains as quality control for commercially available diagnostic tests (such as GeneXpert, MTBDR*plus*)
    c. Panel now incorporated as standard control for tuberculosis laboratories from McGill University Health Centre (MUHC) to the Inuulitsivik Health Centre (Puvirnituq, QC) to Christian Medical College (Vellore, India), and deposited at the Belgian Coordinated Collection of Microorganisms (BCCM) for further distribution.
    d. First to use recombinant BCG panel to systematically evaluate detection of heteroresistance (defined as mixed populations of drug susceptible and drug-resistant bacteria) using phenotypic testing and whole genome sequencing (WGS).
    e. Determination of limit of detection of minority populations for current WGS pipelines in established clinical laboratories in Germany and the Netherlands.
2. First to incorporate the ORBIT system (oligonucleotide-mediated recombineering followed by Bxb1 integrase targeting) in *M. bovis* Ravenel and *M. orygis* 51145
    a. Developed and validated a total of 6 *M. bovis* deletion strains (4 of which were used in this dissertation) and 4 *M. orygis* deletion strains
    b. First to investigate MPT70, MPT83, DipZ and EsxA utilizing the ORBIT system

3. First to perform a secretome analysis of isogenic *M. bovis* strains (*Δmpt70_mpt83, Δmpt70, Δmpt83, ΔesxA*) to determine factors driving phenotypic variance
4. First addition of *M. bovis* isogenic strains (*Δmpt70_mpt83, Δmpt70, Δmpt83*) WGS and *M. orygis Δmpt70_mpt83* WGS to the National Center for Biotechnology Information (NCBI) database
5. First to identify MPT70 and/or MPT83 as species-specific virulence factor
    a. Aerosol infection with *M. bovis* isogenic strains (*Δmpt70_mpt83, Δmpt70, Δmpt83*) revealed a complete reversal of lethal phenotype seen with wildtype strain
    b. Determined that infection with isogenic strain(s) resulted in clearance of bacterial burden from the lung, rather than containment over the course of infection
6. First to experimentally characterize wildtype *M. orygis*
    a. Evaluated growth rates and nutrient requirements to develop standard culturing techniques
    b. Demonstrated the presence of the virulence factor phthiocerol dimycocerosate (PDIM)
    c. First to perform secretomic analysis of wildtype and isogenic *M. orygis* (*Δmpt70_mpt83*)
7. First to experimentally infect C57BL/6 mice with *M. orygis* via the aerogenic route
    a. Demonstrated rapid mortality following *M. orygis* infection that was markedly different from *M. tb* infection using the same route
    b. Determined that death phenotype can be used in translational research, such as time to mortality following vaccination as demonstrated by vaccination with:
        i. BCG Russia

ii. BCG Danish

iii. MPT70 subunit vaccine

iv. ESAT-6 subunit vaccine

8. First to experimentally infect *Bos taurus* calves with *M. orygis*
    a. Performed comparative study of *M. tb, M. bovis* and *M. orygis* in a natural host
    b. Evaluated bacterial burden, gross pathology and histopathology following infection.
    c. Demonstrated that *M. orygis* also manifests enhanced virulence in calf model

CONTRIBUTIONS OF AUTHORS

This thesis was written by Sarah N. Danchuk with input and editing from Marcel A. Behr. This work was prepared as per the guidelines for a traditional thesis provided by McGill University Graduate and Postdoctoral Studies. The contributions of each author to each chapter are described below. Marcel A. Behr designed and supervised all studies.

Chapter I: Literature Review

This chapter was written by Sarah N. Danchuk with guidance and editing from Marcel A. Behr.

Chapter II: The utilization of pNIT:ET in the clinical diagnosis of *Mycobacterium tuberculosis*

This chapter describes in further detail experiments from one published note and one published manuscript. The note entitled, **Bacillus Calmette–Guérin strains with defined resistance mutations: a new tool for tuberculosis laboratory quality control** (Clinical Microbiology and Infection, Volume 26, Issue 3, March 2020) includes authors Sarah N. Danchuk, Fiona McIntosh, Frances B. Jamieson, Kevin May, and Marcel A. Behr. The published manuscript entitled, **Challenging the gold standard: the limitations of molecular assays for detection of *Mycobacterium tuberculosis* heteroresistance** (Thorax, Volume 79, Issue 7, January 2024) includes authors Sarah N. Danchuk, Ori E. Solomon, Thomas A. Kohl, Viola Dreyer, Ivan Barilar, Christian Utpatel, Stefan Niemann, Dick van Soolingen, Richard Anthony, Jakko van Ingen, Joy S. Michael, Marcel A. Behr.

This chapter was written by Sarah N. Danchuk with editing from Marcel A. Behr. Sarah N. Danchuk integrated and validated the pNIT:ET recombineering system in mycobacterial species,

developed the panel of recombinant *M. bovis* BCG strains with defined antibiotic resistance, confirmed the validity of integrated mutation, performed phenotypic drug susceptibility testing on mono-resistant strains, determined the MIC_{90} for each strain, and performed GeneXpert assays at McGill University Health Centre and Lakeshore General Hospital. Sarah N. Danchuk also prepared heteroresistant samples to be assessed using phenotypic and genotypic assays (GeneXpert, GeneXpert Ultra, MTBDR*plus*, and agar proportion method).

Additional contributions to this chapter are as follows: Kevin May performed and interpreted the MTBDR*plus* assay at Public Health Ontario under the supervision of Frances B. Jamieson. Fiona A. McIntosh assisted in running GeneXpert assays at Lakeshore General Hospital. Ori E. Solomon performed phenotypic drug testing on heteroresistant samples of recombinant *M. bovis* BCG strains using the agar proportion method.

Chapter III: Use of mycobacterial recombineering to characterize production of MPT70 and MPT83 by natural and engineered variants of the MTBC

This chapter was written by Sarah N. Danchuk with guidance and editing from Marcel A. Behr. All *in vitro* and *ex vivo* experiments and data analyses discussed in Chapter III were performed by Sarah N. Danchuk with the following exception: proteomic analysis of secretomes was performed by the McGill Proteomic and Molecular Analysis Platform at the Research Institute of the McGill University Health Centre. Sarah N. Danchuk visualized and interpreted this data.

Chapter IV: *Mycobacterium tuberculosis* complex subspecies (MTBC) pathogenesis in a murine model

This chapter describes in further detail experiments in the submitted first author paper entitled **Enhanced virulence of *Mycobacterium orygis* provides new insights into the pathogenesis of tuberculosis.** This submitted paper is a collaboration between: Sarah N. Danchuk, Shannon C. Duffy, Jaryd Sullivan, Syed Beenish Rufai, Fiona A. McIntosh, Andréanne Lupien, Lorne Taylor, Yuhong Wei, Philippe Joubert, Rasmus S. Mortensen, Vivek Kapur, and Marcel A. Behr.

This chapter was written by Sarah N. Danchuk with guidance and editing from Marcel A. Behr. Sarah N. Danchuk performed all aerosol infections in collaboration with Fiona A. McIntosh. Sarah N. Danchuk performed all *in vitro* and *in vivo* experiments and analyzed the data with the following exceptions: Beenish Rufai performed the whole genome sequencing of *M. orygis* 51145 in collaboration with the Pennsylvania State University, and Fiona A. McIntosh performed the ESAT-6/MPT70 subunit vaccination study (vaccine provided by the Statens Serum Institute, Copenhagen, Denmark). Philippe Joubert analyzed and scored histopathology of *M. tb* and *M. orygis* infected groups. Andréanne Lupien assisted Sarah N. Danchuk with *M. bovis* BCG (Russia and Danish) vaccination study. Proteomic analysis was performed by the McGill Proteomic and Molecular Analysis Platform at the Research Institute of the McGill University Health Centre. Sarah N. Danchuk visualized and interpreted this data.

Chapter V: Insights from a natural host

This chapter was written by Sarah N. Danchuk with guidance and editing from Marcel A. Behr. Sarah N. Danchuk provided *M. orygis* 51145 for aerosol infection, assisted with the necropsy of calves at experimental endpoint, photographed gross pathology, determined stages of granulomas on histopathological assessment, and calculated colony forming units per gram in

lungs, mediastinal lymph nodes, and tracheobronchial lymph nodes. This experiment was done in collaboration with Jeffery Chen and the Animal Services department at the University of Saskatchewan (Saskatoon, Saskatchewan). The Animal Services department performed the aerosol infection, necropsy of calves at experimental endpoint, extraction of tissue for histopathology and/or determination of bacterial burden. Jeffery Chen processed and plated extracted materials to determine bacterial burdens.

Chapter VI: Discussion

This chapter was written by Sarah N. Danchuk with guidance and editing from Marcel A. Behr.

CHAPTER I: LITERATURE REVIEW

1: A Brief History

Few diseases have shaped human history as tuberculosis (TB) has. The first written descriptions of TB come from India and China ~2000-3000 years ago; the first physical evidence of TB associated pathology predates this, coming from 8000–10000-year-old human skeletal remains[1–3]. As an 'ancient' disease, TB has held many other names such as phthisis, 'king's evil, 'robber of youth', 'captain of death', white plague, consumption etc.[2,4–6]. Often these names described the disease phenotype, including white, necrotic lesions in the lung (later termed 'tubercles'), cough, bloody sputum, weight loss, pallor, anemia, and fever[2,3]. Beyond these observations, it was also well-established that TB was not only a disease of the lungs, but was also found in the cervical lymph nodes (called scrofula), though this was less common[2,7]. The TB epidemic reached a critical mass between the 17th and 19th centuries in Europe and North America. Historical evidence indicates mortality rates as high as 800-1000 deaths per 100 000 people per year in major European cities (London, Stockholm, Hamburg); in New York and Massachusetts TB was responsible for a quarter of all recorded deaths[3,8–10]. This has been largely attributed to increased population, poor working conditions and socioeconomic factors (overcrowding, inadequate ventilation, malnutrition, poverty etc.) at that time, resulting in the rapid spread of disease[5,9,11]. During this same period, significant advancement was made about the origin, manifestation and transmission of TB. First, in 1720, Benjamin Marten postulated that TB may be an infectious disease, rather than an inherited one, and that it may be caused by microorganisms. Second, in 1819, René Theophile Laennac redefined the clinical features and diagnosis of both pulmonary and extrapulmonary TB (ex: bone, joint, gastrointestinal, central nervous system etc.)[3].

Next, though initially dismissed, in 1865 Jean-Antoine Villemin established that TB is transmissible by subcutaneously infecting rabbits with tissue from a deceased tuberculosis patient (pus and portions of the granuloma)[12,13]. At autopsy, despite no overt signs of clinical disease, the rabbit showed extensive lesions throughout the body, confirming the previous suspicions[12,13]. These efforts culminated in the isolation and identification of tubercle bacilli, the causative agent of tuberculosis, by Robert Koch in 1882[14]. This would subsequently be renamed as *Mycobacterium tuberculosis*.

Shortly after Koch's establishment of *M. tuberculosis* as the key agent of tuberculosis, it became apparent that human-associated TB and cattle-associated TB were fundamentally different in terms of morbidity, and mortality. This suggested that, contrary to the current understanding, there may be more than one causative agent of tuberculosis which affects more than one host. It was already known that milk from diseased cows contained tubercle bacilli and that this disease could be transmitted orally to a number of hosts (guinea pigs, rabbits, pigs, and calves)[10]. Two physicians (Emanuel Klein and Heneage Gibbs, 1883) observed that, following experimental infection, guinea pigs succumbed to infection from both human and bovine tubercle bacilli whereas rabbits only succumbed to infection following exposure to bovine tubercle bacilli[15]. Following this, in 1898, Theobald Smith identified and characterized the bovine tubercle bacillus, known today as *Mycobacterium bovis,* allowing for the parallel analysis of different tubercle bacilli, in different hosts, and, as such, providing the first evidence of differential virulence[16–18].

2: Defining Mycobacteria

Mycobacteria belong to the order Actinomycetales and are the only genus within the family mycobacteriaceae. The Mycobacterium genus was originally named by Lehmann and Neumann in 1896, based on *Mycobacterium tuberculosis*[19]. Broadly, these organisms are defined as acid-fast

positive (AFB+), rod-shaped, non-motile, non-spore forming, aerobic microorganisms, measuring 1.0-10.0 μM in length[20,21]. The doubling time of mycobacterial species varies greatly allowing the genus to be divided into fast growers (colonies appear within 2-5 days on solid media) and slow-growers (colonies appear >7 days on solid media)[22]. One of the defining features of the genus is the composition of the cell wall. Though technically Gram positive, the organization of the mycobacterial cell wall is more similar to Gram negative species[23]. Mycobacteria possess thick, waxy cell walls which contain peptidoglycan, arabinogalactan, mycolic acid, and a multitude of lipids and immunomodulatory structures[20,24]. Notably, mycolic acid acts as a hallmark of the mycobacterial cell wall and is essential for the regulation of bacterial viability and virulence[25]. The unique structure of the cell wall provides inherent resistance to light, acid, alcohol, and heat and plays an essential role in mycobacterial pathogenicity[24,26]. Further, the mycobacterial cell wall is hydrophobic; lipids account for ~40% of its dry mass, in comparison to only 20% in Gram-negative bacteria[27]. At the nucleotide level, mycobacteria are guanine (G) and cytosine (C) rich with an average genomic content of ~62-70% (average prokaryotic GC content= 16-77%)[28,29].

At present, ~200 mycobacterial species have been described, with variable clinical relevance[30]. The Mycobacterium genus can be broadly characterized into three groups: the *Mycobacterium tuberculosis* complex subspecies (MTBCs), *Mycobacterium leprae* and *M. lepromatosis* (the causative agents of leprosy), and non-tuberculous mycobacteria (NTMs)[31,32]. Of note, NTMs make up the largest proportion of the genus and have the greatest genetic diversity between strains. Moreover, whereas the MTBCs, *M. leprae,* and *M. lepromatosis* consist solely of obligate pathogens, the NTMs consist of benign environmental species, opportunistic pathogens, and obligate pathogens[33]. This dissertation will focus on four members of the MTBCs:

Mycobacterium tuberculosis (*M. tb*), *Mycobacterium bovis* (*M. bovis*), *M. bovis* Bacille Calmette-Guérin (BCG), and *Mycobacterium orygis* (*M. orygis*).

3. The Mycobacterium tuberculosis complex subspecies (MTBCs)

Until two decades ago, it was often stated that the tubercle bacillus originated in animals and was transmitted to humans following domestication[34]. Given that animal-associated lineages of the MTBC, such as *M. bovis,* have an extensive host-range whereas *M. tb* is restricted only to humans, this follows logically[35]. However, molecular analysis challenged this evolutionary scenario by showing that *M. tb* had a larger genome and that the *M. bovis* genome was marked by deleted regions. This suggested instead that TB began in humans and evolved in animals[34,36]. Compared to the inferred ancestor, MTBC evolution is reductive, having no evidence of acquisition of new genetic material nor horizontal gene transfer (HGT)[37–39]. Together with the uncertain evolutionary scenario, a contemporary understanding is that the MTBC are tubercle bacilli associated with different mammalian hosts and that phenotypic variation amongst the MTBC is due to either the loss of genes, mutations in genes resulting in altered protein sequences, duplications of genes or the modulation of expression of a conserved gene.

At the nucleotide level, MTBCs are 99.95% conserved, differentiated based on regions of deletion (RDs, ranging from 2-12.7 kb) and strain specific single nucleotide polymorphisms (SNPs)[40–42]. Members of this complex are slow-growing organisms (doubling time > 24 hours), capable of causing tuberculosis in immunocompetent mammalian hosts[43]. Pragmatically, these subspecies can be further divided into human-associated strains, animal-associated strains, and *M. canettii*[43–45]. Though historically cited in literature, the inclusion of *M. canettii* as part of the MTBC has been debated due to genomic size, content, and bacterial physiology of isolates compared to other members of the complex[11]. Additionally, there is evidence of recombination that

differentiates it from the clonal nature of other members of the MTBCs[46]. As such, *M. canettii* will be considered an outgroup in this dissertation.

3.1 Animal-Associated MTBCs

Presently, 10 lineages of *M. tb* (L1-L10) and 10 animal-associated subspecies have been described. The animal-associated subspecies have been binned into clades called A1-A4 (Figure 2). With the exception of A1 members, all animal-associated strains have been documented in at least two animal hosts. As such, the MTBCs can be colloquially divided into single-host specialists (like *M. tb* and A1 organisms) or multi-host generalists (the others) (Figure 2).

Briefly, A1 refers to *M. mungi* (mongoose), *M. suricattae* (meerkat), the Dassie bacillus, and the Chimpanzee bacillus. Notably, members of this clade have to date been detected in a single host and have shown no evidence of human-infection, though these strains are most closely related to L6 and L9 of *M. tb*[11,35]. Additionally, *M. mungi, M. suricattae,* and the Dassie bacillus show unique deletions in 'RD1', whereas the Chimpanzee bacillus shows this region intact[47]. Notably, essential virulence factors (including ESAT-6 and CFP-10, Section 8.1) are encoded by this region[48]. Members of A2 include *M. microti* and *M. pinnipedii*. *M. microti* has a strain specific deletion in RD1 and was previously used as a vaccine strain against *M. tb* (see section 5). Additionally, it can be found in a broad host of wild and domesticated animals (voles, shrew, mice, cats, boar, llamas etc.) though its natural geographic range is likely restricted to Europe[43,49]. *M. microti* infection in humans is rare but has been reported in both immunocompromised and immunocompetent patients[50–52]. Comparatively, *M. pinnipedii* has been isolated from a broad range of hosts including wild and captive pinnipeds (seals, sea lions), dolphins, camels, tapirs, gorillas, leopards, cattle, and immunocompetent humans[53–55]. In fact, MTBC DNA isolated from ~1000-year-old Peruvian human remains is most similar to modern *M. pinnipedii* isolates. This

provides foundational evidence of TB existing in the 'New World' prior to European expansion and supports animal-to-human transmission model from hunting[47,56,57]. Of note, no direct human-to-human transmission of *M microti* or *M. pinnipedii* has been documented though it has been suggested[49,58]. Finally, A3 and A4 lineages have the most extensive host-ranges and include the causative agents of bovine tuberculosis (bTB). Additionally, members of these clades have the greatest contribution to animal and human health globally. A3 consists of *M. orygis* isolates exclusively whereas A4 consists of *M. bovis* (including *M. bovis* BCG vaccine strains), and *M. caprae*[11,43,59]. Lineages A3 and A4 will be further discussed in sections 6 and 7.

4. *Mycobacterium tuberculosis (M. tb)*

In 2022, there were ~10.6 million new cases of TB and 1.3 million deaths. Of these deaths ~167000 could be attributed to HIV + individuals[60]. The great majority of these cases and fatal infections are thought to be due to *M. tb*. Despite being a completely curable disease, TB remains a leading cause of death globally due to a single infectious agent (surpassing COVID-19) and the number one leading cause of death amongst HIV+ people[60]. Thirty countries are responsible for ~87% of the total TB burden, with India being responsible for~27% alone (Indonesia has the next highest burden at ~10%)[60]. The End TB Strategy of the WHO seeks a global case reduction to < 10 cases per 100,000 people by 2035[61]. There are two main barriers that prevent this: 1) lack of available (and accurate) diagnostics and 2) universal access to treatment[61]. For the scope of this dissertation, *M. tb* will only be considered as a comparator species for experimental infections.

4.1 Genome:

The reference strain *M. tb* H37Rv was first sequenced in 1998, revealing a genome ~4.4 MB in size, with an average GC content of ~65.5%. In 2022, this genome was updated and shown to be ~6.4 kB larger[62]. One of the major challenges of *M. tb,* and other members of the MTBC, is

repeated sequences throughout the genome[62]. Further analysis showed that ~50% of the proteome was the result of gene duplication or rearrangement events[11]. Additionally, where gene duplications occurred, they were predominantly involved in secretion (ex: the ESX system, described above), PE/PPE production, fatty acid metabolism, lipid transport[11]. Interestingly, many of these gene duplication events are believed to be associated with virulence and mycobacterial survival[11]. *M. tb* has been divided into 'ancestral' and 'modern' lineages based on the presence or absence of 'TbD1', a region of the genome containing *mmpS6* and a portion of *mmpL6* (suspected to be involved in oxidative stress responses)[63]. Moreover, most TB cases globally can be attributed to the 'modern' lineages (L2-4), though the ancestral lineage 1 is prominent in South Asia[11,64]. Interestingly, there are strain specific variances in bacterial and host phenotypes following natural or experimental TB infection[11,65]. For example, L6 (also known as *M. africanum*) shows a decreased bacterial burden compared to L2 following experimental infection[65]. Similarly, L1 has been reported to be more likely to cause TB meningitis compared to L4[65].

4.2 Pathogenesis:

As described previously, the 'tubercle bacillus' was first discovered to be the causative agent of human tuberculosis in 1882. Although it is a predominantly a pulmonary pathogen, *M. tb* can cause disease anywhere in the body (extrapulmonary TB). Unlike its animal counterparts, the host-range of *M. tb* is restricted to humans[66,67]. Though *M. tb* has been detected in animals (elephants, cattle, dogs, non-human primates) these are considered to be spillover hosts and do not propagate infection[68]. For onward transmission, the estimated burden of bacilli capable of causing infection is estimated to be ~1-3 organisms[65,69]. *M. tb* transmits from human to human via the aerosol route, which can occur during coughing, singing, or even through tidal breathing. Exposure to the bacteria will result in one of two options: 1) clearance or 2) infection. Of those infected,

between 90-95% of infected people will clear or contain *M. tb* infection but ~5-10% of people will develop disease (TB) over their lifetime (typically within 18-24 months of initial infection)[70]. It is this minority that develop disease who are thought to transmit *M. tb*. and propagate the epidemic.

The early events of MTBC infection are complex and depend largely on initial response of the host immune system[71]. The innate system (macrophages, dendritic cells, neutrophils, and natural killer cells) helps restrict the progression of infection until the adaptive system is alerted and mounts a supplementary response. When inhaled *M. tb* is ingested by alveolar macrophages where a cascade of host responses are initiated, including cytokine and chemokine secretion[71]. This response recruits other cells to the site of infection (such as other macrophages, neutrophils, dendritic cells and, at a later point, lymphocytes) and results in the formation of an immune cell rich structure known as a granuloma, considered as the 'hallmark' of TB disease[71]. Though the granuloma acts as one of the main lines of defense against *M. tb,* it also provides a niche for mycobacteria to exploit[72]. If bacterial growth is controlled, bacteria remain within the confines of the structure; however, if there is immune dysregulation (such as an imbalance of pro- and anti-inflammatory cytokines), the centre of the granuloma can undergo necrosis and release bacteria[71]. These bacteria then trigger the formation of additional granulomas in other tissues (both pulmonary and extrapulmonary sites) where the process repeats[71]. The classical *M. tb* granuloma consists of macrophages (naïve and differentiated), multinucleated giant cells (referred to as Langhans giant cells), and lymphocytes (T- and B-cells) in addition to other innate immune cells[72]. Following *M. tb* infection, several types of granulomas can be induced: caseous (in which a central necrotic centre is rimmed by differentiated macrophages, T-cells, and B-cells), non-necrotizing (composed mostly of macrophages), necrotic neutrophilic granulomas, and fibrotic granulomas[72,73]. Of note,

both the host and MTBC strain (ex: *M. tb, M. bovis* and *M. orygis*) influences the granulomatous response and can result in significantly different infection outcomes[18,71,74,75].

4.3 Diagnostics:

As described in the previous section, there are two main outcomes of exposure to *M. tb:* clearance or infection, and of those infected, a minority will progress to disease. Likewise, diagnostics used clinically can be divided into those which test for infection, and those which test for disease. This section will be a brief overview of diagnostic assays currently in use. Several will be discussed more in depth in Chapter II.

4.4 Diagnosis of *M. tuberculosis* infection:

This section outlines two tests commonly used to diagnose *M. tb* exposure and/or infection in humans, rather than the disease (TB). These tests can be used for both the evaluation of contacts of TB cases and routine TB screening for those in higher risk settings such as healthcare or mycobacterial laboratory personnel.

4.4.1 Tuberculin skin test (TST):

The TST uses standardized purified protein derivative (PPD-S), originally isolated from heat killed *M. tb* cultures[76]. If an individual has been previously exposed to mycobacterial antigens (at least 6-8 weeks prior), a delayed-hypersensitivity reaction will occur and can be measured 48-72 hours later[76–78]. This manifests as an induration that can be demarcated and measured with a ruler[78]. Whether a test is positive or not is determined by 'induration cutoffs' of 5, 10, and 15 mm which are applied based on risk factors such as age, immune status, weight, contact with TB patients, or place of residence/work[78]. Accordingly, the specificity of the tests increases as the

diameter of the skin reaction increases but the sensitivity diminishes[79]. Tests read after 72 hours are inaccurate as the size of the skin reaction may be underestimated[78].

One notable drawback of the TST is that antigens used in tuberculin are not specific for *M. tb*; they are also found in BCG and various NTMs, thus increasing the likelihood of a false positive result[77]. In theory, the TST is most useful in areas with low BCG vaccination rates, however in practice, the TST is most commonly used in high burden regions[80]. This may be attributed to its low cost and accessibility in low and middle income countries[78].

4.4.2 Interferon- γ release assay (IGRA):

The IGRA is a blood test that relies on the secretion of the cytokine IFN-γ by T-cells in response to *M. tb* specific antigens that are not present in BCG (ESAT-6, CFP-10, TB7.7). This is particularly attractive for populations in which rates of BCG vaccination are high[81].Currently there are two assays in use clinically: the QuantiFERON-TB Gold (in which an enzyme-linked immunosorbent assay is used to detect IFN-γ secretion from whole blood) and the enzyme-linked immunospot (ELISPOT)-based T-SPOT.TB (in which peripheral mononuclear cells are measured to determine IFN-γ secretion after stimulation)[82]. The benefits of IGRA testing include: no follow-up visits required, results can be provided within 24 hours (depending on laboratory processes), no interpretation required (unlike induration readings), and no false-positive due to prior BCG vaccination. However, due to the expense of these assays, IGRAs are typically used in high income countries with the resources necessary for larger-scale diagnostics[78,81,82].

Neither the TST nor the IGRA are reliable indicators of ongoing infection as they are indirect and rely on the generation of an immune response following a previous exposure to mycobacterial antigens[77]. As such, these tests can only be used for determining if an individual has at one time been infected, not if the infection has been cleared nor will progress to disease.

Moreover, both tests rely on the ability of the individual to mount an adequate immune response; this may be impeded by immunocompromised (ex: HIV+ patients) and immunosuppressed individuals (ex: chronic steroid use, transplant patients etc.).

4.5 Diagnosis of disease:

Broadly, clinical diagnosis of TB may involve a combination of symptomatic assessments, chest X-rays, microscopic examination (ex: acid fast/Kinyoun stain, auramine-rhodamine stain etc.), mycobacterial culturing, and/or molecular screening[83]. Active TB disease is classically described with symptoms such as persistent cough, fever, bloody sputum (hemoptysis), fatigue, weight loss, loss of appetite, and night sweats[84]. On a chest X-ray, TB often presents as opacities, typically in the upper lobes of the lungs[83,85]. Though this is a good indication that there is a lung disease, a chest X-ray alone cannot distinguish TB from other lung diseases such as NTM infection, pneumonia, lung cancer, etc. and must be used in conjunction with other diagnostics[83,85]. Currently, the Canadian Standards of Tuberculosis recommends that "every effort must be made to obtain a microbiological diagnosis"[83]. As such, evidence of *M. tb* (or MTBCs) must be shown through microscopy, culturing (phenotypic testing), and/or molecular testing. AFB staining, described above, determines if the bacterial species is acid fast (likely mycobacteria) but not what the species is. Moreover, microscopy has a limit of detection (LOD) of ~10^5 CFU/mL of sample and bacilli can be overlooked[83]. Mycobacterial culturing (using liquid or solid media) is the most reliable method of *M. tb* detection (LOD ~10 CFU) and remains the 'gold standard' for both identification of MTBC species and drug-susceptibility testing (DSTs)[83,86]. However due to long turnaround time (cultures take between 2-8 weeks depending on the test employed), and specialized requirements for processing, culture-based diagnosis delay adequate patient care [83,86]. The advent of new, molecular tests has been an appealing alternative to culture-based detection.

The WHO currently recommends several nucleic acid amplification assays (NAATs) as initial diagnostic tests[60]. This is largely due to rapid readouts, reduced cost, the ability to detect drug resistant strains in tandem, and overall accessibility in limited-resource settings[60,87]. However, many places (typically low income, high burden countries) in which rapid molecular assays are deployed continue to use outdated tests with lower sensitivity, and thus may overlook both drug-susceptible and drug-resistant *M. tb* cases[86]. Of note, this dissertation will be limited to discussion of the role and limitations of GeneXpert MTB/RIF (Cepheid), GeneXpert ULTRA (Cepheid), and the Hain LifeSciences MTBDR*plus*.

4.6 Treatment:

Effective drugs against *M. tb* have been around since the 1940s. However, with them also came the danger of drug monotherapy. The current treatment recommendations for drug-susceptible *M. tb* by the WHO is ~4-6 months of daily multidrug therapy using rifampin (RIF), isoniazid (INH), pyrazinamide (PZA), and ethambutol (EMB), all frontline TB agents[60]. The Canadian Tuberculosis standards for physicians further divides this into 'intensive' and 'continuous' phases[88]. The intensive phase is defined as the use of 3-4 effective frontline drugs daily for a minimum of 2 months whereas the continuous phase is a daily dosing of a minimum of two effective drugs (for example RIF and INH), though this dosing can be specialized based on patient needs[88]. The biggest challenge in TB treatment is the rise of rifampin-resistant (RR)/multi-drug resistant (MDR)- and extensively-drug resistant (XDR) TB. Broadly, MDR-TB is defined as an isolate resistant to rifampin (RIF) and isoniazid (INH) whereas XDR-TB is defined as an MDR isolate also resistant any fluroquinolone (FQ) and at least one group A drug (bedaquiline, BDQ and/or linezolid, LZN). In 2021, the WHO also expanded their definitions to include 'pre-XDR' in the classification of resistance, defined as a RIF-R isolate also resistant to any FQ. In 2022, it

was reported that RR/MDR-TB cases accounted for 3.3% of all new cases, and 17% of previously treated cases worldwide. Concerningly, it was also reported that just three countries accounted for 42% of RR/MDR-TB cases (India, the Philippines, and the Russian Federation).

Current treatment of DR-TB ranges from 6-20 months, depending on regimen (RR v. MDR v. pre-XDR/XDR-TB). At a baseline, a minimum of 6 months of BDQ, pretomanid, LZN, and MFX is recommended (known as BPaLM); for patients with pre-XDR and XDR, MFX is removed (BPaL). The introduction of a second line injectable may be included for cases of XDR, though this is not ideal. These are extensive treatments with significant side-effects; as such, it is crucial that patients are rapidly- and correctly- diagnosed. In a multi-centre study of several high burden countries, ~72% of isolates studied showed some form of drug resistance (4% of these isolates were XDR-TB)[89]. However, one of the most interesting findings of this study was that ~15% of all patients received the wrong treatment based on local testing compared to WGS[89]. Further, this study also showed a five-fold higher mortality of undertreated versus properly treated patients[89]. A further challenge to TB treatment is heteroresistance, defined as populations of both susceptible and resistant *M. tb* strains within a single sample[86]. Heteroresistance is difficult to reliably detect with current molecular assays and often overlooked[86]. This may contribute to either treatment failure at the individual level or to the propagation of MDR- and XDR-TB at the global level due to the lack of adequate treatment[86,90]. Moreover, this risks the unnecessary exposure of patients to toxic, but ultimately ineffective antibiotics[86].

There are two paths to TB elimination: 1) prevention or 2) detection and treatment. For prevention, this requires the development of new, effective vaccines that surpass the efficacy of *M. bovis* BCG (discussed below). For detection and treatment, this requires the development and/or optimization of phenotypic and genotypic assays in tandem with the expansion of surveillance

globally and access to crucial antibiotics. Of note however, *M. tb* is not the only pathogen that must be overcome for a 'TB free' world (see Sections 6 and 7, below).

5. *Mycobacterium bovis* Bacille Calmette-Guérin (BCG)

BCG is a live, attenuated vaccine derived from virulent *M. bovis* originally derived by Albert Calmette and Camille Guérin. For over 100 years, this vaccine has been employed for protection against TB and remains the only licensed vaccine for TB, with ~100 million doses administered each year[91]. Importantly, BCG typically given within the first few days of life, has a well-established safety profile.

5.1 History

The development of BCG followed the failure of Koch's tuberculin vaccine in 1890, originally thought to be an effective therapeutic agent against TB[92]. This was quickly disproven, though it did prove useful in the diagnosis of *M. tb* infection and continues to be employed today (tuberculin skin test, TST)[93]. Eighteen years and many attempts later, a viable vaccine was still not developed. In response to this, Calmette and Guérin sought to create a strain of mycobacteria with reduced virulence but high immunogenicity. They combined the vaccination strategies of Edward Jenner (utilization of a non-human pathogen) and Louis Pasteur (utilization of attenuated pathogens via long-term bacterial manipulation)[92]. As such, *M. bovis,* originally isolated from a diseased cow in 1902, was passaged >230 times for ~13 years (1908-1921) on potato slices soaked with ox bile and glycerine [94,95]. The resulting strain was attenuated in calves and guinea pigs but could still provide protection against lethal *M. tb* infection[96,97]. It is known now that this attenuation coincided with a 9.5 kb deletion termed 'RD1' that is present in *M. bovis* strains but absent in all BCG strains. RD1 encodes part of the ESX-1 system responsible for the secretion of the '6 kDa early secreted antigenic target' (ESAT-6) and the '10 kDa culture-filtrate protein' (CFP-10). Gene

deletion and complementation studies have shown that a) the RD1 locus is required for the full virulence of *M. tb* and *M. bovis* and b) ESAT-6 and CFP-10 are virulence factors (mentioned above).

BCG was first used to protect infants living in an active TB household. The first oral administration of BCG to a neonate occurred July 18, 1921. Within the year, another 120 infants were vaccinated, and a routine vaccination schedule was established in which BCG was administered every other day within 10 days of birth. By 1927, a total of 21,000 infants had been BCG vaccinated orally[92]. By 1928, the route of administration had been converted from oral to intradermal, still in use today. This became the preferred route of vaccination due to increased dose precision and replicability, and a more consistent response to the Koch's TST. During this initial vaccination phase, it was observed that vaccinated children had significantly less death compared to unvaccinated children (5% versus 16%, respectively)[94].

Following the success of this vaccination campaign, strains of live BCG were sent to ~60 laboratories globally. At the time, the ability to freeze and store viable bacteria was inadequate. As such, between 1924 and 1927, the 'original' BCG strain was exposed to a number of culturing techniques and growth media, as the strain required continual passaging. This resulted in significant *in vitro* evolution i.e. daughter strains with unique antigenic profiles[98–101].

5.2 Features of BCG strains:

BCG strains can be differentiated based on regions of deletion, duplication, and/or lineage specific SNPs. Based on these genetic features, daughter strains can be broadly categorized as early (pre-1927) and late (post-1931) strains. Early strains include BCG Russia, BCG Sweden, BCG Japan, BCG Moreau and BCG Birkhaug; late strains include BCG Prague, BCG Glaxo, BCG Danish, BCG Tice, BCG Connaught, BCG Frappier, BCG Phipps, and BCG Pasteur. Based on

when the strains were obtained, BCG Russia is considered the 'oldest strain' derived in 1924, whereas BCG Pasteur is the most 'modern' strain, derived in 1961[102]. By the 1960s, lyophilization enabled storage of viable bacteria without the need for further passaging[92]. One of the key differences between early and late strains is the expression of MPT64, MPT70, and MPT83; early strains constitutively produce high amounts of these proteins whereas late strains cannot. This coincides with the deletion of the RD2 region as well a mutation in *sigK* that occurred between 1927 and 1931[98,100,103,104]. Due to the decreased immunogenicity of late strains, it has been postulated that these strains may be 1) less virulent than early BCG strains and 2) provide less protection against TB, both of which remain controversial[91,96,97,105–109]. High MPT70/83 expressors have also been associated with higher rates of adverse effects, such as BCG osteitis[110]. This osteitis has been postulated to be in part caused by a conserved osteoblast specific domain in the MPT70 protein, though this has not been proven[110]. Further characterization of MPT70 and MPT83 is discussed in section 6.5. As of 2023, six strains of BCG account for >90% of all vaccination (BCG Pasteur, BCG Danish, BCG Glaxo, BCG Japan, BCG Russia, and BCG Moreau)[111,112].

5.3 BCG in the clinical setting:

The reported efficacy of the overall protection of BCG against pulmonary TB has varied widely between controlled trials, from 0% (Chengalpattu trial) to 80% (UK Medical Research Council trial)[113]. Due to the contested protection of BCG against tuberculosis, many countries have stopped mass vaccination and recommend BCG only in high-risk communities[114]. In Canada, BCG is still routinely administered to 1-month-olds living in Nunavut and Nunavik but is otherwise not part of the standard infant vaccination schedule. For countries in which BCG is administered, the global vaccination rate among 1 year olds is ~87%, with the greatest coverage occuring in Europe (93%), and the lowest coverage occuring in Africa (80%)[115]. Multiple clinical studies have shown

that BCG has the greatest protective efficacy in children < 5 years but is largely ineffective in adolescents and adults. Despite inter-trial variation, BCG protection against miliary or meningeal TB (TB-meningitis) is consistently high, though this protection is limited, often waning beyond 10-15 years[116]. A 2022 systematic review of infant BCG vaccination determined that the overall protection of BCG against all forms of TB was ~18% (analysis of 26 cohort studies in 17 countries), where TB was defined as pulmonary, extrapulmonary, miliary TB, and/or TB-meningitis[117]. However, when stratified for by age, the greatest protection against all forms of TB was seen in children < 5 years with an overall protection of 37%. If restricting to children with a positive TST or IFN-y release assay (IGRA), overall protection was 19%, children under 5 was 32%, and children between 5-9 was 38%. For cohorts with negative TSTs or IGRAs, children < 5 showed ~46% protection. For studies that reported pulmonary versus extrapulmonary infection, overall protection was consistent (19%) but, there was no significant protection against extrapulmonary TB (EPTB, 4%). Studies in which meningeal and miliary TB were reported showed rates of protection between 64-92%[117–119]. This is consistent with other systematic reviews in which overall protection ranged between ~19-50%, and childhood protection is significantly higher[113,119–121]. Additionally, of the studies that do stratify BCG by lineage, there was no significant difference in protection[91,113,121,122]. This latter observation is however limited by the fact that no BCG clinical trials has used an 'early' strain.

Two systematic reviews have reported a significant reduction (>70%) in tuberculosis-related childhood mortality (defined as children < 14 years of age)[117,119]. In contrast, there was no clear relationship between BCG and death in participants > 15 years of age[117]. Emerging evidence suggests that BCG may also reduce infant all-cause mortality, likely due to the induction of non-specific immunity against other pathogens[123–125]. In a recent systematic review, all-cause mortality

in neonates was reduced by 21%, though this effect was abrogated beyond 12 months[123]. Additionally, infection related mortality was reduced by 33% and mortality due to sepsis was reduced by 38%[123]. Risk reduction of respiratory infection (excluding COVID-19) was estimated to be ~44%, though this varied markedly between trials[123]. Protection from non-specific immunity has also been observed with the measles vaccine, oral polio vaccine, and the diphtheria-tetanus-pertussis vaccine, though the exact mechanism of action has yet to be determined[124,126].

5.4 BCG in a laboratory setting:

Three major drawbacks of BCG clinically are 1) genetic diversity between daughter strains 2) variable efficacy across clinical populations (demographically and geographically) and 3) the potential of disseminated disease in immunocompromised individuals. However, these same drawbacks for BCG policy make BCG ideal to study within the laboratory. As discussed, BCG is attenuated, but immunogenic. Moreover, despite *in vitro* evolution, BCG, *M. tb,* and *M. bovis* share >99.9% genomic content. This enables it to be used in select experiments as a laboratory proxy, without the need for a specialized biosafety containment facility. BCG strains also have defined and differential drug profiles, which can be used in diagnostics (as described in this dissertation), investigation of potential drug targets and mechanisms of resistance. For example, strains lacking the RD2 region (such as BCG Danish and BCG Pasteur) show low-level resistance to isoniazid (INH), a frontline antibiotic for TB treatment, and ethionamide (suggesting a common drug target)[127]. Additionally, these same strains are sensitive to clarithromycin, enabling a 'non-TB' drug to be used as frontline treatment[128]. In combination, these observed phenotypic differences between BCG strains, may potentially inform treatment options for disseminated BCG in immunocompromised patients[127].

The second chapter of this dissertation hinges on the ability to use BCG as a well-defined member of the MTBC and, subsequently, create recombinant strains for use in current and future diagnostics. This is especially pertinent as entrance into the 'molecular' era of diagnostics results in the rapid development and enrollment of assays into clinical use, often without the use of proper quality controls.

6. *Mycobacterium bovis (M. bovis):*

Of the animal-associated MTBC members, *M. bovis* is the best studied[43]. Since its discovery by Smith in 1898, the impact of the bovine tubercule on human health has been widely debated. In 1901, though Koch accepted that the tubercle bacilli and the bovine tubercle caused two different diseases, he did not consider cattle to human transmission a cause for concern[16,129]. However, it was clear that 1) the most common route of exposure to *M. bovis* was ingestion of contaminated milk, milk products, and/or contaminated meat and that 2) this exposure led to human disease[130]. In retrospect, this can be considered some of the first evidence of *M. bovis* as a zoonosis, being transmitted not only animal-to-animal, but animal-to-human as well.

Reports of the British Royal Commission between 1904-1911 indisputably established that there were two types of tubercle bacilli and that the bovine one was more virulent than the human variant[131–133]. Additionally, this commission determined that humans must be added to the list of hosts susceptible to the bovine tubercle[17,133]. For many years following this, different virulence, in different hosts was used to determine disease caused by the human tubercle or disease caused by the bovine tubercle, eventually renamed *Mycobacterium bovis* in 1970[131]. The reasons behind differential virulence in humans and animals still remains unknown.

The emergence of *M. bovis* has been postulated to coincide with animal domestication, likely within the last 6000 years[134]. It is suspected that modern *M. bovis* emerged in East Africa

with a later secondary emergence in the 'New World' and Oceania[134–136]. In fact, the earliest evidence of *M. bovis* infection in humans comes from four South Siberian skeletons from the Iron Age (~360 B.C.E -230 C.E.)[135,137]. The transport of cattle and other animals (such as sheep, goat, yaks, horses) likely played a major role in the transmission and spread of *M. bovis;* this is supported by phylogenetic estimations and archeological findings[135,137]. Presently, *M. bovis* infection has been documented in ~85 species including livestock (cattle, pigs, sheep, goats, etc.), wildlife (badgers, deer, wild boar, bison, buffalo etc.), pets (cats, dogs, guinea pigs) and humans[20,138,139]. *M. bovis* transmission has been documented between animal species, from animal-to-human, human-to-animals, and, rarely, between humans. As such, it can be considered both a zoonosis and a reverse zoonosis.

Prior to pasteurization and other bovine control programs (ex: surveillance; test and cull), *M. bovis* constituted a significant portion of total mortality due to tuberculosis, particularly in children[10]. In fact, in the early 1900s, *M. bovis* was estimated to cause up to 25% of all cases of tuberculous meningitis[140]. Though significantly reduced, *M. bovis* is still detrimental to human and animal health. In 2019, an estimated ~140 000 cases and ~11 400 deaths were attributed to zoonotic tuberculosis (zTB)[141,142]. Globally, ~80% of zTB cases in humans are in Africa and South Asia (68 900 and 43 400 cases respectively). For context, these regions account for ~25% and 45% of the global TB burden respectively[143,144]. This provides further cause for concern as a number of high burden TB and zTB countries also have a high prevalence of HIV infection[60,145]. Estimates of zTB worldwide are likely inaccurate, largely due to incorrect definition of the term (zTB verus bovine TB, bTB), lack of reporting, potential co-infection and misdiagnosis[142,146]. This is particularly relevant as the eradication of TB cannot occur without the eradication of zoonotic TB.

6.1 Clinical features:

Tuberculosis caused by *M. bovis* is indistinguishable from *M. tb* clinically and radiographically[147]. Though not geographically restricted, the occurrence of *M. bovis* infection in humans is much less common in countries with rigorous bTB surveillance, control and eradication programs but it can still occur[148,149]. In humans *M. bovis* more commonly manifests as extrapulmonary infection, often considered as a disease of the lymph nodes (lymphadenitis, scrofula) and/or the gastrointestinal tract, though any organ can be affected[150]. Atypical *M. bovis* locations have also been reported in the eye, bones, joints, oral cavity, genitourinary system and the central nervous system (CNS). Case series have also observed that patients with *M. bovis* infection are less likely to have pulmonary involvement when compared to patients with *M. tb*[150]. Whether this is mediated by *M. bovis* virulence, point of pathogen entry, or immune status of the patient, is not clear[151].

Whole genome sequencing (WGS) is the most reliable molecular diagnostic test of *M. bovis* as routine mycobacterial tests such as AFB staining, GeneXpert, skin tests (TST), and IGRAs cannot differentiate between *M. tb* and *M. bovis*[35,147]. This differentiation is crucial as 1) the *M. bovis* treatment regimen is longer and 2) the prognosis of TB due to *M. bovis* infection appears to be worse than TB due to *M. tb*[152]. In frontline TB treatment, PZA acts synergistically with RIF to reduce the length of treatment; however, in *M. bovis* PZA cannot be effectively employed. Canadian guidelines currently recommend a minimum of 9 months of RIF, INH, and EMB treatment for TB patients with *M. bovis,* though this treatment may be extended[88]. This provides a further treatment challenge as complications can and do occur while on therapy (ex: hepatitis, stroke, vasculitis, immune reconstitution inflammatory syndrome etc.)[147,153].

6.2 Transmission:

The pathogenic potential of *M. bovis* cannot be understated. Since the late 1800s there have been reports of transmission via wounds (ex: bites, needle sticks, postmortem examination of diseased animals, pre-existing wounds etc.) which can result in severe disease[15,147,154]. In recent years, the possibility of indirect transmission by environmental contamination has been raised following evidence of bacterial shedding from infected animals (ex: cattle, badgers, deer, and boar)[32,155]. There have also been reports of *M. bovis* persistence in water, feedstuffs, and soil for several months[156,157]. In animals, *M. bovis* may also be transmitted through ingestion of infected carcasses[147]. Though there are several postulated modes of transmission for *M. bovis* only the aerosol and oral routes are considered significant.

Aerosolized *M. bovis* infection is associated with pulmonary presentation and occurs via close contact with diseased animals through occupation, proximity, and cultural practices[35,154]. This is suspected to be the main route of infection between cattle (animal-to-animal) and a rarer route of transmission from animal-to-human. Crucial to public health, there have also been reports of human-to-human *M. bovis* transmission globally and reports of multidrug resistant (MDR) and polydrug resistant strains in both animals and humans[35,158–161]. Further, studies in immunocompromised and immunocompetent patients have demonstrated that a non-negligible amount of *M. bovis* transmission occurs via the aerosol route in healthcare, work, and community settings[15,138,150,162–165]. *M. bovis* infection risk has been more commonly associated with age (<15 years), sex (F>M), and immunosuppressive conditions (ex: patients with human immunodeficiency virus, HIV, or autoimmune diseases requiring glucocorticoids) compared to *M. tb,* though this appears dependent on country of origin[150,151,166–168]. However other high-risk groups for *M. bovis* infection such as those directly handling animals (livestock farmers, veterinarians, butchers, hunters, abattoir workers, wildlife workers, animal husbandry etc.) cannot be

overlooked[154]. Though clinical studies of *M. bovis* are rare, where it has been reported, rates of morbidity and mortality were higher in *M. bovis* patients compared to *M. tb* patients in both HIV– and HIV + cohorts. One systematic review reported mortality between 9-31% in HIV- patients and up to 100% mortality in HIV+ (range 10-100%)[35,152]. In fact, a major challenge in clinical studies of *M. bovis* is the amount of patients who fail treatment and/or succumb to infection[152].

Finally, oral transmission has long been considered the main route of how humans acquire *M. bovis* infection (animal-to-human infection)[35,150,169]. This is largely based on historical trends as well as the mass reduction in *M. bovis* cases following the introduction of pasteurization, TSTs in livestock, and culling[170]. The main driver of *M. bovis* disease in humans is suspected to be through the ingestion of contaminated milk, milk products, or meat products and is the most commonly reported zoonotic link[171]. Globally, it can be observed that bTB burden varies depending on 1) extent of pasteurization, 2) employment of bTB surveillance programs and 3) presence of a dense maintenance host population.

6.3 Laboratory and molecular features:

The reference strain of *M. bovis* (*M. bovis* AF2122/97) was originally isolated in 1997 from an ill-cow presenting with lesions in the lung and bronchomediastinal lymph nodes[172]. In 2003, the first ever *M. bovis* genome was sequenced, allowing direct comparison to the 1998 *M. tb* H37Rv genome[172,173]. With the advent of new sequencing tools, the *M. bovis* reference genome was updated in 2017 and 2020 to include ~616 new ORFs and 69 new gene names[174,175]. From this it was determined that *M. bovis* AF2122/97 has 3989 coding sequences (2026 named) and 488 hypothetical proteins[175]. In 2021, the genome of *M. bovis* Ravenel, a clinical isolate from 1899, was sequenced. This isolate was obtained from the mesenteric lymph node of a Jersey cow by Mazyck Ravenel (thus, later renamed as *M. bovis* Ravenel)[176]. In 1910, this strain was passaged in

rabbits, a non-native host, and frozen[177]. In comparison to the reference genome, 4058 coding sequences were present in *M. bovis* Ravenel (~69 more than *M. bovis* AF2122/97)[178].

The differentiation between human TB (hTB) and bovine tuberculosis (bTB) begins at the subspecies level. Despite sharing 99.95% of the genome at the nucleotide level, *M. bovis* and *M. tb* can be characterized using physical, biochemical and/or molecular techniques. Early categorization utilized physiological and morphological differences between MTBCs. Biochemically, *M. bovis* has been classically characterized as negative for niacin accumulation, negative for nitrate reduction, susceptible to thiophene-2-carboxylic acid hydrazide (TCH), and resistant to PZA whereas the opposite is true to *M. tb.* Morphologically, *M. bovis* presents with dysgonic growth on Lowenstein-Jensen medium (i.e. small, flat, slow-growing colonies) and is microaerophilic (i.e. grows below the surface when plated on Lebek media)[179]. However, these tests can be time consuming, and unreliable due to the wide variation between mycobacterial strains; a single test cannot be used as a confirmation of speciation. For example, *M. bovis* is classically defined by a PncA (H57D) mutation responsible for PZA mono-resistance, yet a number of studies have shown that there are PZA susceptible *M. bovis* strains, with wildtype PncA sequences[179–181]. In fact, one laboratory reported ~5% of all their inhouse *M. bovis* strains were PZA-susceptible[180].

Currently, *M. bovis* and *M. tb* are differentiated at the molecular level through deletion typing, lineage specific single nucleotide polymorphisms (SNPs), spoligotyping, and/or WGS[182]. Both deletion typing and spoligotyping depend on unique genomic patterns; i.e. presence or absence of specific regions of deletions (RDs, deletion typing) or the hybridization pattern of specific spacer oligonucleotides (spoligotyping) whereas lineage specific SNPs and WGS interrogate the genome directly[182]. Some lineage specific SNPs can also be used as a phenotypic

readout such as the *pncA* mutation previously discussed and two missense mutations in *rskA,* a transcriptional regulator[183,184].

6.4 SigK/RskA

The SigK regulon is a genomically conserved system across the MTBCs[185]. Previous work by the Behr laboratory has described the recurrence of *mpt83-rskA-sigK* observed in NTMs, *Rhodococcus equi, Kineococcus radiotolerans, Brevibacterium linens* (broadly related to mycobacteria) and *Yersinia enterocolitica* (an outgroup)[186]. As such, it was proposed that *mpt83-rskA-sigK* are the minimal genes required to respond to external stimuli (effector-regulator-sensor) in this regulon[186]. Transcriptomic comparisons and gene complementation have conclusively shown that SigK controls 10 genes, including *mpt70* and *mpt83* in *M. tb,* coding for the proteins MTP70 and MPT83 (called MPB70 and MPB83 in *M. bovis*)(Figure 3a)[185,186]. The MPB nomenclature is derived by Nagai et al., in which MPB refers to major protein from *M. bovis,* and 70 refers to mobility by electrophoresis[110]. As these genes are identical, this dissertation will refer to these proteins exclusively as MPT70/83 regardless of strain background.

MPT70 and MPT83 are constitutively expressed in *M. bovis, M. caprae,* and *M. orygis,* variably expressed across *M. bovis* BCG strains (discussed in Section 5.2), and inducible in all other members of the MTBC following infection[100,101,103,184–186]. In *M. tb* anti-sigma factor K (RskA) is bound to SigK; following external stimuli (ex: host stress, macrophage activation, hypoxia), RskA dissociates from SigK, mediating transcription[184,187]. However, past studies have shown varying levels of MPT70/83 expression between MTBCs as the direct consequence of independent mutations in RskA. In *M. bovis* (and *M. caprae*) this was due to two missense mutations (D107G and G184E) whereas in *M. orygis* constitutive expression was mediated by a readthrough mutation (X233S)(Figure 3b)[184]. These SNPs either result in a non-functional RskA,

leading to uncontrolled transcription, or they are activator mutations which result in changing the RskA repressor into an activator of transcription. Notably, this overexpression *in vitro* is a defining feature of *M. bovis, M. caprae,* and *M. orygis.*

6.5 MPT70/MPT83

MPT70 was first observed in the 1960s, but was not experimentally characterized for another decade[188]. Structurally, MPT70/MPT83 are exported through the general secretory pathway of mycobacterium (Sec export)[110]. The Sec pathway is essential for all bacteria and conserved globally as it can be found in bacteria, archaea, and eukaryotes[189]. Proteins that are exported through this channel are unfolded and characterized by signal sequences at the N-terminal region[190]. Two signal peptides are responsible for cleavage: signal peptidase I and signal peptidase II. Signal peptidase I cleaves MPT70 following translocation whereas signal peptidase II cleaves MPT83. At the protein level, MPT70 and MPT83 are 73% conserved; whereas MPT70 is a secreted protein, MPT83 is a membrane-bound glycosylated lipoprotein[191]. This is likely due a gene duplication event in which MPT83 lost the lipid branching signal associated with membrane localization[186]. Interestingly, MPT83 exists in two forms with different molecular weights: secreted (~23 kDa) or anchored to the cell surface (~26 kDa)[100,103,110,192]. This presented a challenge in early work as MPT83 was often misidentified as glycosylated MPT70, rather than a distinct but homologous protein[110]. Following purification, two independent groups published the sequences of MPT83, showing that this protein was encoded by a unique gene rather than an MPT70 isotype[193,194]. It has also been experimentally determined that MPT70 and MPT83 do not complex with one another, unlike the canonical virulence factors ESAT-6 and CFP-10 (discussed further below)[110].

Presently, MPT70 is the most well characterized effector of the SigK regulon. Recent work has suggested that MPT70 may have a role in cellular adhesion, aggregation, and the formation of multinucleated giant cells, though this is likely host-mediated[17,195–197]. Natural and experimental observations further support the idea of a 'host-specific' role of MPT70. In animal models, *M. bovis* shows significantly more progressed disease compared to *M. tb;* in *in vitro* models, disease associated phenotypes depend on the cell type infected[195,198,199]. The majority of what is known about MPT70 comes from its immune response. First, MPT70 is an immunodominant antigen[100,101]. It contains multiple bovine, mouse, rabbit, and human T/B-cell epitopes, induces strong pro-inflammatory responses, stimulates delayed hypersensitivity reactions and the formation of antibodies[110,200–202]. In comparative studies downstream, it was determined that MPT83 was more immunogenic compared to MPT70, also inducing potent T- and B-cell responses in animal models. It is postulated that this is likely due to 1) the antigenicity of lipid domains and 2) that it is found in both membrane bound and secreted forms[203]. Further, MPT83 antibodies can be detected in cattle much more rapidly than MPT70 (~4 weeks compared to 15-20 weeks)[204]. In the last decade it has also been postulated that MPT83 may be a proapoptotic gene mediating immune function through controlling the cell-death pathway (bias towards apoptotic rather than necrotic death)[205].

The immunogenicity of both MPT70 and MPT83 have been pragmatically exploited. First, MPT70 has been used as a diagnostic proxy for zoonotic TB in cattle for decades ('reactors' vs. 'non-reactors'). It was quickly discovered that 1) skin testing cattle with bovine PPD stimulated production of MPT70 antibodies and 2) these antibodies were specific to *M. bovis* infection[202]. Cattle in which an induration was observed, were positive for *M. bovis* infection, allowing for the differentiation not only between infected and non-infected but also between *M. bovis* and *M. avium*

paratuberculosis, a common cattle-associated NTM[206]. Second, the cell-mediated and humoral responses of MPT70 and MPT83 suggested they may have a role as vaccine candidates against *M. bovis* or *M. tb.* Since these proteins were first identified, both DNA and protein subunit vaccines have been tested experimentally. However, there has been limited success and conflicting data if MPT70/83 are protective, neutral, or detrimental. For example, Chambers et al. pre-incubated *M. bovis* with MPT83 monoclonal antibodies prior to intravenous infection in BALB/c mice and found that mice had reduced pathology and increased survival compared to untreated groups[207]. In guinea pigs, it was also found that an MPT83-DNA vaccine reduced the severity of lesions, but had no effect on the number of lesions, bacterial burden or spread to the spleen following aerosol infection[208]. In contrast, in its natural host, Wedlock et al. definitively proved there was no effect on infection outcome. Cattle were vaccinated with BCG, MPT70-DNA, MPT83-DNA, or primed with MPT70-DNA followed by a boost with MPT70 protein (suspended in Incomplete Freund's Adjuvant, IFA). Despite moderate protection achieved against *M. bovis* challenge in mice and guinea pigs with MPT83, this did not translate into an observable effect in cattle[207,209]. Beyond this, the 'prime/boosted' calves showed significantly more lesions (in lung and lymph node) and no reduction in bacterial burden[209]. As suggested above, outcome differences may be due to host, infection route, or type of infection though the exact role of MPT70 or MPT83 in MTBC infection- and if that role is the same across species- remains overlooked. Thus, it has been suggested that MPT70 and/or MPT83 may be a species-specific virulence factor, crucial in disease manifestation. An overview of mycobacterial virulence factors and their role in disease outcomes is discussed in Section 8.

6.6 *M. bovis* in animal infections:

M. bovis Ravenel has been used in a number of comparative pathogenesis studies largely due to its historical use in natural experiments and accessibility[177]. This strain has been characterized as fully virulent in small animal hosts (rabbits, guinea pigs, mice) but attenuated in cattle (the natural host)[177,199,210,211]. Though *M. bovis* Ravenel does induce an aggressive immune response, corresponding pathology (ex: formation of granulomatous lesions) is absent in cattle infection models. Recently it has been suggested that the modification of three T-cell epitopes, conserved in other members of the MTBC, may contribute to differential attenuation[211]. Despite this, both *M. bovis* Ravenel and *M. bovis* AF2122/97 are more virulent compared to *M. tb* H37Rv regardless of small animal model studied. For example, in a study using BALB/c mice (an *M. tb* 'resistant' strain) and DBA/2 mice (an *M. tb* 'susceptible' strain), both mice strains infected intravenously with *M. bovis* Ravenel succumbed faster to infection (~2x as fast for the DBA/2 group, and ~4x as fast for the BALB/c group), with evidence of more progressive disease, and more necrosis in the lungs, spleen, liver, kidney, and adrenal glands compared to *M. tb* H37Rv[212]. At endpoint, *M. bovis* infected lung lesions were neutrophil dominated in various states of cellular decay[212]. Further, infection with *M. bovis* Ravenel resulted in uncontrolled growth in the liver and kidneys of BALB/c mice indicating a dissemination phenotype not seen with *M. tb* infected mice (regardless of strain)[212]. This was concordant with earlier studies in which both *M. bovis* strains tested (Ravenel, and a clinical isolate *M. bovis* Branch) showed increased virulence compared to multiple *M. tb* strains, as measured by reduced survival, more extensive lung pathology, and more persistent lung infection compared to *M. tb* strains[199]. In fact, it was reported that *M. bovis* induced such severe immune responses that death occurred before chronic lung pathology could be seen[199]. *M. bovis* Ravenel also showed significantly reduced survival following aerosol infection of C57BL/6 mice (a 'resistant' strain) compared to *M. tb* H37Rv and *M. tb* CDC1551 (a reference

strain)[198]. These findings were also seen in rabbits and guinea pigs (increased raw number of granulomas, increased proportion of granulomas showing caseous necrosis)[210]. Importantly, these results were robust; regardless of the strain tested (ex AF2122/97, Ravenel, Branch, 'N', veterinary isolates) *M. bovis* showed hypervirulence in animal models, when compared to *M. tb.*

In the natural host (cattle), all tested *M. bovis* strains showed this increased virulence; infection outcome (measured by morbidity and mortality) was significantly worse than *M. tb*[16,129,213]. Like small animal studies, this was independent of *M. tb* comparator strain assessed[16,129,176,213,214]. This phenotype extended to other large animal models such as goats (where *M. bovis* was the most virulent, followed by *M. caprae,* and *M. tb*) and domestic pigs[215,216]. Further, in head-to-head cattle infections, it was conclusively shown that *M. bovis* AF2122/97 was more virulent than both a human derived *M. tb* isolate and an *M. tb* isolate (*M. tb* BTB1558) derived from a diseased Ethiopian Zebu bull[213]. These observations may suggest that virulence is an inherent property of the bacterium rather than a by-product of the host it is isolated from[213,214]. Both the reference strain (*M. bovis* AF2122/97) and *M. bovis* Ravenel were utilized through the course of this dissertation, depending on the experiment. *M. bovis* Ravenel was used in *in vitro* characterization studies, both strains were used for *in vivo* virulence studies in a mouse model, and *M. bovis* AF2122/97 was used for comparative virulence studies in cattle.

7. *Mycobacterium orygis (M. orygis)*

M. orygis is overlooked and understudied. A PubMed search for the phrase '*Mycobacterium orygis'* in October 2024 returns only 32 publications, many of which are case reports or case series. In comparison searches for '*Mycobacterium tuberculosis'* and *'Mycobacterium bovis'* return ~92,000 and ~18,000 publications respectively. Whereas *M. tb* and *M. bovis* were characterized by the late 1800s, *M. orygis* was not recognized as a unique member

of the MTBCs until 2012[14,16,59]. The first isolation of *M. orygis* was in two East African oryxes in 1976 from a zoo in Jackson, Mississippi[217]. At the time, this was classified as *Mycobacterium tuberculosis* as it was observed to be pathogenic in guinea pigs but not rabbits (initially 'ruling out' *M. bovis* infection)[217]. In 1987, the 'Oryx bacillus' was described in an oryx in a zoo in the Netherlands, though this was originally described as a rare *M. bovis* strain due to its high number of 'IS6110' copies[218]. At the time of this report, 'IS6110' was commonly used as a genetic marker to differentiate strains of the MTBCs based on copy number and position of the gene[218]. In 2012, the Oryx bacillus was renamed as *M. orygis* (based on its original isolation) and classified as a distinct lineage of the MTBC based on species-specific SNPs (ex: $gyrB^{oryx}$, two unique mutations at positions 1113 (G→A) and 1450 (G→T)), unique regions of deletions (based on presence/absence, size of deletion), and spoligotyping patterns[59,219–221]. Recently, a species-specific SNP in *rskA* (*Rv0444c*) has been implemented to differentiate MTBC lineages[222]. As described in Section 6.5, this SNP (G698C) replaces a stop codon with serine resulting in the overexpression of MPT70 and MPT83, thus providing both genotypic and phenotypic evidence of *M. orygis*[184]. With the implementation of WGS in routine diagnostics, additional species-specific SNPs have been identified, which may improve downstream characterization of *M. orygis*[223]. In 2021, the first genome of *M. orygis* (called *M. orygis* 51145) was published by the Behr laboratory. This isolate originated from a patient with tuberculous meningitis in Canada in 1997 (though it was not correctly classified as the 'oryx bacillus' until 2005)[224]. This allowed for direct comparisons between the human-adapted *M. tb* and the most well characterized animal-adapted lineage, *M. bovis.*

7.1 Clinical, laboratory, and molecular features:

Clinically, the presentation of *M. orygis* is indistinguishable from *M. tb.* Moreover, commonly used diagnostic techniques (both phenotypic and molecular) are often not specific enough for *M. orygis* detection. *M. orygis* presents as an acid-fast organism following ZN staining, present as spots or lesions on a chest x-ray (due to granulomatous reaction), and can be cultured using standard clinical media[150,225,226]. Rapid molecular tests, such as GeneXpert MTB/RIF or the Hain Lifescience GenoType MTBC, also cannot adequately differentiate *M. orygis* from other strains of the MTBC[86,227]. In fact, in one retrospective study, the laboratory acknowledged that using their in-house methodology, *M. orygis* would not have been able to be detected prior to 2007[150]. *M. orygis* is pan-susceptible to frontline anti-tuberculous agents (RIF, INH, PZA, and EMB), showing no evidence of PZA resistance (WT *pncA* gene, unlike *M. bovis*). At present, the most practical diagnostic techniques for *M. orygis* detection are real-time PCRs (rtPCR) based on species specific SNPs and/or deletion typing. WGS (where implemented) will also provide this identification[22,228].

7.2 Transmission:

The host range of *M. orygis* is currently unknown. Like *M. bovis,* there have been reports of animal-to-animal transmission, animal-to-human transmission, and even one case of human-to-animal transmission occurring in New Zealand in which a dairy cow contracted *M. orygis* from an Indian migrant worker during rearing[229]. Though there has been no definitive evidence of human-to-human transmission, a retrospective study in the United Kingdom did detect two pairs of closely related *M. orygis* isolates (0 SNPs and 6 SNPs respectively) which may indicate this possibility[230]. As such, it has been proposed that humans may not be a 'dead-end' host for *M. orygis,* and that infection can be propagated. The modes of transmission of *M. orygis* are suspected to be the aerosol route, the oral route, and/or percutaneous infection (ex: wounds), though this has not been

experimentally assessed. However, due to its similarity to *M. bovis*, broad host range, site of infection, and evidence of spread, these routes of infection are likely[231].

7.3 Epidemiology:

M. orygis appears to be endemic in South Asia, particularly India, Pakistan, Nepal, and Bangladesh, though it has also been reported in South Africa, East Africa, and the Arabian Peninsula in a number of free-roaming animals[150,217,220,229,230,232–241]. To date, *M. orygis* has been found in cattle, captive and wild deer, blue bulls, rhinoceros, water buffalos, water bucks, antelopes, oryxes, bison, rhesus monkeys, and humans[150,217,220,222,229,230,232–241]. In 2024, an outbreak of *M. orygis* was also documented in NHPs (cynomolgus macaques) imported from Southeast Asia for medical research where 26 cases were confirmed and identified in 67% of quarantine rooms[241]. Globally, *M. orygis* human infection has been reported in Canada, the United States, the United Kingdom, Australia, New Zealand, the Netherlands, Norway, and India, though there is a likely a much higher burden. Additionally, there may be a detection bias, as these countries (with the exception of India) have low national rates of tuberculosis[60]. Consistent with *M. bovis, M. orygis* often presents as an extrapulmonary infection, though pulmonary involvement does occur concomitantly[59,150,222,225,240,242]. Reported extrapulmonary sites include but are not limited to lymph nodes (lymphadenitis), spine, central nervous system (CNS), urine, abdomen, gastrointestinal tract, abscesses, and ascitic fluid. Like *M. tb* and *M. bovis, M. orygis* can manifest anywhere in the body. Where *M. orygis* infection in humans has been reported (excluding endemic regions), the greatest epidemiological risk factor was prior residency in South Asia (21/21 cases in Canada, 10/10 cases in the Netherlands, 8/8 cases in the United States, 8/8 in Australia, 5/5 in Norway)[59,150,222,225,230,232,240,242]. Additionally, in a number of studies more females presented with

M. orygis infection compared to males[59,150]. Interestingly, this trend is consistent with risk associated with *M. bovis* infection, but contrasts with risk associated with *M. tb*[150,243].

India is a global hotspot for human and zoonotic tuberculosis due to multiple risk factors[60]. First, there is a high human and animal density; India has the largest cattle herd globally (~300 million, an estimated 21.8 million infected) and no bovine tuberculosis control programs (ex: test and slaughter)[142,244]. Contact with cattle is frequent and it is common to ingest unpasteurized milk and milk products, despite its correlation to tuberculosis infection[142]. Additionally, *M. orygis* may not be detected due to a lack of laboratory capacity and inadequate diagnostics[226]. South Asia also has significant biodiversity and, due to urbanization, significant interaction between humans and animals[226]. It is for these reasons that the emergence of *M. orygis* as a significant zoonotic pathogen cannot be overlooked. If the WHO intends to eradicate TB by 2030, *M. orygis* infection is an unknown barrier that may need to considered. If this pathogen is not well-described, from epidemiology to pathogenesis, ways to combat it, may be challenging, if not impossible.

Much of the research done on *M. orygis* has been by or in collaboration with the Behr laboratory. The first *M. orygis* genome was sequenced here in 2021. The first study of *M. orygis* in a clinical setting, and the determination that *M. bovis* isolates are not found in India, was performed by Shannon Duffy in 2020. The development of the *Rv0444c* rtPCR was also developed by Duffy et al. and implemented into clinical settings. This foundation provided a unique opportunity for this project to go beyond clinical analysis and allow for the characterization of this bacterium using *in vitro, ex vivo,* and *in vivo* experiments (as discussed in Chapters III-V). Further, results from these baseline experiments enabled a reconsideration of mycobacterial virulence and the dynamics between human- and animal-associated MTBCs in both natural and experimental hosts.

8. Virulence factors

The definition of virulence factors is complicated and varies depending on the microbiological field in which they are studied. Broadly, these effectors can be classified into five categories based on their role in infection and disease: 1) membrane proteins, 2) capsule-associated effectors, 3) secretory proteins, 4) cell wall/cell surface components, and 5) other[245]. However, what specifically constitutes a 'virulence factor' is not universally accepted. In some bacteria, colonization factors are considered as 'virulence factors' as they are a requirement for infection; in others survival factors are virulence factors as they are a requirement for disease[246]. In this dissertation, virulence factors will be defined as effectors involved in host-pathogen interaction and directly responsible for causing morbidity and mortality in a natural or experimental host[247]. When these factors are absent or inactivated, a measurable loss of virulence can be observed (ex: survival, pathology, disease progression etc.). As such, virulence will be considered from the 'damage-response' perspective rather than infection alone.

What factors contribute to MTBC virulence is poorly understood, with the role of many effectors still unknown. Unlike other bacteria, members of the MTBC lack 'classical' virulence factors such as pili, toxins, adherence factors, and/or invasion factors[248]. Additionally, MTBC virulence factors are not independently acquired from other bacterial species, as is typical of pathogens like *E. coli* O157[247]. Further, the demonstration of MTBC virulence factors can be complicated by the co-dependence of many mycobacterial effectors[249]. This section will focus exclusively on few well-described virulence factors of the MTBC, specifically *M. tb* and *M. bovis.*

8.1 Type VII Secretion Systems (ESX systems):

Mycobacterial secretion systems include a general secretion system (Sec), a twin-arginine translocation export pathway (Tat), and two specialized secretion systems, the Type VII secretion

system (T7SS), and the accessory SecA2 system[250]. The thick mycobacterial wall acts as an obstacle for protein secretion; though there are multiple virulence associated factors on the outer membrane, specialized secretion systems are required for the full virulence of mycobacteria[250]. Briefly, both Sec and Tat pathways are conserved across a number of bacterial species. Sec plays a role in the secretion of unfolded proteins whereas Tat exports proteins in their folded state[189,250]. Interestingly, the signal sequences that direct protein secretion via these pathways are similar despite differences in translocation machinery[189]. The accessory SecA2 secretion system exports large, glycosylated proteins which may have a role in intracellular growth and inhibition of the host innate immune system[250,251]. However, the most well-studied secretion systems in mycobacteria are the T7SSs, also called ESX systems.

Type VII secretion systems are conserved in other *Actinobacteria* such as *Corynebacterium, Nocardia,* and *Streptomyces,* though their role in infection in unclear[252]. The MTBCs contain 5 ESX secretion systems, called ESX-1 through ESX-5. The first of these systems (ESX-1) was first discovered ~20 years ago, characterized originally as a 'Sec-independent' secretion pathway[253]. In the MTBCs, 3 ESX systems have been associated with bacterial survival during infection and pathogenesis of disease (ESX-1, -3, -5)[254]. ESX systems contain genes encoding 1) structural components of the secretion system (ex: membrane proteins, channel proteins), 2) mycosin (protease) and 3) secreted Esx proteins[255]. With the exception of ESX-4, all mycobacterial T7SSs also encode PE/PPE proteins, which have been postulated to have a role in virulence and bacterial persistence[255]. At present, the roles of ESX-2 and ESX-4 are not well-described, though phylogenetic analysis suggests ESX-4 may be the 'ancestral' secretion system from which other mycobacterial ESX systems are derived[256]. This has been postulated to have occurred through multiple gene duplication and diversification events and/or horizontal gene

transfer[257]. Notably, ESX-4 is the only T7SS found in all identified mycobacterial species (MTBCs and NTMs)[256].

8.1.1 ESX-1

The first ESX-1 associated protein identified was the 6-kDa early secreted antigenic target (also called ESAT-6). Subsequently, it was determined that ESAT-6 secretion depended on the formation of a 1:1 heterodimer with its protein partner, the 10 kDa culture filtrate protein (called CFP-10). The secretion of these proteins is essential to the full virulence of *M. tb* and *M. bovis.* Absence of ESAT-6 and CFP-10 secretion leads to the abrogation of virulence. In fact, the deletion of these genes in *M. bovis* BCG strains brought attention to the genes encoding ESAT-6 and CFP-10 as prime candidates for their attenuation. Comparative genomic analysis revealed a single 9.5 kb locus absent from *M. bovis* BCG, but present in virulent strains of the MTBCs such as *M. tb* and *M. bovis.* This became known as region of difference 1 (RD1) and corresponded to the deletion of 9 genes, including ESAT-6 and CFP-10. Downstream virulence studies demonstrated that deletion of ESAT-6 alone from *M. bovis* resulted in an attenuated phenotype in guinea pigs[258]. Similarly, the deletion of $RD1^{BCG}$ from *M. tb* significantly reduced its pathogenicity whereas restoration of the RD1 region in *M. bovis* BCG, and *M. microti,* a natural ESX-1 mutant, recapitulated virulence, though to a lesser extent than wildtype *M. tb*[253,259,260]. Interestingly, *M. microti, M. mungi, M. suricattae,* and the Dassie bacillus are all members of the MTBC that are naturally deficient in ESAT-6 and CFP-10, a direct result of strain-specific ESX-1 deletions of variable sizes (ex: *M. microti* has a 13 gene deletion in the ESX-1 locus while *M. mungi* has a 3 gene deletion in this same locus)[261].

ESAT-6 and CFP-10 are considered major virulence factors of the MTBCs. ESAT-6 and CFP-10 (called Esx proteins) belong to the WXG100 family, characterized by a conserved

tryptophan-X-glycine domain (WXG) and a length of ~100 amino acids. These proteins are encoded by *esxA* and *esxB* respectively and flanked by additional genes encoding parts of the secretion machinery. There is growing evidence that ESAT-6 and CFP-10 has a multitude of different roles throughout the course of infection including: stimulation of protective immunity, permeabilization and/or rupture of the macrophage phagosome, prevention of phagolysosomal fusion, induction of necrosis, formation of the granuloma, promotion of mycobacterial replication, and mediation pathogen escape from the macrophage[27,247,250,252,253,257,258,262–265]. Broadly, the role of ESX-1 can be defined as 'membrane lysis', as ESAT-6 and CFP-10 act as pore-forming toxins[250]. Additionally, ESAT-6 and CFP-10 are strong T-cell antigens; due to their immunogenic nature, these proteins are often used in vaccine development. The importance of ESAT-6 and CFP-10 is further supported as homologues of these proteins are present in all 5 ESX systems in mycobacteria (called *esxA-esxW*)[266]. Like *esxA* and *esxB,* these genes are arranged in pairs (with the exception of *esxQ*) and form loci containing genes encoding both the substrate and secretion machinery[266].

ESAT-6 and CFP-10 secretion depends on a number of other mycobacterial effectors outside of the RD1 locus, namely EspA, and EspC (encoded by the *espACD* operon)[254,267–269]. This gene cluster is located elsewhere on the chromosome, external to the ESX-1 locus (~260 kb upstream of ESX-1)[265]. Notably, EspD is required for the stabilization of EspA and EspC[267]. The *espACD* operon is induced by *espR* and activated in response to host-stressors via signal transduction by the PhoP-PhoR operon[265]. If the *espACD* operon is not transcribed ESAT-6 and CFP-10 will still be produced, but cannot be exported[265]. Interestingly, *M. bovis* and *M. tb* L6 have a defective PhoP. In these strains, ESAT-6 and CFP-10 secretion is rescued by naturally occurring compensatory mutations in *espACD* and strain-specific deletions[265]. Further, upregulation of the

PhoP operon (via the insertion of a mobile gene element) has been associated with increased human-to-human transmission of *M. bovis,* though the exact mechanism of this remains poorly defined[265]. It has also recently been demonstrated that ESAT-6 secretion is dependent of the production and export of phthiocerol dimycocerosate (PDIM), a cell-surface lipid, though CFP-10 is secreted independently[270]. This relationship is conserved in the secretion of ESX-5 homologues[270]. Notably, the ESX-1 locus is present in non-pathogenic *M. smegmatis* but is not involved in pathogenesis[247].

8.1.2 ESX-3:

The role of ESX-3 in mycobacterial virulence can be defined as the restriction of host defense[247,250]. This locus specifically has been associated with metal ion metabolism (ex: zinc and iron uptake)[247,250,266]. The main effectors of ESX-3 are ESAT-6 and CFP-10 paralogues (called EsxG and EsxH, respectively)[247,250]. It has been reported that the ESX-3 system prevents iron acquisition by host macrophages, impairs the function and repair of the 'endosomal sorting complex' (which is required for transport and degradation of cell products), and interferes with CD4 T-cell activation [247,250]. Additionally, this locus is responsible for the secretion of some PE-PPE proteins, though to a lesser extent than ESX-5 (discussed below)[254].

8.1.3 ESX-5

The ESX-5 system is the most recently evolved mycobacterial T7SSs and only present in slow-growing mycobacterial species[255]. Like ESX-1, ESX-5 has a number of roles in virulence. This system is immunomodulatory and essential for the secretion of a majority of PE/PPE proteins (composing ~10% of the *M. tb* genome)[271,272]. PE/PPE proteins are named after their structure: PE proteins contain a proline-glutamic acid domain, whereas PPE proteins contain a proline-proline-glutamic acid domain[273]. Like the ESX-5 secretion system, these PE/PPE proteins are also mostly

present in slow-growing, pathogenic mycobacteria, though it has been suggested that the emergence of the ESX-5 system predates the expansion of PE/PPE proteins in the *M. tb* genome[267,273]. Notably, not all PE/PPE proteins expressed are secreted; some are localized to the mycobacterial cell surface, suggesting a role in cell permeability and nutrient uptake[250]. The exact role of each PE/PPE protein in mycobacterial virulence has not been determined, though PPE18 (encoded by the ESX-5 system) is used as a component in the M27/AS01E vaccine candidate[267].

ESX-5 is important for a number of cell death pathways and the maintenance of the mycobacterial cell wall[250]. Specifically, ESX-5 has been linked to the inhibition of apoptosis (and conversely, the promotion of necrosis) in macrophages, as well as the initiation of a caspase-independent cell death cascade. This has been suggested to be involved in the spread of *M. tb* to naïve macrophages and other immune cells. Additionally, it has been reported that several genes encoding the structural components of the ESX-5 system are essential for *M. tb* growth[274].

Studies of *M. marinum,* the causative agent of TB in numerous fish species, initially revealed the link between ESX-5 and PE/PPE family protein secretion[255,262,273]. In *M. tb,* the role of ESX-5 in virulence has been shown in both immunocompromised and immunocompetent mouse models, likely due to the abrogation of PE/PPE production and secretion. For example, a disruption of the ESX-5 system in *M. tb* was observed to be attenuated in severe-compromised immunodeficient (SCID) mice; the ESX-5 deficient strain could not replicate in the host[257,275,276]. Likewise, the absence of ESX-5 associated PE/PPE proteins also resulted in attenuation in immunocompetent mice due to the inability to replicate[257,275,276]. In contrast, a transposon mutant resulting in ESX-5 deficient *M. marinum* was observed to be hypervirulent in adult zebrafish, but slightly attenuated in zebrafish embryos[277]. Surprisingly, a deletion of the ESX-5a accessory locus (discussed below) resulted in attenuation in the same adult zebrafish model[272].

In *M. tb*, a four gene stretch of the ESX-5 locus is duplicated an additional 3 times (called ESX-5a, -5b, and -5c, accessory loci). These genomic duplications are of two secreted Esx proteins (called EsxM and EsxN, homologues of EsxA and EsxB respectively) and two adjacent PE/PPE proteins. Notably, these accessory loci do not encode any structural components of the ESX-5 system, only secreted substrates. In total, the ESX-5 and its accessory loci account for 8 out of 13 *esx* genes identified in the *M. tb* genome, arranged in pairs (called EsxM/N, EsxI/J, EsxK/L, and EsxV/W)[255]. Unlike ESX-1, the deletion of EsxM and EsxN alone does not result in the cessation of PE/PPE protein secretion, suggesting that the accessory loci (ESX-5a,b,c) in conjunction with the parental ESX-5 each secrete a specific subset of PE/PPE proteins[255]. Interestingly, *M. tb* PPE38, essential for ESX-5 secretion, is absent in *M. bovis,* due to a genomic deletion (called RD5), and mutated in *M. tb* HN878. As both of these strains may be considered 'hypervirulent' compared to wildtype *M. tb,* it has been speculated that the loss of genes in RD5 may contribute to the increased virulence and pathogenesis observed[278]. This system will be further discussed in Chapter III.

8.2 Phthiocerol dimycocerosate (PDIM)

The mycobacterial cell wall contributes significantly to the intracellular survival of bacteria due to its inherent resistance to host stressors[279]. This is largely mediated by the presence of free lipids, glycolipids, and lipoproteins associated with the cell surface. Phthiocerol dimycocerosate (PDIM) is a complex long-chained, non-polar lipid, bound to the outermost layer of the mycobacterial cell wall[280–282]. The formation of these lipids is metabolically demanding; genes necessary for the biosynthesis of PDIM are clustered in a 70 kb region, corresponding to >1% of the entire MTBC genome[279,283]. Notably, PDIMs are present in slow-growing pathogenic mycobacteria, such as (*M. tb* and *M. bovis*) and absent from non-pathogenic mycobacteria (such

as *M. smegmatis*)[284]. In this dissertation, we have also determined multiple strains of *M. orygis* are PDIM positive.

Numerous studies have demonstrated that PDIM is crucial to the full virulence of pathogenic mycobacteria. For example, in mice (~25 years ago), two independent studies demonstrated the link between the loss of PDIM and subsequent attenuation *in vivo* as measured by a significant reduction (~50-fold) in lung bacterial burden[281,283,285]. These studies supported early observations that aerosol infection of a PDIM negative *M. tb* strain resulted in significantly fewer 'surface tubercles' in the lungs of guinea pigs and that differences between PDIM positive and PDIM negative strains were amplified over the duration of infection[286]. This was consistent in *M. bovis* studies[287]. Aerosol challenge with a PDIM-deficient *M. bovis* strain resulted in significantly reduced lung and spleen bacterial burden, to a level comparable to BCG vaccination[287].

The roles of PDIM can be categorized broadly into 1) survival 2) immune modulation, and 3) cell death[247,257,263,270,280,282,284,288–290]. First, PDIM has been linked to cell permeability, envelope integrity, neutralization of reactive nitrogen and oxygen species, and protection against some antibiotics[263,289]. Second, PDIM can mask pathogen associated molecular patterns (PAMPs) and regulate macrophage uptake and the secretion of pro-inflammatory cytokines (ex: TNF- α, IFN- γ)[279,284]. Third, PDIM is directly involved in *M. tb* escape from infected cells and thus, the spread of infection. This is mediated through phagosomal rupture and modulation of cell death pathways, such as the induction of necrosis[288]. Additionally, it has been shown that PDIM is required for the proper secretion of some ESX associated substrates (ex: ESAT-6, EsxN) but not for others (ex: CFP-10, EsxG, EsxH)[270]. This suggests that interaction with ESX substrates may be dependent on the structure of the lipid[270].

It has long been observed that spontaneous mutations in PDIM associated genes results in the loss of these lipids[283,286,291,292]. Moreover, this loss confers a growth advantage *in vitro*; PDIM negative strains dominate in liquid media compared to PDIM positive strains[283]. In fact, a 2009 study showed that after weekly passaging for 20 weeks in liquid, ~30% of the culture was observed to be PDIM negative[283]. Similarly, a stock culture of *M. tb* H37Rv became 75% PDIM negative following routine passaging on solid media once every 4-6 weeks (~20 passages)[283,293]. Moreover, if the production of PDIM is spontaneously lost, it cannot be reconstituted[283]. This unstable phenotype has been observed in *M. tb* H37Rv, Erdman, HN878, CDC1551 and *M. bovis* BCG strains, suggesting that this loss of PDIM is not restricted to a single species and may be the result of selective pressures (ex: metabolism, nutrient source, etc.)[280,283,289,294]. In mycobacterial virulence research, this implication is obvious: any conclusions about the role of genes of interest in pathogenesis must first verify the presence of PDIM, whether this be through identification by traditional methods (such as C^{14} labelling and thin layer chromatography, TLC) or maintenance by newer culturing methods (such as the routine addition of propionate)[280].

The 'canonical' virulence factors discussed thus far have been common across the MTBCs. However, as described above, there are natural variants which may contribute to differential virulence across the complex such as ESX-1 deletions in some animal-associated lineages, frameshift mutations resulting in the cessation of lipid production (ex: phenolic glycolipids), mutations in 'virulence regulators' (ex: PhoPR), and loss of gene function over course of evolution, amongst others[43,247,262,295,296]. It is evident that despite their similarity, MTBCs are not the same. In order to properly characterize these differences and understand their role in a more 'global' context, molecular and laboratory techniques must be employed.

9. Mycobacterial Recombineering

Genetic manipulation of mycobacterial species has been a challenge of decades. This can be largely attributed to the slow-growing nature of the MTBCs (~18-24 hour doubling time) and/or genomic features of the bacterium that prevent efficient DNA integration[24,28,297]. First, the mycobacterial cell wall is thick, lipid rich, and largely impermeable. Despite being Gram-positive, mycobacterial cell wall structure is similar to that of Gram-negative bacteria in which there is a secondary complex outside the cytoplasmic membrane[298]. This layer contains a complex of free lipids, mycolic acids, peptidoglycan, polysaccharides[298]. Second, there are limited antibiotic markers that can be used for selection without background resistance[297]. And finally, the MTBCs are a clonal population, with limited ability to undergo homologous recombination due to an inherent lack of molecular machinery[37]. Notably, mycobacterial recombineering systems have been dramatically improved by the introduction of phage encoded proteins (~10-100 fold more efficient). These phage-based systems can be categorized into general homologous or site-specific recombination systems[299].

9.1 General homologous recombination systems

General homologous systems defined early recombineering (i.e. genetic engineering using recombination proteins). Chromosomal modifications were facilitated by the incorporation of double-stranded (dsDNA) or single-stranged (ssDNA) into the genome by exogenous proteins[300]. Exchange was facilitated by areas of homology directed towards the gene of interest (GOI), exonucleases, and annealases, in the absence of a integration site (Figure 4a)[301]. General homologous systems have been used in bacterial pathogens such as enterohemorrhagic *E. coli, Salmonella enterica, Shigella flexneri, Pseudomonas aeruginosa, Yersinia pestis,* and *M. tb,* though with variable success[299]. In mycobacteria, the efficacy of general homologous recombineering is limited by the composition of the DNA substrate, physical DNA uptake and

rates of illegitimate recombination[301]. Additionally, slow-growing mycobacterial species have ~5-10-fold reduction in recombineering efficiency compared to fast-growers such as *M. smegmatis*[297]. In gene disruption studies, general homologous recombination hinges on allelic exchange between the dsDNA substrate (such as a vector containing a resistance cassette flanked by regions of homology) and the mycobacterial genome. This requires two rare crossover events to facilitate the insertion of the modified gene target (resistance cassette) in place of the GOI. Moreover, regions of homology are recommended to be longer than 500 bp (up- and downstream of the GOI). Though increased homology corresponds to increased fidelity of recombination, the size of these DNA products significantly reduces the rate of dsDNA substrate uptake[300]. In contrast, phage-encoded systems are most effective at producing point mutations (SNPs) in resistance associated genes; these ssDNA substrates have much higher allelic exchange frequency, and fidelity, compared to dsDNA substrates and require much shorter regions of homology[302]. For the purposes of this dissertation, discussion will be limited to the Che9c (RecET) phage system and its derivative, pNIT:ET.

9.1.1 Che9c (RecET)

The Che9c (RecET) system is derived from the Che9c mycobacteriophage described by Van Kessel et al in 2008. This phage was unique in that it expressed homologues of the well described RecE and RecT recombination proteins, which had already been successfully employed in *E. coli* mutagenesis[303]. RecE (also known as exonuclease VIII) is a 5'→3' exonuclease whereas RecT is a 'single stranded DNA-annealing protein'. When these proteins are complexed together, they initiate a double stranded DNA break repair mechanism. In recombineering, RecE degrades a single strand of dsDNA substrate, exposing a single stranded 3' overhang. RecT, binds will this overhang and promotes recombination by pairing complementary sequences, strand exchange,

and/or strand invasion[301,304]. Compared to *E. coli,* Che9c RecE and RecT are truncated (~30% homology) but function is conserved[301].

In the first iteration of this system, two episomal plasmids were generated: pJV53, designed for dsDNA modifications (ex: knockouts) and pJV62, designed for ssDNA modifications (ex: SNPs)[301,305]. The main difference between these plasmids was the absence of RecE in pJV62, as it was determined only RecT was required for efficient ssDNA substrate integration[301]. RecE and RecT protein expression is controlled by an inducible acetamidase promoter; cultures are induced with acetamide and the ds- or ssDNA substrate is electroporated[297]. For gene deletions, a large, linear fragment of dsDNA is required for integration into the genome (a resistance cassette flanked by 500 bp region of homology up- and downstream) whereas for point mutations (ssDNA) a SNP-containing oligomer (~50-100 bp) is required[306]. Notably, in slow-growing mycobacterial species, van Kessel and Hatfull showed that integration of an oligomer targeting the lagging strand of the replication fork is 10^4-fold more efficient compared to the integration of the leading strand[305]. The main limitation of this system is that point mutations can only easily be screened if they are associated with selectable genes, such as resistance associated drug targets[302].

In 2009, Pandey et al. demonstrated that nitrile inducible promoters could be adapted for use in mycobacteria[307]. Using a green-fluorescent protein (GFP) containing plasmid (pNIT-1) it was determined that the nitrile promoter could induce more gene expression, in a shorter amount of time, under more variable conditions compared to the acetamidase promoter[302,307,308]. This plasmid was then modified to express RecE and RecT rather than GFP and implemented for mycobacterial recombineering (referred to as pNIT:ET). This combined the efficacy of phage-based systems and the inducibility of the nitrile promoter. This pNIT:ET system was used in

Chapter II of this dissertation, showing an affinity for the integration of ssDNA but a complete inability to uptake dsDNA substrates.

9.2 Site-specific recombination

Unlike general homologous recombination systems, site-specific recombination occurs only at specific DNA 'attachment' sites. Specifically, *attP* (a phage attachment site) will recombine with *attB* (a bacterial attachment site) to form a novel product flanked on either side by left (*attL*) and right (*attR*) attachment sites (Figure 4b)[309]. Notably, this reaction can occur bidirectionally, with *attL* and *attR* also capable of recombination, though this may depend on additional host factors (called host-derived integration host factor, mIHF)[302,310]. Exogenous DNA integration into the mycobacterial genome was investigated with number of phage systems (ex: L5, Ms6, Bxb1, and ϕRv1) however, this overview focusses on the utilization of L5, the first well-described mycobacteriophage system, and Bxb1 in gene disruption studies.

9.2.1 L5 integrase

L5 infects both fast- and slow-growing mycobacterial species[311]. The life cycle of the phage depends on the integration into the mycobacterial genome (facilitated by the phage, called Int) and excision from the mycobacterial genome (facilitated by the host via integration host factor, mIHF). Like all site-specific recombination, genetic exchange depends on the recombining of *attP* and *attB*. The L5 integrase is a tyrosine recombinase capable of exchanging genetic information via single stranded breaks. The *attP* is ~413 bp, with a minimal functional cassette of ~252 bp[302,312]. This naturally occurring system was commandeered to make the first recombinant BCG strain via site-specific recombination, successfully integrating a non-replicating shuttle vector and the *attP* site[302]. However, *in vitro* this site-specific recombination could only be successfully facilitated in the presence of exogenous host factors, showing some limitation in genetic manipulations that

could be achieved. As such, this preliminary work led to the discovery, pursuit, and optimization of other mycobacteriophages, such as Bxb1.

9.2.2 Bxb1 integrase:

Bxb1 integrase (Int) is a site-specific serine recombinase derived from mycobacteriophage Bxb1 that coordinates attachment sites and promotes strand exchange[309,313]. In comparison to other mycobacteriophages, this integrase is unique. First, Bxb1 integrase is much smaller compared to other phage integrases such as L5 (~500 amino acid residues). Second, residues within this structure (at the C-terminus) show limited similarity with other serine recombinases[311]. Third, the phage attachment site (*attP*) is only 48 bp, one of the smallest functional *attP* sites[314]. Finally, Bxb1 integrase can function in the absence of additional host factors, but only in a one directional manner. This means that Bxb1 integrase *attP* and *attB* recombine to form *attL* and *attR* flanked products, but the products themselves cannot recombine; thus increasing the efficacy of the integration event[299,310]. This integration is also mediated through dsDNA breakage, rather than ssDNA breakage as observed in L5[314].

In *M. smegmatis,* the naturally occurring location of the *attB* site is within the 3' end of *groEL1,* a well-described chaperonin protein; the *attP* site is encoded on directly upstream of the Bxb1integrase[308,314,315]. To confirm the viability of site-specific recombination via the Bxb1 phage system in mycobacteria, a plasmid carrying Bxb1 integrase and the *attP* site was successfully integrated and maintained, even in the absence of selection. Thus, this system could be further developed for use in efficient genetic disruption, such as in the ORBIT recombineering system

9.2.3 Oligo-mediated recombineering followed by Bxb1 integrase targeting (ORBIT)

In 2018, Murphy et al. first described the ORBIT system, a new recombineering technique that combined two well-established, but inefficient, systems for mycobacterial mutagenesis[299].

ORBIT combines the Che9c RecET and the Bxb1 mycobacteriophage systems (described above) to efficiently facilitate gene disruption studies[299]. This circumvents the need for large, dsDNA PCR products and requires only one homologous recombination step; contrasting directly with previous systems which relied on multiple allelic exchanges and upstream construction of appropriate delivery vectors[299,302,315]. In the current study, over 100 gene modifications were successfully engineered in either *M. smegmatis* or *M. tb,* with rates of efficiency dependent on bacterial strain, gene function, and size of the GOI. The authors report the largest deletion achieved using the ORBIT strain was ~12 kB, though they suspected this is not the absolute limit. However, it was also noted by the authors that regardless of disruption, the ORBIT system still showed ~500-fold less efficacy compared to the incorporation of point mutations[299]. This dissertation is the first to successfully utilize the ORBIT system in *M. bovis* and *M. orygis* to generate genetic knockouts between 150-5500 bp long (Chapter III). Though ORBIT has been described for use in promoter replacements, insertions (ex: C-terminal fusions), and gene knockouts (KOs), for the scope of this project, only the construction of KOs will be discussed.

There are three main components to the ORBIT system: 1) a single stranded oligomer containing *attP* site 2) a non-replicating 'payload' plasmid containing a Bxb1 *attB* site and a selectable marker and 3) an inducible plasmid expressing RecT annealase and Bxb1 integrase. The single-stranded oligo targets the lagging strand of the DNA replication fork to overcome the strand bias observed in mycobacterial recombineering[299]. It contains a 48-bp *attP* site flanked by ~60 bp region of homology upstream of the GOI (including the first 30 bp of the GOI), and ~60 bp of homology downstream of the GOI (including the last 30 bp of the GOI). The homologous arms align the *attP* site with the GOI and dictate insertion site. This is co-electroporated with the 'payload plasmid'. Importantly, this plasmid contains the Bxb1 integrase *attB* site (site-specific

recombination) and a selectable antibiotic cassette. In this dissertation, hygromycin or zeocin were used due to drug susceptibility and availability of plasmid. Lastly, RecT and Bxb1 are under a tetracycline inducible promoter (induction agent= anhydrotetracycline); following stimulation, these genes are highly expressed and mediate the ORBIT reaction. This occurs in two steps. In the first step of the reaction, the *attP* containing oligomer is aligned with the GOI and inserted into the mycobacterial genome via RecT annealase (homologous recombination). In the second step Bxb1 integrase facilitates recombination of *attP x attB*, integrating the antibiotic resistance cassette in place of the GOI (site-specific recombination). The authors reported a high efficacy of integration; ~50% of clones selected were positive, with few clones needing to be selected following the appropriate outgrowth period[299]. Notably, illegitimate recombination in which the antibiotic cassette was integrated but the gene was not knocked out could not be avoided. This is likely to be due to multiple *attB* sites occuring naturally within mycobacterial genomes, as the *attP x attB* reaction has been observed to be promiscuous[314].

The appeal of the ORBIT system is immediately apparent. The requirement of ~3000 bp dsDNA substrates (500 bp homology up- and downstream of the GOI flanking an antibiotic cassette) is replaced with a single stranded oligomer, targeting the replication fork. Additionally, this system does not require the construction of multiple plasmids prior to integration, instead it combines the most efficient components of two phage systems. Chapter III of this dissertation depended entirely on the functionality of the ORBIT system in *M. bovis* and *M. orygis*. Accordingly, the advent and optimization of genetic tools in mycobacteria is vital for the screening of putative virulence factors and the understanding of the mechanism of infection, especially in slow-growing pathogens.

10: Animal Models of Tuberculosis

Since the discovery of the 'tubercle bacillus' and the 'bovine tubercle bacillus', animal models have played a crucial role in tuberculosis research. The utilization of animals allows investigation into the relationship between pathogen and disease; animals are exposed equally to the same pathogen using the same route of infection and monitored until compassionate or experimental endpoints. Further, these animal models can be extended to virulence, vaccine, or treatment studies, depending on the experimental question[18]. Dubé et al outlined several characteristics of an ideal animal model: 1) experimental infection mimics natural disease 2) infection occurs from a biologically relevant dose 3) route of infection mimics natural exposure 4) pathology manifests in relevant organs and/or this pathology is comparable to natural infection, and 5) disease spectrum is comparable to what is seen in a natural host[316]. However, there is no single model that can perfectly recapitulate tuberculosis in humans; the choice of model often depends on the cost, space availability, and biosafety requirements[18,316]. Additionally, different animal models are used to represent different facets of the disease as there is significant variation in susceptibility, presentation, and the course of disease progression depending on the animal studied[18,316]. Further, a 2023 study reported that the most commonly used models in tuberculosis research are mice (~56%), cattle (~27%), and guinea pigs (~5%), however there have also been studies reported in rabbits, non-human primates, rats, zebrafish, pigs, cats, goat, deer etc.[18] For this dissertation, the murine model (Chapter IV) and the bovine (cattle) model (Chapter V) will be used. At the time of this submission, the Behr laboratory has been the only group to propose and validate a murine model of *M. orygis* infection. Additionally, the Behr laboratory, in conjunction with the University of Saskatchewan, has been the only group to perform *M. orygis* infections using a bovine model.

10.1 Murine models:

It is generally agreed upon that inbred mice provide the greatest utility in tuberculosis research, despite limitations in disease manifestation. They act as a fundamental tool for understanding complicated phenotypes. First, mice are small, easy to handle, and accessible. Second, the genetic and immunological background of humans and mice have significant overlap[317]. Moreover, in a mouse model, these backgrounds are clearly defined and can be manipulated (ex: targeted genetic knockouts of mice to assess specific genes involved in the host response to MTBCs)[318]. For example, the development of IFN-γ knockout (-/-) mice unequivocally proved that IFN-γ production was necessary to successfully control bacterial growth and had an essential role in macrophage activation and resistance to *M. tb* infection[319]. Mice can also be engineered to be more representative of the disease process of interest[320,321]. Additionally, due to their abundance in research, many reagents, such as antibodies, have been designed specifically for mice, enabling the in depth study of early immunological processes of infection[322].

Mice are considered a 'tolerant' host compared to other animals (ex: guinea pigs) due to high bacterial burdens that can be withstood. However, the infection outcome is not uniform and can be altered depending on the sex, age, or lineage of the mouse. Infection outcomes also differ significantly depending on route of infection, dose, and type of infectious agent used (ex: *M. tb* versus *M. bovis).* Broadly, mice can be categorized into 'resistant' and 'susceptible' strains, defined typically by length of survival, bacterial burden, induced pathology, and progression of infection[323]. The most commonly used mouse strain for virulence and vaccine studies is BALB/c, followed closely by C57BL/6 mice, though these are often considered 'resistant' strains to *M. tb* infection[18]. For context, in one foundational study ranking susceptibility, the median survival of *M. tb* infected C57BL/6 mice and BALB/c mice was comparable following both aerosol and IV

infection (~239 and 252 days respectively) but distinct from other strains with a median survival of around ~100 days[323]. In both C57BL/6 and BALB/c mice, aerosol, intranasal, intravenous, intraperitoneal, and intratracheal modes of infection have been successfully described, though the aerosol model most accurately mimics the natural route of MTBC infection[18]. Of note, aerosol infection of *M. bovis* in a mouse model is not often reported though this is likely due to the availability of the natural host (calf) to study disease mechanisms and models without the need for a proxy. However, mice studies have shown that, like *M. tb, M. bovis* isolates evoke different immune responses and that survival, bacterial burden, and lung pathology is strain dependent[74].

Despite clear advantages, mouse models are not fully representative of human (or bovine) disease. First, all mice infected with MTBCs will get sick and eventually progress to active TB; in comparison, only 5-10% of humans will progress to active TB[324]. Mouse models may overlook the host-pathogen interactions that must occur to result in clearance, containment or progression. Next, traditional mouse models (such as C57BL/6 or BALB/c mice) do not induce caseating and necrotizing granulomas that are considered a hallmark of tuberculosis[84,325,326]. This is considered to be the greatest disadvantage of the mouse model. Following infection of C57BL/6 or BALB/c mice, only one type of lesion forms; this lesion is non-necrotic, non-hypoxic, and does not cause cavitation[316,327]. However, these mice will still succumb to infection, still have significant bacterial burdens in the lungs, dissemination to the spleen and liver, and manifest a chronic TB infection[316]. Work into the characterization of more susceptible strains (such as DBA/2, C3HeB/FeJ, and 129/SvJ,) has reduced (but not overcome) this challenge. For example, C3HeB/FeJ mice have a mutation within the 'super-susceptibility to tuberculosis-1' locus (*sst1*) that results in progressed disease and uncontrolled bacterial growth[328]. Following aerosol *M. tb* (or *M. bovis*) infection C3HeB/FeJ mice can develop heterogenous, necrotizing lesions that are much more representative

of heterogeneous human infection outcomes[317,328–330]. Overall, mouse models provide the greatest flexibility in experimental design and control. Though there are some limitations, mouse models are a crucial starting point in the characterization of infection and disease manifestation when a proxy is required.

10.2 Bovine models (cattle):

Cattle studies have been essential in understanding the pathology and disease mechanisms of *M. bovis,* as the calf is a natural host. Like mice, calves have a defined genetic background, though comparison between groups (ex: *Bos taurus* versus *Bos indicus*) is uncommon. Due to the longevity of *M. bovis* research, experimental infections have been described using aerosol, oral, intranasal, intratracheal, subcutaneous, intratonsillar, and intravenous routes of transmission[177,331–337]. Notably, the route and dose of infection, drives its outcomes. For example, the minimum dose required to establish infection in the respiratory tract was determined to be ~10^3 times lower than the dose required for oral challenge[338]. In another study, following oral challenge, lesions were more likely to manifest in the digestive tract and show limited dissemination whereas following endotracheal challenge lesions showed the greatest pathology in the lungs and thorax[332]. A review by Pollock et al. also highlighted the relationship between route of infection, dose, and pathology[337]. Overall, high doses (> 10^6 CFU) via the IV, SC, or oral route results in severe, generalized disease whereas low dose aerosol or intratracheal infection (100-10000 CFU) results in pathology more comparable to natural infection[337]. Moreover, cattle studies can be direct (targeted infection) or indirect (animals in contact with source of infection)[337]. This is ideal to evaluate not only host-pathogen interactions, but also transmission rates between animals and minimum infectious dose.

Historically, cattle studies have been performed to investigate the host immune response to *M. bovis*[18,336]. Cattle elicit a comparable granulomatous reaction to humans and respond similarly to BCG administration[336,339]. As such, experimental infection can be used as direct screens for vaccine candidates and/or interventions in real time. From a practical perspective, a number of immunological agents have also been established to study bovine tuberculosis (ex: diagnostic assays, various antibodies, etc.) and, it has been proposed that the study of bovine tuberculosis may be a good proxy for the study of human tuberculosis[322,336]. Perhaps most relevant to my research, as cattle are natural hosts of *M. bovis*- and *M. orygis*-, species-specific virulence factors can also be rapidly evaluated using standardized readouts (for example: bacterial burden, gross pathology, histopathology, etc.).

The largest drawback to cattle as an experimental model is the large size of the animal. These studies are expensive and require specialized infrastructure and staff to be safely performed (ex: a large animal biosafety level 3). As such, sample sizes are smaller and experiments may not be easily repeated, compared to small animal studies. Further, the genetic manipulation of calves is much more complicated compared to mice, hamsters, and guinea pigs meaning that key immunological molecules cannot easily be knocked out. Despite this, the cattle model shows the most complete picture of *M. bovis* infection and disease and has been thoroughly described over the last 100 years.

Having both experimental and natural models of bacterial infection is essential to the characterization of novel pathogens. Moreover, it allows for the simultaneous assessment of infection versus disease, the immune response, and the efficacy of current interventions. Duffy et al. established that *M. bovis* is not the main zoonotic threat in one of the highest TB burden regions

globally; instead, this was determined to be *M. orygis.* As such, new understandings of virulence factors, host-pathogen interactions, infection outcomes, and susceptibility need to be established.

11. Figures

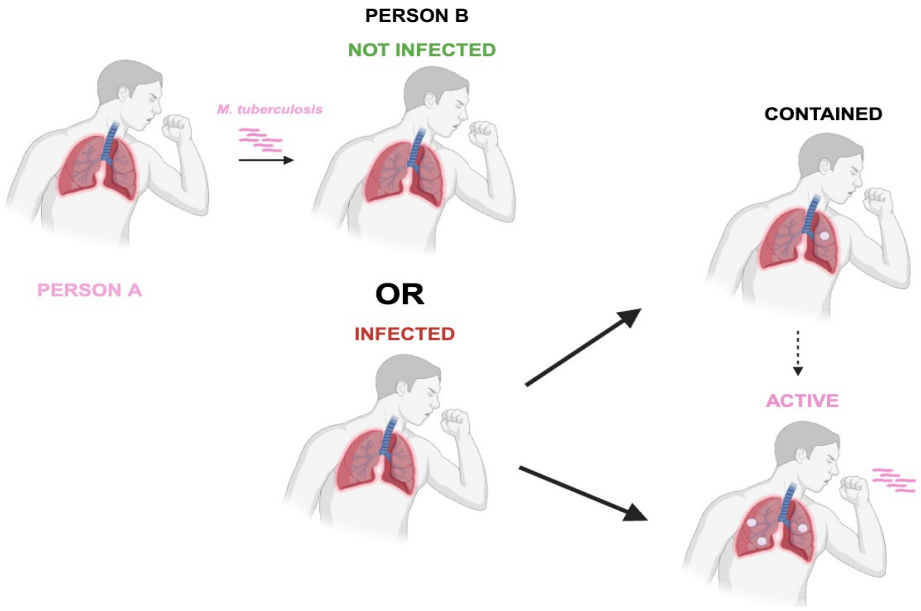

Figure 1. Transmission cycle of *Mycobacterium tuberculosis* (*M. tb*).

Person A is infected by *Mycobacterium tuberculosis* and progresses to active disease. In this state, Person A may present clinically with symptoms such as persistent cough, fever, bloody sputum, weight loss, loss of appetite and/or night sweats. On a chest X-ray, opacities within the lung can be observed. During active disease, bacteria are actively replicating and can be spread via the aerosol route to Person B. Following this exposure, there are two outcomes for Person B: infected or not infected. If Person B is infected, the bacteria can either be contained/cleared by the host immune system (ex: via the formation of granulomas) or the infection progresses to active disease, continuing the transmission cycle.

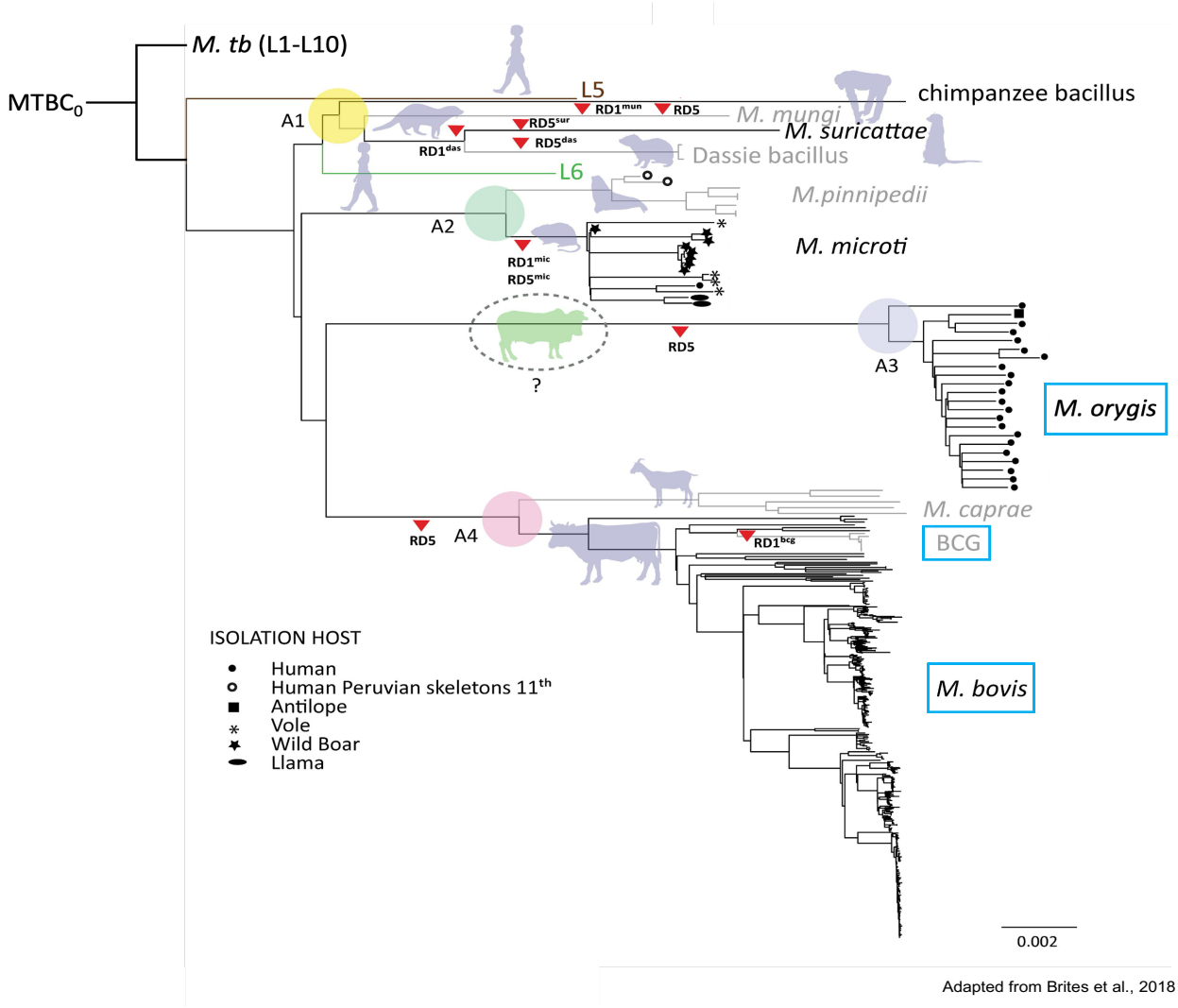

Figure 2. Animal-adapted members of the MTBC subspecies.

Phylogenetic tree of the animal-adapted members of the MTBC (n= 10 strains). Of note, *M. tb* L5 is also commonly referred to as *M. africanum* and included as a separate lineage. Members of the A1 clade are restricted to a single, maintenance host whereas members of clades A2-A4 have broad host ranges and evidence of human infection (immunocompetent and/or immunocompromised hosts). The focus of this dissertation will be on *M. bovis* BCG, *M. bovis*, and *M. orygis* (highlighted in blue). Figure adapted from Brites et al., 2018[47].

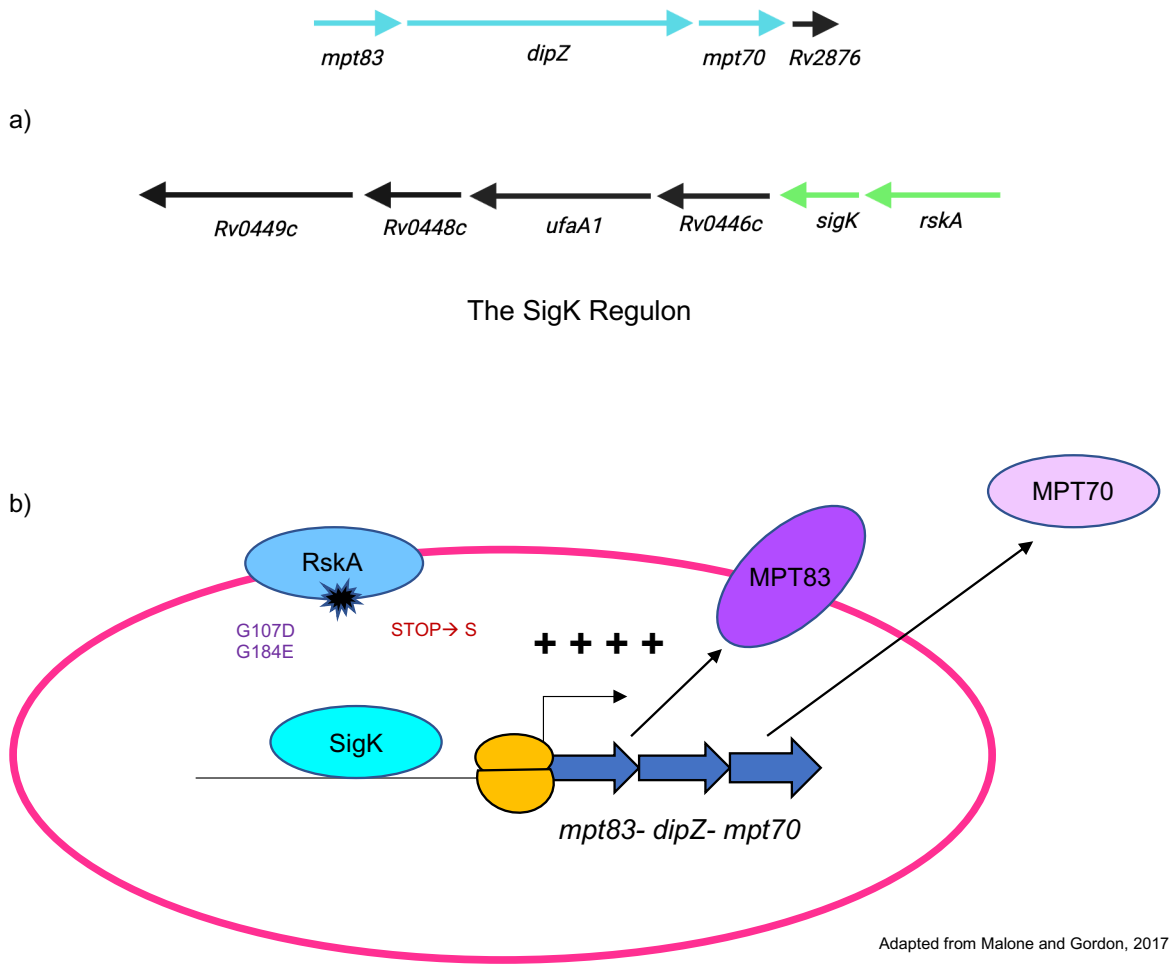

Figure 3. Depiction of the SigK regulon.

a) Genes under the control of the SigK regulon. Regulon composed of a regulatory locus (*sigK*, *rskA*; highlighted in green) and an effector locus (*mpt70, dipZ, mpt83*; highlighted in blue). SigK= sigma factor K, RskA= anti-sigma factor K. b) Schematic of SigK regulon expression in *M. bovis* and *M. orygis*. In this scenario, RskA is unable to bind SigK resulting in constitutive expression of both MPT70 and MPT83. This is caused by two missense mutations in *M. bovis* (purple) or a single readthrough mutation in *M. orygis* (red). In this diagram, the secreted MPT83 is not depicted. In *M. tb*, RskA binds SigK repressing transcription of the SigK regulon. Following host stressors (starvation, hypoxia, etc.) RskA and SigK dissociate, resulting in the expression of MPT70 and

MPT83. Recently, an alternative model of SigK-RskA has been proposed by Veyrier et al. in which RskA acts as a dual activator-inhibitor of SigK activity (not shown)[185]. Cartoon adapted from Malone and Gordon, 2017[43].

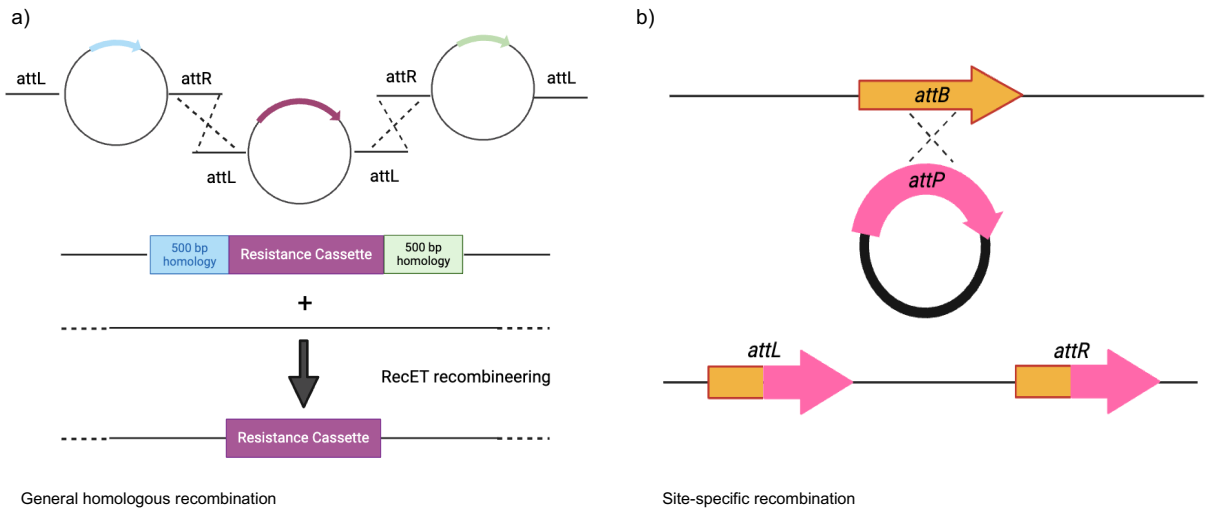

Figure 4. Mycobacterial recombineering techniques used in gene deletion studies.

a) General homologous recombination. A double-stranded DNA (dsDNA) substrate is synthesized using molecular cloning. Three plasmids are recombined using *attB* (bacterial attachment site) and *attP* (phage attachment site) recognition to form a single product consisting of an antibiotic resistance cassette flanked by 500 bp of homology up- and downstream of the gene of interest (GOI). Integration of the dsDNA product is mediated by RecE and RecT and guided by the flanking areas of homology. **b)** Site-specific recombination mediated by *attB x attP* recognition ('BP' reaction). This facilitates the integration of gene(s) of interest (in the case of deletion strains, an antibiotic resistance cassette) into the bacterial genome in the correct location. The resulting product is demarcated in the genome by *attL* and *attR* recombination sites. The role of site-specific recombination is further described in Chapter III of this dissertation (Figure 10).

AIMS AND HYPOTHESES OF RESEARCH

In this thesis I will be bridging a technical challenge with a substantive application. The technical challenge is adapting molecular methods to engineer various mycobacterial strains with specific capacities. The substantive application is to use these strains for targeted investigations of hypothesized virulence factors that have been suggested by associations between genomic variance and differential infection outcomes.

The advent of molecular techniques, such as mycobacterial engineering, has enabled researchers to specifically target the genome for loss-of-function investigations. These tools can be incorporated into the pipeline of *M. tb* diagnostics or be used to investigate 'natural experiments' that have occurred as a consequence of mycobacterial evolution. Though natural variation (such as SNPs and/or regions of deletions) is associated with differential gene and protein expression, much of the genome has not been interrogated. Additionally, virulence studies typically utilize *M. tb* as a default laboratory organism for *in vitro, ex vivo* and *in vivo* studies. Despite greater than 99.9% conservation at the nucleotide level, differential virulence across *Mycobacterium tuberculosis* complex subspecies (MTBCs) has been known for over 100 years. This suggests that *M. tb* may not be representative of the pathogenesis of other mycobacterial species and that investigation of other closely related members, such as *M. bovis* and the recently described *M. orygis,* may aid in the discovery of previously overlooked virulence factors. Finally, both *M. bovis* and *M. orygis,* have been shown to contribute to the global burden of zoonotic TB (zTB). While *M. bovis* has been studied since the late ~1800s, *M. orygis* was only described in 2012. As such, knowledge about the 'new' pathogen (ex: pathogenesis, host range, impact on human health, and infection outcomes) is limited, and techniques used to study *M. tb* have yet to be validated in *M. orygis*.

This dissertation focusses on two aims to address differential virulence and pathogenesis within the MTBCs:

Aim I: Employ mycobacterial engineering to develop isogenic *M. bovis* BCG, *M. bovis,* and *M. orygis* strains

Aim II: Evaluate infection outcomes of wildtype and isogenic strains using *ex vivo* and *in vivo* models

These aims are aligned with three hypotheses:

Hypothesis I: I hypothesize that molecular techniques can be used to engineer isogenic strains in *M. bovis* BCG, *M. bovis,* and *M. orygis.* Further, these strains can be efficiently incorporated in both clinical and laboratory work.

Hypothesis II: I hypothesize that the experimental infection outcome of *M. orygis* may be comparable to *M. bovis,* but distinct from *M. tb,* as defined by the parameters of morbidity and mortality.

Hypothesis III: I hypothesize that the upregulation of effector proteins MPT70 and/or MPT83 in cattle-associated members of the MTBCs contributes to enhanced virulence and that the roles of these proteins may be species-specific.

CHAPTER II: THE UTILIZATION OF pNIT:ET IN THE CLINICAL DIAGNOSIS OF *MYCOBACTERIUM TUBERCULOSIS*

The chapter contains work from my previous publications in both Clinical Microbiology and Infection titled "**BCG strains with defined resistance mutations: a new tool for TB lab quality control"** (Danchuk et al., 2020) and Thorax titled "**Challenging the gold standard: the limitations of molecular assays for detection of *Mycobacterium tuberculosis* heteroresistance"** (Danchuk, Solomon et al., 2024). Here, I focus predominantly on the molecular engineering of mono-resistant *M. bovis* BCG strains and their implementation into clinical laboratory diagnostics (phenotypic and genotypic testing) to ensure the initiation of appropriate antibiotic therapy.

1. Introduction

Tuberculosis eradication efforts have been largely hindered by the emergence of drug-resistant *M. tuberculosis* (DR-TB)[60]. In 2022, ~410 000 cases of multidrug resistant/rifampin resistant TB (MDR-TB/RR-TB) were estimated globally, out of a total of ~10.3 million TB cases (3.2%)[60]. Drug susceptible TB (DS-TB) has a treatment success rate of ~88% whereas DR-TB has a treatment success rate of only 63%. Crucial to the control and management of DR-TB is accurate detection, as misdiagnosis may result in treatment failure at the individual level and onward propagation of DR-TB at the population level[340]. Mycobacterial culturing and drug susceptibility testing remain the gold standard for TB diagnostics (phenotypic testing)[86]. However, these techniques are time-consuming, costly, and have an extended turnaround time, resulting a delay in the initiation of treatment. To address these challenges, rapid molecular testing has been implemented globally to 1) detect the presence of *M. tb* and 2) predict first- and second-line drug susceptibility in the absence of cultures[341]. These tests span from simple tests used in peripheral laboratories (such as the GeneXpert MTB/RIF assay and/or GeneXpert Ultra) to clinical WGS[342].

The development of low complexity molecular tests (such as NAATs) has caused a shift in the diagnostic landscape as testing can now be performed in reference and hospital laboratories ('classical' microbiology laboratories), as well as clinics, outreach programs, and remote polyfunctional settings[343–346]. Initiation of appropriate interventions for DR-TB cases rest on the foundation of reliable laboratory results. Notably, few institutions have the physical and operational capacity to propagate *M. tb* (DS- or DR-TB). Thus, only limited settings in which diagnostics are run, 1) have the ability to assess the concordance of genotypic and phenotypic testing and 2) have an adequate quality control for these tests. It has been well-documented that discordance between local and reference laboratories is associated with under-treatment and a predictor of mortality in DR-TB patients[347]. As such, we engineered a panel mono-resistant BCG strains using the pNIT:ET recombineering system to determine the limitations of molecular testing in the absence of traditional mycobacteriology and provide accessible laboratory controls (Figure 5)[86,348]. BCG strains possess the same phenotypic qualities of *M. tb* (doubling time, morphology on solid agar, microscopic presentation) and, with the exception of PZA, comparable drug susceptibility profiles[24,349]. Moreover, BCG strains have a well-established safety profile already in clinical use, minimizing risk to laboratory technicians[96]. This allows our panel to be used in the validation of genotypic and phenotypic diagnostic testing, as well as detection of protocol oversights (media, procedures, reporting). Additionally, given the importance of DR-TB detection (MDR-, pre-XDR, XDR), our panel specifically targets canonical and non-canonical mutations associated with first- and second-line antibiotic resistance. Since the initial development of this panel in 2018-2019, we have also showed its utility as a quality control in the detection of minority populations of resistant bacteria phenotypically and genotypically.

2. Methods

2.1 Mycobacterial culturing:

All cultures (WT and recombinant) were grown in 7H9 complete media (defined as 7H9, 0.1% Tween80, 0.2% glycerol + 10% albumin, dextrose, and catalase, (ADC)) with or without antibiotic. Cultures were adjusted to OD_{600} of 0.05-0.1 and rolled at 37°C until log-phase (OD_{600}= 0.5-1). Prior to use in downstream experiments, cultures were passaged at least twice, as described above. All bacterial strains used in this chapter are outlined in Table 1.

2.2 Validation of the pNIT:ET system:

M. smegmatis is utilized as the point of validation for recombineering systems due to its rapid doubling time (T= ~4 hours) and biosafety level[350]. The pNIT:ET plasmid was subjected to increasing concentrations of isovaleronitrile (IVN) to determine 1) the efficacy of induction of *recE* and *recT* and 2) subsequent generation of colonies containing resistance-conferring SNPs (Figure 5c,d). Briefly, 20 mL of *M. smegmatis* containing pNIT:ET was grown to late log-phase (OD_{600}= 0.8-0.1) and stimulated with IVN for 2.5 hours at 5 µM, 10 µM, 50 µM and 500 µM concentrations. Following induction, cultures were centrifuged and resuspended in 1 mL of Trizol. RNA was obtained using a phenol-chloroform extraction with subsequent DNAse cleanup (TURBO DNA-free™ kit, Invitrogen); cDNA was derived from purified RNA. A qRT-PCR was performed alongside a 'no induction control' (IVN-free culture) with primers specific to RecE and RecT. Expression was normalized to sigma factor A (SigA, housekeeping control) to determine fold induction (Figure 5c). In *M. smegmatis* induction of RecE and RecT was comparable across concentrations tested. Additionally, pNIT:ET induction was assessed in *M. tuberculosis* using the above-described protocol with the following modifcations: 5 µM IVN was added to 20 mL of log-

phase culture and rolled at 37°C for 16-24 hours to mimic electroporation conditions (Figure 5d). This protocol was subsequently applied for all pNIT:ET containing members of the MTBC used in this chapter.

2.3 Generation of mono-resistant BCG strains:

Mono-resistant BCG strains were engineered as described by Murphy et al[306]. The pNIT:ET plasmid was electroporated into either BCG Russia, BCG Danish, or BCG Pasteur and maintained using 50 μg/mL of kanamycin. At late log-phase, 2M glycine (10% of total culture) and 5 μM of IVN was added to culture and rolled for 16-24 hours at 37°C. Oligomers (70 bp) were electroporated into pNIT:ET containing BCG to generate a resistance-conferring SNP within the gene of interest (such as *rpoB, katG, gyrA* etc.). SNPs were selected based on literature reviews ('canonical' mutations) and case reports ('non-canonical' mutations). Following 5 days of recovery in 7H9 complete media at 37°C, the electroporated culture was plated on 7H10 agar plates containing glycerol, oleic acid, albumin, dextrose, catalase (OADC), and the antibiotic for which resistance was conferred. SNPs were confirmed using conventional PCR, Sanger sequencing (Genome Quebec and Innovation Centre) and subsequent alignment with the GOI against the parental BCG strain (Geneious Prime 2019.2) (Figure 6a,b). Resistance conferring SNPs and correlated antibiotics are outlined in Table 1. In total, six mono-resistant BCG strains and one strain engineered to contain two targeted SNPs (KatG S315T + GyrA D94G) were generated (Table 1). Introduction of the KatG S315T SNP could only be achieved following the electroporation of two resistance conferring oligos (KatG S315T and GyrA D94G) and cross-selection using both INH and MFX. All engineered strains are available in the Belgian Coordinated Collections of Microorganisms (BCCM) repository.

2.4 Molecular resistance prediction:

BCG is a live, attenuated member of the MTBC[47]. As such, it can be safely used as a proxy in clinical laboratories without access to a biosafety containment level 3 (CL3) facility. The engineered strains BCG RpoB S450L, BCG RpoB I491F, and BCG KatGdel428 were used as quality controls for two molecular diagnostic tests: GeneXpert (Cepheid, USA) and GenoType MTBDR*plus* Ver 2.0 (Hain Lifesciences, Germany) (Figure 7,8). Additionally, mixtures of mono-resistant BCG strains were used to determine the efficacy of GeneXpert Ultra (Cepheid, USA) at 5%, 10%, 50%, and 60% resistant populations (Table 2). All molecular resistance prediction assays were performed as per manufacturer protocols with no modifications. GeneXpert studies were performed at the Research Institute of the McGill University Health Centre and the Lakeshore General Hospital (Montreal, Canada). GeneXpert Ultra studies were performed in collaboration with Christian Medical College (Vellore, India); Geneotype MTBDR*plus* assays were performed in collaboration with the Public Health Ontario Laboratory (Toronto, Canada). *Mycobacterium avium hominissuis* (MAH) and/or *Mycobacterium avium paratuberculosis* (MAP) were included as negative controls (non-tuberculous mycobacteria) whereas WT BCG was included as a drug-sensitive MTBC control (Figure 7,8).

2.5 Phenotypic drug susceptibility testing (pDSTs):

Broth microdilution assays were prepared by the addition of 100 µL of antibiotics to 100 µL of bacteria to a final antibiotic concentration of 0.0312-8 µg/mL in a 96-well plate and incubated at 37°C for 7 days (technical triplicate, unless otherwise indicated). A 7H9 complete background control (200 µL media) and 7H9 complete plus antibiotic (100 µL media + 100 µL antibiotic) control was additionally included. Minimum inhibitory concentration ($MIC_{90,}$ the concentration at which 90% of bacterial growth is inhibited) was determined using OD_{600}. Final

OD_{600} values were calculated using the average of the three wells (background OD_{600} removed). Percent (%) inhibition through microdilution was determined formulaically as % inhibition= 1-$(\frac{OD_{mutant\ D7}-OD_{mutant\ D0}}{OD_{wildtype\ D7}-OD_{wildtype\ D0}})$ × 100%. Inhibition was assessed every 24 hours from Day 0 to Day 7. If growth was still observed at the highest concentration, it was reported as > 8 µg/mL. This process was repeated for all mono-resistant BCG strains generated to determine the MIC_{90} (Figure 9). MIC determination was performed as a proof of concept to ensure that resistance-associated SNPs (including disputed mutations) could successfully confer resistance to WT BCG strains (Figure 9). Of note, broth microdilution is not used clinically to determine if a patient isolate is resistant to an antibiotic of interest[351]. Instead, the prescription of anti-tuberculous agents is influenced by critical concentrations and clinical breakpoints. Critical concentration (CC) is defined as the lowest concentration of antibiotic which can inhibit the growth of 99% of wildtype *M. tb* whereas clinical breakpoint is the concentration of antibiotic above critical concentration which can help determine if *M. tb* isolates are susceptible (treatment success likely) or resistant (treatment failure likely)[352]. Importantly, CCs vary depending on the type of culture media, time of reading, and MIC of wildtype bacterial strains[352].

2.6 Preparation of heteroresistant samples:

Mono-resistant BCG strains were combined in different ratios to determine the efficacy of resistance detection at 50%, 10% and 1% resistance on a wildtype background. In accordance with established literature RIF-R samples were prepared to test the limitations of GeneXpert MTB/RIF and GeneXpert Ultra[353,354].

2.7 Agar proportion method (APM):

WT BCG and RIF-R BCG (RpoB S450L) were cultured as described above with the following modification: BCG RIF-R was grown in 1 μg/mL RIF. Cultures were adjusted to 0.5 using the MacFarland standard, serially diluted (10^{-2} and 10^{-4}), and plated on 7H10 + OADC quadrant plates. Quadrants were divided into 1) antibiotic free, 2) 1 μg/mL LFX, 3) 1 μg/mL INH, and 4) 1 μg/mL RIF. Plates were incubated at 37°C for 3 weeks and enumerated. Resistance was defined as CFUs present on an antibiotic containing quadrant at a concentration ≥ 1% of the antibiotic free quadrant[355]. This experiment was performed in collaboration with Ori Solomon.

3. Results

DR-TB can be stratified into three categories: MDR-TB (defined as isolates resistant to both rifampin and isoniazid), pre-XDR TB (defined as isolates resistant to rifampin and/or isoniazid and any fluoroquinolone) and XDR-TB (defined as isolates resistant to rifampin and/or isoniazid, at least one fluroquinolone, and either bedaquiline or linezolid)[60,341]. For this chapter, I will discuss the validation of molecular and phenotypic assays for MDR-TB detection.

The pNIT:ET recombineering system recommends using a 70 bp oligo containing the K43R mutation in RpsL (known to confer streptomycin resistance) as a positive control for determining system efficacy (Figure 5b)[306,356]. Once this Strep-R strain was successfully generated in BCG, the utility of the mono-resistant BCG strains became readily apparent: the incorporation of resistance conferring SNPs could provide an easily accessible, affordable, and customizable quality control for clinical mycobacterial labs. For this we developed a panel of BCG strains resistant to first- and second-line antibiotics to be blindly tested against commonplace molecular and phenotypic assays. The MIC_{90} for all mono-resistant strains engineered was determined using microbroth dilution.

3.1 Molecular testing:

The GeneXpert MTB/RIF targets mutations in the rifampin-resistance determining region (RRDR) of *rpoB*, an 81-bp section of the gene (codons 426-452) accounting for up to 98% of rifampin-resistant *M. tb* strains[353,357]. Five overlapping molecular probes are utilized in a multiplex PCR; if a mutation is present in a region the probe targets (defined as A-E), the probe does not adequately bind and a blunted signal will be recorded[357]. If less than two molecular probes bind, the sample is returned as MTBC negative.

A mutation at codon 450 (S→L) within the RRDR is one of the most common SNPs associated with high-levels of rifampin resistance globally[341,358,359]. In the GeneXpert MTB/RIF assay, this SNP translates to a signal at 'Probe E', corresponding to codons 450-452 within the RRDR. The results of the GeneXpert MTB/RIF assay are outlined in Figure 7a-d. Samples included a) *M. avium hominissuis* b) wildtype BCG, c) BCG RIF-R (RpoB S450L) and d) BCG RIF-R (RpoB I491F). As expected, *M. avium hominissuis* returned the result 'MTB NOT DETECTED' indicating a failure of all RpoB probes (Ct=0.0), whereas WT BCG returned the result 'MTB DETECTED, Rif-resistance NOT DETECTED', in which all RpoB probes passed within two cycles of each other (Ct= 24.7-26.2). In the RpoB S450L strain probes A-D passed within two cycles of each other (MTB DETECTED) but probe E consistently returned a Ct value of 0.0 (Rif-resistance DETECTED). To determine the limitations of this quality control, live or heat-killed bacteria was added to the GeneXpert cartridge at increasing concentrations of bacteria (1000 bacteria/mL, 5000 bacteria/mL, 100 000 bacteria/mL). These parameters had no outcome on the validity of assay readout. Heat-killed RIF-R BCG was further validated by a third-party clinical lab in Puvirnituq, Nunavik (Quebec, Canada).

Similarly, the I491F mutation in RpoB accounts for 1-5% of all rifampin-resistant strains and has been reported globally[360]. This mutation is outside of the RRDR and as such is overlooked by current molecular tests endorsed by the WHO, including GeneXpert and GeneXpert Ultra[361,362]. Additionally, RpoB I491F cannot be detected by the Bactec Mycobacteria Growth Indicator Tube (MGIT), a validated phenotypic assay used in drug susceptibility testing, due to its association with low-level RIF-R resistance[351,363,364]. In 2009, this mutation accounted for 30% of MDR cases in Eswatini[360]. However, following the most recent survey of MDR-cases in 2017, this mutation accounted for ~56% of reported cases[365]. This is of particular concern for neighbouring countries such as South Africa and Mozambique which have some of the highest burdens of MDR/XDR-TB per capita[363]. Moreover, since 2022 DR-TB cases attributed to the I491F have been recorded in Botswana and Myanmar and studies have recently reported additional resistance-conferring mutations in Rv0678 (CFZ, BDQ-R) and KatG (INH-R) within *M. tb* strains already containing the RpoB I491F mutation[361,362,366,367]. As expected, the I491F mutation outside of the RRDR was reported as "MTB DETECTED, Rif resistance NOT DETECTED' following GeneXpert testing on this sample (Figure 7d).

The WHO endorses the GenoType MTBDR*plus* assay for rapid detection of MDR-TB[361]. This assay uses probes for 1) MTBC DNA and 2) common RIF- (*rpoB,* within the RRDR) and INH- (*katG, inhA*) resistance-conferring mutations[368–370]. Unlike GeneXpert, this assay accounts specifically for the KatG S315T mutation, responsible for 23.7% of INH-resistant isolates globally, and four *inhA* promoter mutations (T-8C, T-8A, C-15T, and A-16G)[359,371]. To broaden the utility of this panel beyond RIF mono-resistant strains, we also developed an INH resistant quality control strain as *katG* and *inhA* are well characterized targets of this first line drug. Like GeneXpert, this assay uses probes specific for MTBC DNA, as well as probes specific to common RIF- (*rpoB,*

within the RRDR) and INH- (*katG, inhA*) resistance-conferring mutations[372,368]. Resistance prediction is determined through binding patterns of both wildtype and mutant probes. If one or more wildtype probe is absent in *rpoB, katG* or *inhA*, with or without the presence of other mutant probes, the sample is 'resistant'[372,368]. However, these probes are not designed to capture mutations outside of these regions. In 2018, when this work was first initiated, a non-canonical deletion in amino acid 428 in KatG was identified and determined to confer high-level INH resistance[373] . To broaden the utility of recombinant BCG beyond RIF mono-resistant strains and GeneXpert testing, we incorporated this novel SNP into BCG, as a control for MDR-TB detection. This panel of RIF-R and INH-R strains were validated in collaboration with the Public Health Ontario Laboratories (PHOL). The MTBDR*plus* assay was run against 10 strains, processed as part of routine clinical testing. As expected, the WT BCG strains (BCG Russia; BCG Pasteur) were correctly detected as pan-susceptible and the NTM control strains (MAP; RpsL K43R MAP) were correctly identified as non-MTBC. For canonical mutations, such as RpoB S450L, RIF-R was clearly detected (failure to amplify a WT probe; successfully amplified the mutant probe). In contrast, when evaluating non-canonical mutations -such as RpoB I491F and KatG del428AA- both strains were called as susceptible to RIF and INH respectively (Figure 8).

Beyond monoresistance, we also evaluated the efficacy of currently employed molecular tests in the detection of mixed (heteroresistant) infections, defined as a seemingly homogenous sample that contains multiple bacterial populations[90]. As previously published, the GeneXpert MTB/RIF assay was unable to detect the presence of RIF-R populations $\leq$ 50%[353,354]. It was only when the sample population was increased to 60% that RIF-R was adequately detected. Since its endorsement by the WHO in 2010, a second iteration of GeneXpert (GeneXpert Ultra) was developed with higher sensitivity to mycobacterial DNA and a lower limit of detection[353]. When

the same samples were run using the GeneXpert Ultra, the detection threshold decreased to ≥ 10% (Table 2). However, when the minority population was reduced to 5%, RIF resistance could not be detected (Table 2).

3.2 Phenotypic testing:

3.2.1 Broth microdilution

RIF resistance:

The MIC_{90} of WT BCG was determined to be ~0.03 µg/mL. Comparatively, when assessed by pDST, the S450L RpoB mutation correlated to an MIC_{90} of > 8 µg/mL, the maximum concentration tested (Figure 9a, Table 1). At 8 µg/mL, ~20% inhibition was observed by Day 7. Similarly, the MIC_{90} of the I491F RpoB strain was observed to be ~8 µg/mL. When analyzing the data further, it can be observed that although MIC_{90} is not reached, by 0.5 µg/mL RIF, 50% of the bacteria are inhibited at this concentration (MIC_{50}), indicating that this mutation likely confers intermediate rather than high-level resistance (Figure 9a, Table 1). Notably, the definition of resistant or susceptible isolates depend on type of assay, type of media (ex: MGIT versus 7H9 complete), and readouts used[351,352,374].

INH resistance:

As previously described, the non-canonical KatG del428AA was associated with high levels of INH resistance. Our results correlated with this finding as the MIC_{90} of our engineered strain exceeded the maximal concentration tested (MIC_{90} > 8 µg/mL INH)(Figure 9b). At concentrations at or below 8 µg/mL an inhibition of ~20% was observed. In comparison, the WT BCG control had an MIC_{90} of 0.25 µg/mL INH. The dual-SNP BCG strain (INH-R + FQ-R) was not evaluated using microbroth dilution for the MIC_{90} using either INH or moxifloxacin (MFX).

Second-line antibiotic resistance:

In 2022, the WHO updated its treatment recommendations for DR-TB[375]. The current frontline regimen for MDR-TB is 6-month treatment with bedaquiline (BDQ), pretomanid, linezolid, and moxifloxacin (fluoroquinolones, FQ), known as BPaLM[375]. Previously, ≥ 9 months of treatment was recommended for MDR-TB[348,376]. This included fluoroquinolones (FQ), bedaquiline (BDQ) and linezolid as front-line agents (known as group A drugs) and at least one group B drug (i.e. clofazimine and cycloserine or terizidone)[348,376]. Of the current regimen of MDR-TB drugs, the D94G mutation in GyrA has been associated with high levels of fluroquinolone resistance such as moxifloxacin (MFX), levofloxacin (LFX), and ofloxacin (OFX). Additionally an S63R mutation in Rv0678 has been associated with low-level BDQ and CFZ resistance[359,377,378]. Using the preceding logic for the development of quality controls for molecular testing, we engineered strains containing these mutations and subjected them to microbroth dilutions. The S63R Rv0678 had an MIC_{90} of 1 μg/mL for both CFZ and BDQ, showing a slight increase from the WT BCG MIC_{90} of 0.25 μg/mL for both CFZ and BDQ at the same timepoint (Figure 9c,d). The D94G GyrA mono-resistant strain had an MIC_{90} of ~4 μg/mL (compared to 0.125 μg/mL of the WT BCG strain)(Figure 9e).

3.2.2 Agar proportion method (APM) of heteroresistant mixtures

Samples containing minority populations of RIF resistant BCG (RpoB S450L) were tested using APM and enumerated (Table 2). Resistance was observed in all samples tested, including a minority population of 1%.

4. Discussion

Effectiveness of TB treatment hinges on accurate diagnosis. Without treatment, even drug susceptible TB has a mortality rate ranging from ~20% (culture positive, smear negative) to up to ~70% (smear-positive pulmonary TB)[60]. Though it is crucial to have patients started on antibiotic

therapy as quickly as possible, it is also necessary for this therapy to be correct. As of 2023, there 16 vaccines, 50 diagnostic tests, and 28 drugs under development for the prevention, detection, and treatment of TB[379]. However, these current and developing technologies lack adequate quality controls. If being offered clinically, the analytical limitations of these diagnostics must be assessed. We have developed a panel of mono-resistant BCG strains that can be applied to phenotypic and genotypic diagnostic tests and can be adapted per clinical needs/WHO recommendations. The utilization of live, attenuated strains of BCG as quality controls mitigates technical challenges associated with *M. tb* diagnostics such as the requirement of a CL3 and training of technical staff. Additionally, BCG has a well-established safety profile, being given to over 100 million newborns per annum, and minimizes infection risk to laboratory personnel[94]. The utility of this panel has also been independently confirmed in clinical and outreach settings globally and incorporated into routine use.

BCG strains in which resistance-associated SNPs were incorporated, mimicked resistance profiles seen in their *M. tb* counterparts. With the rising rates of DR-TB globally, the impact of heteroresistant infections, defined as a single sample containing both wildtype (susceptible) and resistant bacterial populations, has become of increasing importance[90,340]. Previous studies have shown that up to 20% of tested clinical isolates contain these mixed populations, though this varies globally[380–383]. Accordingly, heteroresistant populations may be detrimental to patient care. Since the 1960s, the reference method for detecting DR-TB has been the agar proportion method (APM)[355]. This method is founded on the premise that if more than 1% of *M. tb* grows in the presence of the antibiotic of interest (ex: RIF), treatment with that antibiotic is unlikely to be successful[355]. Notably, this 1% is in contrast with other sectors of clinical microbiology laboratories in which 0.1% bacterial growth is indicative of resistance[86,384]. As our panel is

composed of live, attenuated BCG strains, we assessed the robustness of molecular and phenotypic assays in the detection of minority populations. Our results show that phenotypic testing remains the 'gold standard' in clinical diagnostics, with the ability to detect rifampin resistance in populations as low as 1%, though minority populations below this proportion were not assessed. Comparatively, when testing with GeneXpert and GeneXpert Ultra, the limit of detections increased to 60% and 5% respectively. The clinical consequence of this discrepancy has yet to be fully understood.

With the transition to full-genome interrogation in clinical diagnostics (via WGS), this panel also proves its utility in establishing the limit of detection using this technique, particularly in the differentiation between multiple bacterial strains within a single sample. WGS offers the capacity to detect mutations beyond the regions restricted by LPAs such as GeneXpert and MTBDR*plus;* however, without the determination of a reliable limit of detection, the discrepancy between phenotypic and genotypic testing remains. A key obstacle in the current landscape of WGS is a lack of standardization; the application of mono-resistant BCG strains at varying concentrations may highlight potential pitfalls in bioinformatic pipelines from variant detection (identification) to the generation of resistance reports (communication).

To summarize, this chapter is founded on the concept of quality controls in *M. tb* diagnostics. The pNIT:ET recombineering system was optimized and used to generate a panel of live, mono-resistant BCG strains. From this we validated their use in standard phenotypic and molecular assays as quality controls and in several laboratories (nationally and internationally). The use of this panel was then integrated into standard operating procedures. Subsequently, the BCG panel was used to reaffirm the 'gold standard' of phenotypic testing and determine the limitations of GeneXpert (and GeneXpert Ultra), in the detection of heteroresistant infections. This

is particularly important as GeneXpert is commonly used in many high burden TB settings (in the absence of quality controls), being restricted to detection of mutations within the RRDR, and having an LOD of 60% for heteroresistant infections[385,386]. Additionally, as of 2021, the WHO has endorsed the 'GeneXpert MTB/XDR' assay which promises rapid detection of resistance to isoniazid, fluroquinolones, ethionamide, and second line injectable drugs (SLIDs) but not bedaquiline or clofazimine[387]. Though we did not utilize this molecular test, the design of the GeneXpert XDR is conserved: our panel can be easily incorporated as controls for this assay in the detection of mono- or heteroresistant infections.

Ultimately, the implementation of a panel of mono-resistant BCG strains in TB diagnostics can provide greater assurance that a laboratory can confidently detect DR strains of *M. tb,* regardless of the proportion of resistant bacilli within a single isolate. This enables their clinical and public health counterparts to promptly- and correctly- initiate appropriate health interventions. The introduction of new and effective diagnostics is essential for the control and eradication of TB cases worldwide. Despite this, developing quality controls to address non-canonical resistance, and heteroresistance with these diagnostic tools is not prioritized by the WHO, manufacturers, or regulators. Clinical and technical gaps remain: how can new assays be validated? What is the limit of detection? Is this limit of detection clinically relevant? How will a lack of identification affect patient care? Without adequate diagnostics, individual care and public health may be compromised: not only is the patient exposed to the negative side effects of ineffective antibiotics, DR-TB may be selected for at the population level due to inadequate treatment. This may be the most apparent consequence of using assays without known limitations, and instead assuming they will be 'good enough'. Our panel seeks to provide a starting point to address current knowledge gaps and the tools to ensure the proper and immediate patient care. In 2015, the WHO developed

the END TB strategy; a commitment to reduce TB deaths by 95% and TB cases by 90% by 2035[60,388]. Our lab hopes to contribute to these goals by assisting in the laboratory detection of TB and DR-TB, so that patients can receive the appropriate care.

5. Figures

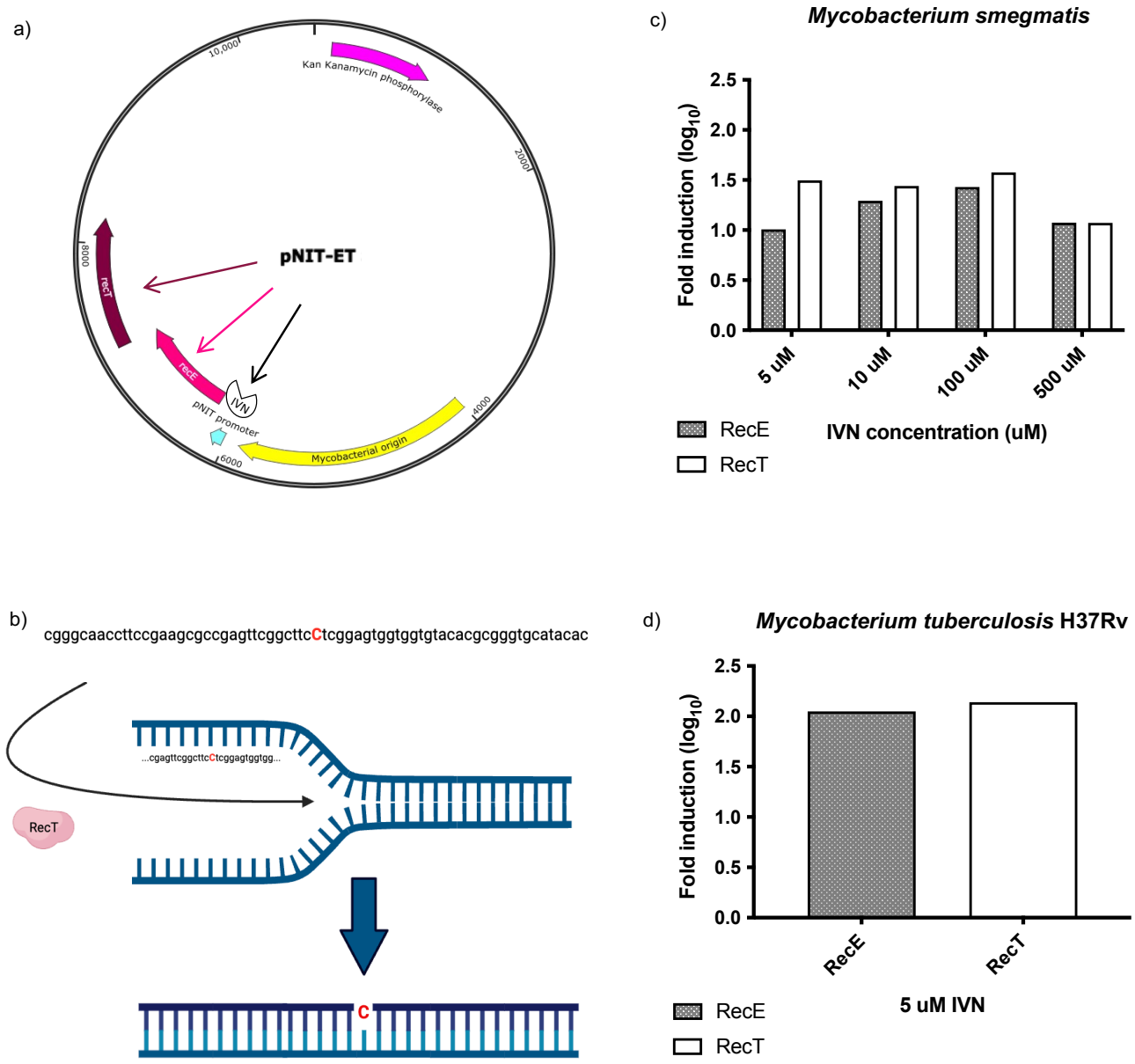

Figure 5. Validation of the pNIT:ET recombineering system.

a) The pNIT:ET plasmid. Expression of RecE and RecT under control of a nitrile promoter, induced by isovaleronitrile (IVN). **b)** Oligo-mediated recombineering used to incorporate streptomycin-conferring mutation (RpsL K43R). ssDNA integration depends on induction and expression of the RecT enzyme from pNIT:ET plasmid. **c)** Fold induction (log_{10}) of RecE and

RecT following stimulation with increasing amounts of IVN (5µM-100 µM; T= 2.5 hour) in *M. smegmatis* culture. **d)** Fold induction (log_{10}) of RecE and RecT following stimulation with 5 µM IVN (T= 16-24 hours) in *M. tuberculosis* H37Rv culture.

a) *Mycobacterium bovis* BCG RpoB S450L

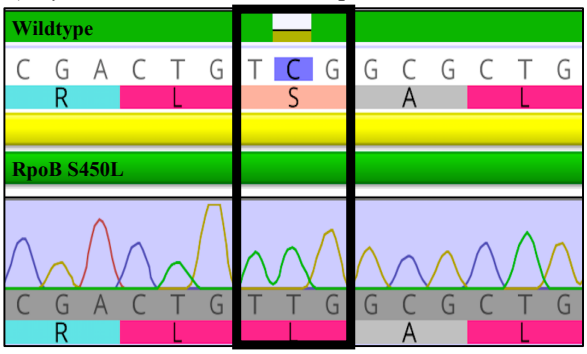

b) *Mycobacterium bovis* BCG RpoB I491F

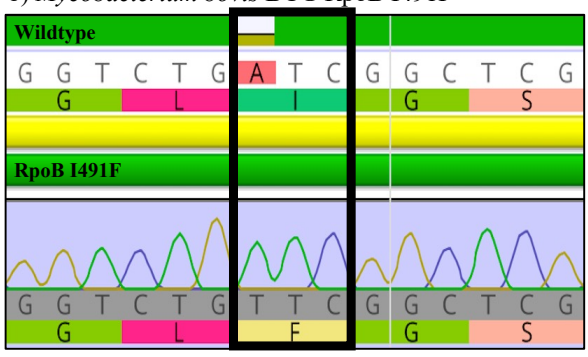

Figure 6. Dideoxynucleotide sequencing electropherograms.

Geneious Prime (v. 2019.2) alignments of wildtype *rpoB* gene; *M. bovis* BCG sequence (top) compared to engineered mutant (below). **a)** *M. bovis* BCG S450L strain. Black box highlights amino acid position 450; conversion of serine (S) to leucine (L). **b)** *M. bovis* BCG I491F strain. Black box highlights amino acid position 491; conversion of isoleucine (I) to phenylalanine (F).

a) *Mycobacterium avium hominissuis*

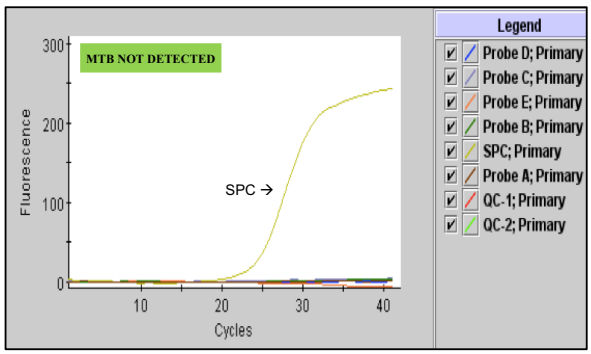

b) Wild-type *Mycobacterium bovis* BCG

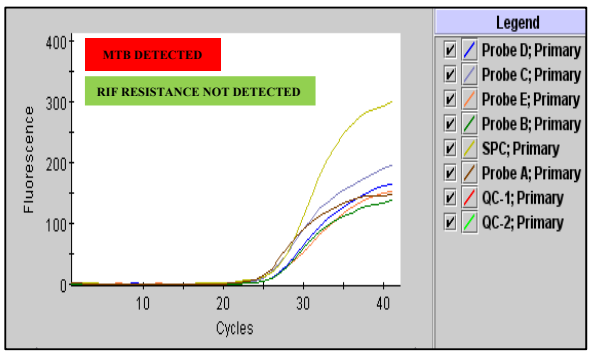

c) *Mycobacterium bovis* BCG RpoB S450L

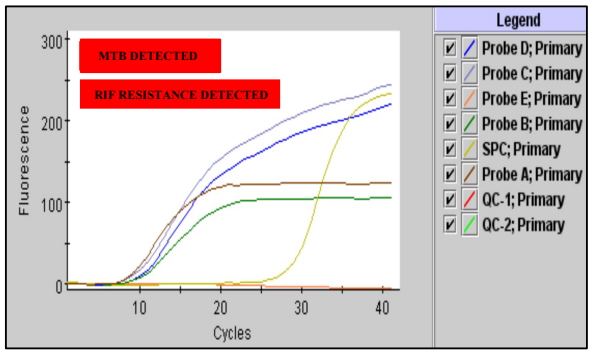

d) *Mycobacterium bovis* BCG RpoB I491F

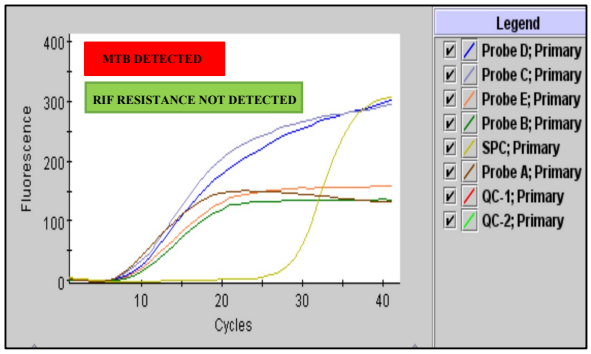

Figure 7. GeneXpert MTB/RIF output.

Probe amplification plots of *M. avium hominisuiss,* wildtype *M. bovis* BCG, and rifampin-resistant mutants. A lack of probe amplification infers *rpoB* mutation and that sample is resistant. Coverage of probes: A → codons 429-430 (brown), B → codons 432-436 (green), C → codon 441 (purple), D → codon 445 (blue), E→ codons 450 and 452 (orange). SPC (yellow) acts as sample processing control. **a)** *M. avium hominisuiss* (MAH) sample (non-tuberculous mycobacterium control). No *rpoB* probe amplification; SPC positive (sample and readout validated). **b)** Wildtype *M. bovis* BCG. Rifampin-sensitive *M. tuberculosis* complex positive control. Probe A-E positive, SPC positive. Final readout: MTB detected, RIF resistance not detected. **c)** *M. bovis* BCG RpoB S450L. Probe A-D positive; probe E negative (Ct= 0). Final readout: MTB detected, RIF resistance detected. **d)** *M. bovis* BCG RpoB I491F. Probe A-E positive. Final readout: MTB detected, RIF

resistance not detected. Failure to detect due to position of mutation as codon 491 is outside of rifampin-resistance determining region (RRDR).

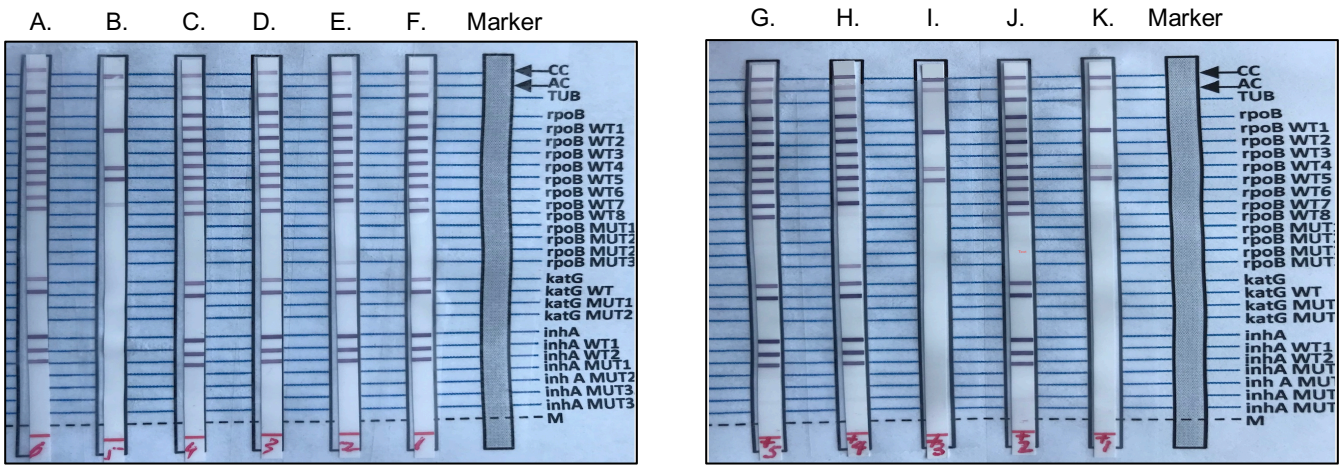

Figure 8. MTBDR*plus* output.

Extracted DNA from mono-resistant *M. bovis* BCG panel sent to Public Health Ontario Laboratory (PHOL) and processed as part of routine clinical testing (blinded to technician). Probe amplification banding patterns indicate presence or absence of resistance mutations in *rpoB, katG,* and *inhA*. Species tested: A→ BCG Russia Rv0678c S63R (BDQ/CFZ-R), B → *M. avium paratuberculosis* (MAP) RpsL K43R, C → BCG Russia KatG AAdel428, D → BCG Russia RpoB I491F, E → BCG Russia S450L, F → *M. tuberculosis* H37Ra, G → wildtype BCG Pasteur, H → BCG Pasteur S450L, I → WT MAP, J → WT BCG Russia, K → MAP RpsL K43R. All WT BCG returned as drug-sensitive, TB probe positive (TUB). All MAP strains returned as TUB negative. Both BCG Russia S450L strains tested negative for one wildtype probe (WT8), and positive for mutant *rpoB* probe (MUT3) (RIF-R positive). BCG RpoB I491F and BCG KatG AAdel428 returned as RIF- and INH-sensitive (respectively) despite resistance profiles.

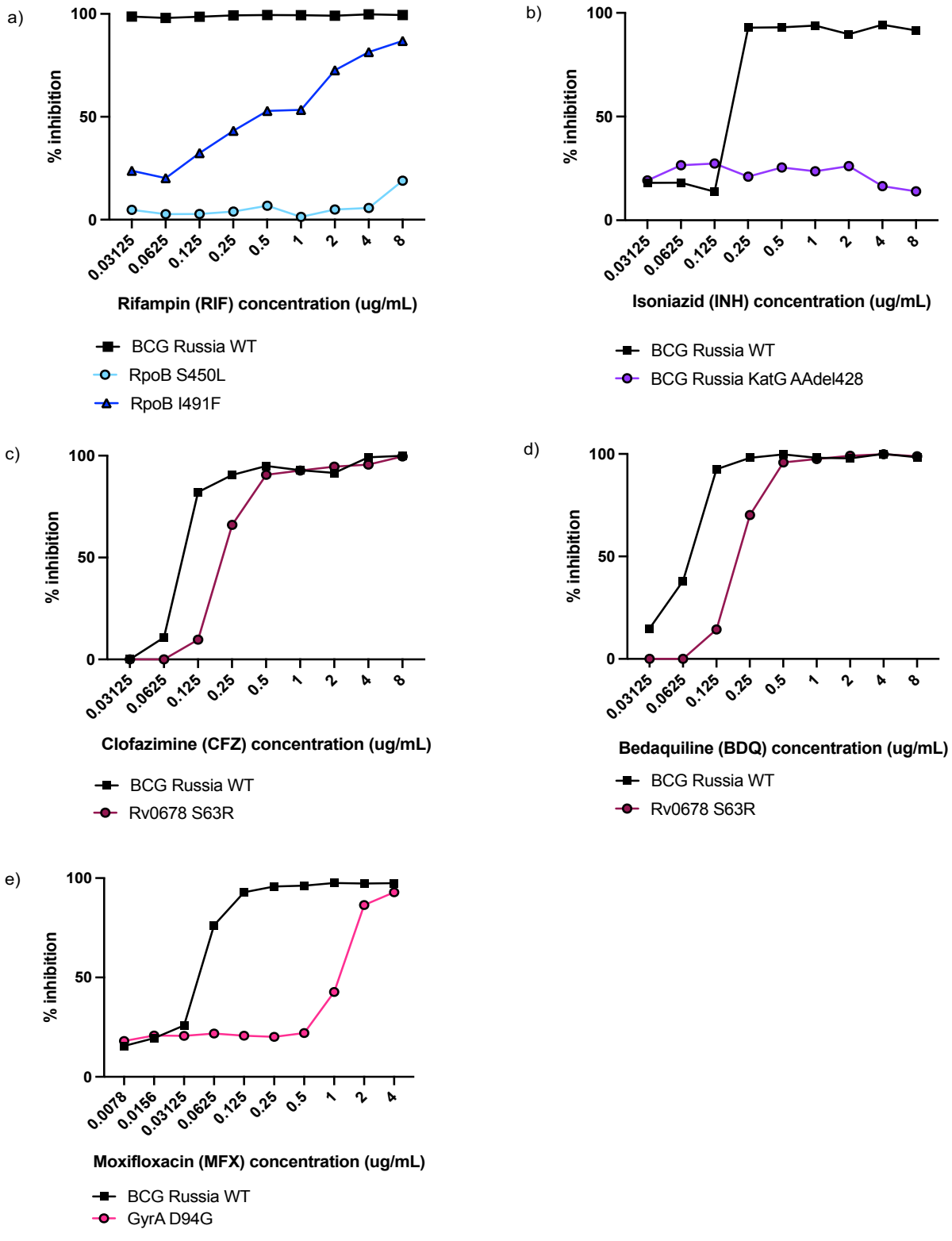
a)
100
50
0
% inhibition
0.03125
0.0625
0.125
0.25
0.5
1
2
4
8
Rifampin (RIF) concentration (ug/mL)
BCG Russia WT
RpoB S450L
RpoB I491F
b)
100
50
0
% inhibition
0.03125
0.0625
0.125
0.25
0.5
1
2
4
8
Isoniazid (INH) concentration (ug/mL)
BCG Russia WT
BCG Russia KatG AAdel428
c)
100
50
0
% inhibition
0.03125
0.0625
0.125
0.25
0.5
1
2
4
8
Clofazimine (CFZ) concentration (ug/mL)
BCG Russia WT
Rv0678 S63R
d)
100
50
0
% inhibition
0.03125
0.0625
0.125
0.25
0.5
1
2
4
8
Bedaquiline (BDQ) concentration (ug/mL)
BCG Russia WT
Rv0678 S63R
e)
100
50
0
% inhibition
0.0078
0.0156
0.03125
0.0625
0.125
0.25
0.5
1
2
4
Moxifloxacin (MFX) concentration (ug/mL)
BCG Russia WT
GyrA D94G

Figure 9. Microbroth dilution curves of engineered BCG strains (MIC_{90}).

MIC_{90} determination by addition of 100 µL antibiotic to 100 µL bacteria in clear 96-well plate. WT BCG Russia control and 7H9 complete media control added to each plate, in tandem with resistant strains (performed in triplicate). % inhibition measured using $OD_{600.}$ RIF→ rifampin, INH → isoniazid, CFZ → clofazimine, BDQ → bedaquiline, MFX → moxifloxacin. Calculation: % inhibition= 1- $\frac{(\mathrm{OD}mutantD7-\mathrm{OD}mutant\mathrm{D0})}{(\mathrm{OD}wildtypeD7-\mathrm{OD}wildtypeD0)}$ x 100%

a) RIF-resistance of WT BCG Russia, RpoB S450L, and RpoB I491F strains. MIC_{90} of WT BCG <0.032 µg/mL. MIC_{90} of RpoB S450L ≥ 8 µg/mL. MIC_{90} of RpoB I491F ~8 µg/mL. Notably, RpoB I491F shows more intermediate resistance compared to S450L; MIC_{50} achieved at ~0.5 µg/mL. **b)** INH-resistance of WT BCG Russia and KatG AAdel428 strains. MIC_{90} of WT BCG ~0.25 µg/mL; MIC_{90} KatG AAdel428 ≥ 8 µg/mL (high-level INH resistance). **c)** CFZ-resistance of WT BCG Russia and Rv0678c S63R strains. MIC_{90} of WT BCG ~0.25 µg/mL; MIC_{90} Rv0678c S63R ~1 µg/mL (low-level CFZ resistance). **d)** BDQ-resistance of WT BCG Russia and Rv0678c S63R strains. MIC_{90} of WT BCG ~0.25 µg/mL; MIC_{90} Rv0678c S63R ~1 µg/mL (low-level CFZ resistance). **e)** MFX-resistance of WT BCG Russia and GyrA D94G strains. MIC_{90} of WT BCG ~0.125 µg/mL; MIC_{90} GyrA D94G ~4 µg/mL.

6. Tables

Strain	Mutation	Conferred Resistance	MIC 90 (µg/mL)
***M. bovis* BCG**	-	Pan-susceptible	-
***M. bovis* BCG RIF-R**	RpoB S450L	RIF (within RRDR)	≥8
***M. bovis* BCG RIF-R**	RpoB I491F	RIF (outside RRDR)	≥8
***M. bovis* BCG INH-R**	KatG AAdel428	INH	≥8
***M. bovis* BCG FQ-R**	GyrA D94G	FQ (MFX)	4
***M. bovis* BCG CFZ/BDQ-R**	Rv0678c S63R	CFZ/BDQ	1; 1
***M. bovis* BCG STR-R**	RpsL K43R	STR	≥8
***M. bovis* BCG INH-R/FQ-R**	KatG S315T/ GyrA D94G	INH/FQ	-

Table 1. Bacterial strains utilized in molecular and phenotypic testing.

RIF= rifampin, RRDR= rifampin resistance determining region, INH= isoniazid, FQ= fluroquinolone, CFZ= clofazimine, BDQ= bedaquiline, STR= streptomycin. Adapted from Danchuk et al., 2020; Danchuk, Solomon et al., 2024.

Strain proportions (R:S)	Phenotypic RIF-susceptibility testing (>1%=R)	Molecular RIF Resistance Prediction	
	APM	**GeneXpert MTB/RIF**	**GeneXpert Ultra**
0:100	Susceptible	Susceptible	Susceptible
1:99	Resistant	-	-
5:95	-	-	Susceptible
10:90	Resistant	Susceptible	Resistant
50:50	Resistant	Susceptible	Resistant
60:40	Resistant	Resistant	Resistant
100:0	Resistant	Resistant	Resistant

Table 2. Phenotypic and molecular detection of RIF-heteroresistance.

‘Resistant’ defined as ≥ 1% growth in antibiotic media compared to antibiotic free media. -: DST platform not tested at this proportion. RIF= rifampin; APM= agar proportion method. Adapted from Danchuk, Solomon et al., 2024.

CHAPTER III: USE OF MYCOBACTERIAL RECOMBINEERING TO CHARACTERIZE PRODUCTION OF MPT70 AND MPT83 BY NATURAL AND ENGINEERED VARIANTS OF THE MTBC

1. Introduction

The MTBCs are more than 99.9% conserved at the nucleotide level. Despite this, differences in virulence, disease presentation, and host range between subspecies have been well-established since the late 1800s[16,129]. *M. tb, M. bovis* and *M. orygis,* are differentiated by lineage-specific SNPs and large polymorphisms termed 'regions of difference'[172,174,184,389]. Unlike other bacterial species, this variation is not mediated by the acquisition of new genes; instead the MTBCs lack the molecular machinery required for horizontal gene transfer (HGT) and possess reduced genomes compared to the most recent common ancestor (MRCA)[390,391]. As such, differential infection outcome and host preference between species has been a key area of research.

The prior chapter explored the use of the pNIT:ET recombineering system for the introduction of resistance-associated SNPs via the incorporation of a modified single-stranded oligomer (ssDNA). However, the generation of knockout strains require the recombination of three delivery vectors (constructed using PCR products) into a final 'destination vector'. This vector consists of a selectable resistance cassette flanked by 500 bp of homology upstream and downstream of the GOI (total size ~3000 bp) (Figure 4). In theory, gene deletions can be successfully conferred using allelic exchange between the modified construct and the genomic GOI (homologous recombination). Initially we sought to develop to develop deletion (knockout) strains of the putative virulence factors MPT70 and MPT83 in *M. bovis* BCG, *M. bovis,* and *M. orygis*. However, due to the complexity of this process, the size of the gene insert, and relatively low homologous recombination rates in mycobacteria, the generation of a single gene knockout is often unachievable. To determine if this was a species, or gene-specific defect, we incorporated

the pNIT:ET system into several mycobacterial species (*M. smegmatis, M. bovis* BCG Russia, and *M. tb*) and incorporated constructs targeting multiple non-essential genes (ex: *sigK, rskA,* and *lppZ*). Additionally, increased doses of IVN had no significant impact on the expression levels of RecE and RecT nor the efficacy of this exchange. Regardless of modifications, deletion strains could not be generated.

To remedy this, we implemented and optimized the "oligonucleotide-mediated recombineering followed by Bxb1 integrase targeting" (ORBIT) system. Following optimization in the non-pathogenic *M. smegmatis,* we implemented the ORBIT recombineering system in slow growing MTBCs (*M. tb, M. bovis, M. bovis* BCG, and *M. orygis*) and successfully generated knockouts for MPT70, MPT83, and the canonical virulence factor ESAT-6. We sought to characterize the properties of these isogenic strains at the *in vitro* and *ex vivo* levels to determine how the loss of two major antigenic proteins would impact bacterial pathogenesis. Subsequently, these strains were employed *in vivo* to evaluate the role of MPT70 and/or MPT83 in the infection outcome of a murine model.

2. Methods

2.1 Bacterial strains:

All bacterial strains used are listed in Table 3.

2.2 Oligo-mediated recombineering followed by Bxb1 integrase targeting (ORBIT)

The ORBIT recombineering system is described in detail in Figure 10. ORBIT recombineering requires 1) the expression of RecT and Bxb1 integrase, 2) a gene specific oligomer (~160-180 bp), and 3) a non-replicative 'payload plasmid' containing a selectable resistance cassette (such as hygromycin or zeocin). The ORBIT plasmid (pKM444) is an exogenous plasmid containing RecT (an annealase) and Bxb1 integrase under a tetracycline inducible promoter. To

facilitate the creation of a gene deletion the following occurs: first, co-expression of RecT and Bxb1 integrase is induced following stimulation with anhydrotetracycline (AtC). Second, the targeted oligo (containing an *attP* recombination site) and the payload plasmid (containing an *attB* recombination site) are co-electroporated. RecT pairs homologous regions of oligomer to the lagging strand of DNA during replication. This results in the alignment of the *attP* site (oligo) in place of the target GOI. In tandem, Bxb1 integrase recombines *attP* and *attB* sites, replacing the GOI with the selectable resistance cassette. ORBIT reduces the introduction of synthetic DNA (i.e. the oligomer) into a single step and bypasses the need for double-stranded DNA (dsDNA) products, significantly improving the efficacy of producing gene deletions.

2.3 Production of isogenic strains via ORBIT recombineering system:

Strains containing targeted gene-deletions were generated using the ORBIT system as described by Sassetti et al. with modifications[299]. Briefly, pKM444-KanR (plasmid containing RecT and Bxb1) was electroporated into log-phase *M. bovis* Ravenel and *M. orygis* 51145 cultures; induction of Bxb1 and RecT was confirmed following exposure to 5 µg/mL anhydrotetracycline (T= 16-24 hours). A 170 bp oligomer was developed containing an *attP* site and 60 bp homologous regions of our genes of interest (*esxA, mpt70_mpt83, mpt70, mpt83*). The oligo was then electroporated alongside either pKM464-HygR or pKM496-ZeoR into *M. bovis* or *M. orygis* cultures containing the pKM444-KanR plasmid (*M. bovis* ORBIT, *M orygis* ORBIT). Cultures were recovered for 6 days in 7H9 complete media following electroporation and incubated on 7H10 complete plates (defined as 7H10 + oleic acid, albumin, catalase, and dextrose (OADC)) containing antibiotics up to 6 weeks at 37□C. Oligomers used in the development of these strains are described in Table 4.

2.4 Deletion strain validation:

All strains generated for downstream studies were validated using an in-house 'knockout pipeline'. Colonies were screened using conventional PCR and confirmed with Sanger sequencing. Junction primers were designed to target the integration site of pKM464 or pKM496. Primers spanned from 150 base pairs (bp) upstream of the GOI into the *oriE* site and from the resistance cassette (Hyg-R or Zeo-R) to 150 bp downstream of the GOI. A qRT-PCR was run to assess expression levels of GOIs compared to a WT positive control and 'no reverse transcriptase' negative controls to determine background detection. Viable candidates were then confirmed using WGS (Illumina NovaSeq 6000, Genome Quebec). Efficacy of knockout varied depending on target GOI. In total, 8 gene-specific knockout strains were generated using the ORBIT recombineering system (4 in *M. bovis* ORBIT, 4 in *M. orygis* ORBIT). Engineered strains were sequenced using Illumina NovaSeq 6000 (Genome Quebec) to confirm fidelity of gene deletions. Sequencing of deletion strains available at NCBI under BioProject PRJNA1141970.

2.5 Proteomic analysis:

Cultures used in secretomic analysis are outlined in Table 3. Cultures were grown in 15 mL 7H9 complete media to mid-log phase (OD_{600}= 0.8-1) and passaged in 30 mL of Sauton minimal media. Cultures were again grown to an OD_{600} of ~0.8 and passaged an additional two times in 30 mL Sauton media. Cultures were centrifuged at 3980 rpm for 15 minutes. Supernatant was filtered twice through 0.22 □M filters and concentrated using centrifugal filter units (Amicon Ultra-15 Centrifugal Unit, 3 kDa cutoff) by spinning at 3980 rpm for 2-3 hours to a final volume of 1 mL. Protein concentration was determined using the Qubit Protein BR Assay per manufacturer instructions. Proteomic analysis was performed by the Proteomic and Molecular Analysis Platform at the Research Institute of the McGill University Health Centre (Lorne Taylor). For each sample,

proteins were loaded onto a single stacking gel band to remove lipids, detergents, and salts. The gel band was reduced with DTT, alkylated with iodoacetic acid, and digested with trypsin. Extracted peptides were re-solubilized in 0.1% aqueous formic acid and loaded onto a Thermo Acclaim Pepmap (Thermo, 75□M ID X 2cm C18 3μM beads) precolumn and then onto an Acclaim Pepmap Easyspray (Thermo, 75□M X 15cm with 2□M C18 beads) analytical column separation using a Dionex Ultimate 3000 □HPLC at 250 nl/min with a gradient of 2-35% organic (0.1% formic acid in acetonitrile) over 3 hours. Peptides were analyzed using a Thermo Orbitrap Fusion mass spectrometer operating at 120,000 resolution (FWHM in MS1) with HCD sequencing (15,000 resolution) at top speed for all peptides with a charge of 2+ or greater. The raw data were converted into *.mgf format (Mascot generic format) for searching using the Mascot 2.6.2 search engine (Matrix Science) against a combined protein sequence database of *M. tb* H37Rv, *M. bovis* AF2122, and *M. orygis* 51145 and a database of common contaminant proteins. The database search results were loaded onto Scaffold Q+ Scaffold_5.2.1 (Proteome Sciences) for statistical treatment and data visualization (ANOVA Benjamini-Hochberg correction, $p < 0.05$; minimal spectra value= 0.5). Samples were prepared in technical triplicate unless otherwise stated. Heatmaps were created using the Z-score of normalized spectra (dominant proteins= top 20) and visualized using GraphPad Prism 10.2.3. Z score defined as: $Z = \frac{(\text{normalized spectra} - \text{mean of population})}{\text{standard deviation of population}}$. Differential expression of proteins was determined using T-test without correction; minimal spectra value= 0.5 ($p < 0.05$).

2.6 Macrophage studies

Bone marrow derived macrophages (BMDMs) were obtained as described by Mendonca et al, with modifications[392]. The long bones (femur and tibia) of uninfected C57BL/6 mice were

cut open at the epiphysis and suspended in R10 (RMPI-1640 supplemented with 10% heat-inactivated fetal bovine serum (FBS), 1% HEPES and 1% non-essential amino acids (NEAA)). Bone marrow was treated using red blood cell lysis buffer, adjusted to a final concentration of $4x10^5$ cells per mL and treated with 1% macrophage colony stimulating factor (M-CSF). 10 mL of whole bone marrow was cultured in a non-tissue culture treated petri dish at 37□C, 5% CO_2. After 72 hours, cells were supplemented with 5 mL R10 containing 1% M-CSF and incubated for a total of 7 days. On day 7 cells were washed with PBS to remove R10 media and non-adherent cells; remaining cells were detached using CellStripper™ and adjusted to $2x10^5$ cells per well in a 96 well plate.

2.6.1 *Ex vivo* infection

Macrophages were infected with isogenic strains at an multiplicity of infection of 5:1 (MOI; bacteria:BMDMs). Briefly, cultures were grown to log phase (OD_{600}= 0.8-1), pelleted, and resuspended in 1 mL 7H9 complete media. Remaining clumps were removed by passing culture through 22G, 25G and 26G needles and adjusted to a final volume of 15 mL R10 media. Subsequently, the culture was filtered using a 5 µM filter and adjusted to a final OD_{600}=0.1 (corresponding to ~$1x10^7$ CFU). 100µL of bacteria was added to 100 µL BMDMs and incubated at 37□C, 5% CO_2 for 4, 24, 48, and 72 hours. At 4 hours, plates were washed with R10 to remove all remaining extracellular bacteria from macrophages. At 4, 24, 48, and 72 hours, cells were lysed with 1% PBS-Triton X-100, serially diluted (10^{-2}, 10^{-3}, 10^{-4}) and plated on 7H10 OADC agar (100 µL). Plates were incubated for 4-6 weeks at 37□C to determine bacterial burden. Strains used in *ex vivo* infection studies are described in Table 3. Bacterial uptake calculated as $\frac{CFU_{T=4}}{CFU_{T=0}}$ x 100%. Bacterial burden calculated relative to T= 4-hour timepoint (relative ratio; $\frac{CFU_{T=X}}{CFU_{T=4}}$).

3. Results

The key objective of this chapter was to generate knockout strains using mycobacterial recombineering, and subsequently characterize these strains using *in vitro* and *ex vivo* assays. In both *M. bovis* and *M. orygis* independent mutation events in RskA (regulator) have resulted in the constitutive expression of MPT70, and the conserved homolog MPT83[103,184,186]. As described previously, in *M. bovis* this was due to two missense mutations (G107D, G184E) whereas in *M. orygis,* differential RskA activity was the result of a readthrough mutation (stop → S; X233S)[46,184,185]. The notion that MPT70, could be a virulence factor has been considered since it was first definitively identified in 1984, largely based on this differential expression between *M. tb* and *M. bovis*[101]. However efforts to characterize this protein have been limited- perhaps because a role during *M. tb* infection has not been identified[393,394]. We developed solo and *en bloc* deletion strains of *mpt70, mpt83* and *dipZ* (the gene between the two effectors) in both cattle-associated strains to determine how alterations to the expression level of two antigenic proteins may change *in vitro* phenotypes and *ex vivo* infection. Deletion of a canonical virulence factor (ESAT-6) was also included as a positive control for both subspecies[250]. Additionally, rather than comparing wildtype strains of *M. bovis* Ravenel and *M. orygis* 51145 to the generated mutants, all experiments in this chapter compared ORBIT containing strains (i.e. *M. bovis* ORBIT and *M. orygis* ORBIT) to the deletion strains (i.e. *M. bovis Δmpt70_mpt83, M. orygis Δmpt70_mpt83,* etc.). This was done to ensure the effect of the deletion strains could be attributed to the gene of interest and not caused by laboratory manipulation.

3.1 *M. bovis* and *M. orygis* show significant differences in protein expression

We assessed two questions in tandem. First, how do the secretomes of *M. bovis* ORBIT and *M. orygis* ORBIT compare to each other? Second, how do isogenic strains- in which major

antigens are deleted- compare to their parental counterparts? As previously reported, the top three proteins in the *M. bovis* secretome are ESAT-6 and CFP-10 (two canonical virulence factors), and MPT70 (a putative virulence factor). As the proteome of *M. orygis* had not previously been investigated, we also confirmed this observation in *M. orygis*. To further characterize the parental *M. bovis* and *M. orygis* strains, we utilized a normalized Z-score cutoff value corresponding to the top 20 proteins. Between the two cattle lineages, the top secreted proteins are conserved at comparable expression levels (13 proteins shared; normalized Z-score). If we focus on the proteins not shared between the two groups, we see that *M. bovis* shows an abundance of immunogenic antigens, associated with the ESX-1 system, whereas *M. orygis* shows an increased abundance of ESX-5 associated proteins (ESX-5 bias) (Figure 11a,b)[250,255].

Proteomic analysis shows there is little *in vitro* difference between parental *M. bovis* and knockout groups, indicating a relatively stable secretome. Major proteins of *M. bovis* isogenic strains are comparable to the parental secretome regardless of the presence or absence of genes of interest. Differences in the spectra of these strains correlate to the isogenic secretome analyzed. As expected, MPT70 spectra were rare in *M. bovis Δmpt70_mpt83* and *M. bovis Δmpt70,* MPT83 spectra were rare in *M. bovis Δmpt70_mpt83* and *M. bovis Δmpt83,* and ESAT-6 spectra were rare in *M. bovis ΔesxA* (Figure 12a,c). The impact of *mpt70* and *mpt83* disruption on other secreted proteins was minimal. When restricted to the top 5% of secreted proteins (normalized Z-score), *M. bovis ΔesxA* shows the greatest variation in shared proteins (6 out of 13), whereas *M. bovis Δmpt70_mpt83* and *M. bovis Δmpt70* share the most proteins with the parental group (10 out of 13). Further, analysis of the entire parental secretome shows a small subset of proteins uniquely expressed compared to isogenic strains. Specifically, RipA (associated with cell wall

biogenesis/degradation) and EftB (associated with electron transport) showed an upregulation compared to knockouts of *mpt70, mpt83,* or *esxA.*

We define differentially expressed proteins as proteins that are either up- or down-regulated following a head-to-head comparison (T-test without correction, $p < 0.05$) (Figure 12, 13). We observed differential expression in 3 of the 4 experimental groups (Figure 12a). The secretome of *M. bovis Δmpt70_mpt83* completely overlapped with *M. bovis* ORBIT (n= 0 unique proteins) (Figure 12b,d). Similarly, *M. bovis Δmpt70* and *M. bovis Δmpt83* shared 257 proteins, uniquely regulating few proteins compared to the parental group (not shown). Overall, *M. bovis ΔesxA* expressed the most unique proteins (n= 47), a majority of which were upregulated compared to *M. bovis* ORBIT (Figure 12e). Unsurprisingly, when *esxA* was absent, MPT70 became the dominant protein in the secretome ($p < 0.05$, Ordinary One-Way ANOVA). The significant variation in *M. bovis ΔesxA* was likely due to the co-dependency of ESAT-6, CFP-10, EspA, and EspC secretion, as a deletion of the single gene *esxA* abrogates the secretion of the ESX-1 system as a whole[48,268,395–398]. While it has been established that MPT70 and MPT83 do not act in an operon, the stability of the *M. bovis* ORBIT secretome in the absence of MPT70 and/or MPT83 further suggests that these antigens do not influence the expression of other proteins (including known virulence factors)[186]. To further account for variance, we performed a principal component analysis (PCA) of parental and isogenic *M. bovis* strains. We saw that *M. bovis ΔesxA* was separated from all other strains in this analysis whereas the parental strain, MPT70 and/or MPT83 deletion strains had significant overlapping of groups (Figure 12b). Moreover, variation in strain distribution could be attributed to the deletion of genes of interest rather than any unique feature of the strains: principal component 1 (PC1, accounting for ~94% of the variance) was driven by differential expression in ESAT-6 and CFP-10 whereas principal component 2 (PC2, accounting

for ~5% of the variance) was predominantly driven by differential expression in MPT70, and to a lesser extent, MPT64. This indicates that differences in very few proteins accounts for ~99% of the observed variance.

In contrast to *M. bovis*, *M. orygis* deletion strains (*Δmpt70_mpt83*; *ΔesxA*) showed striking proteomic differences (Figure 13). Whereas *M. bovis Δmpt70_mpt83* showed no unique expression, *M. orygis Δmpt70_mpt83* uniquely expressed 148 proteins compared to the parental *M. orygis* ORBIT, though the two strains shared 575 proteins (p-value > 0.05). In comparison, *M. orygis ΔesxA* expressed 100 proteins uniquely and shared 655 proteins with *M. orygis* ORBIT (p-value > 0.05) (Figure 13d,e). Despite this, when restricted to the top 5% of proteins detected, the dominant secreted proteins were mostly conserved. *M. orygis* and *M. orygis Δmpt70_mpt83* shared 30 out of 43 proteins whereas *M. orygis ΔesxA* shared 34 out of 43 (normalized Z-score). Within this subset of proteins, virulence associated factors (ex: Esx and PPE proteins) and proteins associated with metabolic processes were most common. Notably, several iron-associated proteins were upregulated in both *Δmpt70_mpt83* and *ΔesxA* strains compared to expression by the parental strain, suggesting a distinct metabolic preference in deletion strains. PCA revealed a separation of *M. orygis Δmpt70_mpt83* and *M. orygis ΔesxA*, with most of PC1 (~86% of total variance) being determined by ESAT-6 and CFP-10 expression. PC2, comparatively, was influenced predominantly by MPT70, EspA, multiple PPE proteins, and ESX-5 secreted components (~11.5% variance) (Figure 13b).

The former observation of different *M. bovis* and *M. orygis* secretome sizes suggests either that one bacteria is actively producing less proteins than the other or, alternatively, that one bacteria is producing such a high quantity of a lesser number of proteins, that those present at a lower frequency are not detected in bulk proteomic analysis. Accordingly, the latter observation that

isogenic mutants result in differential effects across these two bacteria could again be due to different production of the major proteins, such that a discrete loss affects the proteome to different extents, or that MPT70 and MPT83 may have a role in *M. orygis,* that is not recapitulated in *M. bovis.*

3.2 *Ex vivo* infection with isogenic cattle stains does not mediate bacterial uptake or viability

Due to the immunogenic nature of both MPT70 and MPT83, we infected murine bone-marrow derived macrophages (BMDMs) with either WT *M. bovis* or *M. bovis* deletion strains (MPT70 and/or MPT83 absent) at an MOI of 5:1. We hypothesized that constitutive expression of MPT70 and MPT83 may contribute to the efficacy of macrophage infection due to a pre-stimulation of cells by immunogenic proteins. As such, we suspected that isogenic strains in which MPT70 and/or MPT83 were absent, would have a reduced bacterial burden compared to WT group, either due to impaired uptake or more efficient bacterial killing by the cell. Unexpectedly, the deletion of MPT70 and MPT83 had no effect on the bacterial burden. Bacterial uptake was comparable across infection groups, with < 1% of inoculum phagocytosed by T= 4 hours (Figure 14a). Additionally, there were no significant differences in bacterial burden at T= 24, 48, and 72 hours post infection (p.i.) compared to parental *M. bovis* (Figure 14b). When BMDMs were infected with wildtype or isogenic *M. orygis* (*M. orygis Δmpt70_mpt83*) there was no significant difference in bacterial uptake; like *M. bovis* < 1% of bacteria was phagocytosed by 4 hours (Figure 15a). Moreover, bacterial burden between strains was comparable at 24, 48, and 72 hours p.i., though by 72 hours, *M. orygis Δmpt70_mpt83* trended towards a greater bacterial burden compared wildtype *M. orygis* (Figure 15b). These results may suggest that if MPT70/MPT83 mediates infection 1) bacterial burden may not be the correct readout and/or 2) the macrophage may not be the optimal site of action for these proteins (Figure 14b).

4. Discussion:

The constitutive expression of MPT70 and MPT83 in *M. bovis* and *M. orygis* is not a subtle phenotype. The role, if any, of these antigens in pathogenesis has yet to be established. There are three lines of evidence suggesting a putative role of MPT70/MPT83 in successful mycobacterial infection. First, *M. bovis* and *M. orygis* are 'generalist' pathogens with extensive host ranges whereas *M. tb* is a human-adapted 'specialist'[43]. Second, if infection severity is defined by morbidity and mortality, the infection outcomes of *M. bovis* and *M. orygis* appear to be worse in cattle and other mammalian hosts (including humans) compared to their human-adapted counterpart[16,129,225,232]. Third, MPT70 and MPT83 have been twice independently upregulated through mutations in RskA in only the virulent, cattle-associated lineages, yet this was lost following *in vitro* passaging of *M. bovis* BCG[186]. As MTBC evolution is reductive, it follows that if a gene/gene product is not required by the organism to survive in its niche, metabolic resources will not be wasted on maintaining this phenotype[11,40].

Given this, we pursued the following questions: first, can the ORBIT recombineering system successfully generate genomic deletions in *M. bovis,* and *M. orygis*? Second, does disruption of MPT70 and/or MPT83 production affect other protein production by the bacterium? To address the former, we generated 8 knockouts with high efficacy and fidelity specifically targeting these antigens (*en bloc* or solo) To address the latter, we characterized parental and isogenic strains in the absence of a host.

Our data reveal that *M. bovis* and *M. orygis* have different secretomic profiles at baseline and suggests that the role of MPT70 and/or MPT83 may vary depending on the mycobacterial strain. In both strains, ESAT-6, CFP-10, and MPT70 composed the majority of the secretome. However, when compared to parental *M. bovis,* the *M. orygis* secretome 1) was much larger and

2) showed an upregulation of ESX-5 associated proteins. Isogenic strains revealed upregulated proteins for *M. orygis Δmpt70_mpt83* but not for *M. bovis Δmpt70_mpt83*. The variance of the parental strains along with the differences seen with isogenic strains together suggest that, despite genomic similarity, there may be differential effects of the same genes on the outcome of infection.

Of the 5 ESX systems in the MTBCs, only 3 have been associated with pathogenesis and bacterial viability (ESX-1, -3, and -5)[252,271,273,399]. In particular, ESX-5 (and ESX-5 accessory regions) has a role in bacterial growth and nutrient acquisition, secretes the majority of PE/PPE proteins, influences cell death, and mediates pro-inflammatory responses[255,272,275,400–402]. Moreover, this system is the most 'recent' gene expansion of the ESX regions, and is only present in slow-growing, pathogenic mycobacterial species[275,403,404]. Within the ESX-5 system there are 5 pairs of Esx proteins (EsxM/N, EsxI/J, EsxK/L, EsxO/P, and EsxV/W) which are further classified as either ESAT-6 or CFP-10 paralogues, and numerous PE/PPE proteins. The PE/PPE proteins compose ~10% of the entire *M. tb* genome, but their role in host interactions has yet to be fully resolved[252,405] though previous studies have revealed that *M. tb* ESX-5 deficient strains are significantly attenuated in both immunocompromised (SCID) and immunocompetent (C57BL/6 mice)[272,275,406]. Like *mpt70* and *mpt83*, genes within ESX-5 encode strong antigenic proteins with poorly characterized roles in *M. bovis* and *M. orygis*. Given that the proteins upregulated in the *M. orygis* secretome are predominantly Esx or PE/PPE, this suggests the possible use of an alternate virulence strategy, which acts in conjunction with the 'classical' ESX-1 system[399].

Finally, at the cellular level, the success or failure of mycobacterial infection depends a balance of pro- and anti-inflammatory arsenal by the host immune response[407]. Our data reveal that despite differences in protein expression, following macrophage infection, *M. bovis* and *M. orygis* (in which MPT70 and/or MPT83 are absent) present similarly *ex vivo*. However, it should

not be overlooked that when *M. bovis* and *M. orygis* lack strong B- and T-cell antigens, such as MPT70 and/or MPT83, the typical pro-inflammatory cascade initiated by the host is likely impaired. As such, how these proteins act in a natural infection may not be accurately represented using this *ex vivo* model. Instead, perhaps *in vivo* studies are needed to explore the role of MPT70 and/or MPT83 in the context of 'true' infection, namely where the host and pathogen interface.

5. Figures

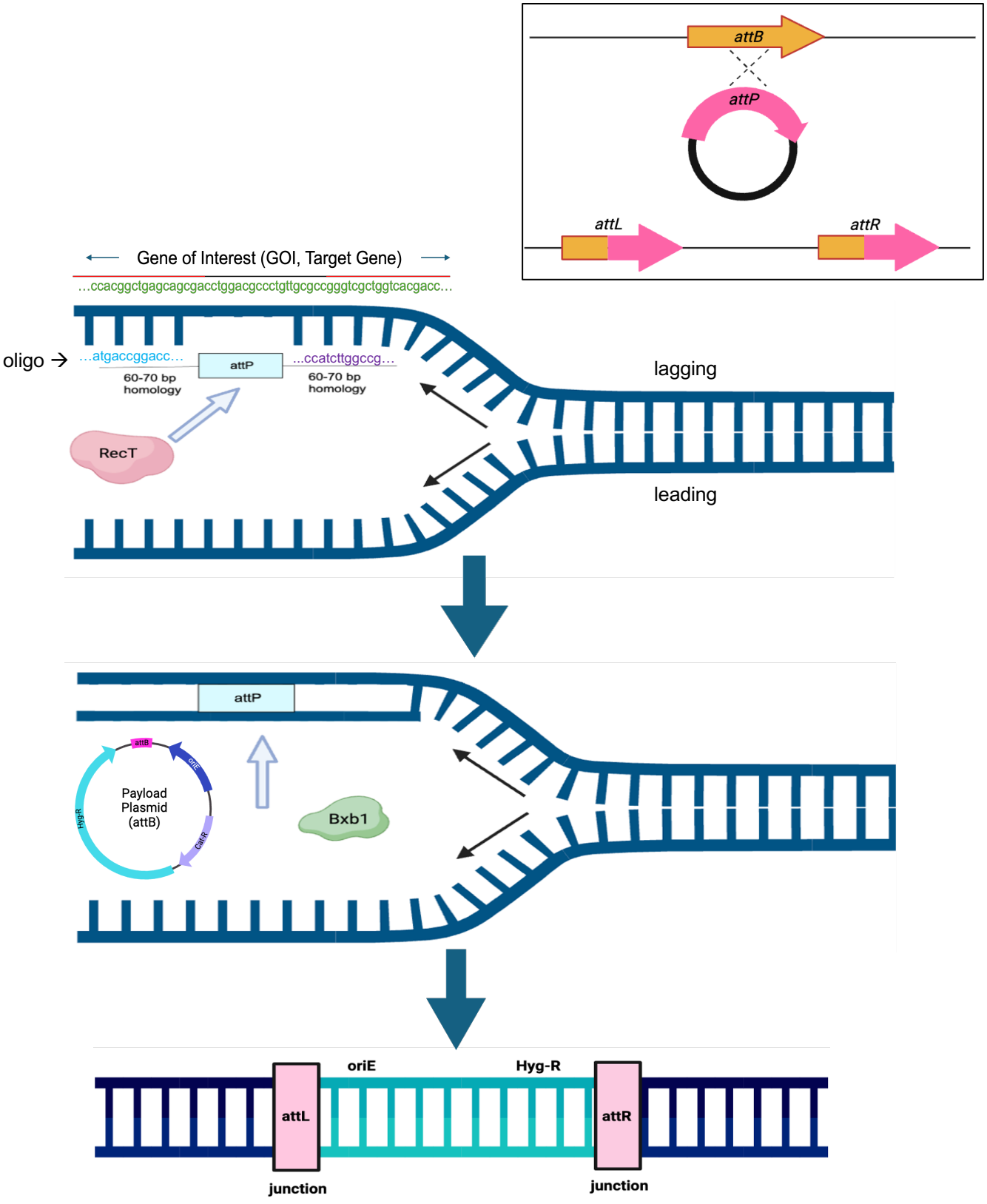
attB
attP
attL
attR
Gene of Interest (GOI, Target Gene)
…ccacggctgagcagcgacctggacgccctgttgcgccgggtcgctggtcacgacc…
oligo
…atgaccggacc…
attP
…ccatcttggccg…
60-70 bp homology
60-70 bp homology
RecT
lagging
leading
attP
attB
oriE
HygR
CatR
Payload Plasmid (attB)
Bxb1
attL
oriE
Hyg-R
attR
junction
junction

Figure 10. Overview of oligonucleotide-mediated recombineering followed by Bxb1 integrase targeting (ORBIT).

RecT annealase and Bxb1 integrase enzymes facilitate the integration of an antibiotic resistance cassette in place of the gene of interest (GOI). A single-stranded oligomer containing an *attP* recombination site and 60 bp of homology (up- and downstream of the GOI) targets the lagging strand of the DNA replication fork. A non-replicating 'payload plasmid' containing the *attB* site and a selectable antibiotic cassette is co-electroporated with the oligomer. Homologous arms of the oligomer align *attP* with the GOI and integrated into the genome via RecT annealase. Bxb1 integrase facilitates *attB x attP* combination to insert the selectable cassette in place of GOI. Schematic adapted from Murphy et al., 2018[299]. Inset: site-specific recombination mediated by *attB x attP* reaction results in new genomic 'product' demarcated by *attL* and *attR* recombination sites.

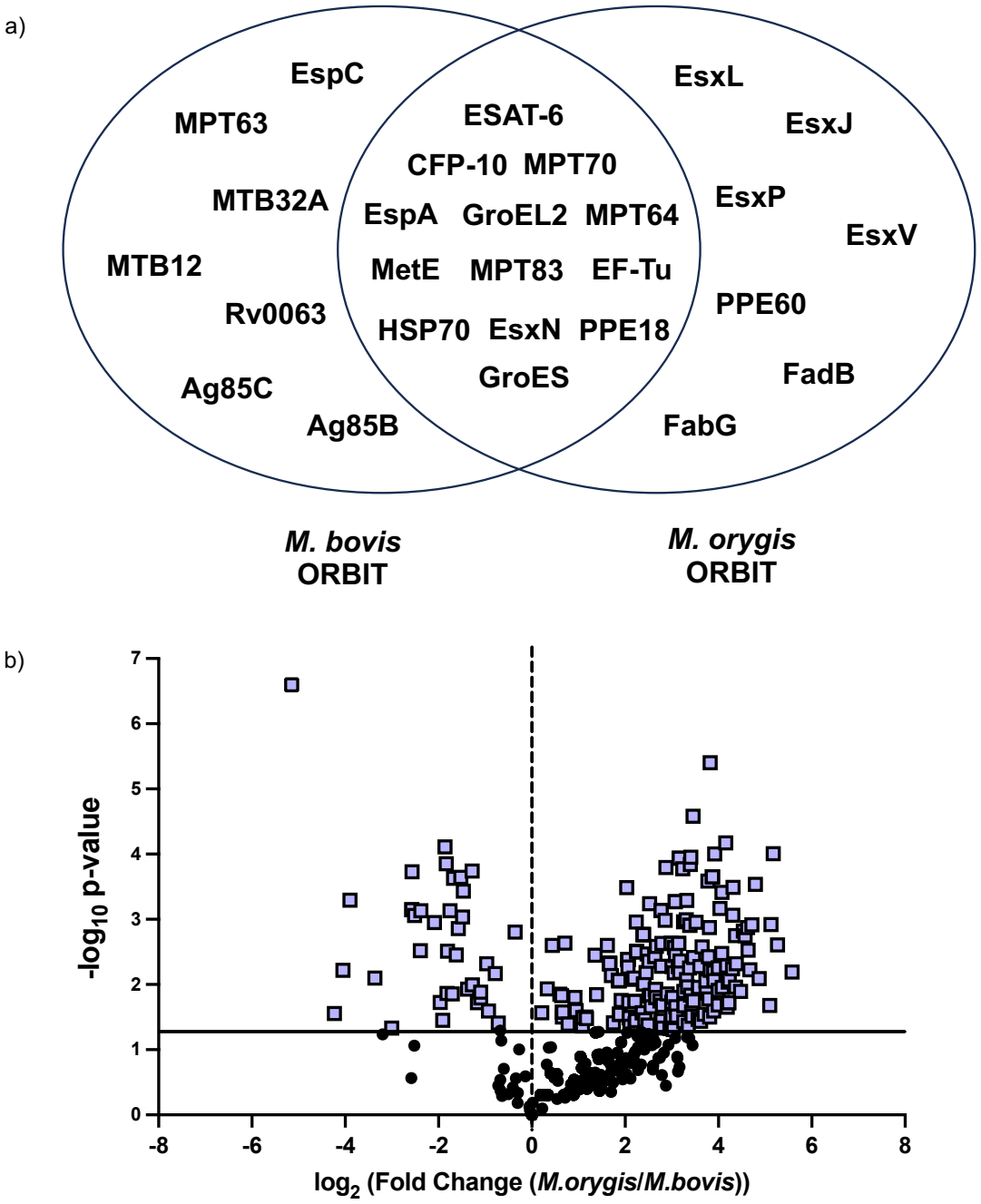

Figure 11. Secretomic comparison of *M. bovis* ORBIT and *M. orygis* ORBIT.

a) Venn diagram of the top 20 proteins of both the *M. bovis* and *M. orygis* secretomes as determined by Z-score. 13 out of 20 of the most dominant secreted proteins are shared between groups. **b)** Volcano plot of *M. bovis* ORBIT and *M. orygis* ORBIT (Scaffold_5.2.1). Values determined by

quantitative profile ($p < 0.05$, no correction). *M. orygis* ORBIT uniquely expresses significantly more proteins compared to *M. bovis* ORBIT.

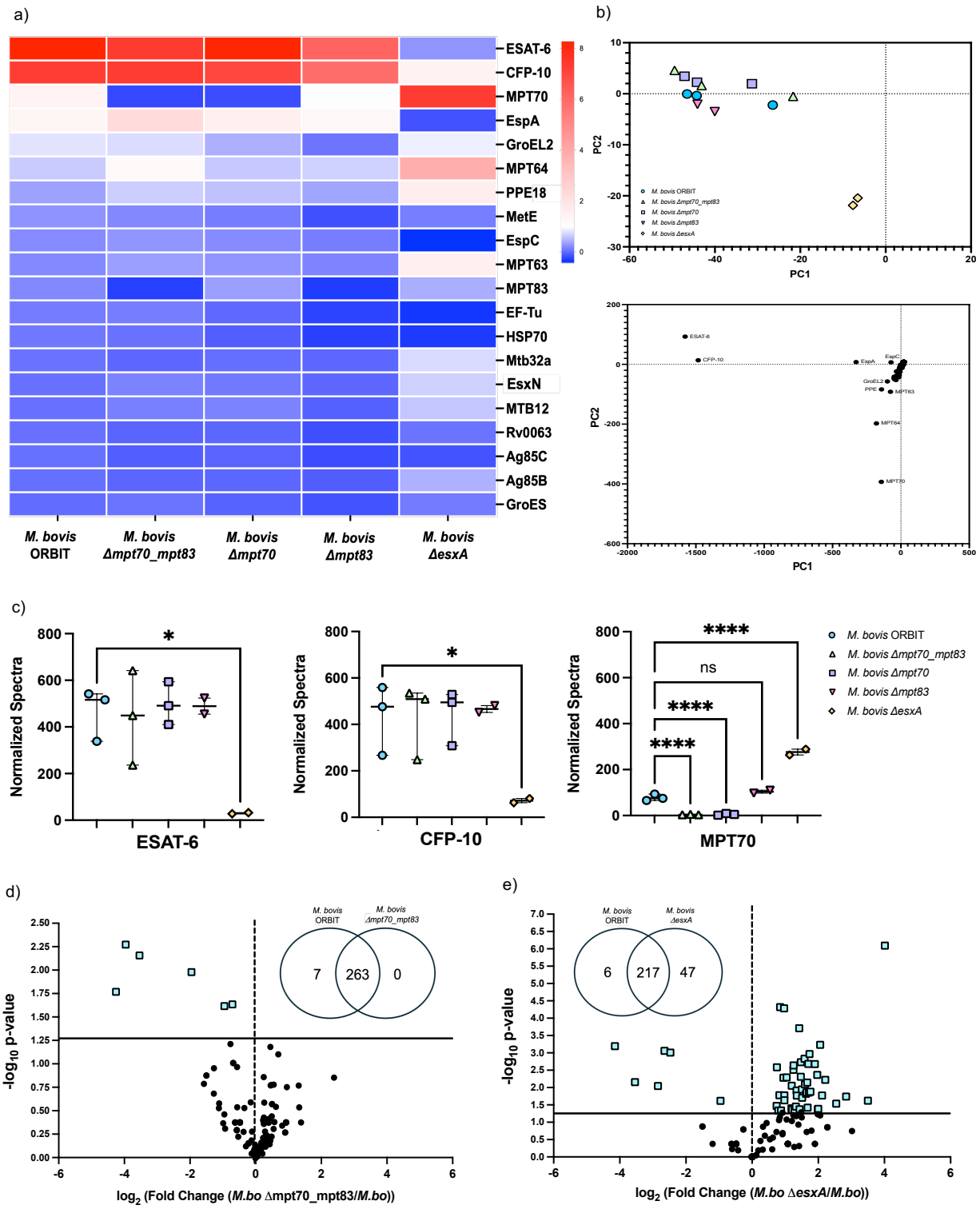

Figure 12. Secretomic analysis of *M. bovis* parental and deletion strains

a) Heatmap of *M. bovis* ORBIT, *M. bovis Δmpt70_mpt83. M. bovis Δmpt70, M. bovis Δmpt83,* and *M. bovis ΔesxA*. Proteins ranked against *M. bovis* ORBIT (Z-score > 0). Proteins correspond to top 8% of the secretome. **b)** Principal component analysis of parental versus deletion strains. PC1 accounts for ~94% of all variance; PC2 accounts for ~5% of all variance. *M. bovis ΔesxA* uniquely clusters away from parental and MPT70 and/or MPT83 deletion strains. **c)** Normalized spectral counts of parental and isogenic *M. bovis* strains in top 3 secreted proteins. As expected, MPT70 spectra rare in *M. bovis Δmpt70_mpt83* and *M. bovis Δmpt70;* ESAT-6 spectra rare in *M. bovis ΔesxA* ($p < 0.05$, Ordinary one-way ANOVA) **d)** Volcano plot of expressed proteins of *M. bovis* ORBIT versus *M. bovis Δmpt70_mpt83* (normalized spectral counts; threshold shown by solid black line). Embedded Venn diagram depicts unique and shared proteins ($p < 0.05$, no correction). *M. bovis* ORBIT uniquely expresses 7 proteins; *M. bovis Δmpt70_mpt83* does not uniquely express any protein. **e)** Volcano plot of expressed proteins of *M. bovis* ORBIT versus *M. bovis ΔesxA* (normalized spectral counts; threshold shown by solid black line). Embedded Venn diagram depicts unique and shared proteins ($p < 0.05$, no correction). *M. bovis* ORBIT uniquely expresses 6 proteins; *M. bovis ΔesxA* uniquely expresses 47

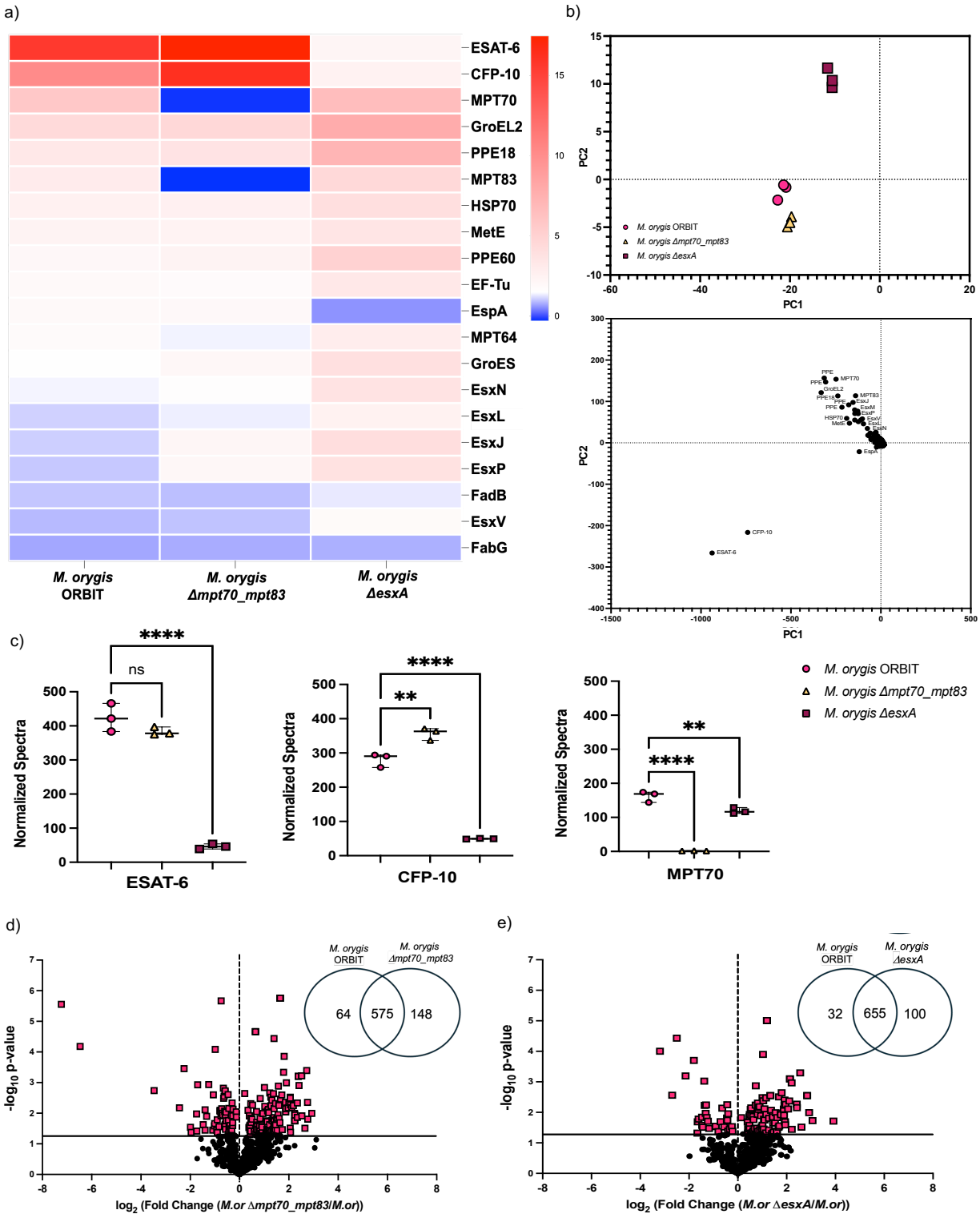

Figure 13. Secretomic analysis of *M. orygis* parental and deletion strains.

a) Heatmap of *M. orygis* ORBIT, *M. orygis Δmpt70_mpt83,* and *M. orygis ΔesxA*. Proteins ranked against *M. orygis* ORBIT (Z-score > 0.7). Proteins correspond to top 2% of the secretome. **b)** Principal component analysis of parental versus deletion strains. PC1 accounts for ~86% of total variance; PC2 accounts for ~11.5% of all variance. All *M. orygis* strains cluster individually with no overlap however, *M. orygis* ORBIT and *M. orygis Δmpt70_mpt83* are more similar than *M. orygis ΔesxA*. **c)** Normalized spectral counts of parental and isogenic *M. orygis* strains. Counts consistent with targeted GOIs; ESAT-6 spectra were rare in *M. orygis ΔesxA;* MPT70 spectra were rare in *M. orygis Δmpt70_mpt83* ($p < 0.05$, Ordinary one-way ANOVA). **d)** Volcano plot of expressed proteins of *M. orygis* ORBIT versus *M. orygis Δmpt70_mpt83* (normalized spectral counts; threshold shown by solid black line). Embedded Venn diagram depicts unique and shared proteins between groups ($p < 0.05$, no correction). *M. orygis* ORBIT uniquely expresses 64 proteins; *M. orygis Δmpt70_mpt83* uniquely expresses 148. **e)** Volcano plot of expressed proteins of *M. orygis* ORBIT versus *M. orygis ΔesxA* (normalized spectral counts; threshold shown by solid black line). Embedded Venn diagram depicts unique and shared proteins ($p < 0.05$, no correction). *M. orygis* ORBIT uniquely expresses 32 proteins; *M. orygis ΔesxA* uniquely expresses 100.

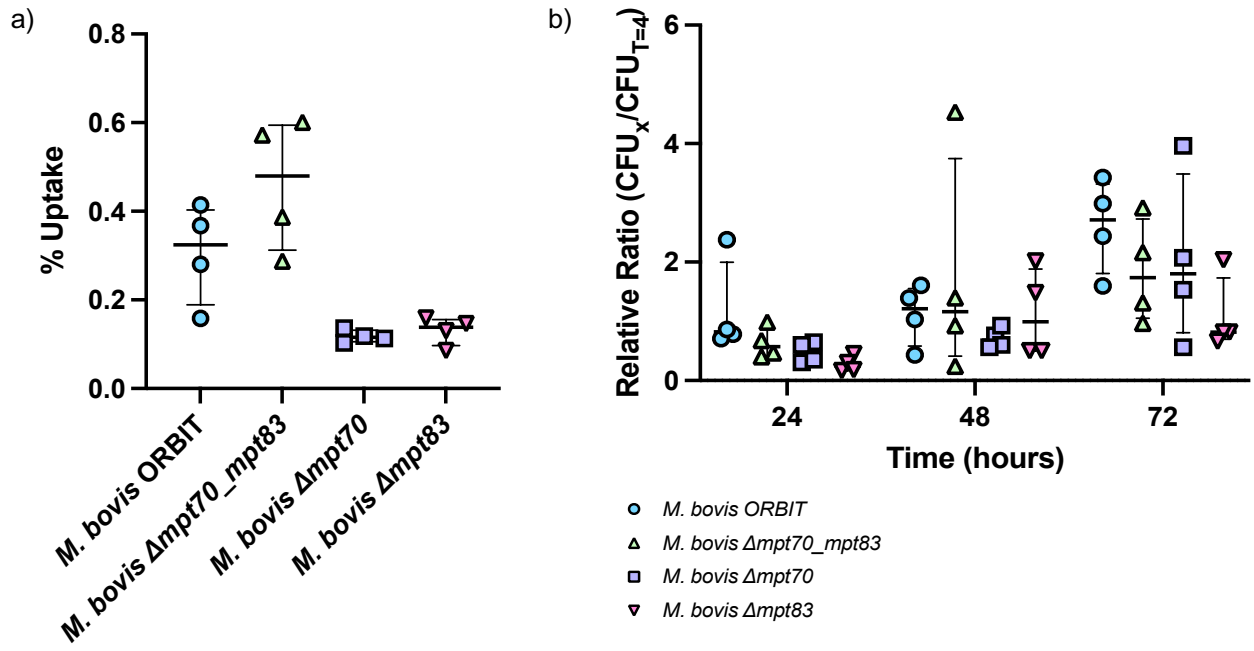

Figure 14. *M. bovis* isogenic and parental strains show comparable bacterial burdens.

Murine bone marrow derived macrophages (BMDMs) were infected with wildtype (ORBIT) or isogenic *M. bovis* strains at a multiplicity of infection (MOI) of 5:1 (bacteria:BMDMs). Infection performed in quadruplicates. **a)** Bacterial uptake of *M. bovis* ORBIT and *M. bovis* deletion strains (%). No significant differences across groups ($p > 0.05$, Kruskal-Wallis test). Bacterial uptake calculated as $\frac{\mathrm{CFU_{T=4}}}{\mathrm{CFU_{T=0}}}$ x 100%. **b)** Relative ratio of *M. bovis* ORBIT and *M. bovis* deletion strains. All bacterial burden calculated relative to T= 4-hour timepoint. No significant differences across experimental groups ($p > 0.05$, 2way ANOVA). Bacterial burden calculated relative to T= 4 hour timepoint (relative ratio; $\frac{\mathrm{CFU_{T=X}}}{\mathrm{CFU_{T=4}}}$).

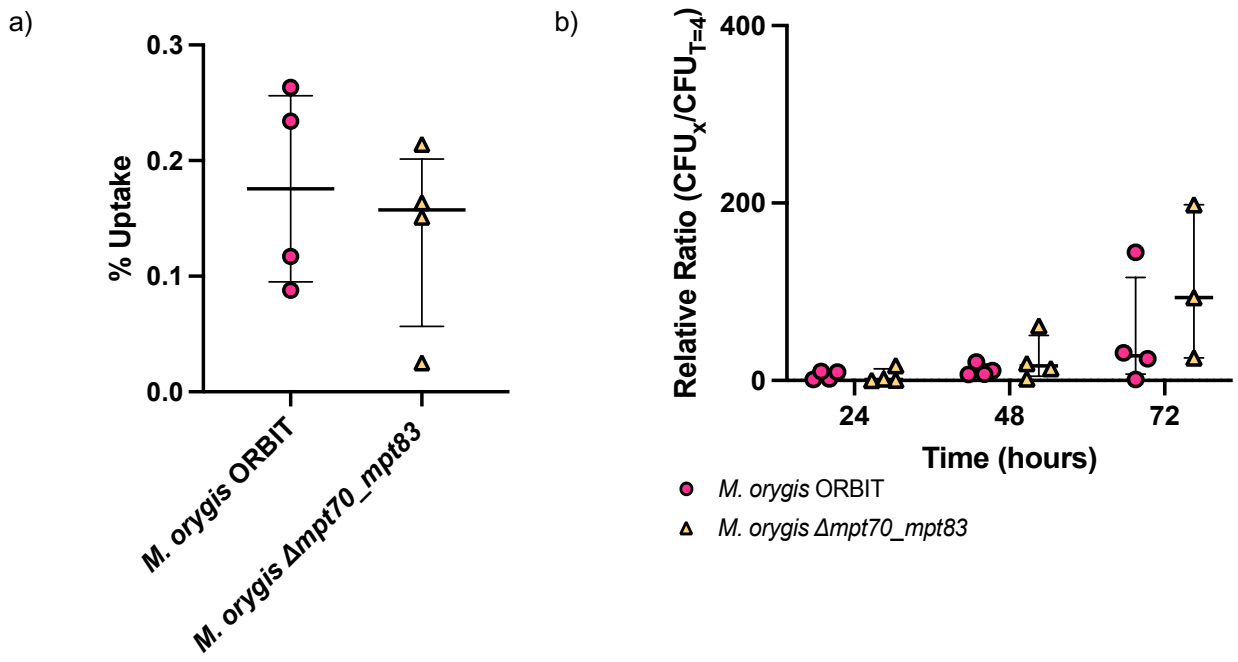

Figure 15. *M. orygis Δmpt70_mpt83* strains show comparable bacterial burden to wildtype.

Murine bone marrow derived macrophages (BMDMs) were infected with *M. orygis* ORBIT or *M. orygis Δmpt70_mpt83* at a multiplicity of infection (MOI) of 5:1 (bacteria:BMDMs). Infection performed in quadruplicates. **a)** Bacterial uptake of *M. orygis* ORBIT and *M. orygis Δmpt70_mpt83* (%). No significant differences across groups ($p > 0.05$, Kruskal-Wallis test). Bacterial uptake calculated as $\frac{CFU_{T=4}}{CFU_{T=0}}$ x 100%. **b)** Relative ratio of *M. orygis* ORBIT and *M. orygis* deletion strains. All bacterial burden calculated relative to T= 4-hour timepoint. No significant differences across experimental groups ($p > 0.05$, 2way ANOVA). Bacterial burden calculated relative to T= 4 hour timepoint (relative ratio; $\frac{CFU_{T=X}}{CFU_{T=4}}$).

6. Tables

***M. bovis* Ravenel**	***M. orygis* 51145**
M. bovis ORBIT (pKM444-KanR)*	*M. orygis* ORBIT (pKM444-KanR)*
M. bovis Δmpt70_mpt83 (pKM464-HygR)*	*M. orygis Δmpt70_mpt83* (pKM496-ZeoR)*
M. bovis Δmpt70 (pKM496-ZeoR)*	*M. orygis Δmpt70* (pKM496-ZeoR)
M. bovis Δmpt83 (pKM496-ZeoR)*	*M. orygis Δmpt83* (pKM496-ZeoR)
M. bovis ΔesxA (pKM496-ZeoR)*	*M. orygis ΔesxA* (pKM496-ZeoR)*

Table 3. Bacterial strains.

Isogenic strains with their respective resistance backgrounds. Kan- kanamycin (pKM444), Hyg- hygromycin (pKM464), Zeo- zeocin (pKM496). *M. bovis* and *M. orygis* containing *mpt70_mpt83* indicates *en bloc* deletion of *mpt70, mpt83* and the gene between them, *dipZ.* *indicates use in secretomic analysis. Isogenic strains derived from *M. bovis* Ravenel and *M. orygis* 51145.

Gene of Interest (GOI)	Oligomer
mpt70_mpt83	ctcgggcgggtcggcggcctccgcggacgattacgccggaggcattagcacgctgtcaat GGTTTGTCTGGTCAACCACCGCGGTCTCAGTGGTGTACG GTACAAACCtgcggccggtttggcctgaacgttgatcatcgcttcgattcctttgcttctg cggcggcg
mpt70	gccgtctccggcagcgaaggagtgaacggcatgaaggtaaagaacacaattgcggcaacc GGTTTGTCTGGTCAACCACCGCGGTCTCAGTGGTGTACG GTACAAACCattgacagcgtgctaatgcctccggcgtaatcgtccgcggaggccgcc gacccgcccgag
mpt83	cgccgccgcagaagcaaaggaatcgaagcgatgatcaacgttcaggccaaaccggccgca GGTTTGTCTGGTCAACCACCGCGGTCTCAGTGGTGTACG GTACAAACCgatacggtgctgatgcccccggcacagtaacgttcggcgcggtcaag gcgaggcagcccg
esxA	cgctaatacgaaaagaaacggagcaaaaacatgacagagcagcagtggaatttcgcgggt GGTTTGTCTGGTCAACCACCGCGGTCTCAGTGGTGTACG GTACAAACCgaaggcaacgtcactgggatgttcgcatagggcaacgccgagttcgc gtagaatagcgaa

Table 4. Oligomers used in the generation of deletion strains

Oligomers used to generate deletion strains. Oligos composed of 60 bp of homology upstream of GOI, *attB* recombination site, and 60 bp homology downstream of GOI.

CHAPTER IV: *MYCOBACTERIUM TUBERCULOSIS* COMPLEX SUBSPECIES (MTBC) PATHOGENESIS IN A MURINE MODEL

1. Preface

The previous chapter explored the development of deletion strains using mycobacterial recombineering and subsequent laboratory testing in two cattle pathogens. Several questions remained; first, using an experimental infection model, what is the outcome of *M. orygis*? Second, how does this compare to *M. tb,* the human adapted pathogen, and *M. bovis,* the cattle adapted pathogen? The following chapter contains content from the submitted first author paper, **Enhanced virulence of *Mycobacterium orygis* provides new insights into the pathogenesis of tuberculosis.** This piece of work was a collaboration between Sarah N. Danchuk, Shannon C. Duffy, Jaryd Sullivan, Syed Beenish Rufai, Fiona A. McIntosh, Andréanne Lupien, Lorne Taylor, Philippe Joubert, Rasmus S. Mortensen, Vivek Kapur, and Marcel A. Behr.

2. Introduction

The MTBCs can be broadly categorized into either a) the human-associated lineages, *M. tuberculosis sensu stricto* and *M. africanum* or b) animal-associated lineages[43,47]. The latter include *M. bovis,* the causative agent of bovine tuberculosis in Europe, Africa and the Americas, and *M. orygis,* the causative agent of bovine tuberculosis in South Asia[43,47,222].

M. tb and *M. bovis* were first described in the late 19th century. Since their discovery more than 120 years ago, they have been largely studied by different investigators using different experimental infection models in different hosts[14,16]. When directly compared in the same host, *M. bovis* has shown greater virulence (defined as the capacity to cause disease in a susceptible host) than *M. tb* in guinea pigs, rabbits, mice, cattle and other species[14,16] The basis for this differential virulence remains unknown, for two major reasons. First, whether *M. bovis* is

hypervirulent or *M. tuberculosis* is attenuated cannot be resolved with a two-pathogen comparison. Second, the large number of genomic differences between these two lineages presents a challenge when dissecting a complex phenotype, such as virulence.

In 2012, 114 years following the characterization of *M. bovis, M. orygis* was described as a member of the MTBC with a deep branch separating it from *M. bovis*[222,59]. Case series indicate that *M. orygis* shares with *M. bovis* a broad host range and the ability to cause disease in humans[226,229,232,233,242,408]. However, experimental infections with *M. orygis* have yet to be described, exempting studies performed in the previous chapter. Given the availability of genomic data and standardized experimental models, we sought to compare *M. orygis* to *M. tb* and *M. bovis*, *in silico, in vitro* and *in vivo.* Our data reveal profound differences in virulence between animal and human-associated tubercle bacilli, a finding with important implications for basic and translational tuberculosis research.

3. Methods

3.1 Whole genome sequencing:

Sequencing of *M. orygis* 51145 reference strain was performed by Beenish Rufai in collaboration with the Pennsylvania State University. The *M. orygis* 51145 genome sequence was corrected using Illumina HiSeq. Raw Illumina reads were screened using FastQC v0.11.9 and quality score of >= 20 was retained. The output of contigs was assembled using the SPAdes genome assembler (v3.9.0) using the default *k-mer* size, annotated using Prokaryotic genome annotation pipeline (PGAP) and submitted in sequence read archive (SRA) under accession number (SRR16643349). Illumina fastq reads were mapped onto the annotated Pacbio sequence and variants were called using Geneious Software v.2021.1. List of variants extracted from Illumina sequenced Orygis 51145 genome in comparison with Pacbio Sequenced Orygis 51145

genome is given in Table 5. The revised *Mycobacterium orygis* 51145 genome was deposited in GenBank under the accession number CP063804.2. Genomic characteristics of *M. tb, M. bovis,* and *M. orygis* presented in Table 6.

3.2 Bacterial strains:

Bacterial strains used in aerosol challenges are listed in Table 7. Deletion strains were constructed using the ORBIT recombineering system, as described by Murphy et al. with modifications (2018) (see Chapter I/ III)[299].

3.3 Phthiocerol Dimycocerosates (PDIM) analysis

The presence of PDIM in our bacterial strains was confirmed prior to all animal infection using the protocol previously described by Reed et al[283]. Briefly, 10 mL cultures of *M. tb, M. bovis* and *M. orygis* were grown to mid-log phase in 7H9 complete media and passaged once. 1 µL of propionic acid (1 mCI/µL) was added to 10 mL of culture and rolled for 48 hours at 37ºC. Following this, cultures were centrifuged at 3800 rpm for 15 minutes at room temperature. Supernatant was discarded and pellet was resuspended in 600 µL of MetOH: 0.3 % NaCl (10:1 ratio). 300 µL of hexanes was added, vortexed for 15 minutes and centrifuged at 15000 rpm for 5 minutes. The aqueous layer was removed and dried overnight before downstream processing. Following extraction, lipids were separated using thin layer chromatography (TLC) and visualized using STORM 840 phosphoimager (Amersham).

3.4 Preparation of aerosol stocks:

Mycobacterial strains were grown in 20 mL of 7H9 complete media (defined as 7H9 + 0.1% Tween80 + 0.2% glycerol + 10% ADC (albumin, dextrose, and catalase)) to mid-log phase (OD_{600}= ~0.8-1) and passaged twice. Following the second passage, cultures were centrifuged at 500 rpm for 5 minutes. Supernatant transferred to new 50 mL conical and centrifuged at 3980 rpm

for 10 minutes. The pellet was resuspended in 1 mL 7H9 complete and passed through a 25g syringe 5 times to remove any remaining clumps. Following this, 19 mL of 7H9 complete was added to a total of 20 mL. 100% sterile glycerol was added to a final concentration of 10% and frozen. Aerosol stocks for all animal experiments were prepared as described above unless otherwise specified.

3.5 Mice:

All mouse experiments used 8–12-week-old female or male C57BL/6 mice from Jackson Laboratories unless otherwise specified. All protocols involving mice followed the guidelines of the Canadian Council on Animal Care (CCAC) and were approved by the ethics committee of the Research Institute of the McGill University Health Centre (RI-MUHC) animal resource division.

3.6 Aerosol infection studies:

3.6.1 MTBC survival:

Frozen aerosol stocks were thawed and diluted to OD_{600} =0.04-0.05 (correlating to ~150-300 CFU) in PBS supplemented with 0.05% Tween80. Eighteen C57BL/6 female mice were exposed to a continuous stream of aerosolized inoculum for 15 minutes (CH Technologies Nose-Only Inhalation exposure system) unless otherwise indicated. Following infection, inoculum was plated (day 0) on 7H10 plates containing polymyxin B, amphotericin B, nalidixic acid, trimethoprim, azlocillin (PANTA, Beckton Dickinson) and supplemented with oleic acid, albumin, dextrose, and catalase (OADC, Beckton Dickinson BBL Middlebrook), and 0.5% glycerol. Three mice per group were sacrificed at either day 1 or day 3 (as specified) to determine initial infectious dose received by mice. Lungs were extracted, homogenized in 2 mL of 7H9 complete media and plated on 7H10 PANTA + OADC + glycerol. Lungs were homogenized using the Omni Tissue Homogeniser and Hard Tissue Omni Tip Plastic Homogenising Probes (Omni International). The

remaining mice were monitored by animal health technicians until compassionate (clinical) or experimental endpoint at which a necropsy was performed on the mouse. Compassionate endpoints were defined as mice which have lost > 20% of weight compared to start of infection, hunched posture, inactive or decreased activity, dehydration, and/or having rapid breathing (Table 8). At necropsy, the right accessory lobe of lung was extracted for downstream hematoxylin and eosin (H&E) or Ziehl-Neelsen (ZN) histological staining where indicated (McGill University Goodman Cancer Research Centre Histology Core). The remaining lungs, spleen, and liver were harvested and homogenized in 1 mL 7H9 complete media. Samples were serially diluted and plated on 7H10 PANTA + OADC + glycerol to determine bacterial burden after 4-6 weeks of incubation at 37□C. This protocol was used for all survival experiments except for *in vivo M. bovis* studies, in which inocula and homogenized organs were plated on 7H11 PANTA + OADC + glycerol plates.

3.6.2 *M. orygis* aerosol infection with pre-defined time-points:

Inoculum was prepared as described above. Thirteen mice (per experimental group) were exposed to either *M. orygis* 51145 or *M. tb* H37Rv via the aerosol route at a standard dose of ~150-200 CFU. Three mice per group were sacrificed to determine initial dose, as described above. The remaining mice were sacrificed at weeks 3 and 4 (n= 5 mice per experimental group per time point). Both lungs and spleen were collected for downstream processing and accessory lobes of infected mice were extracted for histological assessment (H&E or ZN staining where specified). Slides of the right accessory lobe were reviewed, blinded to experimental group. A semiquantitative scale (Table 9) was used to score bronchial/endobronchial, peribronchial, perivascular, interstitial, pleural and intra alveolar inflammation, capillary vascular congestion, and pulmonary edema. Additionally, the tissue quality, percent of lung area affected, and the distribution of lesions were assessed in the consideration of these scores (Table 9).

3.6.3 Vaccination with BCG

Strains of *M. bovis* BCG Russia and *M. bovis* BCG Danish were grown in 7H9 complete media, passaged twice, and processed to remove any remaining clumps, as described above in the preparation of aerosol stocks. Bacterial cultures were then adjusted to an OD_{600} of 0.1. Following this, BCG Russia or BCG Danish was injected via the subcutaneous route (100 µL; n= 12 mice per group) (~10^6 CFUs). Additionally, 12 mice were sham vaccinated with 100 µL of phosphate buffered saline (PBS). At 10-weeks post vaccination, all groups were challenged with aerosolized *M. orygis*. Two mice per group were sacrificed at day 3 to determine initial aerosol dose. At compassionate endpoints, lungs and spleen were harvested and processed as described above. Remaining mice were monitored for signs of clinical disease until experimental endpoint at week 36. At compassionate or experimental endpoint, the right accessory lobe was extracted for histopathological studies.

3.6.4 *M. bovis Δmpt70_mpt83* aerosol challenge with pre-defined timepoints:

Mice were infected via the aerosol route (~200-300 CFU) and randomized to either week 3 (n= 5), week 16 (n= 10), week 32 (n= 7), or week 52 (n= 7), per experimental design. At pre-defined timepoints, mice were sacrificed. The right accessory lobe of lung was extracted for H&E staining; remaining lobes of lung and spleen were processed as described above for CFU enumeration (7H11 + PANTA + OADC plates).

3.6.5 *M. bovis Δmpt70* and *Δmpt83* aerosol challenge with pre-defined timepoints:

Mice were infected via the aerosol route (~100-300 CFU) and randomized into week 3 (n= 3 or 5, as specified) or week 16 (n= 10) experimental groups. *M. bovis Δmpt70* infection was performed twice whereas *M. bovis Δmpt83* was performed once as a proof of concept. At pre-

defined timepoints, the right accessory lobe was extracted for H&E staining but only lungs were processed for CFU enumeration.

3.6.6 Rag -/- C57BL/6 aerosol challenge:

Fifteen Rag -/- C57BL/6 mice (female, 8-12 weeks) were exposed to a continuous stream of aerosolized inoculum for 15 minutes (CH Technologies Nose-Only Inhalation exposure system) as described above (~350 CFU). Following challenge, mice were monitored by animal health technician until compassionate endpoint (Table 8). At euthanasia, lungs were processed and plated on 7H11 + PANTA + OADC + glycerol plates; right accessory lobe was extracted for downstream histopathology and H&E staining.

3.6.7 *M. orygis Δmpt70_mpt83* aerosol challenge with pre-defined timepoints:

Mice were infected via the aerosol route with ~300-500 CFU of *M. orygis* or *M. orygis Δmpt70_mpt83* as previously described and randomized into day 7, day 14, or day 21 timepoints (n=5 mice per timepoint, per group). At pre-defined timepoints, mice were sacrificed as described previously (lungs extracted for CFU enumeration; right accessory lobe allocated for H&E staining).

3.7 Mycobacterial protein extraction and analysis

Proteomics performed as described in Chapter III. Accordingly, MTBC cultures were grow in 10 mL 7H9 complete media (OD_{600}= 0.8-1) and passaged in 30 mL of Sauton minimal media. Cultures were again grown to an OD_{600} of ~0.8, spun down (3980 rpm, 15 minutes), washed with ice-cold PBS, and resuspended in 30 mL Sauton media. This was repeated for a total of 3 passages. Following this, cultures were centrifuged at 3980 rpm for 15 minutes. Culture filtrate was allocated for secretomic analysis; pellet stored at -80°C. For culture filtrate, supernatants were filtered twice

through 0.22 □M filters and concentrated using centrifugal filter units (Amicon Ultra-15 Centrifugal Unit, 3 kDa cutoff) by spinning at 3980 rpm for 2-3 hours to a final volume of 1 mL. Protein concentration was determined using the Qubit Protein BR Assay per manufacturer instruction. Proteomic analysis was performed by the Proteomic and Molecular Analysis Platform at the Research Institute of the McGill University Health Centre as previously described. For each sample, proteins were loaded onto a single stacking gel band to remove lipids, detergents, and salts. The gel band was reduced with DTT, alkylated with iodoacetic acid and digested with trypsin. Extracted peptides were re-solubilized in 0.1% aqueous formic acid and loaded onto a Thermo Acclaim Pepmap (Thermo, 75□M ID X 2cm C18 3□M beads) precolumn and then onto an Acclaim Pepmap Easyspray (Thermo, 75□M X 15cm with 2□M C18 beads) analytical column separation using a Dionex Ultimate 3000 uHPLC at 250 nl/min with a gradient of 2-35% organic (0.1% formic acid in acetonitrile) over 3 hours. Peptides were analyzed using a Thermo Orbitrap Fusion mass spectrometer operating at 120,000 resolution (FWHM in MS1) with HCD sequencing (15,000 resolution) at top speed for all peptides with a charge of 2+ or greater. The raw data were converted into *.mgf format (Mascot generic format) for searching using the Mascot 2.6.2 search engine (Matrix Science) against the protein sequence database of the imputed ancestor of the MTBC (called $MTBC_0$) and a database of common contaminant proteins[409]. The database search results were loaded onto Scaffold Q+ Scaffold_5.2.1 (Proteome Sciences) for statistical treatment and data visualization (AVOVA with Benjamini-Hochberg correction, $p < 0.05$; minimal spectra value= 0.5). Heatmap constructed as described in Chapter III. Protein ranking based on *M. orygis* 51145; Z-score protein cutoff > 1. Z-score defined as: $Z = \frac{(\text{normalized spectra} - \text{mean of population})}{\text{standard deviation of population}}$. Data visualized using GraphPad Prism (v10.0.3). Assessed MTBC strains: *M. orygis* 51145, *M.*

bovis Ravenel, *M. tb* H37Rv (lineage 4), *M. tb* lineage 1 isolate, *M. tb* HN878 (lineage 2), *M. africanum,* and *M. microti.*

3.8 Recombinant antigens and vaccination

ESAT-6 and MPT70 recombinant antigens were produced with a His-tag at the N-terminal end (MHHHHHH-) and purified in accordance with established methods[410]. Codon optimized DNA constructs were inserted into the pJ411 expression vector (ATUM, Menlo Park, CA, USA) and transformed into *E. coli* BL21 (DE3) (Agilent, DK). In 3L liquid cultures, protein expression was induced with 1 mM isopropyl ß-d-1-thiogalactopyranoside and ESAT-6/MPT70 were purified from inclusion bodies by metal chelate chromatography followed by anion-exchange chromatography. Vaccine formulation were prepared by mixing CAF01 with recombinant ESAT-6 or MPT70 and subcutaneously administered as previously described by Clemmensen et al.[410,411] In tandem, mice were vaccinated with BCG Russia or sham-vaccinated with PBS, as described above. Ten weeks post vaccination, mice were challenged with standard dose of *M. orygis* 51145 (150-300 CFU) via the aerosol route and monitored for signs of clinical disease until compassionate or experimental endpoint. Vaccines provided by Statens Serum Institute.

3.9 Statistics:

Statistical analyses were conducted using GraphPad Prism (v10.0.3). Survival curves were constructed and analyzed using the Kaplan-Meier (non-parametric) method. When comparing multiple groups over multiple timepoints, Ordinary 2way ANOVA with Sidak's multiple comparisons test was performed; comparison of multiple groups at specific timepoints was performed using Kruskal-Wallis test. Comparison of 2 groups at a single timepoint was performed using Mann-Whitney U test. Statistical significance was defined as $p < 0.05$. Where applicable, data are shown as individual data points with median and interquartile range**.**

4. Results

4.1 Genomic and proteomic analysis further characterize *M. orygis* 51145 *in vitro*

Genome sequencing of *Mycobacterium orygis* 51145 was previously performed using PacBio single-molecule real-time (SMRT) technology to assemble a single circular chromosome[412]. To verify nucleotide reads, the same DNA aliquot used in Pacbio sequencing was run using the Illumina HiSeq platform. It was determined that *M. orygis* 51145 has a genome size of 4,352,140 bp in length, 32 bp less than previously reported, with an average guanosine cytosine (GC) content of 65.6%[412]. The genome contains 4,089 genes of which 3,788 are coding sequences (CDS). Discrepancies with the previous assembly were found in five genes, including missense mutations and deletions (presence confirmed with Sanger sequencing) (Table 5). Further, genomic comparison of *M. tb* H37Rv, *M. bovis* Ravenel, and *M. orygis* 51145 shows genomes similar in size (~4.4Mb) and predicted gene content (~4100-4200). Of the three, *M. tb* H37Rv had the largest genome whereas *M. orygis* 51145 had the smallest genome (Table 6). In this chapter, *M. tb* H37Rv will be referred to as *M. tb*, *M. bovis* Ravenel will be referred to as '*M. bovis*' and *M. orygis* 51145 will be referred to as '*M. orygis*', unless otherwise specified.

4.2 Experimental *M. orygis* infection results in rapid mortality

The driving hypothesis of this chapter was: if *M. tb* and *M. orygis* are similar at the genomic level, then standardized models used in *M. tb* infection outcome can be applied for the assessment of *M. orygis* pathogenesis. As such, we infected C57BL/6 mice via the aerosol route with the intention of assessing bacterial burden and histopathology at days 21, 42, and 84 post-challenge (Figure 16). Unexpectedly, by day 28, 50% of the *M. orygis* infected group had reached the pre-determined criteria for sacrifice, resulting in a median survival of 28 days (Figure 16b, Table 8). In contrast, the median survival of *M. tb* infected mice could not be reached by day 119.

Interestingly, lung, spleen, and liver bacterial burdens at day 21 were comparable between *M. tb* and *M. orygis*, with no evidence that early mortality was due to disseminated *M. orygis* infection (consistent across 2 independent experiments, Figure 16d). Mice that succumbed to *M. orygis* infection by day 28 showed no increase in bacterial burden compared to day 21, despite extensive pulmonary pathology (Figure 16c).

As the critical point of *M. orygis* infection was between day 21 and 28, we repeated the infection and experimentally assigned mice to be euthanized at these timepoints (n= 5 per group, per timepoint) (Figure 16e). Consistent with previous data, we saw no differences in lung bacterial burdens from day 21 to day 28 (for both *M. orygis* and an *M. tb* control group) (Figure 16f). However, H&E slides from day 21, when there were no overt signs of clinical disease, revealed clear differences in histopathology, with a mean pathology score of 361 in the *M. orygis* group compared to 50 for the *M. tb* group (Figure 16g-h) (Table 9). Furthermore, *M. orygis* infected mice had higher pathology scores at day 21 than *M. tb*-infected mice at day 28 (Figure 16g). By day 28, 3 out of 5 of the *M. orygis* group had already met criteria for compassionate endpoint. As determined by the clinical pathologist, scores following *M. orygis* infection were due to prominent granulomatous and/or neutrophilic inflammation with varying degrees of necrosis not observed after *M. tb* challenge at either day 21 or day 28. This suggests exacerbation of lung damage in *M. orygis* lungs is likely the result of uncontrolled neutrophilic influx and subsequent recruitment of other inflammatory immune cells that is not recapitulated in *M. tb* infected mice[413–415].

Given that TB disproportionately affects males, both male and female mice were exposed to the same *M. orygis* inoculum via the aerosol route[60]. We determined that *M. orygis* infection outcome is sex-independent by measures of median survival (male= 25 days, female= 23.5 days) and bacterial burden (Figure 17a-c). Further, having observed that *M. orygis* is more virulent in

the same host, based on measured time to mortality, we asked whether *M. tb* could result in the same early mortality phenotype using a higher dose (Figure 17d). This permitted 2 sets of comparisons: whether a dose increase changed the intra-strain survival time (*M. tb* v. *M. tb*) and whether an increased dose of *M. tb* overcame the inter-strain differences in survival (*M. tb* v. *M. orygis*). When infected with a ~200 CFU of *M. tb*, median survival occurred at 241.5 days. Comparatively, when infected with ~1300 CFU *M. tb* median survival was expedited to ~95 days ($p < 0.0001$, Mantel-Cox) (Figure 19e). This was still four-times longer than observed with standard-dose *M. orygis* (median survival 24 days; $p< 0.05$, Mantel-Cox). At a comparable dose of *M. orygis* (~1300 CFU), median survival shifted to 20 days, a difference of only 4 days (Figure 17e). Moreover, at 28 days, macroscopic differences were apparent between the lungs of *M. orygis* infected mice (standard dose) and the high-dose *M. tb* group (Figure 17f). By this comparison, we estimate that the lethal dose 50 (LD50) of the two strains differs by at least one order of magnitude.

4.3 *M. orygis* morbidity and mortality is comparable to *M. bovis* but distinct from *M. tb* lineages

To determine if excessive mortality was unique to *M. orygis* infection, we assessed the survival of mice infected with *M. tb* Erdman, (a well-described *M. tb* strain used in pathogenesis studies), *M. bovis* Ravenel, *M. bovis* AF2122/97 (reference strain) and a clinical isolate of *M. orygis* known as '*M. orygis* 2019-352'[175,416]. The median survival time following challenge with either *M. orygis* or *M. bovis* strains was comparable (~24 days- 31 days) whereas median survival for both *M. tb* groups was greater than 30 weeks (Figure 18a). Moreover, like *M. orygis, M. bovis* infected mice showed aggressive lung pathology both micro- and macroscopically.

4.4 *M. orygis* mortality can be postponed, but not overcome

Given that BCG shows a protective effect against *M. tb*, we asked whether BCG vaccination could protect against pulmonary *M. orygis* infection. We utilized two BCG strains

(BCG Russia, an early strain, or BCG Danish, a late strain) as both *M. orygis* and BCG Russia constitutively produce two highly antigenic proteins (MPT70 and MPT83), whereas BCG Danish does not (Figure 18b)[103]. Following *M. orygis* challenge, 40% of the sham-vaccinated PBS group succumbed to infection by week 4 whereas no clinical signs of disease were seen in either BCG vaccinated group at this time point. At week 16, a secondary wave of mortality began, with all PBS-mice reaching compassionate endpoint by week 21 (Figure 18c). As such, BCG vaccination delayed but did not prevent mortality, and there was no difference in the median survival between BCG Russia or BCG Danish vaccinated mice (Figure 18c, 26.5 and 26 weeks respectively, $p >> 0.05$). Notably, prolonged survival in the vaccination groups was not due to prevention of infection or bacterial clearance; at the time of demise, lung bacterial burdens were comparable across groups (Figure 18d,e).

BCG has been proposed to better prevent extrapulmonary TB, although a systematic review of randomized controlled trials also found an effect against pulmonary TB[113]. In our experimental infections, we did not observe a difference in the lung:spleen ratio after vaccination (Figure 18f). Combined, these data indicate that BCG-mediated protection against *M. orygis* challenge is independent of MPT70 (and MPT83) expression in BCG and that protection by BCG acts on control, rather than clearance, of infection.

4.5 Proteome-guided virulence studies identify MPT70 as a non-canonical virulence factor

As discussed, it has previously been shown that *M. orygis*, like *M. bovis*, upregulates the production of the secreted protein MPT70, and the lipoprotein MPT83, due to an independent mutation in the regulator of Sigma Factor K (RskA)[185]. We have further validated this at both the genomic and proteomic level. However, prior studies did not offer information on how these differences compare to variations among other secreted proteins across the MTBC. To evaluate

this further, we compared the culture filtrates of various members of the MTBCs grown in parallel in the same medium, using mass spectrometry (Figure 19a). As previously seen, the dominant proteins of both *M. bovis* and *M. orygis* were ESAT-6, CFP-10, and MPT70. In contrast, whereas ESAT-6 and CFP-10 were still the most abundant proteins in the culture filtrates of all *M. tb* strains and *M. africanum*, MPT70 spectra were rare (Figure 19a). This is concordant with previous studies in which *M. tb mpt70* is only induced following infection[187,393]. As expected ESAT-6, CFP-10, and MPT70 spectra were rare in *M. microti,* a natural variant of ESAT-6/CFP-10[49,417]. Notably, we included *M. tb* HN878 in this study, as it is regarded as a 'hypervirulent' *M. tb* strain (though this phenotype may be impaired following multiple passages) and *M. microti,* as a naturally attenuated, animal-associated strain[418–420,421].

Given the *in vitro* and *ex vivo* results described in Chapter III, we employed these *M. orygis* and *M. bovis* deletion strains in downstream *in vivo* infection studies. As a positive control, we generated *esxA* mutants, to disrupt the canonical virulence factor ESAT-6, and indirectly, CFP-10[422,423]. Accordingly, mice infected with either *M. bovis ΔesxA* or *M. orygis ΔesxA* via the aerosol route showed no mortality events until experimental endpoint (~42 weeks post-challenge) (Figure 19b; survival curves superimposed). When performing head-to-head studies, *M. orygis ΔesxA* infected mice showed ~1 $\log_{10}$ less bacteria in the lung compared to WT *M. orygis* as early as day 7, ~2 $\log_{10}$ less burden by day 14 and ~3 $\log_{10}$ less burden by day 21 (Figure 19c). These data suggest that for *M. orygis*, like *M. tb* and *M. bovis*, the disruption of ESAT-6 results in significant attenuation.

Whether MPT70 is a virulence factor for *M. bovis* has yet to be formally demonstrated[424]. To determine if the effect of MPT70 and/or MPT83 is host-mediated, mice were first infected with an *M. bovis* strain disrupted for three genes: *mpt70, mpt83,* and *dipZ*, the gene in between the two

putative effectors (*M. bovis Δmpt70_mpt83*) (Figure 20a). Strikingly, the disruption of these three genes resulted in a reversal of the mortality phenotype observed in wildtype *M. bovis* studies, with only one event seen by experimental endpoint (Figure 20b). As early as week 3, mice showed ~1 $\log_{10}$ reduced bacterial burden and significantly milder pathology (reduced inflammation, smaller lesions, limited consolidation) compared to WT *M. bovis* despite comparable doses at initial aerosol (Figure 20c-e). Moreover, there was a 5-$\log_{10}$ decrease in *M. bovis Δmpt70_mpt83* burden between week 3 and 52, with a subset showing bacterial elimination from the lungs after one year, although bacteria were still present in the spleen (Figure 20f-i).

To narrow down the potential virulence factor, both *M. bovis Δmpt70* and *M. bovis Δmpt83* were generated. By experimental endpoint (T=24 weeks post challenge), only 2 out of 45 mice had succumbed to *M. bovis Δmpt70* infection (Figure 20b). Additionally, *M. bovis Δmpt70* infected mice showed ~1 $\log_{10}$ reduced lung burden compared to WT *M. bovis* infected mice at week 3 and a further ~3 $\log_{10}$ reduction between weeks 3 and 16 (Figure 20c,d), with mild histopathology (Figure 20e). These results were also seen following aerosol challenge with *M. bovis Δmpt83*. By experimental endpoint, 1/15 mice had succumbed to infection (Figure 20b). Like *M. bovis Δmpt70* infected mice, a ~1 $\log_{10}$ reduced lung burden was observed in *M. bovis Δmpt83* infected mice compared to WT *M. bovis* at the same timepoint (week 3, n= 3). Moreover, a further ~2 $\log_{10}$ reduction was observed between weeks 3 and 16 (Figure 20c,d). Histopathology was mild compared to WT *M. bovis* infected lungs (at week 3) (Figure 20e).

4.6 *M. bovis Δmpt70_mpt83* prolongs survival in the absence of the adaptive immune system

By day 21, the host adaptive immune system is fully functional. RAG1 -/- mice lack mature B- and T- cells due to an impairment in the activation of V(D)J recombination and as such, lack an adaptive immune system[425]. To further investigate how MPT70 and/or MPT83 mediates the early

events of host immune response, RAG1 -/- mice were infected with comparable doses of either *M. bovis* or *M. bovis Δmpt70_mpt83* and monitored for clinical disease (Figure 20j). In stark contrast to immunocompetent mice where median survival could not be reached, all mice in the *M. bovis Δmpt70_mpt83* experimental group succumbed before day 50 (Figure 20k). The absence of MPT70 and MPT83 continues to show protection compared to *M. bovis* WT infection, though to a much lesser extent. We can consider this at two levels: first, *M. bovis Δmpt70_mpt83* survive longer than *M. bovis* infected mice (median survival 39 days v. 30 days, respectively; $p < 0.05$). Second, though infection in general is much more poorly controlled compared to wildtype C57BL/6 mice, *M. bovis Δmpt70_mpt83* still shows a slight reduction in bacterial burden at experimental endpoint (~1/3 $\log_{10}$; $p < 0.05$) (Figure 20l). These data demonstrate that MPT70 and MPT83 are prime virulence factors of *M. bovis* and may have a role in infection chronicity.

4.7 *M. orygis* shows distinct virulence profile compared to *M. bovis*

When *M. orygis* was disrupted for either *mpt70* alone, *mpt83* alone, or *mpt70_mpt83,* the reversal of the lethal phenotype could not be recapitulated (Figure 21a). Additionally, no reduction of bacterial burden can be observed at days 7, 14, or 21 compared to wildtype *M. orygis* (Figure 21b). As proposed in Chapter III, this latter *in vivo* result may suggest that the role of these genes in the overall virulence of *M. orygis* differs from that of *M. bovis*, and/or that *M. orygis* is more virulent in this host, such that disruption of one locus is insufficient to reverse early mortality.

Notably, it has been shown that ESAT-6, but not MPT70, confers protection against *M. tb* challenge[411]. As an alternative means to test for a role of *mpt70* on the outcome of *M. orygis* infection, we asked whether vaccination with an MPT70 subunit vaccine could confer protection against disease (Figure 21c,d). PBS-sham vaccinated, and BCG Russia-vaccinated mice served as negative and positive controls, respectively, with median mortalities of 24- and 171-days post-

infection (Figure 21d). Consistent with the established role of ESAT-6 in vaccination and its newly shown role in *M. orygis* virulence, the ESAT-6 vaccine extended survival to 112 days. Interestingly, mice subcutaneously vaccinated with MPT70 also manifested a similar survival of 119 days (Figure 21d). This observation that MPT70 alone prolongs survival with the same efficacy of ESAT-6 vaccination indirectly supports a role of MPT70 in the pathogenesis of *M. orygis* disease.

5. Discussion

M. orygis is overlooked and understudied. Our data on this pathogen provide a new perspective to investigate the evolution of MTBC virulence, beyond *M. tb* and *M. bovis*. We utilized the standard aerosol infection model to evaluate *M. orygis* outcomes in comparison to more well-established pathogens[327]. In doing so, we are the first to demonstrate that *M. orygis* is a hypervirulent member of the MTBC subspecies, like *M. bovis*. Whether using relative virulence or pathogenic potential as a measure of the ability of a microorganism to cause disease, aerosol infection with *M. orygis* leads to faster mortality, at a lower dose, compared to *M. tb* in the same host. Due to the severity of this phenotype, our study may provide a new experimental approach for the study of tuberculosis pathogenesis. Three advantages emerge immediately from our data. First, the experimental endpoint is objective — mortality cannot be misinterpreted. Second, the experimental read-out is based on host outcome, rather than bacterial counts. Third, the experimental conclusion is fast —attenuation of candidate virulence factors can be inferred sooner than the time it takes to count colonies from the first timepoint after infection.

We see that there is a ‘critical inflection point’ following aerosol infection which occurs between day 21 and 28. Based on when mortality occurs temporally, we speculate that this may be dictated by 1) activation, or hyper-activation, of the innate and adaptive immune cells, 2) a ‘threshold’ of host-pathogen damage that can be withstood or 3) a combination of both. Immune

cell populations present in the lung differ between mice which succumb to infection by 28 days when compared to mice which succumb to infection by 4 months (112 days). Neutrophils dominate the lungs of the early mortality cohort, whereas macrophages predominate the late mortality cohort (not shown). This lends itself to the idea of the host-damage threshold. Importantly, it has been established that neutrophils act as the sentinels for early *M. tb* infection and stimulate the activation of additional immune cells such as monocytes, dendritic cells and T-cells[426]. It has also been well-established that neutrophils cause significant inflammation and damage as a product of this 'protective' mechanism[413–415,426]. A cornerstone of *M. tb* infection is the ability to evade and exploit the host immune system[427]. However, as previously shown, one of the essential differences between *M. tb, M. bovis* and *M. orygis* is the secretion of the highly antigenic, MPT70[185]. Based on our data, it may be feasible that *M. orygis*- and *M. bovis*- antagonize innate immune cells, resulting in a cycle of uncontrolled inflammation and immune cell recruitment. As such, we speculate that the first inflection point (mortality at 28 days) in our model is largely caused by immune recruitment whereas the second inflection point (mortality at 4 months) seen in both *M. bovis* and *M. orygis* is likely due to immune exhaustion[428]. This may be further supported by chronic *M. tb* infection, as mice begin to succumb to infection at the same 4-month timeframe, as well as our long-term vaccination studies.

Moreover, *M. bovis* aerosol infection is not commonly done using a mouse model. In our study, mice infected with *M. bovis* in which MPT70 and/or MPT83 are absent show significant reduction in inflammation and pathology both macro- and microscopically compared to wildtype. This is likely due to the absence of MPT70/83 antagonism i.e. the host-immune system is not exposed to antigens prior to pathogen uptake and may be able to better modulate pro-inflammatory responses. In tandem, when MPT70 and/or MPT83 are missing, infection is cleared over time,

though the mechanism for this is still unknown. To our knowledge, this is a unique phenotype that has not been seen in knockout studies of other virulence factors; however, this 'clearance phenotype' has been seen in natural infections[429,430].

Translationally, this infection model poses two challenges for vaccine research while also providing opportunities for their study. Can a candidate vaccine overcome early mortality? If so, can this vaccine protect better than the current 'gold standard' (BCG)? Due to the severity of this phenotype, we suggest that our experimental model may serve in the up- or down-selection of new vaccine candidates. As shown in Figures 3 and 5, within 8-12 weeks, the potential efficacy -and thus, viability- of vaccines can be compared. Clemmensen et al. previously published that an MPT70 expressing vaccine conferred lower levels of protection than an ESAT-6 expressing vaccine against WT *M. tb* infection but that this protection was significantly increased when challenged with *M. tb* overexpressing MPT70[411]. Our data is concordant with these results: antigen-driven vaccines protected *M. orygis* challenged mice from early mortality but could only partially recapitulate the effect of BCG. As such, our data also supports the possibility that tailored vaccines may be required to protect against different members of the MTBC and reinforces a key limitation of current vaccines in this experimental model, which is that they modulate disease but do not prevent the establishment of infection.

Much of our understanding of virulence within the MTBC is derived from studies of a single human-adapted strain, *M. tb*, or less commonly, from the study of a single animal-associated strain, *M. bovis*. These reference points provide useful contrasts but are insufficient to fully elucidate the evolution of MTBC pathogenicity. Presently, the MTBCs are pragmatically divided into virulent clinical strains, such as *M. tb,* versus attenuated vaccine strains, such as BCG and *M. microti*[417]. Our data suggest a third level of virulence which we call 'hypervirulence'. As shown

with our *M. bovis* gene deletion strains, virulence factors may be overlooked when using H37Rv as the parent strain, due to their absence or low-level of expression in *M. tb in vitro*[431]. Accordingly, our model could be useful in the discovery and investigation of other non-canonical virulence factors. By using proteomic analysis of 3 MTBC strains, candidate virulence factors could be identified and subject to gene deletion studies, with the impact on infection outcome seen within 4 weeks of aerosol exposure. Moreover, we provide data supporting the existence of both across-MTBC virulence factors as well as MTBC subspecies-specific virulence factors. The former is supported by the *M. bovis* or *M. orygis* lacking *esxA*, where no mortality was documented until experimental endpoint. Though expected, this experiment showed that *M. orygis,* like *M. tb* and *M. bovis,* depends on ESAT-6 for full virulence. As suggested previously, the notion that MPT70 could be a virulence factor has been considered since it was adequately characterized in 1984[101], yet efforts to characterize this protein have been limited- perhaps because a role during *M. tb* infection has not been identified[393,394]. Using *in vitro* and *ex vivo* techniques, we found that differences between wildtype and knockout strains were subtle, with no indication of a significant role in the mediation of virulence. However much like ESAT-6, the absence of MPT70 from *M. bovis* results in significant attenuation. Moreover, our gene disruption studies in *M. bovis* indicate that MPT70 contributes to long-term infection persistence, as both the *Δmpt70_mpt83* and *Δmpt70* strains showed a trend towards bacterial elimination over time. Based on our data, we propose that MPT70 contributes to the hypervirulence of *M. bovis* but that there may be additional partners contributing to the hypervirulence of *M. orygis.* Unlike *M. bovis Δmpt70_mpt83,* the effect of MPT70 and/or MPT83 disruption was insufficient to rescue *M. orygis* lethality during the acute phase of infection. However, vaccination with MPT70 alone did delay mortality following *M. orygis* challenge, to the same extent as ESAT-6, suggesting the need for further study of MPT70

and/or MPT83 in *M. orygis* infection. This is further supported by secretomic differences such as bias towards ESX-5 in *M. orygis,* but not *M. bovis.* As many canonical virulence factors include lipids and lipid-associated proteins, lipidomics may provide further insights into differential virulence[247,263,432].

The definition of bacterial virulence varies by the context in which it is applied. Traditionally, it is defined as the manifestation and severity of disease pathology, including death, in a susceptible host[247]. In this chapter, we define virulence accordingly, as the severity of infection outcome following the same infection, measured in the same host. Our three-way comparative findings build upon a century of observations where *M. bovis* has been observed to be more virulent than *M. tb* across many host species, such as mice, guinea pigs, and rabbits[16,198,433]. It has been difficult to resolve a two-bacteria comparison (*M. bovis* vs. *M. tb*), without a third comparator species. Our findings present at least two possible evolutionary scenarios, which are not mutually exclusive. Either *M. tb* has suffered attenuation of virulence since their common ancestor, and/or *M. orygis* and *M. bovis* have both incurred a gain-of-virulence since their common ancestor (Figure 22). Despite the longevity of tuberculosis research, we still do not know why MTBC members have different niches and differential infection outcomes, nor why *M. tb* is largely restricted to humans while *M. orygis* and *M. bovis* have much broader host ranges. The inclusion of *M. orygis* in TB research may help address these and other knowledge gaps and provide new opportunities for MTBC pathogenesis research.

6. Figures

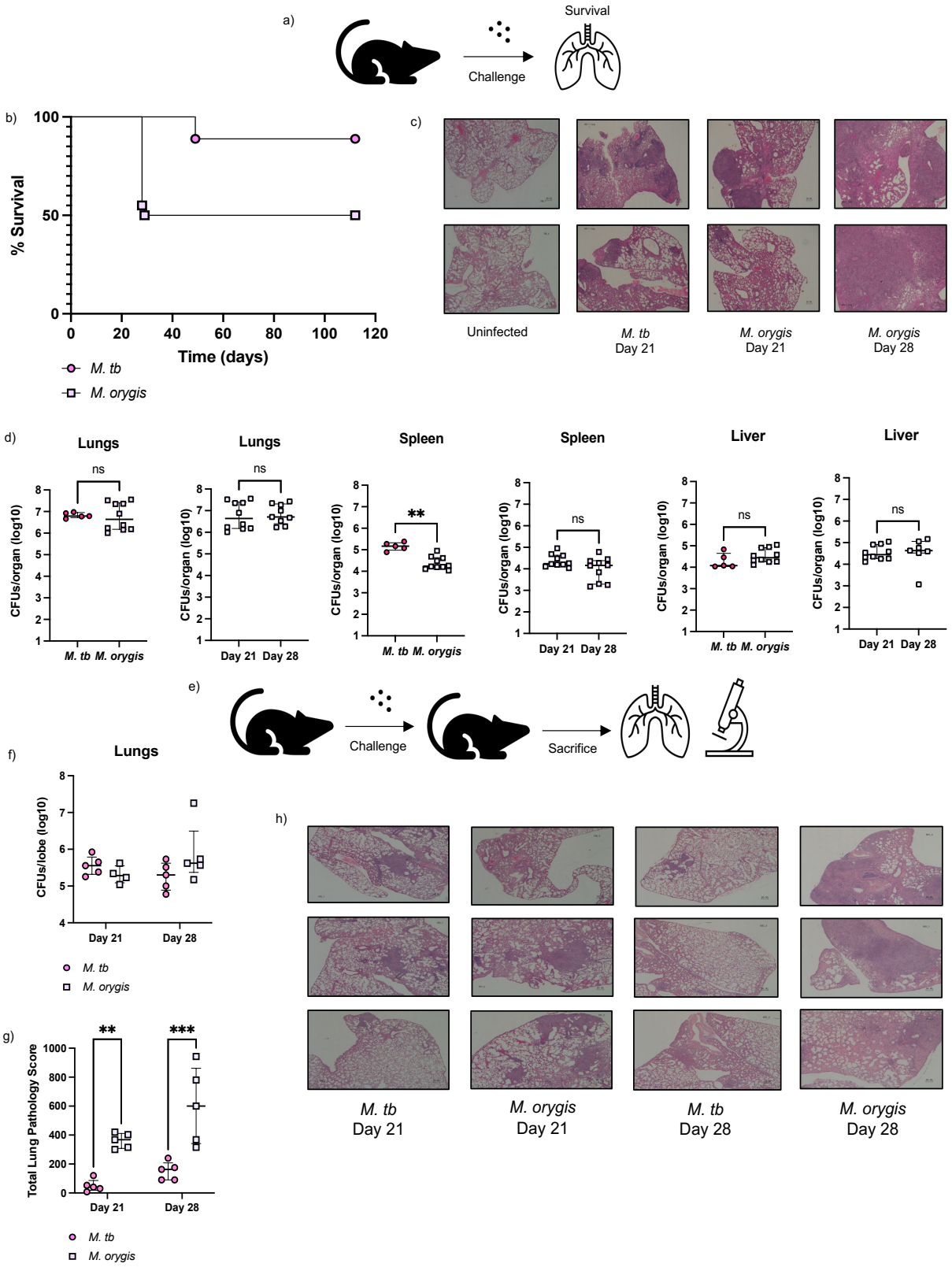
a)
Challenge
Survival
b)
% Survival
Time (days)
M. tb
M. orygis
c)
Uninfected
M. tb Day 21
M. orygis Day 21
M. orygis Day 28
d)
Lungs
Lungs
Spleen
Spleen
Liver
Liver
CFUs/organ (log10)
ns
**
M. tb M. orygis
Day 21 Day 28
e)
Challenge
Sacrifice
f)
Lungs
CFUs/lobe (log10)
Day 21
Day 28
M. tb
M. orygis
g)
Total Lung Pathology Score
**
***
h)
M. tb Day 21
M. orygis Day 21
M. tb Day 28
M. orygis Day 28

Figure 16. *M. orygis* results in progressive fatal disease following aerosol infection of C57BL/6 mice.

a) Schematic of aerosol challenge. C57BL/6 mice were exposed to ~200 CFU of either *M. tb* H37Rv or *M. orygis* 51145 (n= 2 experiments). *M. tb* H37Rv infection group n= 18 mice, *M. orygis* 51145 infection group n= 36. Three mice per experiment were tested to verify initial dose. Five mice per experiment were sacrificed at T= 21 days. The remaining 10 mice were monitored for signs of clinical disease until compassionate endpoint or experimental endpoint (n= 112 days) **b)** Kaplan-Meier survival curve following aerosol. *M. orygis* median survival= 28 days. *M. tb* H37Rv median survival could not be determined by experimental endpoint. (Mantel-Cox test, p= 0.047). **c)** Hematoxylin and eosin (H&E) staining of right accessory lobe of lung for both experimental groups. **d)** Comparison of lung, spleen, and liver bacterial burdens. *M. tb* and *M. orygis* showed comparable lung and liver bacterial burdens at T= 21 days, with increased splenic burden in *M. tb* group (p= 0.013, Mann-Whitney U-test). Between day 21 and day 28 there was no significant difference in lung, spleen, or liver burdens within the *M. orygis* infected group. **e)** Schematic of targeted lung infection. Mice were challenged with ~200 CFU of either *M. tb* H37Rv of *M. orygis* 51145. Five C57BL/6 mice were randomized to be sacrificed at either day 21 or day 28 timepoints (n= 10 mice per group). **f)** Lung bacterial burden of *M. tb* and *M. orygis* infected groups at week 3 and 4. **g)** Total lung pathology score. *M. orygis* group resulted in greater pathology than *M. tb* at both day 21 and day 28 (Two-way ANOVA, p= 0.0062, p= 0.0002 respectively). The lowest *M. orygis* pathology score at 21 days was higher than the maximum pathology score of *M. tb* at 28 days. **h)** Associated hematoxylin and eosin (H&E) staining of right accessory lobe of lung at day 21 or day 28. Featured slides representative of material sent to pathologist for assessment.

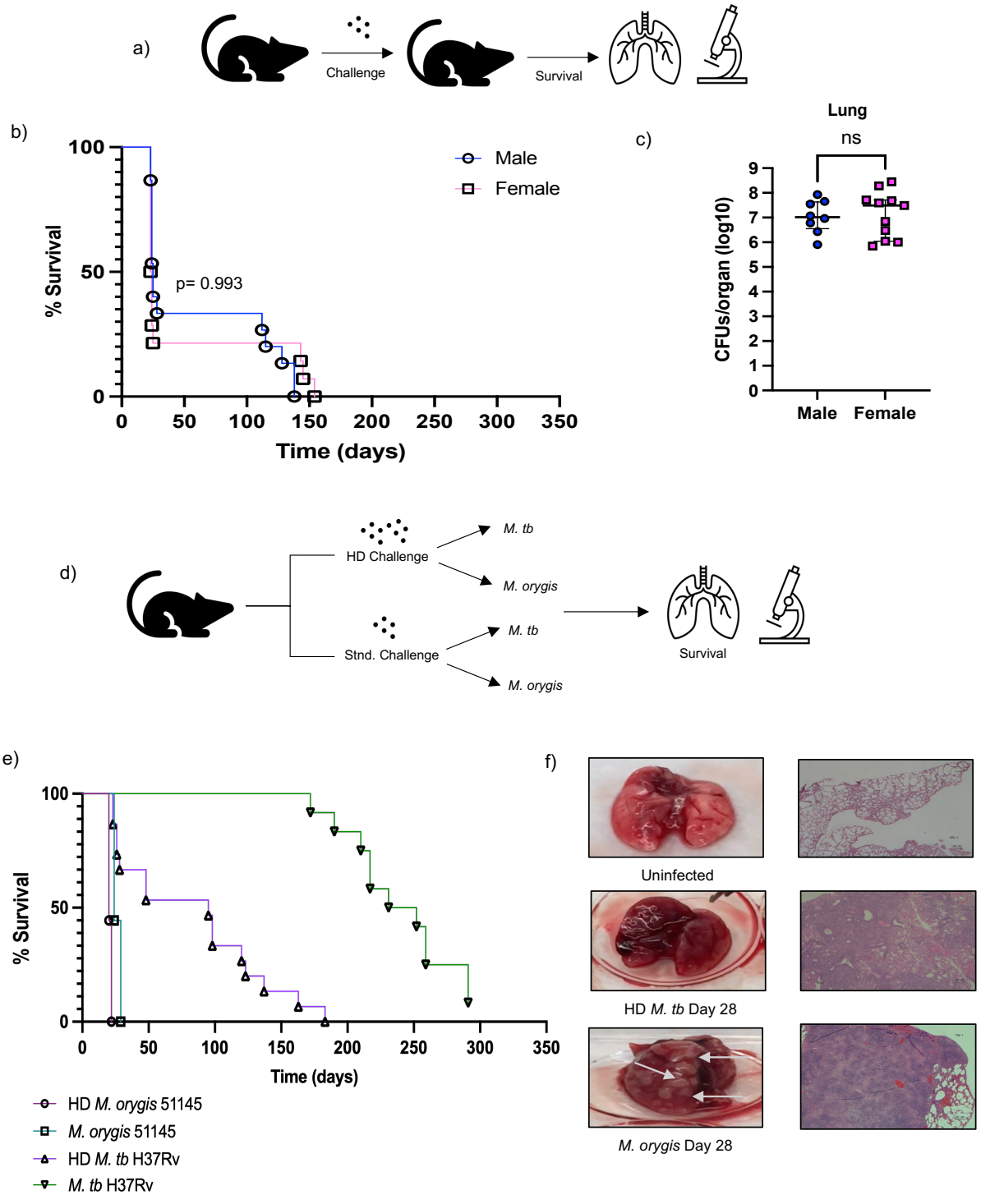

Figure 17. *M. orygis* infection outcome is sex- and dose-independent

a) Overview of survival experiment. Given that *M. tb* disproportionately affects males, both male and female mice were infected to assess potential differences in survival outcomes and lung

bacterial burdens. Male and female C57BL/6 mice were exposed to ~150-300 CFU of *M. orygis* via the aerosol route (n= 18 mice per experimental group; 3 mice per group sacrificed to determine initial dose). Remaining mice were monitored for clinical signs of disease until compassionate endpoint was reached. **b)** Kaplan-Meier survival curve following aerosol infection. Median survival of males= 25 days; median survival of females= 23.5 days (Mantel-Cox test, p= 0.993). **c)** Lung bacterial burdens at compassionate endpoint. Regardless of when mice succumbed to infection, bacterial burden was not significantly different (Mann-Whitney test, p= 0.778). **d)** Overview of dosing experiment. Mice divided into four arms: *M. tb* standard dose (stnd), *M. orygis* standard dose (stnd), *M. tb* high dose (HD), *M. orygis* high dose (HD) and monitored until compassionate endpoint. **e)** Kaplan-Meier survival curve of *M. tb* H37Rv and *M. orygis* 51145 at a standard dose compared to high dose (HD) *M. tb* and HD *M. orygis* (~1300 CFU). Standard *M. tb* curve generated from independent experiment (Fig. 20, n=12 mice). Median survival of standard *M. orygis* = 24 days (n= 9 mice). Median survival of HD *M. tb* = 95 days (n=15 mice). Median survival of HD *M. orygis*= 20 days (n= 9 mice). Median survival of standard *M. tb*= 241 days. Survival of HD *M. tb* infected mice is significantly longer compared to *M. orygis* infected mice at a standard dose (Mantel-Cox test, p = 0.0072). **f)** Macroscopic photos of lungs following euthanasia with corresponding hematoxylin and eosin (H&E) staining of right accessory lobe of lung at same timepoint. *M. orygis* at a standard dose (~200 CFU) showed more extensive pathology compared to HD *M. tb* (~1300 CFU).

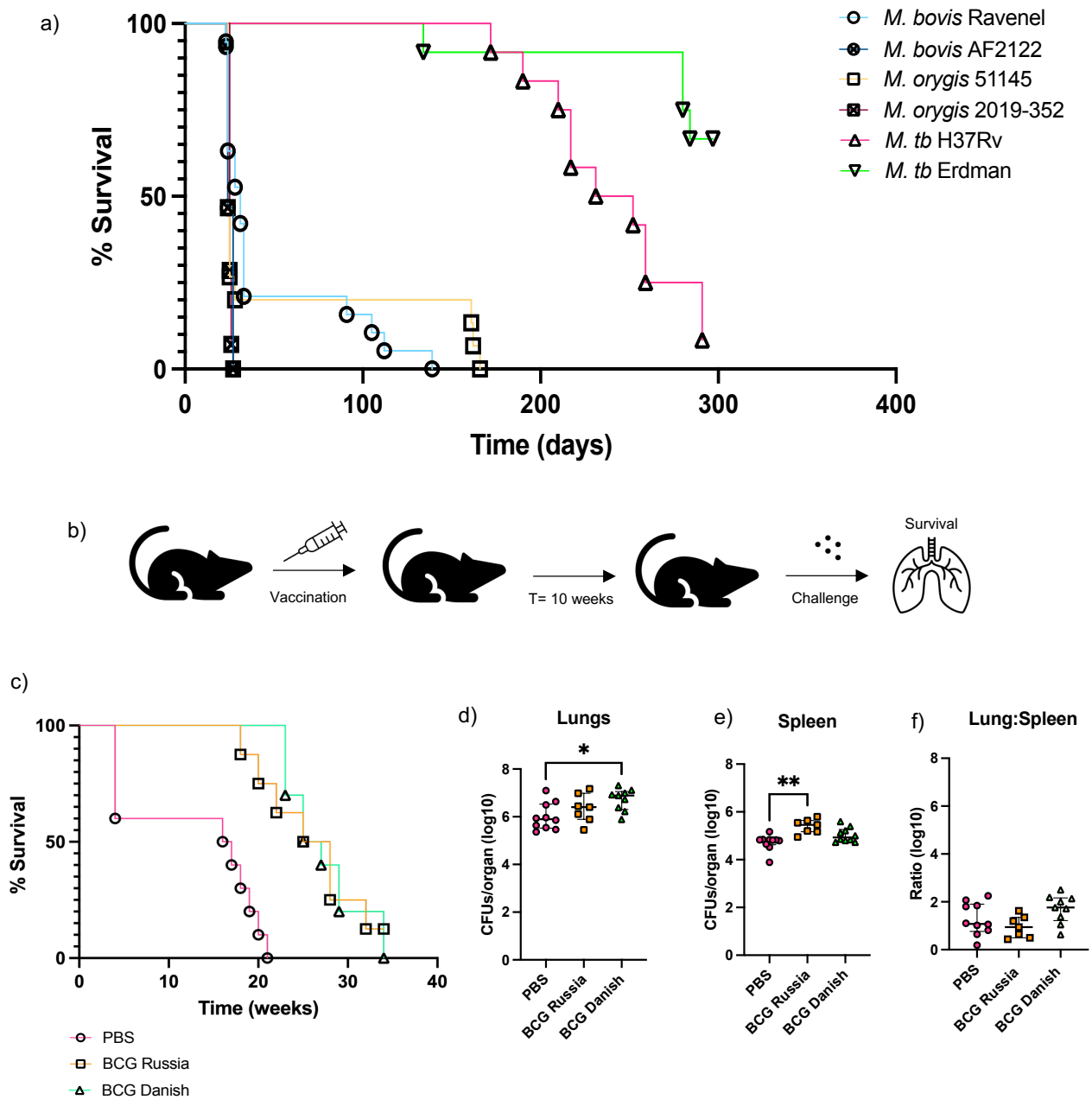

Figure 18. *M. orygis* mortality is comparable to *M. bovis*, distinct from *M. tuberculosis,* but can be postponed by BCG vaccination.

a) Kaplan-Meier survival curves of standard dose *M. orygis* 51145 (reference strain), *M. orygis* 2019-352, *M. bovis* Ravenel, *M. bovis* AF2122/97 (reference strain), *M. tb* H37Rv (reference strain) and *M. tb* Erdman. *M. orygis* 2019-352 is a clinical isolate from the Public Health Ontario

Laboratory. Mice were exposed to ~200 CFU of various members of the *Mycobacterium tuberculosis* complex subspecies (*M. bovis* Ravenel*, M. bovis* AF2122/97, *M. orygis* 51145*, M. or* 2019-352: n= 18 mice; *M. tb* H37Rv and *M. tb* Erdman: n= 15 mice). Median survival: *M. bovis* Ravenel = 31 days, *M. bovis* AF2122/97= 25 days, *M. orygis* 51145 = 24 days, *M. orygis* 2019-352 = 25 days; *M. tb* H37Rv = 241 days. Median survival could not be determined by experimental endpoint for *M. tb* Erdman. **b)** Schematic overview of vaccination. C57BL/6 mice were subcutaneously vaccinated with BCG Russia and BCG Danish (~10^6 CFU) alongside a PBS sham-vaccinated control. 10 weeks post vaccination, mice were challenged with ~200 CFU of *M. orygis* and monitored until compassionate or experimental endpoint (T= 34 weeks). **c)** Kaplan Meier survival curve of PBS sham-vaccinated mice, BCG Russia, and BCG Danish vaccinated mice (n= 10 mice per group). Median survival: PBS = 16 weeks, BCG Russia= 26.5 weeks, BCG Danish= 26 weeks. One BCG Russia vaccinated mouse survived until experimental endpoint (n= 34 weeks). **d)** Lung bacterial burden at compassionate endpoint. BCG Danish vaccinated group had increased burden compared to the PBS sham-vaccinated group (Kruskal-Wallis test, p= 0.030). **e)** Spleen bacterial burden at compassionate endpoint. BCG Russia vaccinated mice had increased burden at endpoint compared to PBS-sham vaccinated mice (Kruskal-Wallis test, p= 0.002). **f)** Lung:spleen ratio of PBS, BCG Russia and BCG Danish vaccinated mice, showing no significant difference across groups.

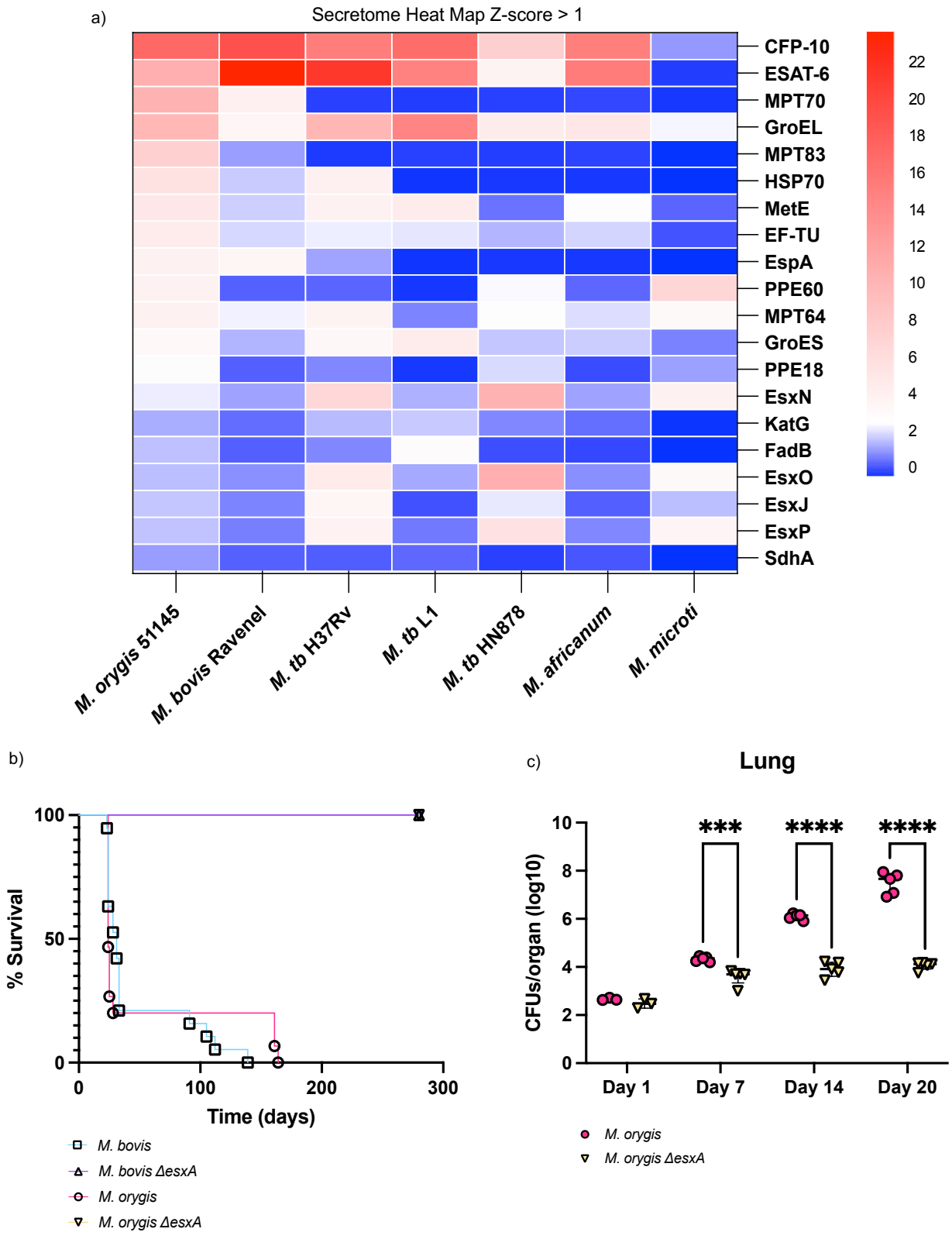

Figure 19. Proteomic comparisons yield insight into *M. orygis* virulence.

a) Comparative heat-map of various MTBC secretomes (*M. orygis* 51145, *M. bovis* Ravenel, *M. tb* H37Rv, *M. tb* lineage 1, *M. tb* HN878, *M. africanum,* and *M. microti).* Proteins of interest ranked using *M. orygis* (Z-score > 1). Each row represents a specific protein; each column represents average of triplicate samples (expect for *M. tb* H37Rv in which this is a duplicate). Colour intensity indicative of abundance of protein based on raw Z-scores. Heatmap made using GraphPad Prism v10.0.3. **b)** Kaplan-Meier survival curve of two cattle-associated isogenic strains (*M. bovis ΔesxA* and *M. orygis ΔesxA*) compared to wildtype *M. bovis* Ravenel and *M. orygis* 51145 until experimental endpoint (T~300 days, n= 15 mice per isogenic group). Isogenic survival curves overlayed. *M. bovis* and *M. orygis* survival curves representative of independent experiments. **c)** Lung bacterial burden at Day 1, 7, 14 and 20 of *M. orygis* (51145) and *M. orygis esxA*. Despite comparable initial dosing, divergence in bacterial burden between groups was evident as early as Day 7, with the greatest difference occurring at 20 days (n= 5 mice per timepoint, per group) (2-way ANOVA, $p < 0.001$ at all timepoints).

Figure 20. *mpt70* disruption reverses lethality in *M. bovis*

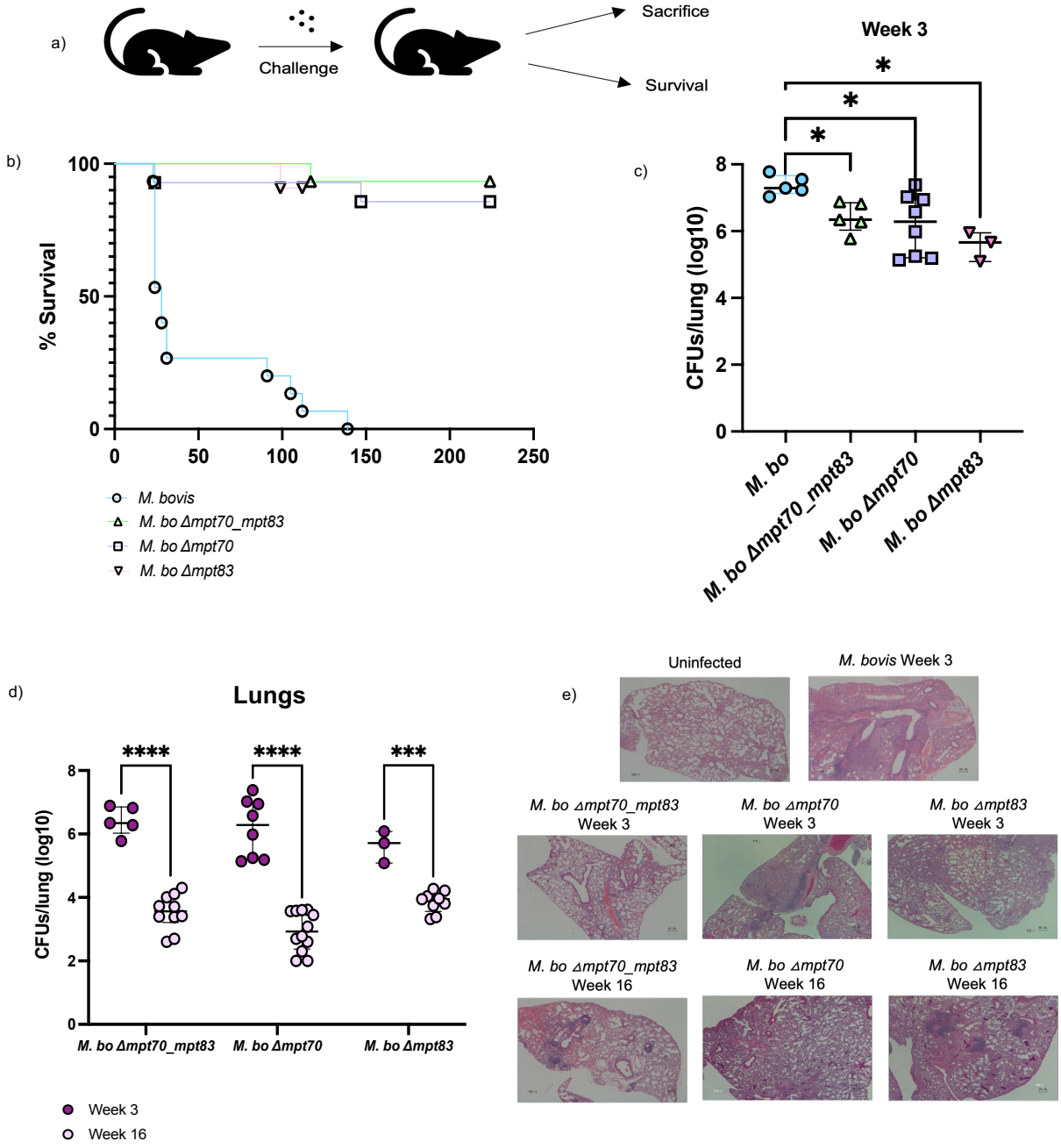

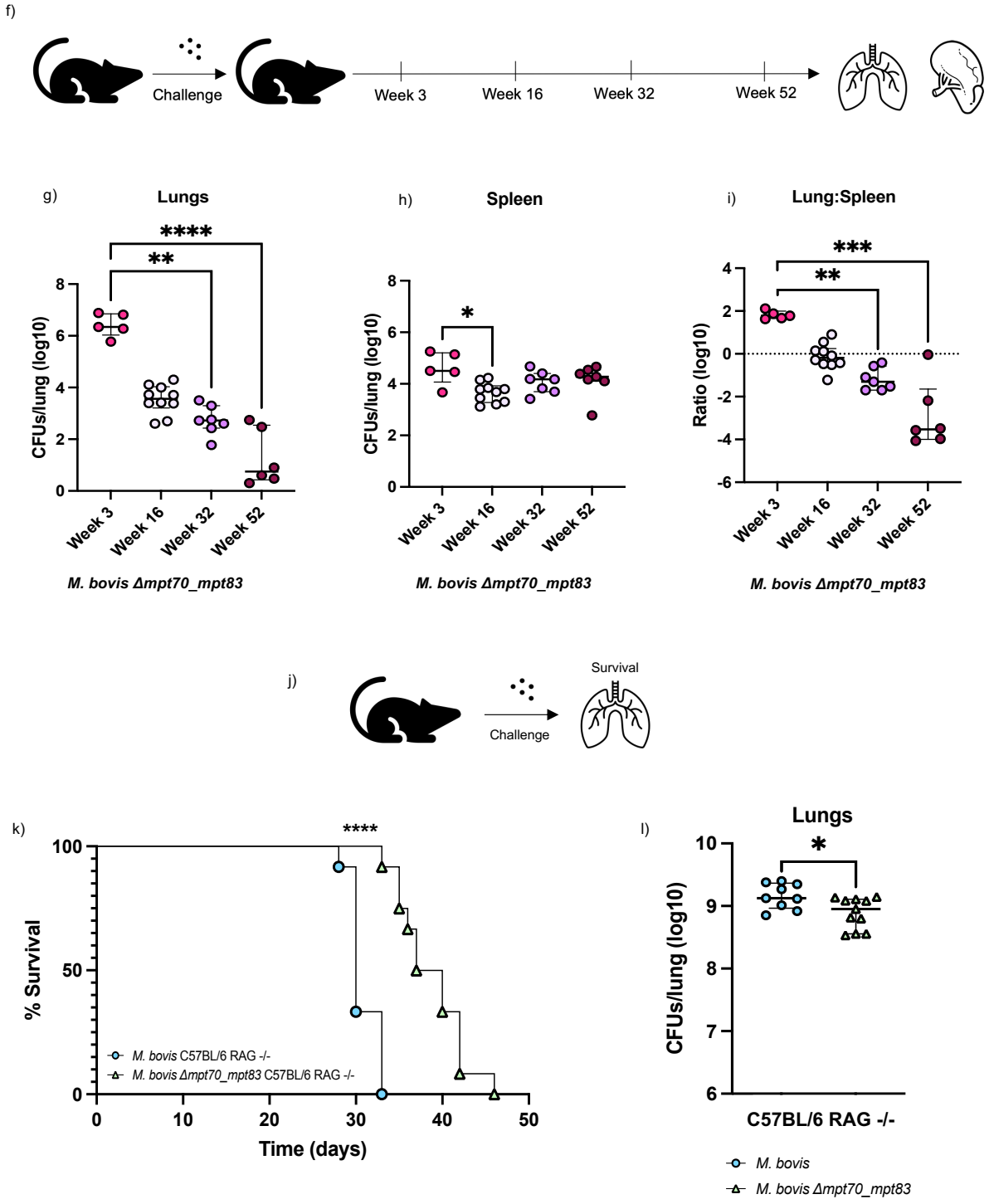

Figure 20. ***mpt70*** **disruption reverses lethality in** ***M. bovis***

a) Schematic of experimental infection. Mice were either randomly assigned for assessment at experimental timepoints or monitored for clinical disease until compassionate/experimental

endpoint. **b)** Kaplan-Meier survival curve of *M. bovis, M. bovis Δmpt70_mpt83*, *M. bovis Δmpt70,* and *M. bovis Δmpt83*. *M. bovis* curve representative of control experiment. Experimental endpoint of *M. bovis Δmpt70_mpt83* and *Δmpt70*= 32 weeks (224 days); experimental endpoint of *M. bovis Δmpt83*= 16 weeks (112 days). Dosing: WT *M. bovis* ~170 CFU, *M. bovis Δmpt70_mpt83* ~250 CFU, *M. bovis Δmpt70* ~300, *M. bovis Δmpt83* ~350 CFU **c)** Lung bacterial burden at week 3. *M. bovis* and *M. bovis Δmpt70_mpt83* infected groups n= 5 mice/group; *M. bovis Δmpt70* group n= 8 mice (2 experiments); *M. bovis Δmpt83* group n= 3 mice (proof of concept). All isogenic strains showed significantly reduced burden following aerosol infection (Kruskal-Wallis test; *M. bovis Δmpt70_mpt83*: p= 0.030, *M. bovis Δmpt70*: p= 0.012; *M. bovis Δmpt83*: p=0.002). **d)** Lung burden of *M. bovis Δmpt70_mpt83, M. bovis Δmpt70,* and *M. bovis Δmpt83* at 3- and 16-weeks. A ~3 log reduction was observed by endpoint in all isogenic strains ($p < 0.0001$, 2-way ANOVA). **e)** Histopathology of right accessory lobe at week 3 and week 16 compared to uninfected control (H&E stain, n= 5 mice/group). Photos representative of overall mouse pathology. **f)** Schematic of *M. bovis Δmpt70_mpt83* aerosol infection. Mice were randomly selected for euthanasia at week 3, 16, 32, or 52. Results representative of n= 2 independent experiments. At experimental endpoint, lungs and spleen were evaluated for bacterial burden; right accessory lobe of lung was extracted for histopathological assessment. **g)** Lung burden of *M. bovis Δmpt70_mpt83* at week 3, 16, 32 and 52. Bacterial burden reduced by ~5 logs between week 3 and 52 ($p < 0.0001$, 2-way ANOVA). **h)** Splenic bacterial burden of *M. bovis Δmpt70_mpt83* monitored at weeks 3, 16, 32 and 52 following aerosol infection. Spleens showed no significant reduction in bacterial burden at week 32 or 52 compared to week 3 burden (2-way ANOVA, $p > 0.05$). **i)** Corresponding lung:spleen ratio over time; by week 52, splenic burden was greater than lung bacterial burden (Kruskal-Wallis test, p= 0.0001). **j)** Overview of experimental design. **k)** Kaplan-Meier survival curve of C57BL/6 RAG

-/- mice infected with either WT *M. bovis* or *M. bovis Δmpt70_mpt83.* Median survival: *M. bovis* WT= 30 days, *M. bovis Δmpt70_mpt83*= 39 days (~350 CFU in both experimental groups). *M. bovis Δmpt70_mpt83* shows prolonged survival compared to *M. bovis* WT ($p < 0.01$). **l)** Associated lung bacterial burden at compassionate endpoint. WT *M. bovis* infected mice have significantly higher burden compared to *M. bovis Δmpt70_mpt83* at compassionate endpoint ($p = 0.03$, Mann-Whitney). Lung bacterial burden is increased in both experimental groups in RAG -/- mice compared to WT C57BL/6 mice.

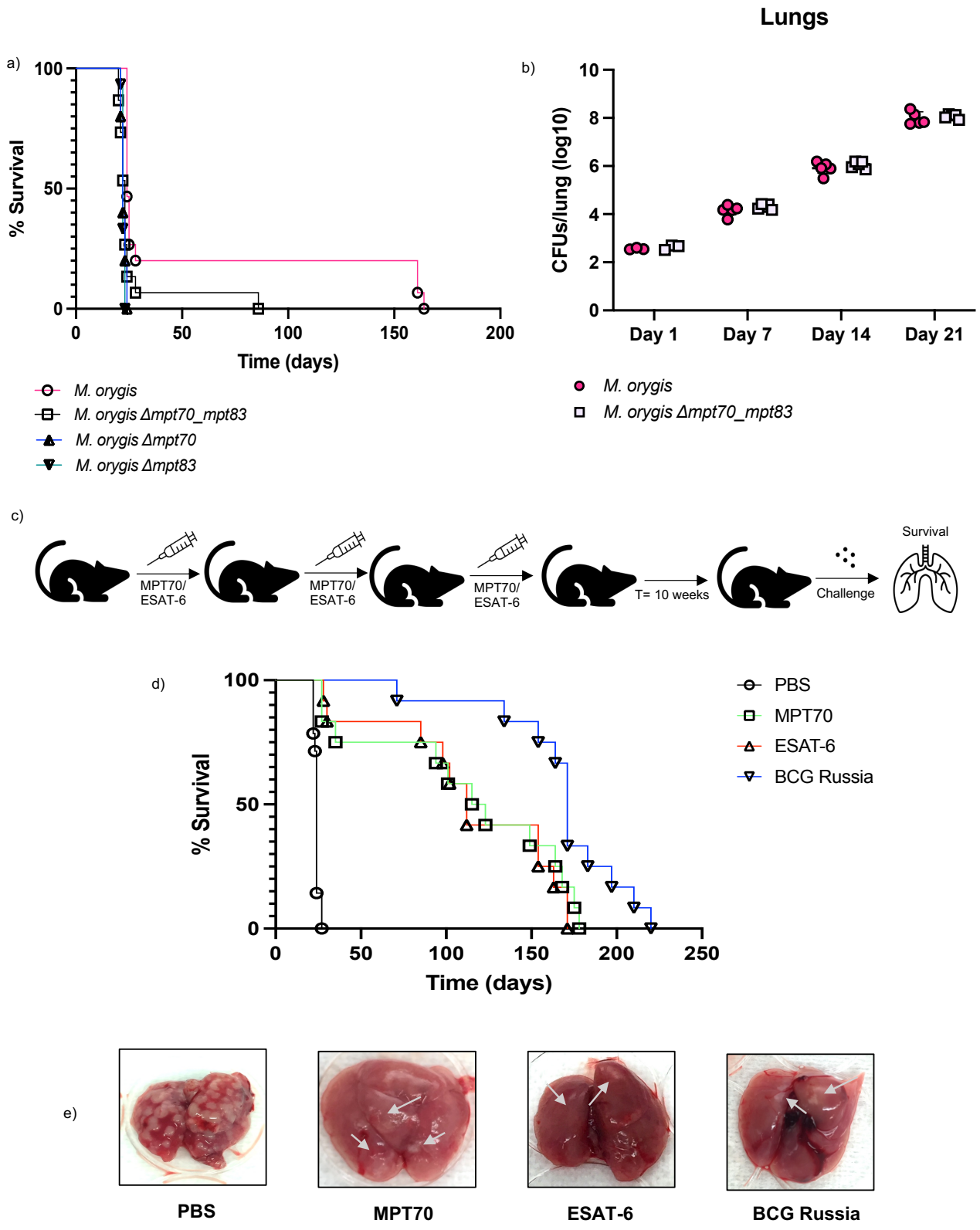

Figure 21. *mpt70* immunization prolongs survival following *M. orygis* aerosol challenge.

a) Kaplan-Meier curve of WT *M. orygis* compared to *M. orygis Δmpt70_mpt83* (2 experiments, n= 30 mice), *M. orygis Δmpt70* (1 experiment, n= 15 mice) and *M. orygis Δmpt83* (1 experiment, n= 15 mice) following aerosol infection. *M. orygis* WT curve representative of control experiment. Median survival of *M. orygis* WT = 24 days; *M. orygis Δmpt70_mpt83* = 23 days; *M. orygis Δmpt70* and *M. orygis Δmpt83*= 22 days, Dosing: *M. orygis Δmpt70_mpt83* ~180 CFU; *M. orygis Δmpt70* and *M. orygis Δmpt83* ~400 CFU. **b)** Lung bacterial burden of WT *M. orygis* versus *M. orygis Δmpt70_mpt83* at day 7, 14, and 21 (n= 5 mice per timepoint per group; independent experiment). No significant differences between groups at any timepoint observed. Day 1 included to show comparable dose (~300 CFU). **c)** Experimental overview of subunit vaccination followed by aerosol challenge with *M. orygis* 51145. BCG Russia vaccination and PBS-sham vaccination performed in tandem as previously described (Fig. 20b). **d)** Kaplan-Meier survival curve. Mice vaccinated with either PBS, MPT70, ESAT-6 or BCG Russia were challenged with *M. orygis* via the aerosol route and monitored for signs of clinical disease (n= 15 mice/group). Median survival of MPT70 and ESAT-6 immunized mice did not significantly differ (T= 119 days and 112 days respectively, p= 0.598). Median survival of PBS-sham vaccinated mice= 24 days, median survival of BCG Russia vaccinated mice = 171 days. **e)** Representative macroscopic images of lung at compassionate endpoint per experimental group. The extent of lesions observed in PBS-infected lungs is not recapitulated in vaccinated groups, though few lesions at endpoint are present (grey arrows).

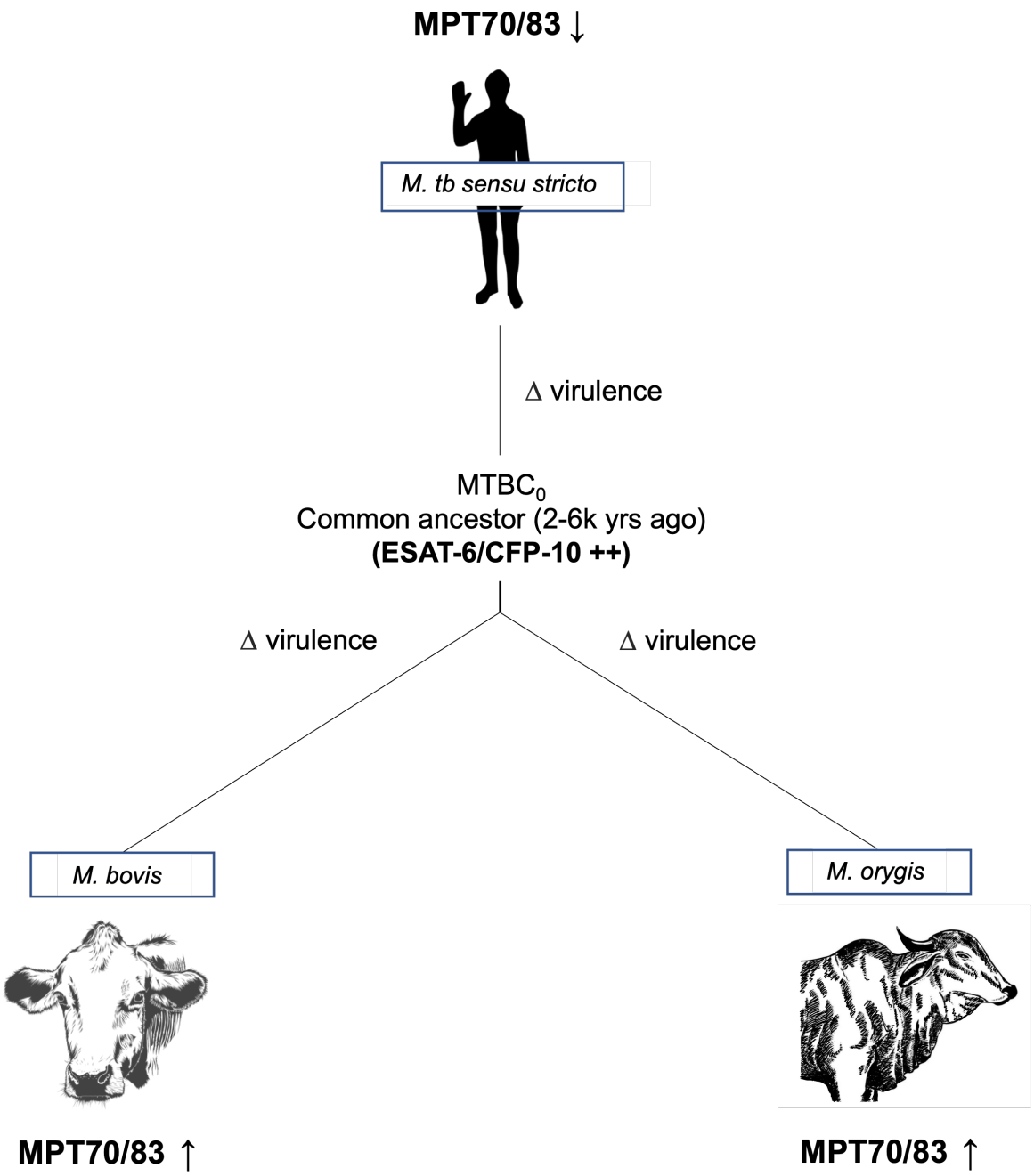

Figure 22. Conceptual overview.

Evolutionary scenario for the three *Mycobacterium tuberculosis* complex organisms studied. *M. tuberculosis* (sensu stricto) forms a distinct lineage from the cattle-associated pathogens, *M. bovis* and *M. orygis*, who share a short branch before being separated by deep branches. *M. tb, M. bovis* and *M. orygis* are all positive for ESAT-6 and CFP-10 production but show different

expression levels of MPT70 (and MPT83). Since the inferred common ancestor of *M. tuberculosis* complex organisms, the data suggest either a) an attenuation of virulence in *M. tuberculosis*, and/or b) a gain-of-virulence in *M. bovis* and *M. orygis.*

7. Tables

Position	PacBio	Illumina	Codon change	Sanger	Locus_Tag	Gene name
2017392	T	C	p.Met507Thr	**C**	RJtmp_001858	eccC5
577991	TT	T	.	**T**	RJtmp_000510	mshA
2093004	T	G	p.Asp38Ala	**G**	RJtmp_001924	Rv1856c
3161714	CC	C	.	**C Del**	gene_RJtmp_002996	Rv2905 (lppw)
3161737	GTC	T	.	G Del	gene_RJtmp_002996	Rv2905 (lppw)
3161754	A	G	.	A Del	gene_RJtmp_002996	Rv2905 (lppw)
3161764	TT	T	.	T Del	gene_RJtmp_002996	Rv2905 (lppw)
3161772	AA	A	.	A Del	gene_RJtmp_002996	Rv2905 (lppw)
3161779	TT	T	.	T Del	gene_RJtmp_002996	Rv2905 (lppw)
3161790	CC	C	.	C Del	gene_RJtmp_002996	Rv2905 (lppw)
3161799	TTT	T	.	T Del	gene_RJtmp_002996	Rv2905 (lppw)
3161811	AA	A	.	A Del	gene_RJtmp_002996	Rv2905 (lppw)
3161818	CC	C	.	C Del	gene_RJtmp_002996	Rv2905 (lppw)
3161828	AA	A	.	A Del	gene_RJtmp_002996	Rv2905 (lppw)
3161834	GG	G	.	G Del	gene_RJtmp_002996	Rv2905 (lppw)
3161843	TT	T	.	T Del	gene_RJtmp_002996	Rv2905 (lppw)
3161850	AA	A	.	A Del	gene_RJtmp_002996	Rv2905 (lppw)
3161881	CC	C	.	C Del	gene_RJtmp_002996	Rv2905 (lppw)
3161889	AA	A	.	A Del	gene_RJtmp_002996	Rv2905 (lppw)
3161898	CGGA	GG	.	C Del	gene_RJtmp_002996	Rv2905 (lppw)
3161929	CC	C	.	C Del	gene_RJtmp_002996	Rv2905 (lppw)
3161940	CC	C	.	C Del	gene_RJtmp_002996	Rv2905 (lppw)
3161947	CC	C	.	C Del	gene_RJtmp_002996	Rv2905 (lppw)
3161967	AA	A	.	A Del	gene_RJtmp_002996	Rv2905 (lppw)
3161979	AA	A	.	A Del	gene_RJtmp_002996	Rv2905 (lppw)
3162155	TT	T	.	**T Del**	gene_RJtmp_002997	Rv2906c(trmD)
3162210	GTC	T	.	**T Del**	gene_RJtmp_002997	Rv2906c(trmD)
3162228	AA	A	.	**A Del**	gene_RJtmp_002997	Rv2906c(trmD)
3162245	GG	G	.	**G Del**	gene_RJtmp_002997	Rv2906c(trmD)
3162282	CC	C	.	**C Del**	gene_RJtmp_002997	Rv2906c(trmD)
3162291	GG	G	.	**G Del**	gene_RJtmp_002997	Rv2906c(trmD)
3162299	CC	C	.	**C Del**	gene_RJtmp_002997	Rv2906c(trmD)
3162303	GGC	G	.	**G Del**	gene_RJtmp_002997	Rv2906c(trmD)
3162311	TT	T	.	**T Del**	gene_RJtmp_002997	Rv2906c(trmD)

Table 5. Genomic corrections following Illumina HiSeq

	M. tuberculosis H37Rv	*M. bovis* Ravenel	*M. orygis* 51145
Genome Size (bp)	4417942	4371545	4352140
GC content (%)	65.5	65.5	65.6
Genes	4206	4109	4089
CDSs	3857	3866	3788
Hypothetical proteins	475	449	422
Pseudogenes (total)	147	192	250
Transposases (total)	44	28	79
tRNA	45	45	45
PPE-family	55	45	41
PE-family	63	80	75

Table 6. Genomic characteristics of *Mycobacterium tuberculosis* complex subspecies (MTBCs).

Wildtype strains	Isogenic mutants
M. orygis 51145 (*M. or;* reference)	*M orygis ΔesxA*$^{+}$
M. orygis 2019-352 (clinical isolate)	*M. orygis Δmpt70_mpt83*$^{+}$
M. bovis Ravenel (*M. bo*)	*M. orygis Δmpt70*
M. tuberculosis H37Rv (*M. tb;* reference)	*M. orygis Δmpt83*
M. tuberculosis Erdman	*M. bovis ΔesxA*$^{+}$
M. tuberculosis HN878	*M. bovis Δmpt70_mpt83**$^{+}$
M. bovis BCG Russia	*M. bovis Δmpt70* $^{+}$
M. bovis BCG Danish	

Table 7. Bacterial strains used in virulence studies.

* indicative of hygromycin resistance cassette. All other isogenic mutants listed contain the zeocin resistance cassette. + indicates use in secretomic studies (Chapter III).

Behavior (B)

Clinical Sign	Score
BAR (Bright, alert and responsive)	0
Active but hunched posture	1
Less active when observed outside of cage but active when stimulated	2
Inactive even when stimulated (no respond to touch, no righting reflex)	3

Appearance (A)

Clinical Sign	Score
Normal (hair coat and posture, eyes open)	0
Slightly hunched, piloerection, eyes partially closed	1
Moderately hunched, piloerection, eyes moderately closed, pale mucous membranes	2
Ruffled coat, very hunched, eyes completely closed, pale mucous membranes	3

Respiration (R)

Clinical Sign	Score
Normal	0
Increased respiratory rate, mild abdominal breathing	1
Dyspnea (severely increased respiratory rate, open-mouth and abdominal breathing)	2

Dehydration (D)

Clinical Sign	Score
Normal (pinching the skin over the shoulder blades, the skin will quickly return to its original shape)	0
Moderate (Delay in skin return to its normal position after pinching the skin over the shoulder blades)	1
Severe (sunken eyes, skin stay bunched up)	2

Body Condition (BC)	Score
Mouse is emaciated; skeletal structure extremely prominent, vertebrae distinctly segmented	1
Mouse is under-conditioned; segmentation of vertebral column evident, dorsal pelvic bones are easily palpable	2
Normal; mouse is well-conditioned. Vertebrae and dorsal pelvis not prominent but palpable with light pressure	3
Mouse is over-conditioned; vertebrae palpable only with firm pressure	4
Mouse is obese; bone structure disappears under flesh and subcutaneous fat	5

Table 8. Clinical assessment of mice.

If behaviour/appearance reached score of 3 or respiration/dehydration reached score of 2, animal was euthanized. If body condition score (BCS) is < 2 or body weight loss > 20%, animal was euthanized.

Parameter	Score			
Quality control	**0**	**1**	**2**	**3**
Tissue quality	Inadequate	Good	Very good	Excellent
Distribution of lesions	Bronchial/Peribronchial	Parenchymal		
% affected area	0-100%			
Inflammation intensity	**0**	**1**	**2**	**3**
Bronchial/endobronchial	Normal/absent	Mild	Moderate	Marked
Peribronchial	Normal/absent	Mild	Moderate	Marked
Perivascular	Normal/absent	Mild	Moderate	Marked
Interstitial	Normal/absent	Mild	Moderate	Marked
Pleural	Normal/absent	Mild	Moderate	Marked
Intra-alveolar	Normal/absent	Mild	Moderate	Marked
Inflammatory cellular infiltrate	**N/A**	**A**	**C**	**AC**
Type of cellular infiltrate	Not applicable	Acute (neutrophils)	Chronic (lymphohistiocytic)	A and C
Vascular damages	**0**	**1**	**2**	**3**
Hemorrhages				
Endothelialitis				
Capillary vascular congestion	Absent	Mild	Moderate	Marked
Pulmonary edema	**0**	**1**	**2**	**3**
Pulmonary edema	Absent	Mild	Moderate	Marked

Table 9. Semiquantitative scoring scale of histological parameters.

For inflammation intensity, vascular damages, and pulmonary edema fractions of points were also allowed. Very mild= 0.5, mild to moderate= 1.5, and moderate to marked= 2.5

CHAPTER V: INSIGHTS FROM A NATURAL HOST

1. Introduction

Prior to this dissertation, the infection outcome of *M. orygis* had never been formally assessed in an animal model. In the previous chapter, we showed that *M. orygis* infection using a standardized aerosol model results in significant morbidity and expedited mortality compared to *M. tb* infected C57BL/6 mice[317,434,435]. Moreover, we concluded that, like *M. bovis*, *M. orygis* is a hypervirulent member of the MTBC. The main caveat of this conclusion is that it is informed from experimentation with mice and may not be representative about the natural pathology and progression of *M. orygis* infection and/or disease. As such, our main objective for this chapter was to evaluate the outcome of *M. orygis* infection in a well-defined maintenance host (*Bos taurus*) following aerosol exposure (experiment performed in collaboration with Jeffery Chen and the Animal Services Department at the University of Saskatchewan). Three possibilities emerge: either *M. orygis* recapitulates the *M. tb* phenotype, *M. orygis* recapitulates the *M. bovis* phenotype, or *M. orygis* acts uniquely within a cattle host. In murine studies, there was a clear divide between the survival of mice experimentally infected with animal-associated or human-associated pathogens. We hypothesized that the disease phenotype of *M. orygis* infected cattle is comparable to *M. bovis,* but markedly more severe than *M. tb.*

2. Methods

2.1 Aerosol challenge in a natural host:

Aerosol challenge was performed in collaboration with the University of Saskatchewan Vaccine and Infectious Disease Organization (VIDO) in an agricultural biosafety containment level 3 (CL3) facility. Bacteria were resuspended in 4 mL of saline solution and nebulized. Fifteen *Bos taurus* calves (age= 6-7 weeks, post-weaned) were randomized into *M. orygis* 51145, *M. bovis*

AF2122, and *M. tb* H37Rv infection groups (n= 5) and challenged with ~10^4 CFU/calf via the aerosol route (Figure 23a). Following infection, calves were monitored by the Animal Services Department at VIDO through both physical examination and CCTV footage. Inoculum from each group was plated on 7H10 + OADC agar to determine initial challenge material (100 µL). For the remainder of this chapter *M. orygis* 51145 will be referred to as *M. orygis, M. bovis* AF2122 will be referred to as *M. bovis*, and *M. tb* H37Rv will be referred to as *M. tb.*

2.2 Gross pathology:

Fifteen weeks (~105 days) post infection, calves were euthanized in three randomized batches. At necropsy, myself and the VIDO CL3-Agriculture staff extracted whole lungs, spleen, liver, and lymph nodes (tracheobronchial, TBLN; mediastinal, MLN. Prior to necropsy, 2 calves succumbed to 'free bloat' (*M. bovis; M. orygis* infected calves), 1 calf succumbed to suspected co-infection with *Mycoplasma bovis (M. bovis* infected calf) resulting in the final experimental groups of: *M. tb* n= 5, *M. bovis* n= 3, and *M. orygis* n= 4. For the remaining cattle, individual lobes of lungs were visually inspected and palpated to determine a final lesion score (0-5 per lung, total pathology score= 40). Parameters of lesion scoring are described in Table 10[333]. A score of 0 indicates no gross lesions seen and/or palpated whereas a score of 5 indicates numerous coalescing lesions of varying sizes observed (Figure 23b,c; Table 10)[333]. Spleen, liver, TBLNs, and MLNs were visually assessed for the presence or absence of lesions but not scored (marked as + or -; Table 11). Weight at endpoint was recorded for each calf (Figure 23d). Lungs corresponding to greatest lung pathology in *M. tb, M. bovis,* and *M. orygis* infected cattle depicted in Figure 23e.

2.3 Histopathology:

3 x 3 x 3 cm pieces of tissue were allocated for histopathology (left or right cranial, mid, and caudal lobes of lung; TBLN and MLN). Tissue was stored in 10% neutral buffered formalin

and processed by the Goodman Cancer Research Centre Histology Core (McGill University) using standard parafilm embedding protocols. 4 μM slices were cut and transferred to slides to be H&E or ZN stained as indicated. Due to the heterogeneity of the bovine granuloma, traditional scoring criteria described by Wangoo et al. was modified to include 'atypical' granuloma presentation observed in young calves (~4 months or younger) with the main changes to the schema being the presence/absence of a capsule[75,436,437]. Due to the age of the calves in this study, we defined granulomas as the following: stage I granulomas (including satellite granulomas) consist of epithelioid macrophages, with or without areas of necrosis and/or the presence of neutrophils. Langhans giant cells (multinuclear cell composed of fused epithelioid macrophages) and lymphocytes may also be present. Stage II granulomas are larger than stage I granulomas and dominated by epithelioid macrophages, a higher frequency of giant cells, lymphocytes, and areas of necrosis. Stage III granulomas are larger than stage II and have large necrotic areas, often demarcated by a capsule, with a peripheral layer of macrophages, lymphocytes, and neutrophils. In young calves, granulomatous borders may be poorly defined and were also considered as part of stage III. Stage IV granulomas are similar to stage III granulomas at the cellular level but have multiple foci of caseous necrosis and/or mineralization dominating the structure. These are large, irregular, and/or encapsulated. Healthy lung tissue was defined as preserved airway (intact alveoli) with no inflammation. Examples of granuloma staging are depicted in Figure 24. Staging and disease progression were confirmed by a trained pathologist blinded to experimental group (Philippe Joubert, Institut Universtaire de Cardiologie et de Pneumologie de Québec). Lower limit of detection of acid-fast bacilli (AFB) by ZN stain ~5x 10^3 CFU/mL[21] (AFB visualized in Figure 25). In this chapter, Langhans giant cells will be referred to as multinucleated giant cells (MNGCs).

2.4 CFU enumeration:

Tissue was extracted from each lobe of lung (both right and left cranial lobes, mid lobes, and caudal lobes), TBLN, MLN, spleen, and liver using a sterile biopsy punch (~1 g) and plated on 7H10 PANTA OADC plates. For CFU interpretation, any raw bacterial counts under 10 were excluded from CFU quantification in lung, MLN, and TBLN. Due to the size of calf, burden in all organs processed is calculated as CFU/g (log_{10}). Lung bacterial burden is presented as the sum of left and right caudal, middle, and cranial lobes (CFU/g).

2.5 Statistics:

Statistical analysis was conducted using GraphPad Prism (version 10.0.3). Due to distribution and variability of calves, Kruskal-Wallis test (Dunn's multiple comparison test, non-parametric) was used unless otherwise indicated. Statistical significance was defined as $p < 0.05$. Where applicable, data are shown as individual points with median and interquartile range.

3. Results

In this study, *M. tb* infected cattle at necropsy were unremarkable. Lungs had an average pathology score of 1.6 (out of 40, range between 0 and 3) with good colouration and tissue integrity (pink and spongy) (Figure 23e, Figure 26a). Of cattle where lesions were recorded, they could only be detected by palpation rather than visual inspection (3/5). Moreover, lesions were not present in either lymph node (TBLN, MLN), spleen, or liver (Table 11). Comparatively, both *M. bovis* and *M. orygis* infected cattle showed severe disease at necropsy, evidenced by extensive lesions, and significantly enlarged lymph nodes. The mean pathology score of *M. bovis* infected cattle was 16.7 (out of 40; range: 9-30) whereas the mean pathology score of *M. orygis* was 24.3 (range: 12-36) with *M. orygis* trending towards greater gross pathology than *M. bovis* (Figure 23c). Contrary to *M. tb* infected cattle, all *M. orygis* and *M. bovis* infected cattle showed the presence of lesions in the lymph nodes (TBLN, MLN) with no visible splenic lesions (Table 11). Notably, only two calves

showed macroscopic evidence of lesions in the liver- both of which were infected with *M. orygis* (Table 11; calf 33, 41). If ranking cattle by gross pathology, there was an obvious division between the cattle-associated strains (*M. bovis* and *M.* orygis) and the human-associated strain (*M. tb*), concordant with what has been observed historically and what was observed in our mouse model. *M. orygis* infected cattle ranked first and third (pathology scores 36 and 28) whereas 1 *M. bovis* infected calf ranked second (pathology score 30). Gross pathologic differences between experimental groups outlined in Figure 23. Weight at experimental endpoint was comparable across groups and could not be used as a proxy for disease progression (Figure 23d).

3.1 *M. tb* infected calves:

Concordant with gross pathology of the lungs, TBLNs and MLNs of *M. tb* infected calves were unremarkable (Figure 26a, 27a, *M. tb* infected lymph nodes representative of experimental group). Further, no areas of necrosis were observed microscopically, though areas of minor thickening (inflammation) were noted. Few early granulomas (~stage I) could be observed following H&E staining; ZN staining could not identify AFB+ bacteria in the lungs or lymph nodes. Though viable bacteria could be observed in a portion of the *M. tb* infected calves (lungs, lymph nodes) these were sporadic, and below the threshold of quantification. Comparative bacterial burdens of lung, lymph nodes, spleen and liver are described in Figure 28.

3.2 *M. bovis* infected calves:

All calves were positive for lesions in the lung, TBLN, and MLN but negative for lesions in the spleen and liver (3/3) (Figure 26a,27a; Table 11). Despite this, only 1/3 calves were considered 'positive' for CFU in the lungs, as determined by our limit of quantification (calf 37) (Figure 28a). At necropsy, lungs of all calves were poor quality, typically paler than their *M. tb* infected counterparts, with evidence of surface lesions (the extent of which varied depending on

the calf). Lesions were most evident following transverse slicing of the lung (whitish grey crystal-like structures) and by palpation of lung (Figure 26). As expected, *M. bovis* infection presented predominantly as a lymphatic disease, with minimal lung involvement[438–441]. This was particularly evident in calf 37 which had the largest TBLNs and MLNs of all experimental groups (MLN >> TBLN) (Figure 27). Gross inspection revealed that solid, coalescing areas of nodules (granulomatous lymphadenitis, shown in white) composed the entire lymph node with evidence of damage to the structure of the lymph nodes (holes). Further, granulomatous regions were segmented by thick pale connective tissue and both the TBLN and MLN were completely engulfed by granulomatous formations (Figure 27). At 9 weeks post-infection, calf 37 required surgical intervention due to chronic bloat (rumenostomy). The moderate bloat was likely due to compression of the vagus nerve due to the size of the lymph nodes extracted[442]. Moreover, calf 37 was the only calf to present with lung involvement above limit of quantification, though this was limited to the left middle lobe (Figure 28a). This result may be due to a sampling bias, as only 1 g of tissue was obtained per lobe of lung. At necropsy, calves 32 and 38 showed comparable lung pathology (pathology score 9 versus 12 respectively) as well as TBLN and MLN pathology. Both TBLN and MLN were enlarged with extensive nodules interspersed throughout the lymph nodes and significant hemorrhage. However, in calf 38 the MLN was larger than the TBLN whereas in calf 32, the opposite was observed.

Histopathology revealed significantly more advanced disease in both the TBLN and MLN compared to the lungs (Figure 26b, 27b). This was determined through two lines of evidence: first, the staging of the granuloma, second, the number of necrotic foci. The lung tissue of calf 37 and 38 showed preserved airways/intact alveoli, with minor regions of atelectasis and inflammation. Early-stage granulomas (stage I), lymphocyte infiltrates, and MNGCs were observed sporadically.

Despite calf 37 having a much higher gross pathology score, calf 38 showed more extensive inflammation and pockets of lymphocytic infiltrates (Figure 26b). Surprisingly, calf 32 showed the greatest extent of lung injury microscopically. The mid-lobe of the lung was dominated by a large, stage IV granuloma. A central necrotic core was surrounded by layers of innate and adaptive cells and encapsulated by a thin, fibrous capsule. There was a clear separation between recruited macrophages, neutrophils, and lymphocytes forming three distinct borders and within the central core, with acellular regions (Figure 26b). This phenotype was restricted only to the mid-lobe of lung; in the caudal and cranial lobes inflammation was minimal, though lymphocytic pockets were observed (Figure 26b). As suggested previously, this difference may be due to the random sampling of the lung at necropsy and not fully representative of disease progression. Comparatively, the TBLN and MLN of all three calves showed much more extensive pathology due to infection (Figure 27b). 3/3 MLNs and 2/3 TBLNs had at least one stage III or higher granuloma (Table 11). Satellite stage I granulomas were also common. Concordant with gross pathology, the MLN of calf 37 showed the most progressed granulomas (stage III and IV). Tissue was disorganized with multiple necrotic foci, acellular regions, and numerous MNGCs surrounding the necrotic core. Dense regions of lymphocytes were limited compared to *M. tb* infected lymph nodes and instead, granulomas dominated the structure (n= 8 necrotic foci). In the TBLN, only 2 necrotic cores were observed, however extensive acellular regions, ill-defined borders, and a decreased lymphocyte population was apparent (pale purple colour). Calf 32 and 38 also showed significant lymphatic pathology in the MLN but, of the two, only calf 32 showed necrosis in the TBLN (calf 38 has a dominant lymphocyte population with no evidence of late-stage granulomas) (Figure 27b). Both TBLN and MLN were AFB+, though bacilli detection was infrequent. Bacteria harboured in the necrotic centre of granulomas showed markedly different

morphology compared to bacteria harboured in MNGCs and early-stage granulomas when detected. Bacteria in necrotic core did not manifest the traditional bacilli formation, instead being clustered with some evidence of shearing[443,444]. No bacteria could be observed in lung tissue by microscopy.

Bacterial burden of *M. bovis* infected cattle was concordant with histopathological and macroscopic findings. Lung bacterial burden could only be quantified in 1/3 calves (calf 37) whereas MLN and TBLN bacterial burden were quantified in all 3 calves (Figure 28a-c). Only one calf showed evidence of liver involvement (calf 32, no surface lesions visible at necropsy) and splenic involvement was not observed in any of the *M. bovis* infected cattle (0/3) (Table 11). Calf 38 had the lowest bacterial burden in the TBLN (300 CFU/g); in the same animal, the MLN burden was ~2 $\log_{10}$ higher per gram (Figure 28b,c). Calf 37 had the greatest bacterial burden in both the MLN and the TBLN (~1-2 $\log_{10}$ higher per gram) compared to other members of the *M. bovis* infected group. Additionally, calf 37 had the greatest lymphatic burden across all experimental groups- correlating well with the size and pathology of lymph nodes at necropsy (MLN= ~10^5 CFU/g; TBLN= ~$7x10^4$ CFU/g). On average, the MLN housed ~2x more bacteria per gram compared to the TBLN. These results are supported by the recent report that *M. bovis* infection induces increased proinflammatory responses in young calves, resulting advanced granulomatous lesions, necrosis, and increased bacterial burden due to decreased mycobactericidal activity[445].

3.3 *M. orygis* infected calves:

Lesions were seen macroscopically and felt by palpitation, showing extensive disease at necropsy. Multiple calves showed the formation of granulomas and had visible areas of necrosis, particularly evident following transverse slicing of the lungs (Figure 29a). Two calves (calf 35, 45) had significantly discoloured, fluid-filled lungs and expelled foam from the trachea following

euthanasia (likely independent of disease). As in the *M. bovis* infected group, one calf required a rumenostomy, also suspected to be caused by a compression of the vagus nerve due lymphatic enlargement[442] (calf 41, n= 9 weeks post infection). All *M. orygis* infected calves presented with significantly enlarged TBLNs and MLNs compared to the *M. tb* group, correlative to the pathology rank of the calf (Figure 30a). As expected, calf 45 had the most extensive lymph node pathology. Within the TBLN and MLN, a thick, fibrous, connective tissue encapsuling areas of caseous necrosis (composed of coalescing nodules; white in colour) could be observed with evidence of microhemorrhage (Figure 30a). This calf had the largest LNs collected from all *M. orygis* infected cattle and showed the greatest clinical progression. Subsequently, in calves 41 and 35, thick connective tissue was observed surrounding areas of granulomatous lymphadenitis (white, solid nodules). In calf 35, both the TBLN and MLN showed evidence of hemorrhage in addition to lesions. Calf 33 had mild granulomatous formations, with small, white nodules dispersed throughout the LNs. Of the calves which showed liver involvement (calf 33, 41), a small, white, surface nodule was evident.

Histopathology of the lungs, TBLN, and MLN was concordant with macroscopic observations (Figure 29b, 30b). Limited healthy tissue was observed microscopically, though this varied depending on the lobe of lung assessed. Stage III or higher granulomas were observed in at least one lobe of all *M. orygis* infected lungs (4/4 calves). This was distinct from *M. tb* infected calves where airways were predominantly conserved, showed limited granuloma formation, and/or no acellular features (5/5 calves). Additionally, the frequency of granulomas was significantly increased in the *M. orygis* infected group compared to the *M. tb* control group; often many granulomas contained multiple necrotic foci with nearby satellite granulomas (Figure 26b, 29b). In both the TBLN and MLNs stage III or higher granulomas were seen in all *M. orygis* infected

calves (Figure 30b). Interestingly, despite having the greatest gross pathology, calf 45 did not show the same areas of progressive necrosis/mineralization observed in other *M. orygis* infected cattle. In general, *M. tb* and *M. orygis* infected lymph nodes can be easily differentiated by colouration of the H&E staining. Due to the cell populations and pathology caused by infection, *M. orygis* lymph nodes present with significantly fewer patches of lymphocytes (stained purple nuclei) and more advanced granulomatous features (ex: necrosis, disorganization, acellular regions) compared to *M. tb* infected nodes (Figure 27b, 30b). Both TBLN and MLN were AFB+ by ZN staining. Like *M. bovis* infected cattle, bacilli at the centre of necrotic cores were clustered and/or fragmented, though in a subset of samples, rod-shaped bacilli were also observed (heterogeneous morphology; bacilli not restricted to the empty centre of the core). Additionally, bacilli were more frequently detected by microscopy in the *M. orygis* experimental group compared to either *M. tb* or *M. bovis* groups. Intracytoplasmic bacilli were apparent. Due to limit of detection, lungs were AFB- with microscopy.

When assessing lung bacterial burden, all *M. orygis* cattle had bacteria present in at least one lobe of lung, the MLN, and the TBLN (4/4 calves) (Figure 28a-c). This contrasts directly to *M. bovis* infected cattle- in which bacterial burden was above the LOD in the lungs of only one calf- as well as *M. tb* infected cattle. In the lungs, burden directly correlated with gross pathology, however this was not consistently observed in the MLN or TBLN. Additionally, bacteria could be cultured from the liver and spleen of calf 33 and 41 (2/4, liver burden > splenic burden) (Figure 28d,e). Like *M. bovis*, *M. orygis* presented predominantly as a lymphatic disease as lymph nodes contained ~1-2 $\log_{10}$ more bacteria compared to lungs. On average, the MLNs housed roughly ~1.5x more bacteria per gram compared to the TBLN, despite the respective sizes of the lymph nodes (TBLN > MLN). Notably, calf 45 (highest lung pathology score) had significantly more

lung and MLN burden compared to other *M. orygis* infected cattle, however TBLN burden was comparable to calf 41.

3.4 Considerations

Despite the robustness of this data, we must be aware of the following caveats. First, three calves were lost prior to completion of the study (2 due to free bloat caused by premature weaning and a lack of roughage in their food supply; 1 euthanized due to suspected co-infection with *Mycoplasma bovis*). *Mycoplasma bovis* is a common bovine pathogen responsible for pneumonia, respiratory disease, osteitis, arthritis, and other chronic illness in young calves (termed *Mycoplasma bovis* associated disease). In western Canada, up to 30% of feedlot/auction cattle are treated for bovine respiratory disease (BRD) though field cases of *Mycoplasma bovis* have also been recorded[446,447]. Gross pathological findings of the calf euthanized due to co-infection, indicated that *Mycobacterium bovis* infection was not the sole cause of death- though the extent to which this agent played a role is unknown. Notably these calves were only lost from our zoonotic experimental groups (*M. bovis* and *M. orygis*). This resulted in a reduced sample size and subsequently, less statistical power. As such, though the trends in this experiment are evident, they cannot be definitively proven as significant. Second, this experiment used aerosol (inhalation) as the route of infection. Though this has been largely accepted as the most common route of infection in cattle, there still is significant debate over the contribution of other transmission routes such as ingestion[332,441,448]. In *M. bovis* infected cattle, an aerogenic route of transmission is correlated to the presence of lesions in the upper and lower respiratory tracts and their associated lymph nodes (such as the tracheobronchial and mediastinal lymph nodes). Comparatively, exposure to *M. bovis* through ingestion (the oral route) is correlated to involvement of lymph nodes associated with the digestive system, seldom disseminating to the lungs[332]. Accordingly, it has been suggested that the

infection outcome, and progression of disease, is associated with how/where the bacilli come into contact with the host[332,441,449,450]. Our experimental outcomes are only representative of disease progression following inhalation and do not account for differences in disease manifestation due to differences in route of exposure. Moreover, the transmission route of *M. orygis* has yet to be formally demonstrated; instead, it can only be inferred from case series and data about well-established members of the MTBC[232,239,242,408]. This means that 1) *M. orygis* may be spread via aerosolized droplets, ingestion, and (more rarely), transplacental, mammary, or genital transmission and 2) the most common route of infection may not be via aerosol[332]. Lastly, *M. orygis* is the causative agent of bovine tuberculosis in South Asia whereas *M. bovis* is the causative agent of bovine tuberculosis in Europe, Africa, and the Americas[59,222,232,234,239]. Correspondingly, the cattle populations differ in these locations: *Bos indicus* (Zebu-like cattle) in South Asia and *Bos taurus* in the 'Western world'[222]. Our study utilized a well-established aerosol model in *Bos taurus* cattle, which means that results may not fully recapitulate the host-pathogen interactions in *Bos indicus*[337]. Moreover, in studies of *M. bovis* infected cattle, induction of pro-inflammatory responses are differentially expressed depending on the bacterial strain and the breed of cattle[177,451].

4. Discussion

M. tb is a specialist pathogen that predominantly transmits from human-to-human, and occasionally, human-to-animal. Infection of mammalian hosts (other than humans) are considered to represent spillover infections, rather than host preference, and no animal-to-animal transmission of *M. tb* has been recorded[452]. It has been well-documented that disease and infection outcome depends on host-pathogen interactions. In humans, *M. tb* most often presents as a pulmonary infection with extensive lesions, bloody sputum, fever, and weight loss; however where reported

in cattle, *M. tb* is attenuated, often showing no outward signs of clinical disease[213,16,129,453]. Typically, this has occurred in regions of the world where *M. tb* is endemic, contact with cattle herds is common, and is considered a 'dead-end' infection[454]. Comparatively, in humans, livestock, and wild animals naturally infected with *M. bovis* or *M. orygis* similar disease phenotypes are observed, often presenting with severe extrapulmonary infection, granulomatous lesions in the lung/lymph nodes and lymphadenitis (scrofula)[166,232,239,408,436]. Moreover, *M. bovis* and *M. orygis* can be maintained in both animal- and human-populations without re-infection.

Historically, our understanding of virulence has come from post-mortem examination of naturally infected hosts. In 1901, it was established that *M. tb* is attenuated in animal hosts, such as cattle, pigs, donkeys, sheep and goats[129]. Regardless of route of infection, when cattle were infected with 'human tuberculosis', no gross pathology could be observed at necropsy[15,16,129]. Conversely, when infected with 'bovine tuberculosis', cattle showed extensive lesions (site of infection, lymph nodes, lung, spleen etc.), weight loss, fever, and in a subset of cattle: mortality[129]. Since then, this observation has been repeatedly validated[213,452]. The pathogenesis of *M. bovis* in mammalian hosts (including humans) has been investigated for over a century, though driving forces behind differences in disease presentation have yet to be fully understood[16,129,213]. In their natural hosts (*M. tb*= humans; *M. bovis*= cattle), progression from infection to disease parallel each other. Though we successfully used a C57BL/6 mouse aerosol model to compare *M. tb, M. bovis* and *M. orygis* survival, this does not perfectly recapitulate natural infection, largely due to the absence of 'classic' necrotizing granulomas[317]. The granuloma is the hallmark of tuberculosis disease and the early events of granuloma formation determine infection outcome (proliferation, containment, and/or clearance)[325,455–457]. This structure acts as a host defense mechanism by physically containing mycobacteria, however, the recruitment and activation of immune cells

result in increased cell-to-cell contact, providing a niche for mycobacteria to exploit (Figure 24)[458]. The classical granuloma consists of a mycobacterial centre surrounded by an inner core of macrophages and an outer core of lymphocytes (predominantly T-cells)[75,459]. Depending on the stage of granuloma, the inner 'innate' layer may also include MNGCs (Langhans), neutrophils, dendritic cells, and natural killer cells, in varying proportions[75,459,460]. As such, the establishment and control of *M. tb* and *M. bovis* infection by the host depends on a balance between the production of proinflammatory cytokines (such as TNF-α, IFN-γ, IL-2) and anti-inflammatory cytokines (such as IL-10, TGF-β) during the initiation of granuloma formation[325]. Crucial to the survival of both *M. tb* and *M. bovis* is the ability of MTBCs to counteract and manipulate the 'killing' mechanisms of the host, often by (though not limited to) the prevention of phagolysosomal fusion, acidification, and inhibition of controlled cell death (apoptosis)[461]. Despite these similarities, the infection outcome of *M. tb* and *M. bovis* diverge, allowing us to categorize one as attenuated (*M. tb*) and one as virulent (*M. bovis*). Our study demonstrates this same categorization for *M. orygis.*

In Chapter IV we proposed that a host-damage threshold was a key determinant of the mortality and morbidity of C57BL/6 mice; this result is echoed in *Bos taurus* cattle and informed by *M. bovis* virulence studies in mammalian hosts (calves, mice, goats, camels etc.)[15,16,129,462]. In this study, *M. orygis* and *M. bovis* show a comparable disease phenotype following aerosol infection. However, the role and composition of the granuloma has yet to be studied following *M. orygis* infection. We know from experimental cattle infections with *M. bovis* that the cellular composition of the granuloma differs depending on tissue type (ex: lung versus lymph node), mycobacterial growth, and/or time post infection suggesting the influence of a local microenvironment on disease control[463]. The breakdown of the granuloma is a crucial determinant

in the progression of both *M. tb* and *M. bovis* infection. Advanced necrosis and mineralization lead to the collapse of the granuloma centre and the release of mycobacteria to adjacent cells whereas the formation of multinucleated giant cells contain it[71,464]. Thus, signalling and recruitment correspond to either increased 'host control' of infection (low grade encapsulated granulomas) or increased 'bacterial-control' (high grade, extensively necrotic granulomas)[465]. Moreover, if excessive amounts of proinflammatory cytokines are produced, a hyperinflammatory state is induced, resulting in irreparable tissue damage to the host[463]. In this experiment, we observe that late-stage granulomas dominate the lungs and lymph nodes of *M. orygis* infected cattle, indicating a poorly controlled, hyperinflammatory infection by the host; this concordant with post-mortem examination of ungulates which naturally succumbed to *M. orygis* infection (cattle, black bucks, buffalo, deer etc.) and comparable to our C57BL/6 model[237]. When compared to another animal-associated strain (*M. bovis*), *M. orygis* infected cattle had increased bacterial burdens in the lungs, but similar TBLN and MLN burdens (Figure 28a-c). Moreover, both *M. orygis* and *M. bovis* experimental groups presented with significantly more advanced granulomas compared to *M. tb* infected cattle microscopically and more frequent, hardened, coalescing lesions macroscopically. This corresponds to what has been previously reported in surveillance studies: *M. bovis* infected cattle frequently present with lesions in the TBLN and MLN, but sparingly present with lesions in the lung[213,438–440,466].

How *M. orygis* utilizes the host immune response is unknown. However, it has been postulated that the difference between *M. tb* and *M. bovis* pathogenesis in cattle may be attributed to host- and pathogen-specific factors. At the level of the host, modifications to early immune events correlate to differences in infection outcome. These include variation within granuloma cell populations (such as an increase in neutrophils and MNGCs), increased proinflammatory cytokine

profiles, or differential conversion from a T-helper I (Th1) response to a T-helper-2 (Th2) response over the course infection[195,334,426,451,467]. Concordantly, an 'inflammation signature' (CCL4, IL-1β, IL-6 and TNF-α) and the upregulation of both inflammatory processes and autophagy have been previously described following *M. bovis,* but not *M. tb* infection in a bovine host[334,451]. Additionally, in our study, MNGCs (including stage I satellite granulomas) were most commonly seen in *M. orygis* and *M. bovis* experimental groups but seldom observed in *M. tb* infected cattle. This is concordant with the observation that *M. tb* does not efficiently induce multinucleated giant cells in bovine macrophages whereas in *M. bovis* granulomas these cells act as indicators of lesion severity[195]. Accordingly, these host responses are mediated at the level of the pathogen. Though it would be unwise to use *M. bovis* as a proxy for *M. orygis* infection, it provides a starting point for further research into the similarities, or differences between MTBCs, building upon what has already been established. 'Cattle-associated' factors (host or pathogen) which dictate the infection outcome of *M. bovis,* may also have a role in *M. orygis* survival and could explain the difference between *M. orygis, M. bovis,* and *M. tb* disease presentation in calves. Additionally, our recent characterization of the *M. orygis* secretome (chapter III) may allow further investigation the host-pathogen interaction and delineate factors associated with 'generalist' versus 'specialist' pathogens driving differential virulence.

This study is the first to interrogate the pathogenesis of *M. orygis* in a natural host using an experimental animal model[337]. By all markers of morbidity within this study, cattle infected with *M. orygis* had significantly worse experimental outcomes compared to *M. tb* infected cattle. This correlates well to the binary distribution observed in our established murine model. Both *M. bovis* and *M. orygis* infected mice have more severe pathology and significantly expedited median survivals when compared to *M. tb* infected mice. This experiment underscores that result; though

infection with *M. bovis* and *M. orygis* does not result in calf mortality, differences in morbidity are readily observed compared to *M. tb* infection. Previously, our group has suggested that *M. tb* H37Rv should not be used alone as the main resource in virulence studies, as non-canonical virulence factors may be inadequately represented *in vitro.* Accordingly, the potential role of these factors may not be systematically evaluated *in vivo.* Two arguments are often posed against this suggestion; first that this data comes from mice considered 'resistant' to mycobacterial infection, and second, that if *M. bovis*- and *M. orygis*- were more virulent, they would outcompete *M. tb* and be the causative agent of tuberculosis in humans[296,323]. The infection outcome of *M. orygis* in a natural host (against two well-studied members of the MTBC) dispels this. We focussed on readouts of morbidity, mortality, and bacterial burden to compare *M. tb, M. bovis* and *M. orygis* and determined that in both cattle and mice, *M. orygis* mimics *M. bovis.* Moreover, *M. orygis* trends towards increased disease severity compared to *M. bovis* in its natural host as increased pulmonary involvement and lung burden is also observed. Next, in humans, *M. tb* is virulent but in cattle- and mice- this is not the case. If we define virulence traditionally as the morbidity and mortality attributed to the pathogen, *M. bovis* and *M. orygis* have worse infection outcomes compared to *M. tb.* If we include transmission as a measure of virulence in this definition, within the cattle host, *M. bovis* and *M. orygis* are still more virulent, as there has been no reported animal-to-animal transmission of *M. tb* whereas *M. bovis* and *M. orygis* commonly cause outbreaks. Why *M. bovis* is not the causative agent of tuberculosis in humans remains unknown. Ultimately, observing differential virulence in two unrelated, animal hosts (one experimental, one natural) with two different bacteria further emphasizes that the pathogenesis of *M. tb* may need to be revisited. Whether *M. orygis* and *M. bovis* have had a gain-of-virulence or *M. tb* has undergone attenuation since their common ancestor remains an open question.

5. Figures

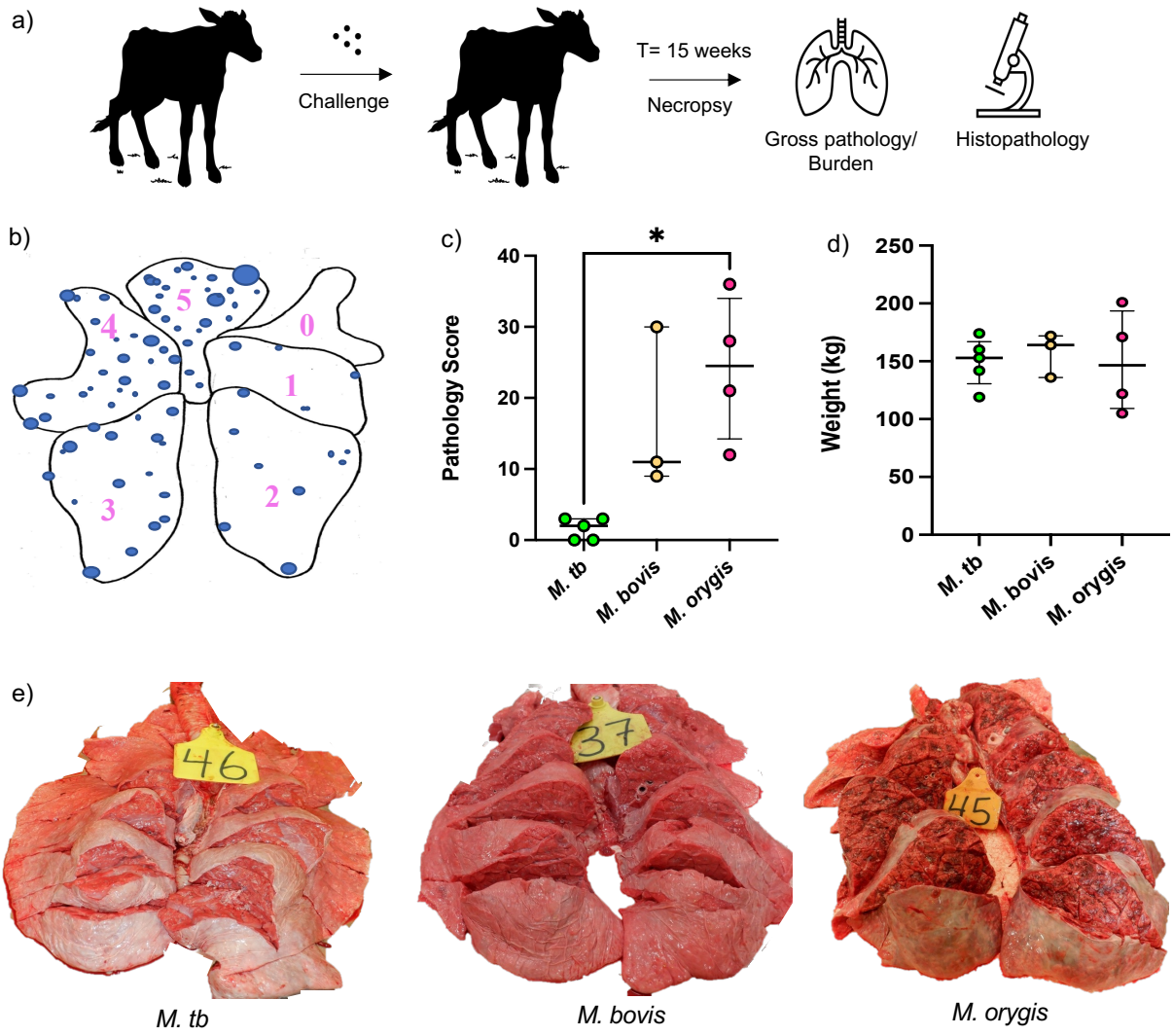

Figure 23. Experimental overview

a) Schematic overview of calf aerosol infection. *Bos taurus* calves were randomized into *M. tb* H37Rv, *M. bovis* AF2122, and *M. orygis* 51145 experimental groups (~10^4 CFU/calf). At week 15, organs were harvested for pathology studies and bacterial burden. **b)** Pathology score determination. Each lobe of lung was measured on a scale of 0-5 based on size, frequency, and distribution of lesions. Maximal pathology score= 40. **c)** *M. orygis* infected cattle have significantly greater lung pathology compared to the *M. tb* experimental group (p= 0.01, Kruskal-

Wallis test). *M. tb* pathology range = 0-3 (out of 40), *M. bovis* pathology range= 9-30, and *M. orygis* pathology range = 12-36. **d)** Weight of cattle at experimental endpoint **e)** Gross pathology of lungs at necropsy for *M. tb* H37Rv*, M. bovis* AF2122, and *M. orygis* 51145 infected cattle (transverse slice). Lungs presented correspond to cattle with the highest overall pathology score in their respective experimental group. Calf 46= *M. tb,* total pathology score = 3; Calf 37= *M. bovis,* total pathology score= 30, Calf 45= *M. orygis,* total pathology score= 36

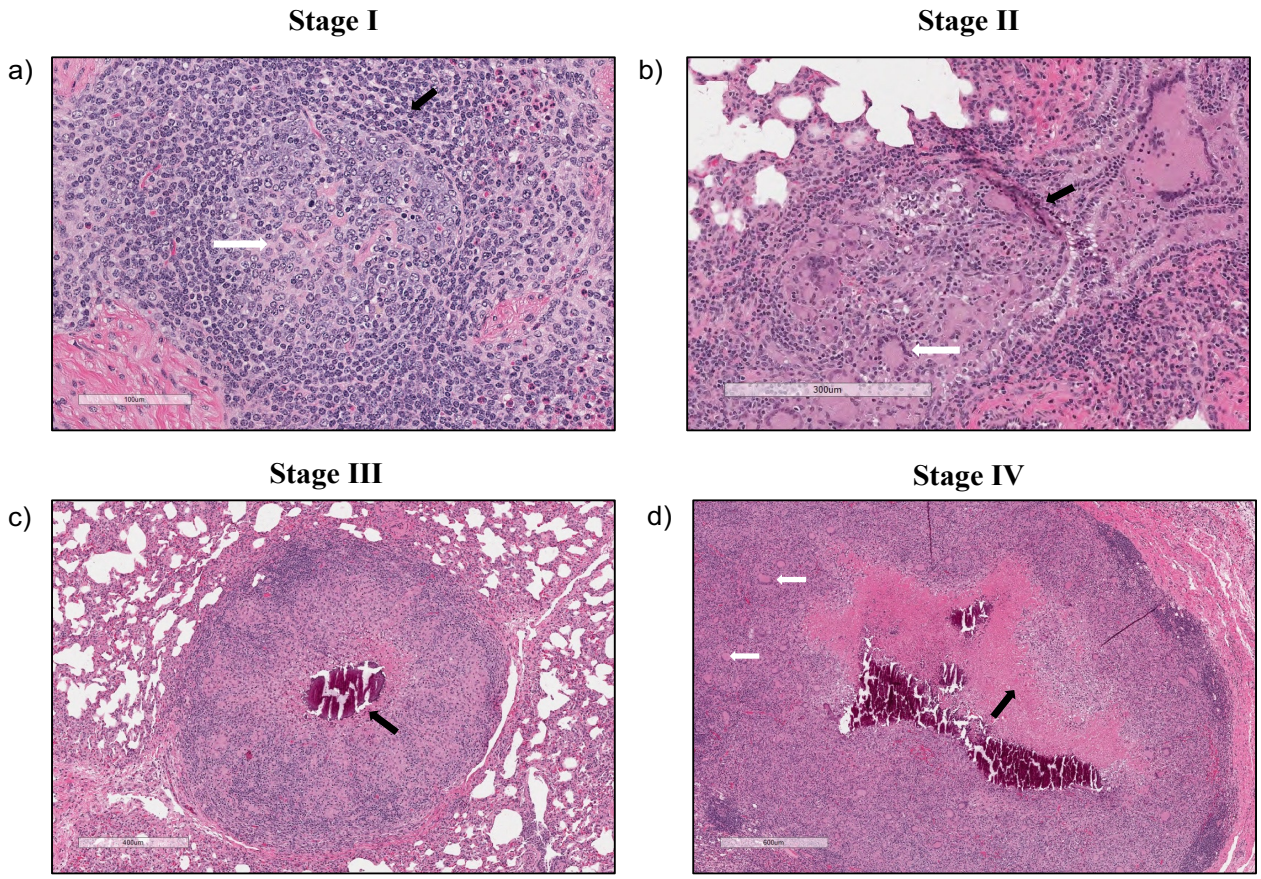

Figure 24. Classification of four stages of granulomas in infected calves.

Scoring criteria based on previously established parameters by Wangoo et al.,[437] and Carrisoza-Urbina et al[39]. Tissues stained with hematoxylin and eosin (H&E). **a) Stage I:** initial formation of the granuloma. Macrophages (typically epithelioid) cluster to form a centre (white arrow). Debris may or may not be present in the centre of structure. No multinucleated cells observed; no necrosis. Lymphocytes surround structure (black arrow). **b) Stage II:** Larger structure than stage I. Significant increase in frequency of multinucleated giant cells (MNGCs, Langhans) (white arrow) with partial encapsulation (black arrow). Depending on progression of granuloma, minimal areas of necrosis may be present. Lymphocytic infiltrates evident. **c) Stage III**: Central necrotic core surrounded by acellular region (caseous necrosis, with or without mineralization; black arrow). Cellular debris observed. Granuloma encapsulated and distinct from surrounding tissue. Mixture

of macrophages, MNGCs, and lymphocytes among other cell populations. **d) Stage IV**: Furthest progressed granuloma. Extensive necrosis; often multiple necrotic foci fused together. Cell debris within centre of the structure; mineralization usually evident. Necrotic cores + debris surrounded by acellular region (black arrow). MNGCs frequent throughout structure; typically presenting as satellite granulomas (white arrow). Structure encapsulated; central hemorrhage observed.

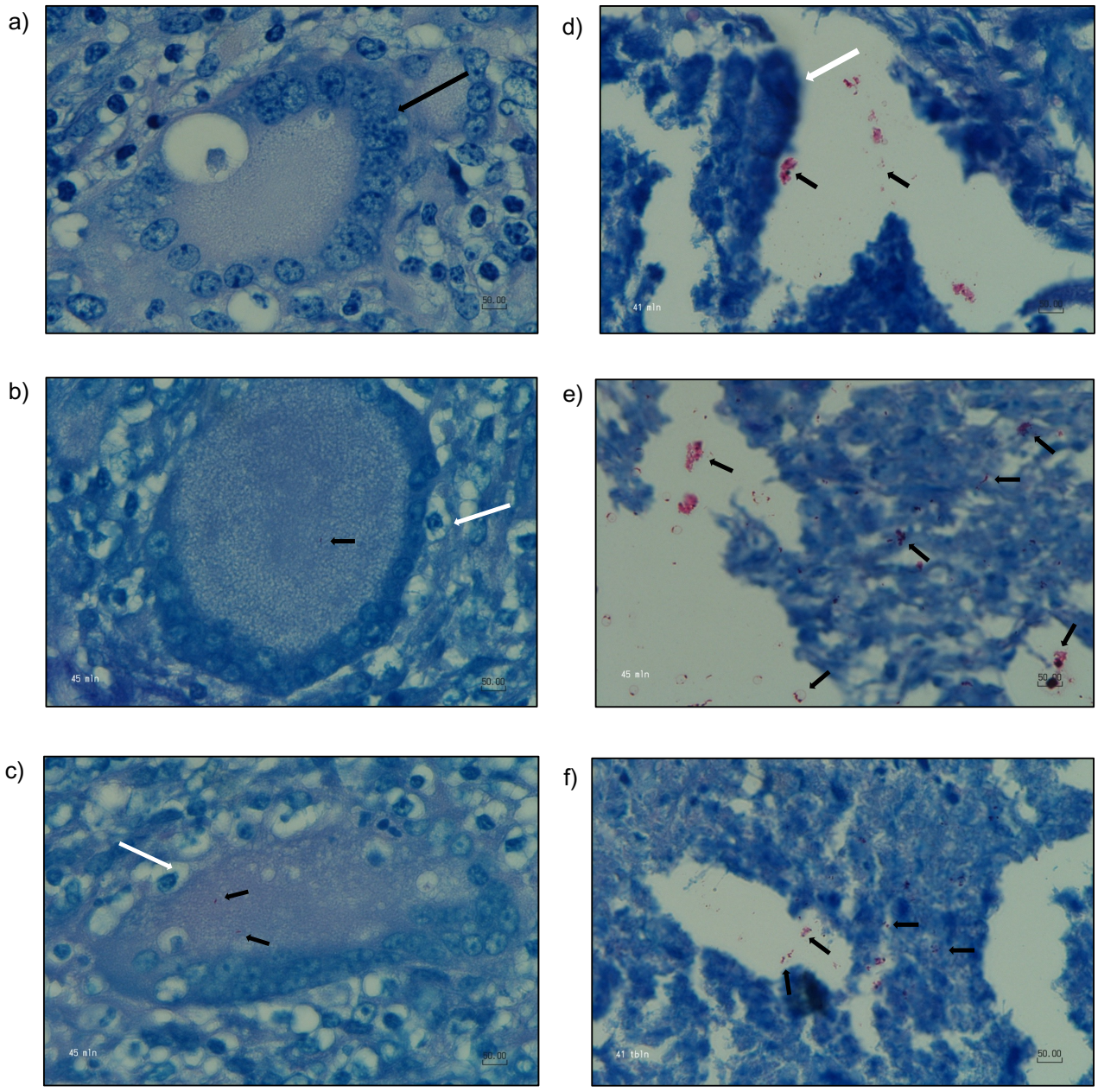

Figure 25. Ziehl-Neelsen (ZN) staining of infected lymph nodes.

a) 100x magnification of multinucleated giant cell (MNGC; Langhans). Structure formed by the fusion of activated epithelioid macrophages; nuclei arranged in circular/ovoid pattern at cell periphery (indicated by black arrow). **b-c) Black arrow**: MNCG showing intracytoplasmic mycobacteria (fuchsia; rod-shaped bacilli). MNGC delineated by border of nuclei. 100x magnification. **White arrow**: pro-inflammatory foamy macrophage surrounding MNGC.

Cytoplasm of cell composed predominantly of lipids (white, 100x magnification). **d-f)** Variable morphology of mycobacteria within the necrotic core of stage IV granuloma (black arrows; 100x magnification). Mycobacteria presented as rod-shaped, clustered, fragmented, and/or circular (fuchsia). This was seen both within the same tissues, and between calf samples. **White arrow**: mineralization/debris within necrotic core. 100x magnification.

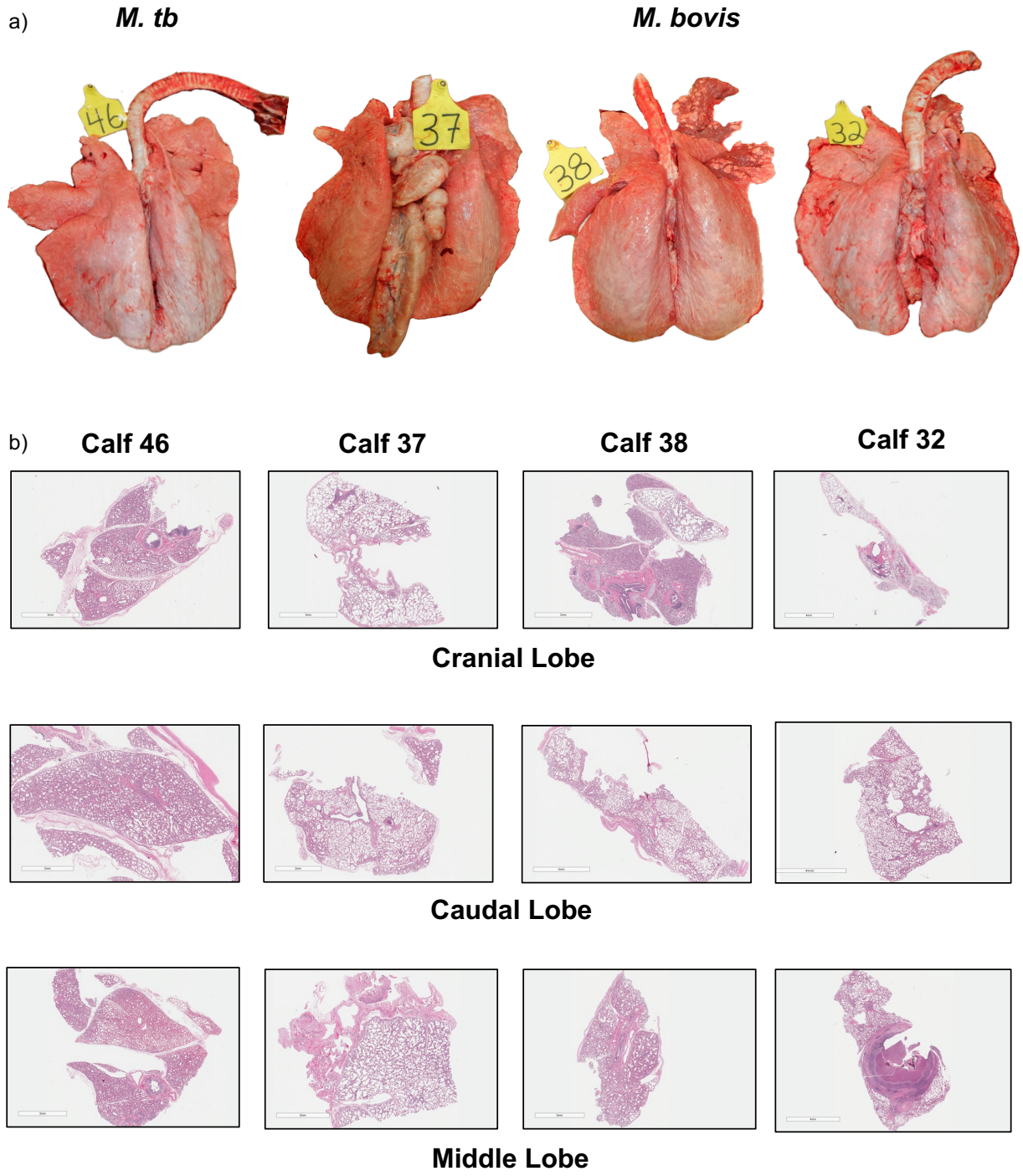

Figure 26. *M. bovis* presents with progressed lung disease compared to *M. tb.*

a) Gross pathology of infected cattle at necropsy. Left: lungs of *M. tb* infected calf corresponding to highest pathology rank (calf 46). Right: lungs of *M. bovis* infected cattle in decreasing order of pathology rank (calf 37 > calf 38 > calf 32). Additionally pathological features: calf 37 presents

with significantly enlarged lymph nodes; calf 38 and 32 present with collapsed lung due to aspiration (cause independent of infection). **b)** Corresponding histopathology of *M. tb* and *M. bovis* infected lungs. Presented overview of cranial, caudal, and middle lobe of lung. 3 x 3 x 3 cm pieces of lung were extracted from lobe of interest and stained with hematoxylin and eosin (H&E) and assessed for presence/absence of granulomatous structures.

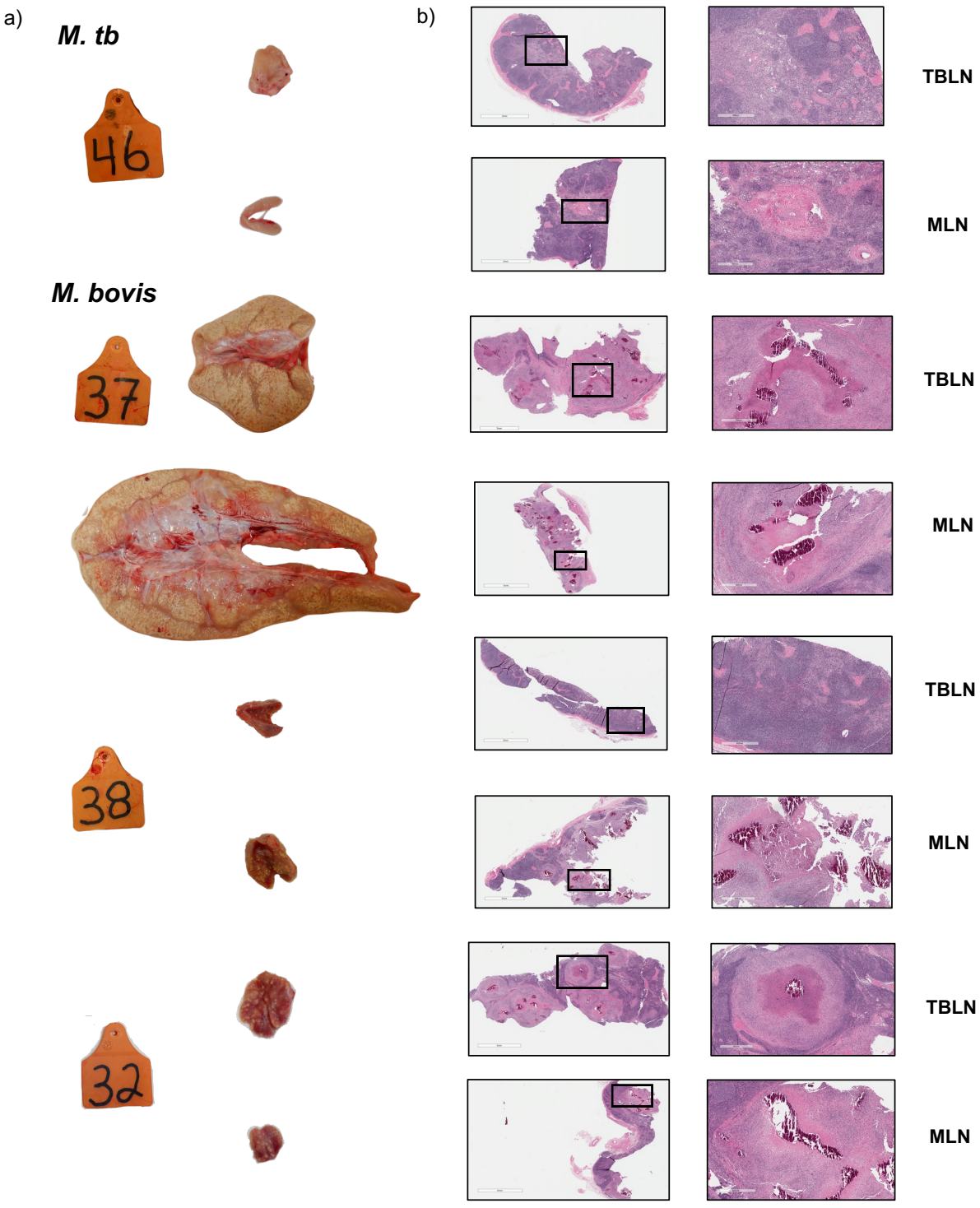

Figure 27. *M. bovis* presents as severe lymphatic disease.

a) Gross pathology of tracheobronchial (TBLN) and mediastinal lymph nodes (MLN) following either *M. tb* or *M. bovis* infection. Whole, encapsulated TBLN/MLN sliced transversely to assess

lesion distribution. Top: *M. tb* infected TBLN/MLN negative for lesions (no lymphatic involvement). Bottom: *M. bovis* infected TBLN/MLN. Calves in order or decreasing pathology (37 > 38 > 32). Calf 37 TBLN and MLN most significantly enlarged. Indistinguishable, coalescing lesions observed following transverse slice of encapsulated node. Regions of lesions segregated by thin margins. In centre of node, white, connective tissue covers portion of lesions (web-like presentation); hemorrhage observed. Two small holes evident at necropsy. **b)** Corresponding histopathology to *M. tb* and *M. bovis* infected lymph nodes. Left side: overview of lymph node architecture (TBLN, MLN). Right side: higher magnification of areas of interest (indicated by black box). 3 x 3 x 3 cm pieces of lung were extracted from TBLN/MLN and stained with hematoxylin and eosin (H&E).

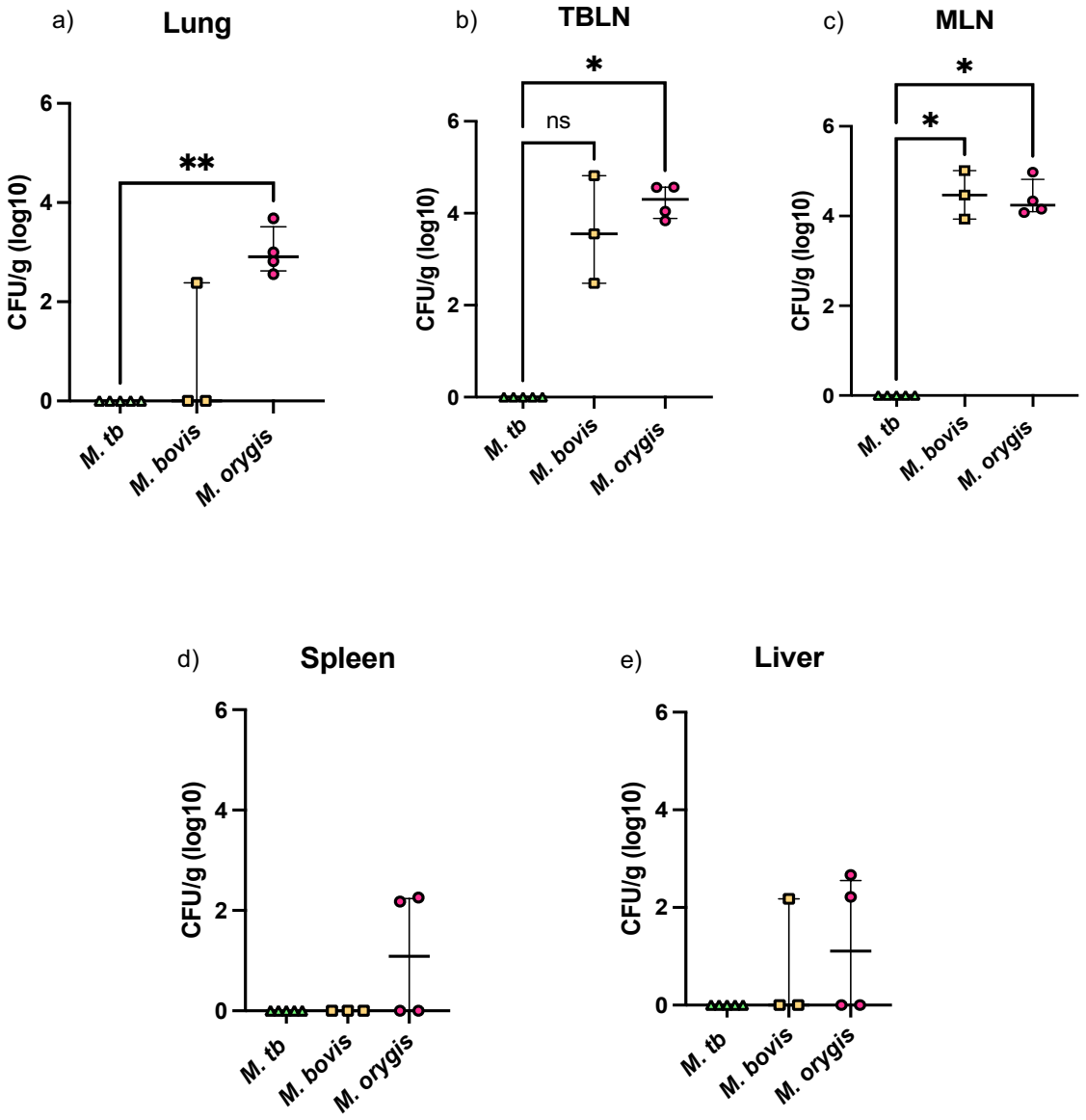

Figure 28. Comparative bacterial burdens

a) Lung bacterial burden (CFU/g). *M. orygis* infected cattle have significantly greater lung burden compared to *M. tb* infected cattle ($p < 0.05$, Kruskal-Wallis test). Additionally, compared to *M. bovis* infected cattle, there is a trend for greater lung involvement in *M. orygis* infected cattle ($p \sim 0.07$, Kruskal-Wallis; not statistically significant). Bacterial burden calculated as CFU/g ($\log_{10}$). 1 g per lobe extracted by sterile biopsy punch and plated (left + right cranial, caudal, and middle lobes). **b)** Bacterial burden of *M. tb, M. bovis* and *M. orygis* infected tracheobronchial lymph nodes

(TBLNs). 1 g of TBLN was extracted by sterile biopsy punch and plated. *M. orygis* infected calves show significantly greater burden compared to *M. tb* infected calves ($p < 0.05$, Kruskal-Wallis test). No significant difference in burden was observed between *M. tb* and *M. bovis* infected cattle ($p= 0.11$, Kruskal-Wallis) nor *M. bovis* and *M. orygis* ($p>0.99$, Kruskal-Wallis). Burden calculated as CFU/g ($\log_{10}$). **c)** Bacterial burden of *M. tb, M. bovis,* and *M. orygis* infected mediastinal lymph node (MLN). Both *M. orygis* and *M. bovis* infected cattle show significantly greater bacterial burden in the MLN compared to *M. tb* infected cattle ($p < 0.05$, Kruskal-Wallis test) but comparable burden to each other (*M. bovis* v. *M. orygis*). **d)** Splenic burden of *M. tb, M. bovis* and *M. orygis* infected cattle. No significant differences between experimental groups. CFU above limit of quantification in spleen only observed following *M. orygis* infection. **e)** Liver burden of *M. tb, M. bovis* and *M. orygis* infected cattle. No significant differences between experimental groups. CFU above limit of quantification in liver only observed following *M. orygis* infection.

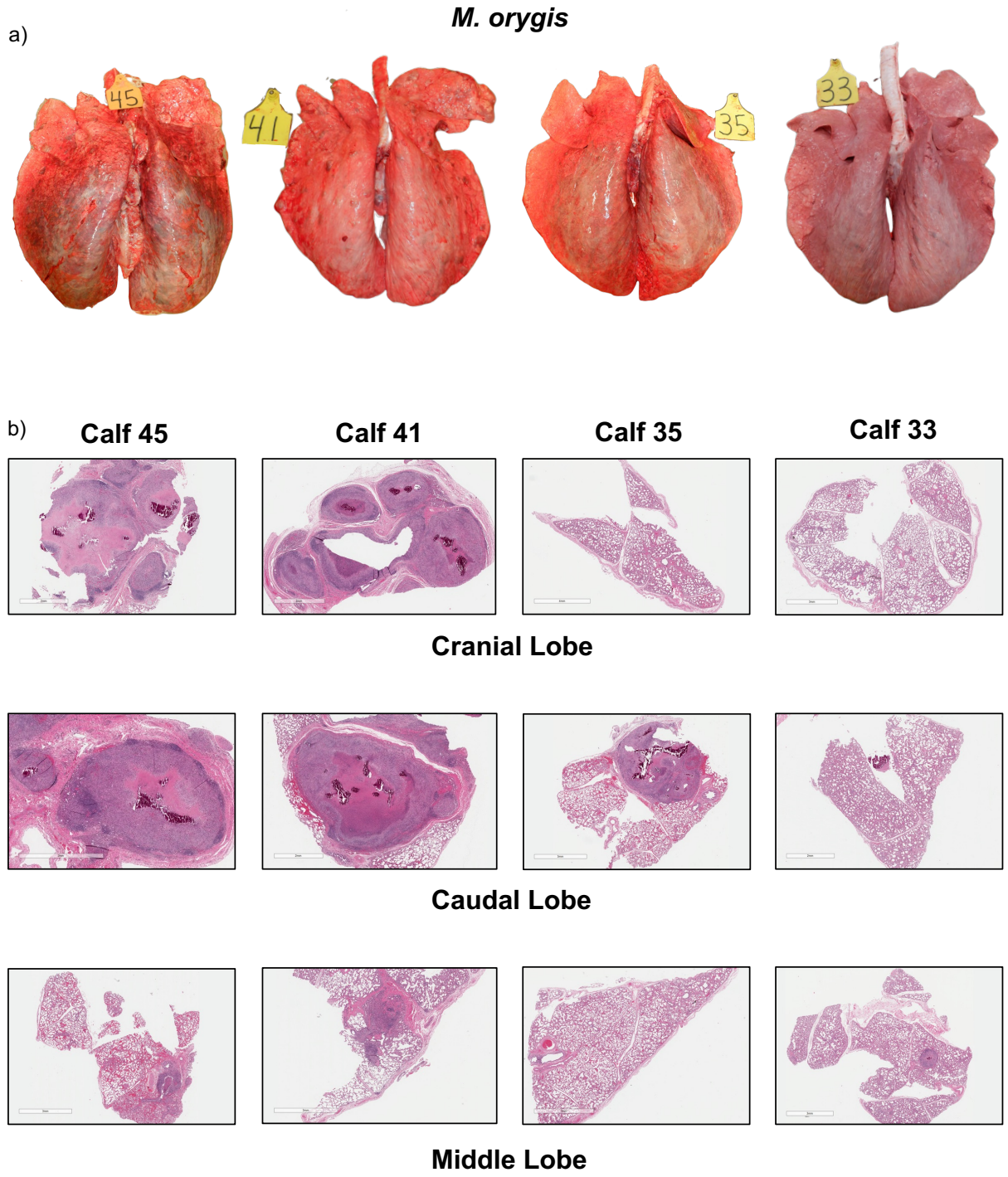

Figure 29. *M. orygis* infected lungs present with significantly worse pathology compared to *M. tb* and *M. bovis* infected cattle.

a) Gross lung pathology of *M. orygis* infected cattle. Far left: highest pathology score (calf 45; pathology score= 36); far right: lowest pathology score (calf 33; pathology score= 12). Calves organized in decreasing pathology (calf 45 > 41 > 35 > 33). Additional pathological features include visible surface lesions, edema (calf 35, 45), and tracheal foam (calf 35, 45; independent of infection) **b)** Corresponding histopathology of *M. orygis* infected lungs. 3 x 3 x 3 cm pieces of lung were extracted from lobe of interest and stained with hematoxylin and eosin (H&E) and assessed for the presence/absence of granulomatous structures.

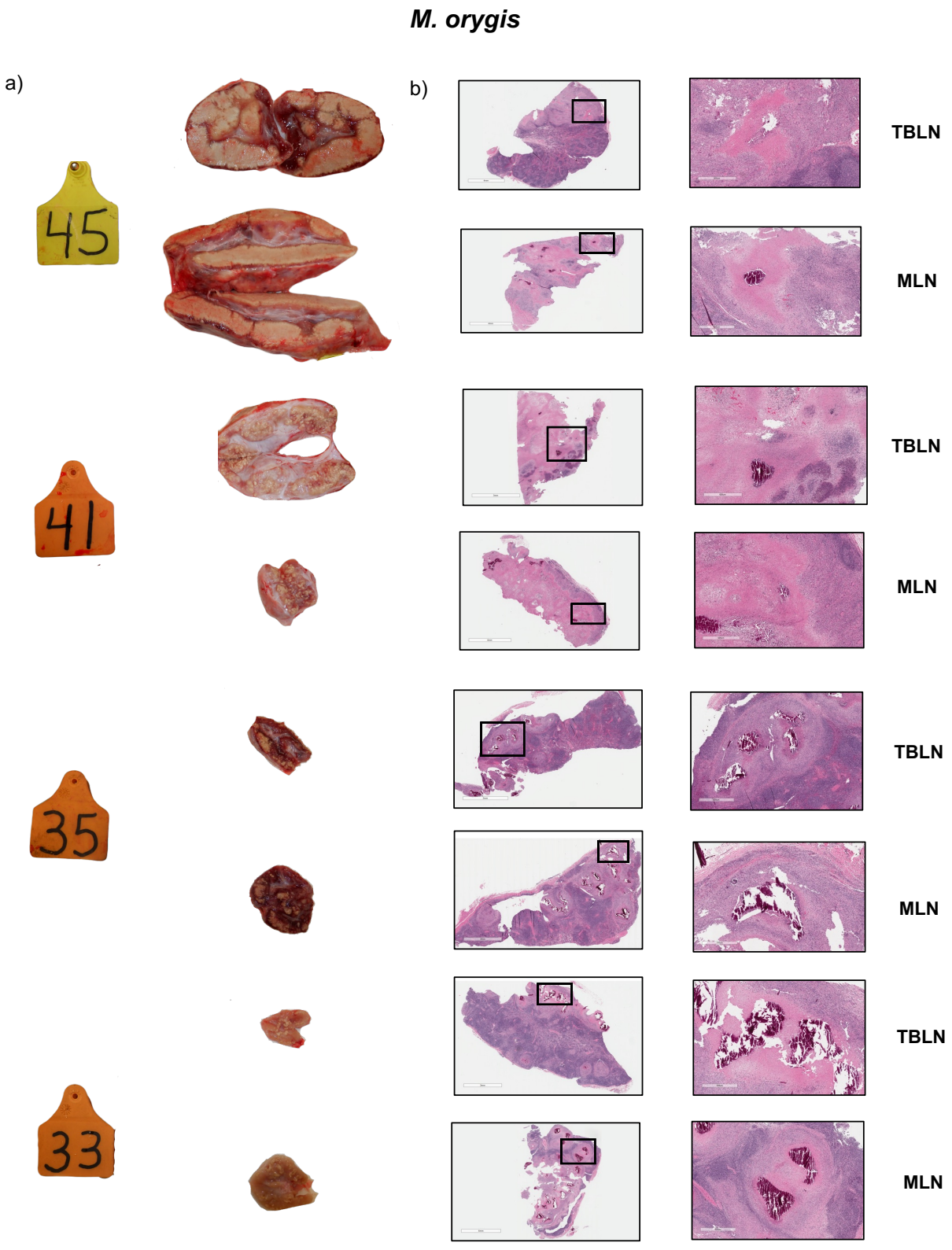

Figure 30. *M. orygis* lymphatic disease is distinct from *M. tb* but comparable to *M. bovis*

a) Gross pathology of *M. orygis* infected tracheobronchial (TBLN) and mediastinal lymph nodes (MLN). Whole, encapsulated TBLN/MLN sliced transversely to assess lesion distribution. All *M. orygis* infected lymph nodes positive for granulomatous lesions. Calf 45 shows a complete consolidation of lesions, with limited margins between lesion foci (2/4 sides of opened lymph node show no distinction between lesions). In the centre of the node there is extensive necrosis and hemorrhage, as well as thin connective tissue (similar to calf 37). Calf 41 MLN lymphadenitis clear; individual lesions beginning to fuse throughout the node but are not as progressed as calf 37 or 45. Additionally, thick margins of connective tissue segregate foci of lesions. Severe hemorrhage observed in calf 35 TBLN/MLN. **b)** Corresponding histopathology of *M. orygis* infected TBLN/MLN. Left side: overview of lymph node architecture (TBLN, MLN). Right side: higher magnification of areas of interest (indicated by black box). 3 x 3 x 3 cm pieces of lung were extracted from TBLN/MLN and stained with hematoxylin and eosin (H&E). All sections of *M. orygis* TBLN/MLN contained at least one stage III-IV granuloma with or without mineralization.

6. Tables

Score	Description
0	No gross lesions
1	≤ 10 lesions AND/OR All lesions < 10 mm in diameter
2	6-10 lesions AND/OR Rare (≤ 2) lesions between 10-20 mm in diameter
3	11-20 lesions AND/OR Occasional (3-5) lesions between 10-20 mm in diameter
4	≥ 20 lesions AND/OR Frequent (> 5) between 10-20 mm in diameter
5	Numerous and coalescing lesions AND/OR ≥ 50% lesions > 10 mm ≥ Identification of any lesions > 20 mm

Table 10. Lung pathology scoring criteria.

Adapted from Dr. Jeffery Chen, University of Saskatchewan; Waters et al. 2014[333]

	M. tb	*M. bovis*	*M. orygis*
Lungs	3/5 (60%)	3/3 (100%)	4/4 (100%)
TBLN	0/5 (0%)	3/3 (100%)	4/4 (100%)
MLN	0/5 (0%)	3/3 (100%)	4/4 (100%)
Spleen	0/5 (0%)	0/3 (0%)	0/4 (0%)
Liver	0/5 (0%)	0/3 (0%)	2/4 (50%)

Table 11. Lesion presentation.

Infected calves positive for gross lesions in the lungs, lymph nodes, spleen or liver at necropsy. TBLN: tracheobronchial lymph nodes; MLN= mediastinal lymph nodes. Lungs considered positive if lesions were detected in any lobe.

CHAPTER VI: DISCUSSION

In this thesis, I describe how experimental tools and models can be used to investigate MTBCs, whether they are new or poorly defined. I first aimed to use mycobacterial engineering in *M. bovis* BCG, *M. bovis,* and *M. orygis* strains. For this, I utilized the pNIT:ET system to generate mono-resistant BCG strains, and the ORBIT system to generate deletion strains in *M. bovis* and *M. orygis.* I then used these strains to determine infection outcomes of WT and isogenic strains using *ex vivo,* and *in vivo* models. Additionally, I used standard murine and calf models to investigate a novel pathogen (*M. orygis*) and understand how it presents compared to the human associated *M. tb* and the cattle-associated *M. bovis.* I sought to investigate why MTBCs show such significant differences in virulence and the genes that may be responsible for this.

In my project, I went from *in vitro* characterization to *in vivo* infection outcomes. My work emphasized how natural experiments can inform fundamental research. Specifically, it shows how mutations occurring due to mycobacterial evolution, on a 'micro' scale as seen in response to antibiotic exposure, or on a 'macro' scale as is evidenced across the MTBCs, can be recreated using current molecular techniques. For decades, the inability to engineer the MTBC complicated fundamental research, however tools are no longer the 'limiting reagent' for these studies. Instead, we are limited by the questions we choose to investigate.

In chapter II, I implemented mono-resistant BCG strains as quality controls for diagnostics. The panel developed in this chapter was a by-product of the failure of the pNIT:ET recombineering system. Initially, pNIT:ET was employed for the development of mycobacterial gene deletions. However, given its reliance on general homologous recombination, a deletion strain could not be generated. Notably, the RpsL K43R mutation was suggested by the authors as a positive control for the efficacy of this system and became the first mono-resistant BCG strain I developed. The

high fidelity of the K43R mutation led to the idea that pNIT:ET could be repurposed for the generation of any resistance conferring SNP and that this may be useful to both clinicians and patients. This addressed a technical gap in the clinic and highlighted the need for robust tools as the diagnostic landscape shifts from phenotypic to genotypic testing. There is growing demand for better, faster tools in order to detect and treat *M. tb* globally, but there are no controls in place to properly confirm these claims. My panel is designed to be expanded upon; resistance-conferring mutations from a variety of sources (such as patient isolates, clinical trials, the WHO mutation catalogue, etc.) can be engineered in the laboratory. In fact, since its conception, a new strain containing a targeted mutation both in GyrA (D94G) and KatG (S315T) has been added to the panel. As these strains are alive, two benefits are apparent: 1) if a mutation truly confers drug resistance can be confirmed and 2) controls can be modified to keep pace with new diagnostics. This is particularly important as a recent study of over 15,000 *M. tb* isolates identified 492 SNPs across 13 antibiotics, including all first-line anti-mycobacterial agents (except PZA), and 8 drugs from the current MDR-TB treatment recommendation[468]. After proving the utility of my work, the panel described in chapter II was implemented as a standard control at the McGill University Health Centre (Montréal, QC), Inuulitsivik Health Centre (Puvirnituq, QC), and Centre de Santé Tulattavik de l'Ungava (Kuujjuaq, QC), and Christian Medical College (Vellore, India) for routine TB testing. It was then deposited in the Belgian Co-ordinated Collection of Microorganisms (BCCM, Brussels) to allow other laboratories globally to request this panel. The work in this chapter can be summarized by the concept of 'bench-to-bedside'. I used common laboratory tools to develop strains that can be implemented in the clinic to address a critical oversight in current diagnostic tests.

As described, the pNIT:ET system was initially employed to engineer deletion strains. However, due to the low rates of general homologous recombineering and the size of the insert, this was not feasible. Instead, the ORBIT system- which combined the most efficient components of mycobacterial recombineering- was implemented. This supports the overarching theme of this dissertation that as molecular tools develop, previously uncharacterized differences between mycobacterial strains can be experimentally investigated. My work in chapters III and IV enabled me to identify MPT70 and MPT83 as non-canonical virulence factors. I determined that in *M. bovis* MPT70 and/or MPT83 were necessary for full virulence whereas in *M. orygis* MPT70 and/or MPT83 continue to have unknown roles. As such, MPT70/MPT83 can be further characterized as 'species-specific' virulence factors. These findings were supported by data at the *in vitro* level (proteomics), the *ex vivo* level (macrophage infections), and the *in vivo* level (murine infections). I also confirmed the role of *esxA* in *M. orygis* virulence, establishing this for the first time. Perhaps the most obvious limitation in this thesis is that my knockouts were not complemented, due to time limitations. As an attempt to determine if there were off-target mutations, I did WGS on my deletion strains to verify the absence of mutations outside of the targeted genes. Additionally, the PCAs performed in these studies supported that the main drivers of variance in *M. bovis* could be attributed to differential expression of the proteins whose genes were deleted. In the murine infection model, the phenotype is severe (i.e. death versus survival) and as such, we suspected that a complement may not fully restore lethality, as complements in mouse models often only partially restore the bacteriological phenotype. This remains to be tested. However, a complement may provide useful insights at the *in vitro* and *ex vivo* levels. For example, the MTBCs have an overwhelming arsenal of effectors designed to resist and evade host stressors including factors involved in lipid and fatty acid metabolism and/or synthesis, cell envelope proteins, and complex

free lipids[247,262]. As MPT83 is a lipoprotein and has been associated with modifications to the cell death pathway, it may be interesting to restore MPT83 without its lipid anchor and determine if and/or how this impacts immunogenicity. Further, infection with *M. bovis Δmpt83* showed increased pathology at week 16 compared to infection with either *M. bovis Δmpt70* and *M. bovis Δmpt70_mpt83* (ex: increased regions of consolidation, cellular infiltrates, etc.); it may be pertinent to investigate if MPT70 or MPT83 mediates a pro-inflammatory cascade, such as neutrophil recruitment, that leads to this pathology. In chapter IV, I explored differential survival between *M. tb, M. bovis,* and *M. orygis*. For *M. bovis* and *M. orygis* it was observed that if mice survived beyond day 28, they stabilized until a second 'cliff' of mortality, occurring at ~120 days (week 16). However, following infection with *M. bovis* in which MPT70 and/or MPT83 are absent this cliff appeared to be circumvented. This poses two questions: first, does MPT70 and/or MPT83 play a role in immune exhaustion? Second, as lung bacterial burden at week 16 showed significant reduction compared to week 3, is bacterial burden the main mediator of mortality? This could be further informed by infection with *Mycobacterium caprae,* a member of the MTBC which harbours the same two missense mutations in RskA as *M. bovis*[103,186].

Throughout the MTBC it is often seen that virulence factors act in tandem with other partners. This may be a potential explanation as to why *M. orygis* mortality cannot be prevented the way it is in *M. bovis* following the deletion of MPT70 and/or MPT83. For example, in *M. orygis,* there is increased expression of ESX-5 associated proteins, many of which are poorly characterized. It may be possible that MPT70 and/or MPT83 either interact or work in concert with these proteins to generate high level virulence. Further, though the role of MPT70 and MPT83 is most evident in the context of *M. bovis,* it cannot be overlooked that vaccination with an MPT70 based subunit vaccine delayed the mortality 'cliff' of *M. orygis* infected mice until ~16 weeks (12

weeks longer than expected) and at a comparable level to that of an ESAT-6 based subunit vaccine. At the time of submission, there is an ongoing *M. orygis* aerosol infection comparing naïve (PBS) mice to H107e-vaccinated mice. The H107e subunit vaccine (Statens Serum Institute, Copenhagen, Denmark) contains 8 *M. tb* antigens, including ESAT-6, MPT70, and MPT83, and has shown some protective effect against *M. tb* aerosol infection when co-administered with BCG[469]. The goal of this experiment is to determine if *M. orygis* mortality can be overcome and if this vaccine can result in clearance rather than containment of infection.

The hypotheses of this thesis hinge on my studies with bacterial strains in which MPT70 and/or MPT83 is absent (*Δmpt70, Δmpt83,* and *Δmpt70_mpt83*). The latter deletion strain disrupts not only *mpt70* and *mpt83*, but also the intermediate gene, *dipZ*[186]. This gene is broadly characterized as an integral membrane protein and associated with cytochrome biogenesis. It has been suggested that DipZ is a fused protein, composed of protein subunits homologous to CcdA and TlpA[186]. Interestingly, DipZ, in its full length, is only found in slow-growing, pathogenic mycobacteria; in other bacterial species CcdA and TlpA are separated. DipZ is controlled by SigK/RskA regulation[186]. Accordingly, like MPT70 and MPT83, DipZ is constitutively expressed in *M. bovis* and *M. orygis*[186]. In chapter IV, I demonstrated that in *M. bovis,* deletion of MPT70 and MPT83 alone showed attenuation comparable to a deletion of MPT70, DipZ, and MPT83. The comparison of *ΔdipZ* to *Δmpt70* and *Δmpt83* may provide insights into the mechanism of MPT70 and MPT83 in infection outcomes. By engineering *ΔdipZ* both MPT70 and MPT83 proteins remain intact; if attenuation is not recapitulated following aerosol infection, this supports that MPT70 and/or MPT83 mediate the host reaction to *M. bovis* infection and pathology. It would also be interesting to determine if the bacterial clearance phenotype observed following *Δmpt70,*

Δmpt83 and *Δmpt70_mpt83* is maintained in the absence of DipZ. This could indicate that recognition of MPT70 and/or MPT83 mediates the establishment of infection.

Additionally, it cannot be overlooked that *ex vivo* studies in this dissertation relied on murine BMDMs, which may not be representative of the immune mechanisms following natural infection. This may account for why bacterial burden does not differ between WT and isogenic strains. As such, it may be more appropriate in future to evaluate *M. bovis* and/or *M. orygis* in bovine alveolar macrophages to determine if the presence or absence of MPT70 and MPT83 results in a host-mediated phenotype, as described in chapter IV.

The exact mechanisms of MPT70 and/or MPT83 remain elusive; however, they may be uncovered through a variety of molecular microbiology methods, either by using the MTBC mutants already generated or studying orthologues in *M. marinum* by using a zebrafish experimental infection model[470]. It has been well-established that *M. marinum* is the causative agent of tuberculosis-like disease in fish and frogs[471]. Moreover, it can infect both immunocompromised (ex: HIV+ patients) and immunocompetent humans via contaminated wounds (often called 'fish tank granulomas')[470,472]. *M. marinum* is closely related to the MTBCs and possesses 4 ESX systems (ESX-1, -3, -4, and -5) and a conserved SigK regulon (in which only MPT83 is absent). Like *M. tb* the SigK regulon of *M. marinum* is induced in response to host-stressors such as hypoxia and starvation[185]. The zebrafish model has been employed for decades as a proxy to study mycobacterial virulence, as *M. tb* and *M. marinum* share pathogenic mechanisms (enabling the intracellular growth and survival in macrophages), are conserved at the amino acid level (~85%), and present with similar pathology[470,471,473]. Moreover, this is a level two pathogen, bypassing the need for a CL3 facility.

Zebrafish are transparent as embryos and larvae, and in early stages of development rely solely on the innate immune system[470]. In chapter IV, I showed that in the absence of an adaptive immune response (RAG -/- mice), mice infected with *M. bovis Δmpt70_mpt83* showed a delay in mortality and a reduced bacterial burden at compassionate endpoint compared to mice infected with wildtype *M. bovis.* Infecting zebrafish with a fluorescent strain of *M. marinum* could allow an investigation into the interplay between MPT70 and the innate system, the localization of infection (providing insight into a potential dissemination phenotype), as well as the role of MPT70 alone, as MPT83 is naturally absent from the genome. Further, both pNIT:ET and ORBIT recombineering systems could be combined to investigate differences in infection outcomes that can be directly attributed to MPT70. This could be accomplished by engineering *M. marinum* expressing no MPT70 (*M. marinum Δmpt70*) and *M. marinum* overexpressing MPT70 (*M. marinum::rskA*$_{Orygis}$). As described in chapter I, the constitutive expression of *M. orygis* can be attributed to a single SNP (X233S). Accordingly, this is an ideal candidate for oligo-mediated recombineering (via pNIT:ET). In *M. marinum* RskA is conserved genomically (100% identity). Like the panel of mono-resistant BCG strains, the *M. orygis* SNP can be introduced into *M. marinum* using pNIT:ET. As this is not a resistance conferring mutation, this oligomer can be combined with the control oligomer (RpsL K43R) to increase selection of a viable candidate. This would allow a simultaneous comparison of three *M. marinum* strains in an *in vivo* model, one in which MPT70 is inducible (WT), one in which MPT70 is absent, and finally one in which MPT70 is constitutively expressed. As suggested above, *M. marinum ΔdipZ* could also be engineered to explore its role in *M. marinum* virulence. As ESX-1, 3, and 5 are conserved, if there are any partners acting in tandem with MPT70, these too can be investigated. At the time of submission,

M. bovis ΔdipZ, M. marinum ORBIT, and *M. marinum Δmpt70* have been constructed and verified (not shown).

In chapters IV and V, I described the novel pathogen (*M. orygis*) using proteomics, macrophage infections, and both murine and cattle models. Through these studies, it was determined that this pathogen is fundamentally different from *M. tb* and warrants further investigation. I have definitively shown that *M. orygis* can be used in virulence studies and that these insights may be translated into *M. tb* research by providing a third comparator species. Additionally, though not described in this dissertation, I have used single-cell imaging mass cytometry (SC-IMC) to evaluate the immune composition of *M. tb* and *M. orygis* infected lungs at 21- and 28-days. Unlike flow cytometry, SC-IMC uses heavy metal conjugated antibodies to label cell populations expressing the markers of interest[474]. Preliminary data indicates that at both day 21 and 28, *M. orygis* elicits a more robust immune response compared to *M. tb* infected mice at the same timepoints (Figure 31a). Moreover, this immune response is hyper-inflammatory, dominated by neutrophils (evidenced by excessive production of myeloperoxidase) and macrophages (Figure 31b). The SC-IMC data is consistent with the microscopic evaluation by a trained pathologist described in chapter IV showing that the *M. orygis* infected mouse with the lowest pathology score shows significantly more inflammation than the highest scored *M. tb* infected mouse. The SC-IMC data also provides insights into potential immune populations of interest. For example, myeloperoxidase (MPO) is a key component of neutrophilic extracellular traps (NETs); based on the preliminary data, we posit that the consolidation and exacerbation of lung damage in *M. orygis* infected mice may be the result of uncontrolled neutrophilic influx, NETosis, and/or subsequent recruitment of other inflammatory immune cells rather than a phenotype mediated by the bacteria[413–415]. Moreover, MPO was observed as early as day 21, which

may be indicative of future mortality. The presence of this MPO-rich histopathologic phenotype was not recapitulated following *M. tb* infection at either day 21 or 28, supporting the hypothesis that *M. orygis* is hypervirulent compared to *M. tb,* in the same host. It is well established that susceptibility to mycobacterial infection is controlled by the balance of pro- and anti-inflammatory responses and that immunopathology is caused by dysregulation of these responses[475]. Accordingly, it is evident that in murine infections, pathology is mediated by the host rather than uncontrolled infection. At both day 21 and day 28, *M. tb* and *M. orygis* bacterial burden was comparable. This was observed in the lungs and liver though *M. tb* spleen burden was significantly greater than *M. orygis*. Further, at day 28 (the point at which mortality was first observed) *M. orygis* showed no increased lung burden compared to *M. orygis* infected mice at day 21, supporting that death is not caused by burden alone. This highlights that neutrophils- a key contributor to host pathology- may be a pertinent *ex vivo* model and can be used to assess differences, such as cytokine secretion, bacterial uptake and/or bacterial burden following WT infection (ex: *M. tb v. M. bovis v. M. orygis*) or isogenic infection (ex: *M. bovis v. M. bovis Δmpt70_mpt83*).

Given the severity of infection observed in WT C57BL/6 mice following *M. orygis* infection, and its significant divergence from *M. tb* infection, it may be interesting to assess the outcome of mice deficient in '*M. tb*- associated' immune receptors following *M. orygis* infection. Specifically, those associated with susceptibility and resistance (prolonged survival). The objective of this experiment would be to determine how (if at all), the mortality curve shifts and if there is a host-receptor integral to propagating *M. orygis* infection. For example, it has been previously shown that C57BL/6 mice lacking the receptor for type I interferons (IFNAR) have prolonged survival and reduced lung burden compared to WT mice, though this may be dependent on strain of mouse utilized (i.e. 'susceptible' v. resistance' strains)[476]. In *M. tb* infection, type I interferons

(IFNs) induce pro-inflammatory cascades via the recruitment of innate immune cells, such as monocytes, macrophages, and neutrophils[476–478]. Whether type I IFNs are beneficial to the pathogen (promotes infection) or beneficial to the host (controls infection) appears to be context dependent, though it has been suggested that there is a relationship between increased secretion of type I IFNs and increased *M. tb* virulence[476–478]. This is particularly relevant in *M. orygis* infection, as hyperinflammation correlates with expedited mortality of the mice. Accordingly, preliminary data of an ongoing survival study has demonstrated that IFNAR -/- mice (C57BL/6 background) exposed to *M. orygis* do not reach median survival until 128 days post infection, consistent with the second 'cliff' of mortality observed in previous WT infection studies (Figure 32). As type I IFNs have limited impact on T-cells, this provides further evidence that the second cliff may be mediated by a loss of control by the adaptive immune system (ex: immune exhaustion)[477]. However, all work with murine models remains limited, as it may not be representative of infection in a natural host.

Finally, in chapter V, it was observed that, in contrast to murine infection, gross- and histopathology correlated to bacterial burden in the lungs and lymph nodes. Notably, this infection was in *Bos taurus* cattle rather than *Bos indicus,* the host most commonly associated with *M. orygis*[222]. As such we do not know if this correlation of bacterial burden and pathology is time-dependent (i.e. calves survived beyond day 28) or host dependent. Previously, it has been reported that bTB arose following the divergence of *Bos taurus* and *Bos indicus* cattle and that *Bos indicus* cattle are more resistant to bTB infection (defined by incidence of bTB, containment/resolution over time, and differences in gross pathology of the lung and/or lymph nodes)[475,479,480]. Interestingly, this trend is not limited to bTB; epidemiological observations also show that *Bos taurus* cattle are more susceptible to bovine tropical Theileriosis (a parasitic infection caused by

Theileria annulata) when compared to *Bos indicus* breeds[479]. This, of course, poses the questions of if resistance is mediated by genetic differences of the host and its response to mycobacteria, once again emphasizing the importance of context in infection. Presently, there are few studies in which genetic loci mediating resistance have been investigated. Where candidate genes were assessed, almost all genes reported were associated with the innate immune system and major innate signalling pathways[475,479]. Moreover, these studies were not based on experimental infection but instead on observational studies[475]. Given these differences, the chapter V cattle study should be repeated in *Bos indicus* cattle with a timepoint for one group at week 4 and secondary timepoint at week 15 (as described in the pilot study). This would allow comparison of the week 4 timepoint across experimental hosts (mice and calves) and establish if an early phenotype, such as differences in burden and/or pathology, occurs. Additionally, this would separate the study into 'acute' v. 'chronic' phases of infection, enabling different arms of the immune system to be studied. The main readout of this experiment would be *M. orygis* infection outcome. As described in chapter V, in *Bos taurus* calves, *M. orygis* infection presented with increased gross and histopathology in both the lungs and lymph nodes, and increased lung burden compared to *M. tb* and *M. bovis.* It would be interesting to see if these trends are maintained in *Bos indicus* calves or if this host is 'specialized' for *M. orygis.* For example, if infection it *Bos indicus* calves is less severe, perhaps this promotes transmission between herds and at the human-animal interface. Further, as the cattle model is well established, it may also be interesting to assess differences in burden (lung, lymph nodes) and/or pathology following infection with WT and isogenic *M. bovis* strains. This would enable direct observation of the roles of MPT70 and/or MPT83 in the context of a natural infection and thus, bovine specific immune responses.

1. Figures

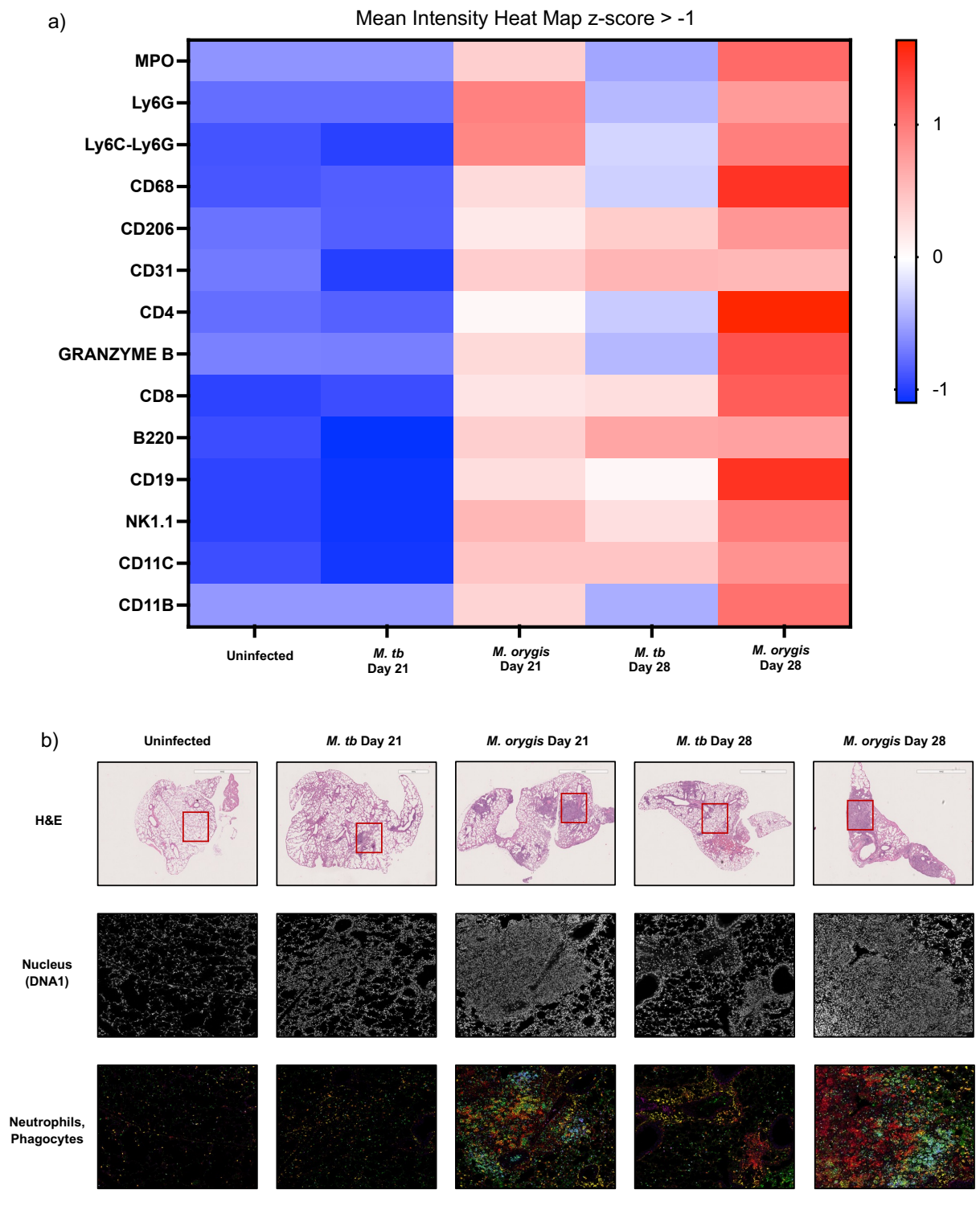

Figure 31: *M. orygis* mounts an early and aggressive immune response

a) Comparative heatmap of uninfected, *M. tb* and *M. orygis* experimental groups at pre-determined experimental endpoint (day 21 and 28) as determined by Z-score. Markers associated with neutrophil (MPO, Ly6G, Ly6C-Ly6G), macrophage (CD206), and phagocyte (CD68) responses. Colour intensity indicative of strength of response. Heatmap generated using GraphPad Prism v.10.0.3. **b)** Single cell and mass cytometry readouts (SC-IMC). H&E staining of right accessory lobe following *M. tb* or *M. orygis* infection at pre-defined timepoints (day 21 or day 28). Uninfected control obtained from age-matched C57BL/6 female mouse on day 21. Red square representative of 1 mm^2 region of interest (ROI) acquired. Images shown are representative of median pathology score per experimental group reported in Fig. 20g). Uninfected= 2.5, *M. tb* (day 21)= 40, *M. orygis* (day 21) = 367.5, *M. tb* (day 28)= 162.5, *M. orygis* (day 28)= 600. Populations of interest: nuclear DNA (DNA1), and neutrophils/phagocytes. Population markers and respective colours in Table 12. Images generated with MCD™ Viewer v.1.0.560.6 (post-acquisition pseudo-colouring).

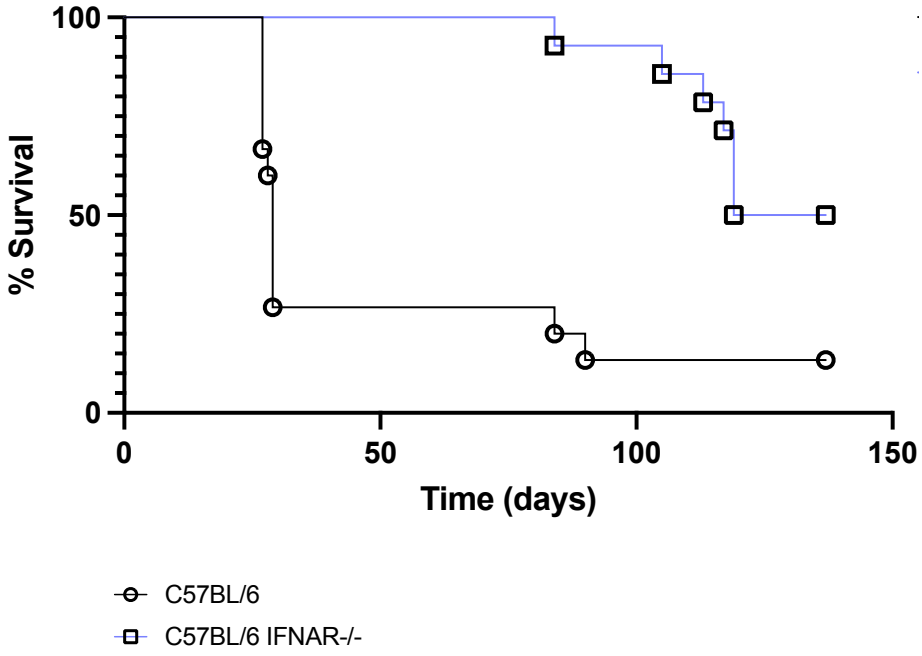

Figure 32: Mice lacking IFNAR show prolonged survival compared to WT C57BL/6.

Kaplan-Meier survival curve of WT and IFNAR -/- C57BL/6 mice. Male and female mice were challenged with *M. orygis* via the aerosol route (n= 18 mice per group; 3 mice sacrificed at day 1 for initial dosing). IFNAR -/- mice showed significantly prolonged survival compared to WT C57BL/6. Median survival IFNAR -/- C57BL/6 = 128 days; WT C57BL/6= 29 days (p= 0.0005, Mantel-Cox). Mortality in IFNAR -/- group observed beginning at day 84 compared to day 27 in the WT group. At time of submission, experiment is still ongoing (n= 7 IFNAR -/- mice remaining; n= 2 WT mice remaining).

2. Tables

Cell Population	Metal-Tag	Conjugated Antibody	Colour
Nuclei	191Ir	DNA1	White
Neutrophils	151Eu	Ly6G	Blue
Neutrophils	176Yb	Ly6C-Ly6G	Pink
Neutrophils (major) Monocytes (minor)	163Dy	Myeloperoxidase (MPO)	Green
Phagocytes	165Ho	CD68	Red
Macrophages	169Tm	CD206	Yellow

Table 12. Markers for single-cell imaging mass cytometry (SC-IMC)

Conjugated antibodies used in immune cell profiling and their respective metal-tags. Colours correspond to Fig. 33b pseudo-colouring. DNA1 included as nuclear control. Markers for T-cell, B-cell, natural killer cells, and dendritic cells also included in SC-IMC panel (not shown).

SUMMARY AND FINAL CONCLUSIONS

In this thesis, I had two aims. The first, to utilize current molecular tools to develop isogenic MTBC strains. I did this using two different recombineering systems: pNIT:ET (for resistance-conferring SNPs) and ORBIT (for creating genetic knockouts). The second, to evaluate infection outcomes using a subset of these strains using *ex vivo* and *in vivo* models. In total, I generated a panel of six isogenic BCG strains, four *M. bovis* deletion strains, and four *M. orygis* deletion strains. Accordingly with my first hypothesis, I was able to implement strains developed by these tools into multiple clinical settings (both nationally and internationally) and utilize deletion strains to investigate putative virulence factors, and in the process discovered a role for MPT70 and MPT83 in *M. bovis* infection. Further, for the first time, I investigated how *in vivo* infection outcomes of *M. orygis* compared to *M. bovis* and *M. tb* and experimentally characterized this overlooked and understudied pathogen. As hypothesized, cattle-associated strains showed increased pathology and decreased survival compared to multiple *M. tb* strains in the same host (mice and cattle). This may suggest that over the course of mycobacterial evolution, *M. tb* may have lost virulence, allowing an increased transmission between human hosts, and/or *M. bovis* and *M. orygis* gained virulence, perhaps enabling spread to multiple animal hosts. Moreover, I showed how the overexpression of MPT70 and MPT83 (a phenotype exclusive to *M. bovis, M. caprae,* and *M. orygis*) contributes to the enhanced virulence of *M. bovis* but unfortunately, does not alter *M. orygis* infection outcomes. However, it was observed that vaccination with MPT70 alone can significantly prolong survival. This enables future research into potential virulence partners which may act in tandem with MPT70 and/or MPT83, such as ESX-5 associated proteins. Additionally, my work in this dissertation has established that the study of *M. orygis* may result in translational applications and could be foundational to future pathogenesis studies. Despite this progress, many

questions still remain. Why is the host range of *M. tb* limited? Why do two independent mutations in a conserved regulon lead to the same overexpression phenotype? Why does this overexpression phenotype result in divergent infection outcomes? And finally, across mycobacterial evolution, why are certain genes upregulated while other genes are lost entirely?

Ultimately, between MTBC subspecies there is ~0.05% difference at the genomic level. This thesis focuses on what the relevance of this difference may be and highlights that, despite conservation, the MTBCs cannot be treated as the same pathogen at either the micro- or global-level. Moreover, I have shown that even a single SNP may be informative to understanding how *M. tb, M. bovis,* and *M. orygis* remain public health threats. Further investigations building upon this work may provide the basis for new diagnostics, vaccines, and/or treatment, and broaden the reference species used in MTBC virulence studies.

BIBLIOGRAPHY

1. BUZIC, I. & GIUFFRA, V. The paleopathological evidence on the origins of human tuberculosis: a review. *J. Prev. Med. Hyg.* **61**, E3–E8 (2020).
2. Barberis, I., Bragazzi, N. L., Galluzzo, L. & Martini, M. The history of tuberculosis: from the first historical records to the isolation of Koch's bacillus. *J. Prev. Med. Hyg.* **58**, E9–E12 (2017).
3. Daniel, T. M. The history of tuberculosis. *Respir. Med.* **100**, 1862–1870 (2006).
4. Saviola, B. & Bishai, W. The Genus Mycobacterium--Medical. in *The Prokaryotes: Volume 3: Archaea. Bacteria: Firmicutes, Actinomycetes* (eds. Dworkin, M., Falkow, S., Rosenberg, E., Schleifer, K.-H. & Stackebrandt, E.) 919–933 (Springer, New York, NY, 2006). doi:10.1007/0-387-30743-5_34.
5. Barbier, M. & Wirth, T. The Evolutionary History, Demography, and Spread of the Mycobacterium tuberculosis Complex. *Microbiol. Spectr.* **4**, 10.1128/microbiolspec.tbtb2-0008–2016 (2016).
6. Natarajan, A., Beena, P. M., Devnikar, A. V. & Mali, S. A systemic review on tuberculosis. *Indian J. Tuberc.* **67**, 295–311 (2020).
7. Grzybowski, S. & Allen, E. A. History and importance of scrofula. *The Lancet* **346**, 1472–1474 (1995).
8. Keshavjee Salmaan & Farmer Paul E. Tuberculosis, Drug Resistance, and the History of Modern Medicine. *N. Engl. J. Med.* **367**, 931–936 (2012).
9. Frith, J. History of Tuberculosis. Part 1- Phthisis, consumption and the White Plague. *JMVH* **22**, (2014).

10. Good, M., Bakker, D., Duignan, A. & Collins, D. M. The History of In Vivo Tuberculin Testing in Bovines: Tuberculosis, a “One Health” Issue. *Front. Vet. Sci.* **5**, (2018).
11. Orgeur, M., Sous, C., Madacki, J. & Brosch, R. Evolution and emergence of Mycobacterium tuberculosis. *FEMS Microbiol. Rev.* **48**, fuae006 (2024).
12. Daniel, T. M. Jean-Antoine Villemin and the infectious nature of tuberculosis. *Int. J. Tuberc. Lung Dis.* **19**, 267–268 (2015).
13. De la virulence et de la spécificité de la tuberculose / by par J.A. Villemin. *Wellcome Collection* https://wellcomecollection.org/works/ah48qcuz/items.
14. Koch, R., Brock, T. D. & Fred, E. B. The Etiology of Tuberculosis. *Rev. Infect. Dis.* **4**, 1270–1274 (1982).
15. Palmer, M. V. & Waters, W. R. Bovine Tuberculosis and the Establishment of an Eradication Program in the United States: Role of Veterinarians. *Vet. Med. Int.* **2011**, 816345 (2011).
16. Smith, T. A COMPARATIVE STUDY OF BOVINE TUBERCLE BACILLI AND OF HUMAN BACILLI FROM SPUTUM. *J. Exp. Med.* **3**, 451–511 (1898).
17. Mitermite, M., Elizari, J. M. U., Ma, R., Farrell, D. & Gordon, S. V. Exploring virulence in Mycobacterium bovis: clues from comparative genomics and perspectives for the future. *Ir. Vet. J.* **76**, 26 (2023).
18. Li, H. & Li, H. Animal Models of Tuberculosis. in *Vaccines for Neglected Pathogens: Strategies, Achievements and Challenges : Focus on Leprosy, Leishmaniasis, Melioidosis and Tuberculosis* (ed. Christodoulides, M.) 139–170 (Springer International Publishing, Cham, 2023). doi:10.1007/978-3-031-24355-4_7.

19. Meehan, C. J., Barco, R. A., Loh, Y.-H. E., Cogneau, S. & Rigouts, L. Reconstituting the genus Mycobacterium. *Int. J. Syst. Evol. Microbiol.* **71**, 004922 (2021).
20. Borham, M. *et al.* Review on Bovine Tuberculosis: An Emerging Disease Associated with Multidrug-Resistant Mycobacterium Species. *Pathogens* **11**, 715 (2022).
21. Shingadia, D. & Burgner, D. Chapter 39 - Mycobacterial Infections. in *Pediatric Respiratory Medicine (Second Edition)* (eds. Taussig, L. M. & Landau, L. I.) 597–614 (Mosby, Philadelphia, 2008). doi:10.1016/B978-032304048-8.50043-8.
22. Bachmann, N. L. *et al.* Key Transitions in the Evolution of Rapid and Slow Growing Mycobacteria Identified by Comparative Genomics. *Front. Microbiol.* **10**, (2020).
23. Daffé, M. & Marrakchi, H. Unraveling the Structure of the Mycobacterial Envelope. *Microbiol. Spectr.* **7**, 10.1128/microbiolspec.gpp3-0027–2018 (2019).
24. Gordon, S. V. & Parish, T. Microbe Profile: Mycobacterium tuberculosis: Humanity's deadly microbial foe: This article is part of the Microbe Profiles collection. *Microbiology* **164**, 437–439 (2018).
25. Vilchèze, C. Mycobacterial Cell Wall: A Source of Successful Targets for Old and New Drugs. *Appl. Sci.* **10**, 2278 (2020).
26. Starke, J. R. CHAPTER 107 - TUBERCULOSIS. in *Feigin and Cherry's Textbook of Pediatric Infectious Diseases (Sixth Edition)* (eds. Feigin, R. D., Cherry, J. D., Demmler-Harrison, G. J. & Kaplan, S. L.) 1426–1469 (W.B. Saunders, Philadelphia, 2009). doi:10.1016/B978-1-4160-4044-6.50112-6.
27. Bunduc, C. M., Bitter, W. & Houben, E. N. G. Structure and Function of the Mycobacterial Type VII Secretion Systems. *Annu. Rev. Microbiol.* **74**, 315–335 (2020).
28. Cook, G. M. *et al.* Physiology of Mycobacteria. *Adv. Microb. Physiol.* **55**, 81–319 (2009).

29. Aliperti, L. *et al.* r/K selection of GC content in prokaryotes. *Environ. Microbiol.* **25**, (2023).

30. Tortoli, E. Microbiological Features and Clinical Relevance of New Species of the Genus Mycobacterium. *Clin. Microbiol. Rev.* **27**, 727–752 (2014).

31. González-Martínez, A. *et al. Mycobacterium* infections. in *Encyclopedia of Infection and Immunity* (ed. Rezaei, N.) 703–718 (Elsevier, Oxford, 2022). doi:10.1016/B978-0-12-818731-9.00216-0.

32. Allen, A. R., Ford, T. & Skuce, R. A. Does Mycobacterium tuberculosis var. bovis Survival in the Environment Confound Bovine Tuberculosis Control and Eradication? A Literature Review. *Vet. Med. Int.* **2021**, 8812898 (2021).

33. Sharma, S. K. & Upadhyay, V. Epidemiology, diagnosis & treatment of non-tuberculous mycobacterial diseases. *Indian J. Med. Res.* **152**, 185–226 (2020).

34. Smith, N. H., Hewinson, R. G., Kremer, K., Brosch, R. & Gordon, S. V. Myths and misconceptions: the origin and evolution of Mycobacterium tuberculosis. *Nat. Rev. Microbiol.* **7**, 537–544 (2009).

35. Kanipe, C. & Palmer, M. V. Mycobacterium bovis and you: A comprehensive look at the bacteria, its similarities to Mycobacterium tuberculosis, and its relationship with human disease. *Tuberculosis* **125**, 102006 (2020).

36. Gagneux, S. Host–pathogen coevolution in human tuberculosis. *Philos. Trans. R. Soc. B Biol. Sci.* **367**, 850–859 (2012).

37. Reva, O., Korotetskiy, I. & Ilin, A. Role of the horizontal gene exchange in evolution of pathogenic Mycobacteria. *BMC Evol. Biol.* **15**, S2 (2015).

38. Veyrier, F. J., Dufort, A. & Behr, M. A. The rise and fall of the *Mycobacterium tuberculosis* genome. *Trends Microbiol.* **19**, 156–161 (2011).

39. Xia, X. Horizontal Gene Transfer and Drug Resistance Involving Mycobacterium tuberculosis. *Antibiotics* **12**, 1367 (2023).

40. Bespiatykh, D., Bespyatykh, J., Mokrousov, I. & Shitikov, E. A Comprehensive Map of Mycobacterium tuberculosis Complex Regions of Difference. *mSphere* **6**, e00535-21.

41. Brosch, R. *et al.* A new evolutionary scenario for the Mycobacterium tuberculosis complex. *Proc. Natl. Acad. Sci. U. S. A.* **99**, 3684–3689 (2002).

42. Coscolla, M. & Gagneux, S. Consequences of genomic diversity in *Mycobacterium tuberculosis*. *Semin. Immunol.* **26**, 431–444 (2014).

43. Malone, K. M. & Gordon, S. V. Mycobacterium tuberculosis Complex Members Adapted to Wild and Domestic Animals. in *Strain Variation in the Mycobacterium tuberculosis Complex: Its Role in Biology, Epidemiology and Control* (ed. Gagneux, S.) 135–154 (Springer International Publishing, Cham, 2017). doi:10.1007/978-3-319-64371-7_7.

44. Coscolla, M. *et al.* Phylogenomics of Mycobacterium africanum reveals a new lineage and a complex evolutionary history. *Microb. Genomics* **7**, 000477 (2021).

45. Guyeux, C. *et al.* Newly Identified Mycobacterium africanum Lineage 10, Central Africa. *Emerg. Infect. Dis.* **30**, 560–563 (2024).

46. Supply, P. *et al.* Genome analysis of smooth tubercle bacilli provides insights into ancestry and pathoadaptation of the etiologic agent of tuberculosis. *Nat. Genet.* **45**, 10.1038/ng.2517 (2013).

47. Brites, D. *et al.* A New Phylogenetic Framework for the Animal-Adapted Mycobacterium tuberculosis Complex. *Front. Microbiol.* **9**, 2820 (2018).

48. Wong, K.-W. The Role of ESX-1 in Mycobacterium tuberculosis Pathogenesis. in *Tuberculosis and the Tubercle Bacillus* 627–634 (John Wiley & Sons, Ltd, 2017). doi:10.1128/9781555819569.ch29.

49. Orgeur, M. *et al.* Pathogenomic analyses of Mycobacterium microti, an ESX-1-deleted member of the Mycobacterium tuberculosis complex causing disease in various hosts. *Microb. Genomics* **7**, 000505 (2021).

50. van de Weg, C. A. M. *et al.* The tough process of unmasking the slow-growing mycobacterium: case report of Mycobacterium microti infection. *Access Microbiol.* **2**, e000074 (2020).

51. Emmanuel, F. X. *et al.* Human and Animal Infections with Mycobacterium microti, Scotland. *Emerg. Infect. Dis.* **13**, 1924–1927 (2007).

52. Panteix, G. *et al.* Pulmonary tuberculosis due to Mycobacterium microti: a study of six recent cases in France. *J. Med. Microbiol.* **59**, 984–989 (2010).

53. Silva-Pereira, T. T. *et al.* Genome sequencing of Mycobacterium pinnipedii strains: genetic characterization and evidence of superinfection in a South American sea lion (Otaria flavescens). *BMC Genomics* **20**, 1030 (2019).

54. Alba, P. *et al.* Genomics insights into a Mycobacterium pinnipedii isolate causing tuberculosis in a captive South American sea lion (Otaria flavescens) from Italy. *Front. Microbiol.* **14**, (2023).

55. Roe, W. D. *et al.* Pathology and molecular epidemiology of Mycobacterium pinnipedii tuberculosis in native New Zealand marine mammals. *PLoS ONE* **14**, e0212363 (2019).

56. Bos, K. I. *et al.* Pre-Columbian mycobacterial genomes reveal seals as a source of New World human tuberculosis. *Nature* **514**, 494–497 (2014).

57. Macedo, R. *et al.* Animal-to-human transmission of Mycobacterium pinnipedii. *Eur. Respir. J.* **56**, (2020).

58. Vågene, Å. J. *et al.* Geographically dispersed zoonotic tuberculosis in pre-contact South American human populations. *Nat. Commun.* **13**, 1195 (2022).

59. van Ingen, J. *et al.* Characterization of Mycobacterium orygis as M. tuberculosis Complex Subspecies. *Emerg. Infect. Dis.* **18**, 653–655 (2012).

60. World Health Organization. Global Tuberculosis Report 2023. (2023).

61. Drain, P. K. *et al.* Incipient and Subclinical Tuberculosis: a Clinical Review of Early Stages and Progression of Infection. *Clin. Microbiol. Rev.* **31**, e00021-18 (2018).

62. Chitale, P. *et al.* A comprehensive update to the Mycobacterium tuberculosis H37Rv reference genome. *Nat. Commun.* **13**, 7068 (2022).

63. Arumugam, P., Shankaran, D., Bothra, A., Gandotra, S. & Rao, V. The MmpS6-MmpL6 Operon Is an Oxidative Stress Response System Providing Selective Advantage to Mycobacterium tuberculosis in Stress. *J. Infect. Dis.* **219**, 459–469 (2019).

64. Senghore, M. *et al.* Evolution of Mycobacterium tuberculosis complex lineages and their role in an emerging threat of multidrug resistant tuberculosis in Bamako, Mali. *Sci. Rep.* **10**, 327 (2020).

65. Saelens, J. W., Viswanathan, G. & Tobin, D. M. Mycobacterial Evolution Intersects With Host Tolerance. *Front. Immunol.* **10**, (2019).

66. Brites, D. & Gagneux, S. Co-evolution of Mycobacterium tuberculosis and Homo sapiens. *Immunol. Rev.* **264**, 6–24 (2015).

67. Pai, M. *et al.* Tuberculosis. *Nat. Rev. Dis. Primer* **2**, 1–23 (2016).

68. Ghodbane, R. & Drancourt, M. Non-human sources of *Mycobacterium tuberculosis*. *Tuberculosis* **93**, 589–595 (2013).

69. Chandra, P., Grigsby, S. J. & Philips, J. A. Immune evasion and provocation by Mycobacterium tuberculosis. *Nat. Rev. Microbiol.* **20**, 750–766 (2022).

70. Behr, M. A., Edelstein, P. H. & Ramakrishnan, L. Revisiting the timetable of tuberculosis. *BMJ* **362**, k2738 (2018).

71. Guirado, E. & Schlesinger, L. S. Modeling the Mycobacterium tuberculosis Granuloma – the Critical Battlefield in Host Immunity and Disease. *Front. Immunol.* **4**, 98 (2013).

72. Silva Miranda, M., Breiman, A., Allain, S., Deknuydt, F. & Altare, F. The Tuberculous Granuloma: An Unsuccessful Host Defence Mechanism Providing a Safety Shelter for the Bacteria? *J. Immunol. Res.* **2012**, e139127 (2012).

73. Huynh, K. K., Joshi, S. A. & Brown, E. J. A delicate dance: host response to mycobacteria. *Curr. Opin. Immunol.* **23**, 464–472 (2011).

74. Aguilar León, D. *et al.* Mycobacterium bovis with different genotypes and from different hosts induce dissimilar immunopathological lesions in a mouse model of tuberculosis. *Clin. Exp. Immunol.* **157**, 139–147 (2009).

75. Palmer, M. V., Kanipe, C. & Boggiatto, P. M. The Bovine Tuberculoid Granuloma. *Pathogens* **11**, 61 (2022).

76. Yang, H., Kruh-Garcia, N. A. & Dobos, K. M. Purified protein derivatives of tuberculin — past, present, and future. *FEMS Immunol. Med. Microbiol.* **66**, 273–280 (2012).

77. Use of the TST and IGRAs for the diagnosis of TB infection. in *WHO consolidated guidelines on tuberculosis: Module 3: Diagnosis – Tests for tuberculosis infection* (World Health Organization, 2022).

78. Pahal, P., Pollard, E. J. & Sharma, S. PPD Skin Test. in *StatPearls* (StatPearls Publishing, Treasure Island (FL), 2024).

79. Pagaduan, J. V. & Altawallbeh, G. Advances in TB testing. *Adv. Clin. Chem.* (2023) doi:10.1016/bs.acc.2023.03.003.

80. Christopher, D. J. *et al.* Tuberculin test using Indian indigenous purified-protein derivative (PPD) shows only moderate agreement with international standard PPD. *J. Clin. Tuberc. Mycobact. Dis.* **34**, 100404 (2024).

81. Gilani, B. & Sergent, S. R. Interferon Test. in *StatPearls* (StatPearls Publishing, Treasure Island (FL), 2024).

82. Executive summary. in *Use of Tuberculosis Interferon-Gamma Release Assays (IGRAs) in Low- and Middle- Income Countries: Policy Statement* (World Health Organization, 2011).

83. Behr, M. A. *et al.* Chapter 3: Diagnosis of tuberculosis disease and drug-resistant tuberculosis. *Can. J. Respir. Crit. Care Sleep Med.* **6**, 33–48 (2022).

84. Alsayed, S. S. R. & Gunosewoyo, H. Tuberculosis: Pathogenesis, Current Treatment Regimens and New Drug Targets. *Int. J. Mol. Sci.* **24**, 5202 (2023).

85. Verma, D. *et al.* An efficient framework for identification of Tuberculosis and Pneumonia in chest X-ray images using Neural Network. *Procedia Comput. Sci.* **171**, 217–224 (2020).

86. Danchuk, S. N. *et al.* Challenging the gold standard: the limitations of molecular assays for detection of Mycobacterium tuberculosis heteroresistance. *Thorax* (2024) doi:10.1136/thorax-2023-220202.

87. Lee, H. J. *et al.* Multicenter Testing of a Simple Molecular Diagnostic System for the Diagnosis of Mycobacterium Tuberculosis. *Biosensors* **13**, 259 (2023).

88. Brode, S. K., Dwilow, R., Kunimoto, D., Menzies, D. & Khan, F. A. Chapter 8: Drug-resistant tuberculosis. *Can. J. Respir. Crit. Care Sleep Med.* **6**, 109–128 (2022).

89. Zürcher, K. *et al.* Mortality from drug-resistant tuberculosis in high-burden countries comparing routine drug susceptibility testing with whole-genome sequencing: a multicentre cohort study. *Lancet Microbe* **2**, e320–e330 (2021).

90. El-Halfawy, O. M. & Valvano, M. A. Antimicrobial Heteroresistance: an Emerging Field in Need of Clarity. *Clin. Microbiol. Rev.* **28**, 191–207 (2015).

91. Schaltz-Buchholzer, F. *et al.* Early Vaccination With Bacille Calmette-Guérin-Denmark or BCG-Japan Versus BCG-Russia to Healthy Newborns in Guinea-Bissau: A Randomized Controlled Trial. *Clin. Infect. Dis.* **71**, 1883–1893 (2020).

92. Tagliabue, A., Boraschi, D., Leite, L. C. C. & Kaufmann, S. H. E. 100 Years of BCG Immunization: Past, Present, and Future. *Vaccines* **10**, 1743 (2022).

93. Barnes, D. S. Historical perspectives on the etiology of tuberculosis. *Microbes Infect.* **2**, 431–440 (2000).

94. Lange, C. *et al.* 100 years of *Mycobacterium bovis* bacille Calmette-Guérin. *Lancet Infect. Dis.* **22**, e2–e12 (2022).

95. Romero-Feregrino, R. *et al.* Report of 16 Years of the BCG Vaccine under the Expanded Program on Immunizations in Mexico (2006–2021). *Vaccines* **11**, 337 (2023).

96. Ritz, N. *et al.* The Influence of Bacille Calmette-Guérin Vaccine Strain on the Immune Response against Tuberculosis. *Am. J. Respir. Crit. Care Med.* **185**, 213–222 (2012).

97. Ritz, N., Hanekom, W. A., Robins-Browne, R., Britton, W. J. & Curtis, N. Influence of BCG vaccine strain on the immune response and protection against tuberculosis. *FEMS Microbiol. Rev.* **32**, 821–841 (2008).

98. Mostowy, S., Tsolaki, A. G., Small, P. M. & Behr, M. A. The in vitro evolution of BCG vaccines. *Vaccine* **21**, 4270–4274 (2003).

99. Behr, M. A. *et al.* Comparative Genomics of BCG Vaccines by Whole-Genome DNA Microarray. *Science* **284**, 1520–1523 (1999).

100. Harboe, M. *et al.* Properties of proteins MPB64, MPB70, and MPB80 of Mycobacterium bovis BCG. *Infect. Immun.* **52**, 293–302 (1986).

101. Harboe, M. & Nagai, S. MPB70, a Unique Antigen of Mycobacterium bovis BCG. *Am. Rev. Respir. Dis.* **129**, 444–452 (1984).

102. Behr, M. A. & Small, P. M. A historical and molecular phylogeny of BCG strains. *Vaccine* **17**, 915–922 (1999).

103. Charlet, D. *et al.* Reduced expression of antigenic proteins MPB70 and MPB83 in Mycobacterium bovis BCG strains due to a start codon mutation in sigK. *Mol. Microbiol.* **56**, 1302–1313 (2005).

104. Behr, M. A., Schroeder, B. G., Brinkman, J. N., Slayden, R. A. & Barry, C. E. A Point Mutation in the mma3 Gene Is Responsible for Impaired Methoxymycolic Acid Production in Mycobacterium bovis BCG Strains Obtained after 1927. *J. Bacteriol.* **182**, 3394–3399 (2000).

105. Zhang, L. *et al.* Variable Virulence and Efficacy of BCG Vaccine Strains in Mice and Correlation With Genome Polymorphisms. *Mol. Ther.* **24**, 398–405 (2016).

106. Fine, P. E. M. Variation in protection by BCG: implications of and for heterologous immunity. *The Lancet* **346**, 1339–1345 (1995).

107. Bottai, D. & Brosch, R. The BCG Strain Pool: Diversity Matters. *Mol. Ther.* **24**, 201–203 (2016).

108. Abdallah, A. M. *et al.* Genomic expression catalogue of a global collection of BCG vaccine strains show evidence for highly diverged metabolic and cell-wall adaptations. *Sci. Rep.* **5**, 15443 (2015).

109. Brosch, R. *et al.* Genome plasticity of BCG and impact on vaccine efficacy. *Proc. Natl. Acad. Sci.* **104**, 5596–5601 (2007).

110. Wiker, H. G. MPB70 and MPB83 – Major Antigens of Mycobacterium bovis. *Scand. J. Immunol.* **69**, 492–499 (2009).

111. Asadian, M., Hassanzadeh, S. M., Safarchi, A. & Douraghi, M. Genomic characteristics of two most widely used BCG vaccine strains: Danish 1331 and Pasteur 1173P2. *BMC Genomics* **23**, 609 (2022).

112. Elton, L. *et al.* Mapping the phylogeny and lineage history of geographically distinct BCG vaccine strains. *Microb. Genomics* **9**, 001077 (2023).

113. Mangtani, P. *et al.* Protection by BCG Vaccine Against Tuberculosis: A Systematic Review of Randomized Controlled Trials. *Clin. Infect. Dis.* **58**, 470–480 (2014).

114. Faust, L., Schreiber, Y. & Bocking, N. A systematic review of BCG vaccination policies among high-risk groups in low TB-burden countries: implications for vaccination strategy in Canadian indigenous communities. *BMC Public Health* **19**, 1504 (2019).

115. GHO | By category | BCG - Immunization coverage estimates by WHO region. *WHO* https://apps.who.int/gho/data/view.main.81500?lang=en.

116. Moliva, J. I., Turner, J. & Torrelles, J. B. Prospects in Mycobacterium bovis Bacille Calmette et Guérin (BCG) Vaccine Diversity and Delivery: Why does BCG fail to protect against Tuberculosis? *Vaccine* **33**, 5035–5041 (2015).

117. Martinez, L. *et al.* Infant BCG vaccination and risk of pulmonary and extrapulmonary tuberculosis throughout the life course: a systematic review and individual participant data meta-analysis. *Lancet Glob. Health* **10**, e1307–e1316 (2022).

118. Trunz, B. B., Fine, P. & Dye, C. Effect of BCG vaccination on childhood tuberculous meningitis and miliary tuberculosis worldwide: a meta-analysis and assessment of cost-effectiveness. *The Lancet* **367**, 1173–1180 (2006).

119. Colditz, G. A. *et al.* Efficacy of BCG Vaccine in the Prevention of Tuberculosis: Meta-analysis of the Published Literature. *JAMA* **271**, 698–702 (1994).

120. Roy, A. *et al.* Effect of BCG vaccination against Mycobacterium tuberculosis infection in children: systematic review and meta-analysis. *The BMJ* **349**, g4643 (2014).

121. Abubakar, I. *et al. Systematic Review and Meta-Analysis of the Current Evidence on the Duration of Protection by Bacillus Calmette–Guérin Vaccination against Tuberculosis*. (NIHR Journals Library, 2013).

122. Brewer, T. F. & Colditz, G. A. Relationship between Bacille Calmette-Guérin (BCG) Strains and the Efficacy of BCG Vaccine in the Prevention of Tuberculosis. *Clin. Infect. Dis.* **20**, 126–135 (1995).

123. Trunk, G., Davidović, M. & Bohlius, J. Non-Specific Effects of Bacillus Calmette-Guérin: A Systematic Review and Meta-Analysis of Randomized Controlled Trials. *Vaccines* **11**, 121 (2023).

124. Higgins, J. P. T. *et al.* Association of BCG, DTP, and measles containing vaccines with childhood mortality: systematic review. *BMJ* **355**, i5170 (2016).

125. Quinn, M. *et al.* Non-specific effects of BCG and DTP vaccination on infant mortality: An analysis of birth cohorts in Ghana and Tanzania. *Vaccine* **40**, 3737–3745 (2022).

126. Aaby, P., Netea, M. G. & Benn, C. S. Beneficial non-specific effects of live vaccines against COVID-19 and other unrelated infections. *Lancet Infect. Dis.* **23**, e34–e42 (2023).

127. Ritz, N. *et al.* Susceptibility of Mycobacterium bovis BCG Vaccine Strains to Antituberculous Antibiotics. *Antimicrob. Agents Chemother.* **53**, 316–318 (2009).

128. Buriánková, K. *et al.* Molecular Basis of Intrinsic Macrolide Resistance in the Mycobacterium tuberculosis Complex. *Antimicrob. Agents Chemother.* **48**, 143–150 (2004).

129. Koch, R. An Address on the Fight against Tuberculosis in the Light of the Experience that has been Gained in the Successful Combat of other Infectious Diseases. *Br. Med. J.* **2**, 189–193 (1901).

130. The Report Of The Royal Commission On Tuberculosis. *Br. Med. J.* **1**, 945–948 (1895).

131. KARLSON, A. G. & LESSEL, E. F. Mycobacterium bovis nom. nov. *Int. J. Syst. Evol. Microbiol.* **20**, 273–282 (1970).

132. Tuberculosis in Animals and Man: A Study in Comparative Pathology. *J. Am. Med. Assoc.* **168**, 133 (1958).

133. Francis, J. The work of the British Royal Commission on Tuberculosis, 1901–1911. *Tubercle* **40**, 124–132 (1959).

134. Inlamea, O. F. *et al.* Evolutionary analysis of Mycobacterium bovis genotypes across Africa suggests co-evolution with livestock and humans. *PLoS Negl. Trop. Dis.* **14**, e0008081 (2020).

135. Zimpel, C. K. *et al.* Global Distribution and Evolution of Mycobacterium bovis Lineages. *Front. Microbiol.* **11**, (2020).

136. Loiseau, C. *et al.* An African origin for Mycobacterium bovis. *Evol. Med. Public Health* **2020**, 49–59 (2020).

137. Taylor, G. M., Murphy, E., Hopkins, R., Rutland, P. & Chistov, Y. First report of Mycobacterium bovis DNA in human remains from the Iron Age. *Microbiology* **153**, 1243–1249 (2007).

138. Ramanujam, H. & Palaniyandi, K. Bovine tuberculosis in India: The need for One Health approach and the way forward. *One Health* **16**, 100495 (2023).

139. Refaya, A. K. *et al.* A review on bovine tuberculosis in India. *Tuberculosis* **122**, 101923 (2020).

140. Griffith, A. S. Bovine Tuberculosis in the Human Subject. *Proc. R. Soc. Med.* **31**, 1208–1212 (1938).

141. Duffy, S. C., Marais, B., Kapur, V. & Behr, M. A. Zoonotic tuberculosis in the 21st century. *Lancet Infect. Dis.* **24**, 339–341 (2024).

142. Kock, R. *et al.* Zoonotic Tuberculosis – The Changing Landscape. *Int. J. Infect. Dis.* **113**, S68–S72 (2021).

143. Tuberculosis SEARO. https://www.who.int/southeastasia/health-topics/tuberculosis.

144. Tuberculosis (TB). *WHO | Regional Office for Africa* https://www.afro.who.int/health-topics/tuberculosis-tb (2024).

145. Cosivi, O. *et al.* Zoonotic tuberculosis due to Mycobacterium bovis in developing countries. *Emerg. Infect. Dis.* **4**, 59–70 (1998).

146. Silva, M. R. *et al.* Tuberculosis patients co-infected with Mycobacterium bovis and Mycobacterium tuberculosis in an urban area of Brazil. *Mem. Inst. Oswaldo Cruz* **108**, 321–327 (2013).

147. Sunstrum, J. *et al.* Human Disease due to *Mycobacterium bovis* Linked to Free-Ranging Deer in Michigan. *Clin. Infect. Dis.* **78**, 637–645 (2024).

148. Taye, H. *et al.* Global prevalence of Mycobacterium bovis infections among human tuberculosis cases: Systematic review and meta-analysis. *Zoonoses Public Health* **68**, 704–718 (2021).

149. Petel, D., Waters, V. & Kitai, I. Disseminated Mycobacterium bovis infection presenting with cervical lymphadenitis in a 15-year-old girl. *CMAJ* **195**, E1155–E1156 (2023).

150. Riopel, N. D. *et al.* Characterization of Mycobacterium orygis, Mycobacterium bovis, and Mycobacterium caprae Infections in Humans in Western Canada. *J. Infect. Dis.* jiae124 (2024) doi:10.1093/infdis/jiae124.

151. Torres-Gonzalez, P. *et al.* Human tuberculosis caused by Mycobacterium bovis: a retrospective comparison with Mycobacterium tuberculosis in a Mexican tertiary care centre, 2000–2015. *BMC Infect. Dis.* **16**, 657 (2016).

152. Lan, Z., Bastos, M. & Menzies, D. Treatment of human disease due to Mycobacterium bovis: a systematic review. *Eur. Respir. J.* (2016) doi:10.1183/13993003.00629-2016.

153. Clifford, K. M. & Szumowski, J. D. Disseminated Mycobacterium bovis Infection Complicated by Meningitis and Stroke: A Case Report. *Open Forum Infect. Dis.* **7**, ofaa475 (2020).

154. Vayr, F. *et al.* Occupational exposure to human Mycobacterium bovis infection: A systematic review. *PLoS Negl. Trop. Dis.* **12**, e0006208 (2018).

155. Olea-Popelka, F. *et al.* Zoonotic tuberculosis in human beings caused by Mycobacterium bovis —a call for action. *Lancet Infect. Dis.* **17**, e21–e25 (2017).

156. Fine, A. E., Bolin, C. A., Gardiner, J. C. & Kaneene, J. B. A Study of the Persistence of Mycobacterium bovis in the Environment under Natural Weather Conditions in Michigan, USA. *Vet. Med. Int.* **2011**, 765430 (2011).

157. Tanner, M. & Michel, A. L. Investigation of the viability of M. bovis under different environmental conditions in the Kruger National Park. *Onderstepoort J. Vet. Res.* **66**, 185–190 (1999).

158. Sunder, S. *et al.* Human-to-Human Transmission of Tuberculosis Caused by Mycobacterium bovis in Immunocompetent Patients. *J. Clin. Microbiol.* **47**, 1249–1251 (2009).

159. Guerrero, A. *et al.* Nosocomial transmission of Mycobacterium bovis resistant to 11 drugs in people with advanced HIV-1 infection. *Lancet Lond. Engl.* **350**, 1738–1742 (1997).

160. de Val, B. P. *et al.* Polyresistant Mycobacterium bovis Infection in Human and Sympatric Sheep, Spain, 2017–2018. *Emerg. Infect. Dis.* **27**, 1241–1243 (2021).

161. Rivero, A. *et al.* High Rate of Tuberculosis Reinfection during a Nosocomial Outbreak of Multidrug-Resistant Tuberculosis Caused by Mycobacterium bovis Strain B. *Clin. Infect. Dis.* **32**, 159–161 (2001).

162. Buss, B. F. Possible Airborne Person-to-Person Transmission of Mycobacterium bovis — Nebraska 2014–2015. *MMWR Morb. Mortal. Wkly. Rep.* **65**, (2016).

163. LoBue, P. A., LeClair, J. J. & Moser, K. S. Contact investigation for cases of pulmonary Mycobacterium bovis. *Int. J. Tuberc. Lung Dis.* **8**, 868–872 (2004).

164. Etchechoury, I. *et al.* Molecular Typing of Mycobacterium bovis Isolates in Argentina: First Description of a Person-to-Person Transmission Case. *Zoonoses Public Health* **57**, 375–381 (2010).

165. Evans, J. T. *et al.* Cluster of human tuberculosis caused by Mycobacterium bovis: evidence for person-to-person transmission in the UK. *The Lancet* **369**, 1270–1276 (2007).

166. Scott, C. *et al.* Human Tuberculosis Caused by Mycobacterium bovis in the United States, 2006-2013. *Clin. Infect. Dis. Off. Publ. Infect. Dis. Soc. Am.* **63**, 594–601 (2016).

167. Rodwell, T. C., Moore, M., Moser, K. S., Brodine, S. K. & Strathdee, S. A. Tuberculosis from Mycobacterium bovis in Binational Communities, United States. *Emerg. Infect. Dis.* **14**, 909–916 (2008).

168. Davidson, J. A. *et al.* Epidemiology of Mycobacterium bovis Disease in Humans in England, Wales, and Northern Ireland, 2002–2014. *Emerg. Infect. Dis.* **23**, 377–386 (2017).

169. Dürr, S. *et al.* Differences in Primary Sites of Infection between Zoonotic and Human Tuberculosis: Results from a Worldwide Systematic Review. *PLoS Negl. Trop. Dis.* **7**, e2399 (2013).

170. de la Rua-Domenech, R. Human *Mycobacterium bovis* infection in the United Kingdom: Incidence, risks, control measures and review of the zoonotic aspects of bovine tuberculosis. *Tuberculosis* **86**, 77–109 (2006).

171. Rowe, M. T. & Donaghy, J. Mycobacterium bovis: the importance of milk and dairy products as a cause of human tuberculosis in the UK. A review of taxonomy and culture methods, with particular reference to artisanal cheeses. *Int. J. Dairy Technol.* **61**, 317–326 (2008).

172. Garnier, T. *et al.* The complete genome sequence of Mycobacterium bovis. *Proc. Natl. Acad. Sci. U. S. A.* **100**, 7877–7882 (2003).

173. Cole, S. T. *et al.* Deciphering the biology of Mycobacterium tuberculosis from the complete genome sequence. *Nature* **393**, 537–544 (1998).

174. Malone, K. M. *et al.* Updated Reference Genome Sequence and Annotation of Mycobacterium bovis AF2122/97. *Genome Announc.* **5**, e00157-17 (2017).

175. Farrell, D., Crispell, J. & Gordon, S. V. Updated functional annotation of the Mycobacterium bovis AF2122/97 reference genome. *Access Microbiol.* **2**, acmi000129 (2020).

176. Ravenel, M. P. The Comparative Virulence of the Tubercle Bacillus from Human and Bovine Sources1Read before the British Congress on Tuberculosis, Section on Pathology and Bacteriology, London, July 23-26, 1901. *J. Comp. Med. Vet. Arch.* **23**, 65–81 (1902).

177. Hadi, S. A. *et al.* Mycobacterium bovis Strain Ravenel Is Attenuated in Cattle. *Pathogens* **11**, 1330 (2022).

178. Hadi, S. A. *et al.* Genome Sequences of Mycobacterium tuberculosis Biovar bovis Strains Ravenel and 10-7428. *Microbiol. Resour. Announc.* **10**, e00411-21.

179. Kubica, T. *et al.* Mycobacterium bovis Isolates with M. tuberculosis Specific Characteristics. *Emerg. Infect. Dis.* **12**, 763–765 (2006).

180. Niemann, S., Richter, E. & Rüsch-Gerdes, S. Differentiation among Members of the Mycobacterium tuberculosis Complex by Molecular and Biochemical Features: Evidence for Two Pyrazinamide-Susceptible Subtypes of M. bovis. *J. Clin. Microbiol.* **38**, 152–157 (2000).

181. Marianelli, C. *et al.* Multiple drug-susceptibility screening in *Mycobacterium bovis:* new nucleotide polymorphisms in the *embB* gene among ethambutol susceptible strains. *Int. J. Infect. Dis.* **33**, 39–44 (2015).

182. Merker, M., Kohl, T. A., Niemann, S. & Supply, P. The Evolution of Strain Typing in the Mycobacterium tuberculosis Complex. in *Strain Variation in the Mycobacterium tuberculosis Complex: Its Role in Biology, Epidemiology and Control* (ed. Gagneux, S.) 43–78 (Springer International Publishing, Cham, 2017). doi:10.1007/978-3-319-64371-7_3.

183. Scorpio, A. *et al.* Rapid differentiation of bovine and human tubercle bacilli based on a characteristic mutation in the bovine pyrazinamidase gene. *J. Clin. Microbiol.* **35**, 106–110 (1997).

184. Saïd-Salim, B., Mostowy, S., Kristof, A. S. & Behr, M. A. Mutations in Mycobacterium tuberculosis Rv0444c, the gene encoding anti-SigK, explain high level expression of MPB70 and MPB83 in Mycobacterium bovis. *Mol. Microbiol.* **62**, 1251–1263 (2006).

185. Veyrier, F. J. *et al.* RskA Is a Dual Function Activator-Inhibitor That Controls SigK Activity Across Distinct Bacterial Genera. *Front. Microbiol.* **11**, 558166 (2020).

186. Veyrier, F., Saïd-Salim, B. & Behr, M. A. Evolution of the Mycobacterial SigK Regulon. *J. Bacteriol.* **190**, 1891–1899 (2008).

187. Schnappinger, D. *et al.* Transcriptional Adaptation of Mycobacterium tuberculosis within Macrophages. *J. Exp. Med.* **198**, 693–704 (2003).

188. Lind, A. Immunologic analysis of mycobacterial antigens. *Am. Rev. Respir. Dis.* **92**, 54–62 (1965).

189. Natale, P., Brüser, T. & Driessen, A. J. M. Sec- and Tat-mediated protein secretion across the bacterial cytoplasmic membrane—Distinct translocases and mechanisms. *Biochim. Biophys. Acta BBA - Biomembr.* **1778**, 1735–1756 (2008).

190. Pal, R., Bisht, M. K. & Mukhopadhyay, S. Secretory proteins of Mycobacterium tuberculosis and their roles in modulation of host immune responses: focus on therapeutic targets. *FEBS J.* **289**, 4146–4171 (2022).

191. Tucci, P., Portela, M., Chetto, C. R., González-Sapienza, G. & Marín, M. Integrative proteomic and glycoproteomic profiling of Mycobacterium tuberculosis culture filtrate. *PLoS ONE* **15**, e0221837 (2020).

192. Harboe, M. *et al.* MPB70 and MPB83 as Indicators of Protein Localization in Mycobacterial Cells. *Infect. Immun.* **66**, 289–296 (1998).

193. Hewinson, R. G., Michell, S. Ll., Russell, W. P., Mcadam, R. A. & Jacobs Jr, W. R. Molecular Characterization of MPT83: a Seroreactive Antigen of Mycobacterium tuberculosis with Homology to MPT70. *Scand. J. Immunol.* **43**, 490–499 (1996).

194. Matsuo, T. *et al.* Cloning and sequencing of an MPB70 homologue corresponding to MPB83 from Mycobacterium bovis BCG. *Scand. J. Immunol.* **43**, 483–489 (1996).

195. Queval, C. J. *et al.* Macrophage-specific responses to human- and animal-adapted tubercle bacilli reveal pathogen and host factors driving multinucleated cell formation. *PLoS Pathog.* **17**, e1009410 (2021).

196. Ulstrup, J. C., Jeansson, S., Wiker, H. G. & Harboe, M. Relationship of secretion pattern and MPB70 homology with osteoblast-specific factor 2 to osteitis following Mycobacterium bovis BCG vaccination. *Infect. Immun.* **63**, 672–675 (1995).

197. Park, S.-Y., Jung, M.-Y. & Kim, I.-S. Stabilin-2 mediates homophilic cell–cell interactions via its FAS1 domains. *FEBS Lett.* **583**, 1375–1380 (2009).

198. North, R. J., Ryan, L., LaCource, R., Mogues, T. & Goodrich, M. E. Growth Rate of Mycobacteria in Mice as an Unreliable Indicator of Mycobacterial Virulence. *Infect. Immun.* **67**, 5483–5485 (1999).

199. Dunn, P. L. & North, R. J. Virulence ranking of some Mycobacterium tuberculosis and Mycobacterium bovis strains according to their ability to multiply in the lungs, induce lung pathology, and cause mortality in mice. *Infect. Immun.* **63**, 3428–3437 (1995).

200. Tollefsen, S., Pollock, J. M., Lea, T., Harboe, M. & Wiker, H. G. T- and B-cell epitopes in the secreted Mycobacterium bovis antigen MPB70 in mice. *Scand. J. Immunol.* **57**, 151–161 (2003).

201. Al-Attiyah, R., Shaban, F. A., Wiker, H. G., Oftung, F. & Mustafa, A. S. Synthetic Peptides Identify Promiscuous Human Th1 Cell Epitopes of the Secreted Mycobacterial Antigen MPB70. *Infect. Immun.* **71**, 1953–1960 (2003).

202. Harboe, M. *et al.* Protein G-based enzyme-linked immunosorbent assay for anti-MPB70 antibodies in bovine tuberculosis. *J. Clin. Microbiol.* **28**, 913–921 (1990).

203. Becker, K. & Sander, P. Mycobacterium tuberculosis lipoproteins in virulence and immunity – fighting with a double-edged sword. *FEBS Lett.* **590**, 3800–3819 (2016).

204. Fifis, T., Costopoulos, C., Radford, A. J., Bacic, A. & Wood, P. R. Purification and characterization of major antigens from a Mycobacterium bovis culture filtrate. *Infect. Immun.* **59**, 800–807 (1991).

205. Wang, L. *et al.* Mycobacterium tuberculosis Lipoprotein MPT83 Induces Apoptosis of Infected Macrophages by Activating the TLR2/p38/COX-2 Signaling Pathway. *J. Immunol.* **198**, 4772–4780 (2017).

206. Wiker, H. G. *et al.* Immunochemical Characterization of the MPB70/80 and MPB83 Proteins of Mycobacterium bovis. *Infect. Immun.* **66**, 1445–1452 (1998).

207. Chambers, M. A., Gavier-Widén, D. & Glyn Hewinson, R. Antibody bound to the surface antigen MPB83 of Mycobacterium bovis enhances survival against high dose and low dose challenge. *FEMS Immunol. Med. Microbiol.* **41**, 93–100 (2004).

208. Chambers, M. A. *et al.* Vaccination of Guinea Pigs with DNA Encoding the Mycobacterial Antigen MPB83 Influences Pulmonary Pathology but Not Hematogenous Spread following Aerogenic Infection with Mycobacterium bovis. *Infect. Immun.* **70**, 2159–2165 (2002).

209. Wedlock, D. N. *et al.* Vaccination with DNA vaccines encoding MPB70 or MPB83 or a MPB70 DNA prime-protein boost does not protect cattle against bovine tuberculosis. *Tuberculosis* **83**, 339–349 (2003).

210. Via, L. E. *et al.* Tuberculous Granulomas Are Hypoxic in Guinea Pigs, Rabbits, and Nonhuman Primates. *Infect. Immun.* **76**, 2333–2340 (2008).

211. Brenner, E. P. & Sreevatsan, S. Attenuated but immunostimulatory Mycobacterium tuberculosis variant bovis strain Ravenel shows variation in T cell epitopes. *Sci. Rep.* **13**, 12402 (2023).

212. Medina, E., Ryan, L., LaCourse, R. & North, R. J. Superior virulence of *Mycobacterium bovis* over *Mycobacterium tuberculosis* (Mtb) for Mtb-resistant and Mtb-susceptible mice is manifest as an ability to cause extrapulmonary disease. *Tuberculosis* **86**, 20–27 (2006).

213. Villarreal-Ramos, B. *et al.* Experimental infection of cattle with Mycobacterium tuberculosis isolates shows the attenuation of the human tubercle bacillus for cattle. *Sci. Rep.* **8**, 894 (2018).

214. Ameni, G. *et al.* Mycobacterium tuberculosis infection in grazing cattle in central Ethiopia. *Vet. J. Lond. Engl. 1997* **188**, 359–361 (2011).

215. Bezos, J. *et al.* Goats challenged with different members of the *Mycobacterium tuberculosis* complex display different clinical pictures. *Vet. Immunol. Immunopathol.* **167**, 185–189 (2015).

216. Niroula, N. *et al.* Domestic pigs experimentally infected with Mycobacterium bovis and Mycobacterium tuberculosis exhibit different disease outcomes. 2021.10.25.465759 Preprint at https://doi.org/10.1101/2021.10.25.465759 (2021).

217. Lomme, J. R., Thoen, C. O., Himes, E. M., Vinson, J. W. & King, R. E. Mycobacterium tuberculosis infection in two East African oryxes. *J. Am. Vet. Med. Assoc.* **169**, 912–914 (1976).

218. van Soolingen, D. *et al.* Use of various genetic markers in differentiation of Mycobacterium bovis strains from animals and humans and for studying epidemiology of bovine tuberculosis. *J. Clin. Microbiol.* **32**, 2425–2433 (1994).

219. Huard, R. C. *et al.* Novel Genetic Polymorphisms That Further Delineate the Phylogeny of the Mycobacterium tuberculosis Complex. *J. Bacteriol.* **188**, 4271–4287 (2006).

220. Gey van Pittius, N. C. *et al.* Infection of African buffalo (Syncerus caffer) by oryx bacillus, a rare member of the antelope clade of the Mycobacterium tuberculosis complex. *J. Wildl. Dis.* **48**, 849–857 (2012).

221. Pittius, N. C. G. van, Helden, P. D. van & Warren, R. M. Characterization of Mycobacterium orygis - Volume 18, Number 10—October 2012 - Emerging Infectious Diseases journal - CDC. doi:10.3201/eid1810.120569.

222. Duffy, S. C. *et al.* Reconsidering Mycobacterium bovis as a proxy for zoonotic tuberculosis: a molecular epidemiological surveillance study. *Lancet Microbe* **1**, e66–e73 (2020).

223. Islam, M. R. *et al.* Whole genome sequencing-based identification of human tuberculosis caused by animal-lineage Mycobacterium orygis. *J. Clin. Microbiol.* **61**, e00260-23.

224. Rufai, S. B. *et al.* Complete Genome Sequence of Mycobacterium orygis Strain 51145. *Microbiol. Resour. Announc.* **10**, 10.1128/mra.01279-20 (2021).

225. Sumanth, L. J. *et al.* Clinical features of human tuberculosis due to Mycobacterium orygis in Southern India. *J. Clin. Tuberc. Mycobact. Dis.* **32**, 100372 (2023).

226. Thapa, J., Gordon, S. V., Nakajima, C. & Suzuki, Y. Threat from Mycobacterium orygis-associated tuberculosis in south Asia. *Lancet Microbe* **3**, e641–e642 (2022).

227. Loiseau, C. *et al.* Revised Interpretation of the Hain Lifescience GenoType MTBC To Differentiate Mycobacterium canettii and Members of the Mycobacterium tuberculosis Complex. *Antimicrob. Agents Chemother.* **63**, 10.1128/aac.00159-19 (2019).

228. Maqsood, R. *et al.* Molecular detection and characterization of the Mycobacterium tuberculosis complex subspecies responsible for bovine tuberculosis in Punjab, Pakistan. *Microbiol. Spectr.* **12**, e02692-23.

229. Dawson, K. L. *et al.* Transmission of Mycobacterium orygis (M. tuberculosis Complex Species) from a Tuberculosis Patient to a Dairy Cow in New Zealand. *J. Clin. Microbiol.* **50**, 3136–3138 (2012).

230. Lipworth, S. *et al.* SNP-IT Tool for Identifying Subspecies and Associated Lineages of Mycobacterium tuberculosis Complex. *Emerg. Infect. Dis.* **25**, 482–488 (2019).

231. Ayalew, S. *et al.* Zoonotic tuberculosis in a high bovine tuberculosis burden area of Ethiopia. *Front. Public Health* **11**, 1204525 (2023).

232. Marcos, L. A. *et al.* Mycobacterium orygis Lymphadenitis in New York, USA. *Emerg. Infect. Dis.* **23**, 1749–1751 (2017).

233. Refaya, A. K. *et al.* Tuberculosis caused by Mycobacterium orygis in wild ungulates in Chennai, South India. *Transbound. Emerg. Dis.* **69**, e3327–e3333 (2022).

234. Love, D. M. *et al.* TUBERCULOSIS CAUSED BY MYCOBACTERIUM ORYGIS IN A GREATER ONE-HORNED RHINOCEROS (RHINOCEROS UNICORNIS): FIRST REPORT IN THE WESTERN HEMISPHERE. *J. Zoo Wildl. Med.* **50**, 1000–1004 (2020).

235. Sharma, M. *et al.* Emergence of Mycobacterium orygis–Associated Tuberculosis in Wild Ruminants, India. *Emerg. Infect. Dis.* **29**, 661–663 (2023).

236. Refaya, A. K. *et al.* Whole-Genome Sequencing of a Mycobacterium orygis Strain Isolated from Cattle in Chennai, India. *Microbiol. Resour. Announc.* **8**, e01080-19 (2019).

237. Jawahar, A., Dhinakar Raj, G., Pazhanivel, N. & Karthik, K. Gross and histopathological features of tuberculosis in cattle, buffalo and spotted deer (*Axis axis*) caused by *Mycobacterium orygis*. *J. Comp. Pathol.* **208**, 15–19 (2024).

238. Karthik, K. *et al.* Whole genome sequencing and comparative genomics of Mycobacterium orygis isolated from different animal hosts to identify specific diagnostic markers. *Front. Cell. Infect. Microbiol.* **13**, 1302393 (2023).

239. Rahim, Z. *et al.* Tuberculosis Caused by Mycobacterium orygis in Dairy Cattle and Captured Monkeys in Bangladesh: a New Scenario of Tuberculosis in South Asia. *Transbound. Emerg. Dis.* **64**, 1965–1969 (2017).

240. Lavender, C. J. *et al.* Epidemiology and control of tuberculosis in Victoria, a low-burden state in south-eastern Australia, 2005–2010. *Int. J. Tuberc. Lung Dis.* **17**, 752–758 (2013).

241. Swisher, S. D. Outbreak of Mycobacterium orygis in a Shipment of Cynomolgus Macaques Imported from Southeast Asia — United States, February–May 2023. *MMWR Morb. Mortal. Wkly. Rep.* **73**, (2024).

242. Eldholm, V., Rønning, J. O., Mengshoel, A. T. & Arnesen, T. Import and transmission of Mycobacterium orygis and Mycobacterium africanum, Norway. *BMC Infect. Dis.* **21**, 562 (2021).

243. Horton, K. C., MacPherson, P., Houben, R. M. G. J., White, R. G. & Corbett, E. L. Sex Differences in Tuberculosis Burden and Notifications in Low- and Middle-Income Countries: A Systematic Review and Meta-analysis. *PLoS Med.* **13**, e1002119 (2016).

244. Yasobant, S., Memon, F., Shah, H. & Saxena, D. Can One Health achieve the target of end TB strategy: perspective from zoonotic TB prevention and control in India. *PAMJ - One Health* **8**, (2022).

245. Wu, H.-J., Wang, A. H.-J. & Jennings, M. P. Discovery of virulence factors of pathogenic bacteria. *Curr. Opin. Chem. Biol.* **12**, 93–101 (2008).

246. Hill, C. Virulence or Niche Factors: What's in a Name? *J. Bacteriol.* **194**, 5725–5727 (2012).

247. Echeverria-Valencia, G. *et al.* Virulence Factors and Pathogenicity of Mycobacterium. in *Mycobacterium - Research and Development* (IntechOpen, 2017). doi:10.5772/intechopen.72027.

248. Peterson, J. W. Bacterial Pathogenesis. in *Medical Microbiology* (ed. Baron, S.) (University of Texas Medical Branch at Galveston, Galveston (TX), 1996).

249. Collins, D. M. Virulence factors of *Mycobacterium bovis*. *Tuberculosis* **81**, 97–102 (2001).

250. Roy, S., Ghatak, D., Das, P. & Bosedasgupta, S. ESX secretion system: The gatekeepers of mycobacterial survivability and pathogenesis. *Eur. J. Microbiol. Immunol.* **10**, 202 (2020).

251. Kurtz, S., McKinnon, K. P., Runge, M. S., Ting, J. P.-Y. & Braunstein, M. The SecA2 Secretion Factor of Mycobacterium tuberculosis Promotes Growth in Macrophages and Inhibits the Host Immune Response. *Infect. Immun.* **74**, 6855–6864 (2006).

252. Gröschel, M. I., Sayes, F., Simeone, R., Majlessi, L. & Brosch, R. ESX secretion systems: mycobacterial evolution to counter host immunity. *Nat. Rev. Microbiol.* **14**, 677–691 (2016).

253. Stanley, S. A., Raghavan, S., Hwang, W. W. & Cox, J. S. Acute infection and macrophage subversion by Mycobacterium tuberculosis require a specialized secretion system. *Proc. Natl. Acad. Sci. U. S. A.* **100**, 13001–13006 (2003).

254. Houben, E. N. G., Korotkov, K. V. & Bitter, W. Take five — Type VII secretion systems of *Mycobacteria*. *Biochim. Biophys. Acta BBA - Mol. Cell Res.* **1843**, 1707–1716 (2014).

255. Shah, S. & Briken, V. Modular Organization of the ESX-5 Secretion System in Mycobacterium tuberculosis. *Front. Cell. Infect. Microbiol.* **6**, (2016).

256. Wang, Y. *et al.* Crosstalk between the ancestral type VII secretion system ESX-4 and other T7SS in *Mycobacterium marinum*. *iScience* **25**, 103585 (2022).

257. Madacki, J., Mas Fiol, G. & Brosch, R. Update on the virulence factors of the obligate pathogen *Mycobacterium tuberculosis* and related tuberculosis-causing mycobacteria. *Infect. Genet. Evol.* **72**, 67–77 (2019).

258. Wards, B. J., de Lisle, G. W. & Collins, D. M. An *esat6* knockout mutant of *Mycobacterium bovis* produced by homologous recombination will contribute to the development of a live tuberculosis vaccine. *Tuber. Lung Dis.* **80**, 185–189 (2000).

259. Lewis, K. N. *et al.* Deletion of RD1 from Mycobacterium tuberculosis Mimics Bacille Calmette-Guérin Attenuation. *J. Infect. Dis.* **187**, 117–123 (2003).

260. Pym, A. S. *et al.* Recombinant BCG exporting ESAT-6 confers enhanced protection against tuberculosis. *Nat. Med.* **9**, 533–539 (2003).

261. Alexander, K. A. *et al.* Emerging Tuberculosis Pathogen Hijacks Social Communication Behavior in the Group-Living Banded Mongoose (Mungos mungo). *mBio* **7**, e00281-16 (2016).

262. Forrellad, M. A. *et al.* Virulence factors of the Mycobacterium tuberculosis complex. *Virulence* **4**, 3–66 (2013).

263. Ly, A. & Liu, J. Mycobacterial Virulence Factors: Surface-Exposed Lipids and Secreted Proteins. *Int. J. Mol. Sci.* **21**, 3985 (2020).

264. Kurenuma, T. *et al.* The RD1 Locus in the Mycobacterium tuberculosis Genome Contributes to Activation of Caspase-1 via Induction of Potassium Ion Efflux in Infected Macrophages. *Infect. Immun.* **77**, 3992–4001 (2009).

265. Anes, E., Pires, D., Mandal, M. & Azevedo-Pereira, J. M. ESAT-6 a Major Virulence Factor of Mycobacterium tuberculosis. *Biomolecules* **13**, 968 (2023).

266. Bitter, W. *et al.* Systematic Genetic Nomenclature for Type VII Secretion Systems. *PLOS Pathog.* **5**, e1000507 (2009).

267. Kroesen, V. M., Madacki, J., Frigui, W., Sayes, F. & Brosch, R. Mycobacterial virulence: impact on immunogenicity and vaccine research. *F1000Research* **8**, F1000 Faculty Rev-2025 (2019).

268. Fortune, S. M. *et al.* Mutually dependent secretion of proteins required for mycobacterial virulence. *Proc. Natl. Acad. Sci.* **102**, 10676–10681 (2005).

269. Ates, L. S. & Brosch, R. Discovery of the type VII ESX-1 secretion needle? *Mol. Microbiol.* **103**, 7–12 (2017).

270. Barczak, A. K. *et al.* Systematic, multiparametric analysis of Mycobacterium tuberculosis intracellular infection offers insight into coordinated virulence. *PLOS Pathog.* **13**, e1006363 (2017).

271. Abdallah, A. M. *et al.* Type VII secretion — mycobacteria show the way. *Nat. Rev. Microbiol.* **5**, 883–891 (2007).

272. Shah, S., Cannon, J. R., Fenselau, C. & Briken, V. A Duplicated ESAT-6 Region of ESX-5 Is Involved in Protein Export and Virulence of Mycobacteria. *Infect. Immun.* **83**, 4349–4361 (2015).

273. Abdallah, A. M. *et al.* PPE and PE_PGRS proteins of Mycobacterium marinum are transported via the type VII secretion system ESX-5. *Mol. Microbiol.* **73**, 329–340 (2009).

274. Luca, M. D. *et al.* The ESX-5 Associated eccB5-eccC5 Locus Is Essential for Mycobacterium tuberculosis Viability. *PLOS ONE* **7**, e52059 (2012).

275. Bottai, D. *et al.* Disruption of the ESX-5 system of Mycobacterium tuberculosis causes loss of PPE protein secretion, reduction of cell wall integrity and strong attenuation. *Mol. Microbiol.* **83**, 1195–1209 (2012).

276. Sayes, F. *et al.* Strong Immunogenicity and Cross-Reactivity of *Mycobacterium tuberculosis* ESX-5 Type VII Secretion -Encoded PE-PPE Proteins Predicts Vaccine Potential. *Cell Host Microbe* **11**, 352–363 (2012).

277. Weerdenburg, E. M. *et al.* ESX-5-deficient Mycobacterium marinum is hypervirulent in adult zebrafish. *Cell. Microbiol.* **14**, 728–739 (2012).

278. McEvoy, C. R., van Helden, P. D., Warren, R. M. & van Pittius, N. C. G. Evidence for a rapid rate of molecular evolution at the hypervariable and immunogenic Mycobacterium tuberculosis PPE38 gene region. *BMC Evol. Biol.* **9**, 237 (2009).

279. Rens, C., Chao, J. D., Sexton, D. L., Tocheva, E. I. & Av-Gay, Y. Roles for phthiocerol dimycocerosate lipids in Mycobacterium tuberculosis pathogenesis. *Microbiology* **167**, 001042 (2021).

280. Mulholland, C. V. *et al.* Propionate prevents loss of the PDIM virulence lipid in Mycobacterium tuberculosis. *Nat. Microbiol.* **9**, 1607–1618 (2024).

281. Cox, J. S., Chen, B., McNeil, M. & Jacobs, W. R. Complex lipid determines tissue-specific replication of Mycobacterium tuberculosis in mice. *Nature* **402**, 79–83 (1999).

282. Camacho, L. R. *et al.* Analysis of the Phthiocerol Dimycocerosate Locus ofMycobacterium tuberculosis: EVIDENCE THAT THIS LIPID IS INVOLVED IN THE CELL WALL PERMEABILITY BARRIER *. *J. Biol. Chem.* **276**, 19845–19854 (2001).

283. Domenech, P. & Reed, M. B. Rapid and spontaneous loss of phthiocerol dimycocerosate (PDIM) from Mycobacterium tuberculosis grown in vitro: implications for virulence studies. *Microbiol. Read. Engl.* **155**, 3532–3543 (2009).

284. Vincent, A. T. *et al.* The Mycobacterial Cell Envelope: A Relict From the Past or the Result of Recent Evolution? *Front. Microbiol.* **9**, (2018).

285. Camacho, L. R., Ensergueix, D., Perez, E., Gicquel, B. & Guilhot, C. Identification of a virulence gene cluster of Mycobacterium tuberculosis by signature-tagged transposon mutagenesis. *Mol. Microbiol.* **34**, 257–267 (1999).

286. Goren, M. B., Brokl, O. & Schaefer, W. B. Lipids of Putative Relevance to Virulence in Mycobacterium tuberculosis: Phthiocerol Dimycocerosate and the Attenuation Indicator Lipid 1. *Infect. Immun.* **9**, 150–158 (1974).

287. Hotter, G. S. *et al.* Transposon Mutagenesis of Mb0100 at the ppe1-nrp Locus in Mycobacterium bovis Disrupts Phthiocerol Dimycocerosate (PDIM) and Glycosylphenol-

PDIM Biosynthesis, Producing an Avirulent Strain with Vaccine Properties At Least Equal to Those of M. bovis BCG. *J. Bacteriol.* **187**, 2267–2277 (2005).

288. Quigley, J. *et al.* The Cell Wall Lipid PDIM Contributes to Phagosomal Escape and Host Cell Exit of Mycobacterium tuberculosis. *mBio* **8**, 10.1128/mbio.00148-17 (2017).
289. Block, A. M. *et al.* Mycobacterium tuberculosis Requires the Outer Membrane Lipid Phthiocerol Dimycocerosate for Starvation-Induced Antibiotic Tolerance. *mSystems* **8**, e00699-22.
290. Jones, B. S. *et al.* The loss of the PDIM/PGL virulence lipids causes differential secretion of ESX-1 substrates in Mycobacterium marinum. *mSphere* **9**, e00005-24 (2024).
291. Daffé, M. & Laneelle, M. A. Distribution of phthiocerol diester, phenolic mycosides and related compounds in mycobacteria. *J. Gen. Microbiol.* **134**, 2049–2055 (1988).
292. Reed, M. B., Domenech, P., Manca, C., Su, H. & al, et. A glycolipid of hypervirulent tuberculosis strains that inhibits the innate immune response. *Nature* **431**, 84–7 (2004).
293. Andreu, N. & Gibert, I. Cell population heterogeneity in *Mycobacterium tuberculosis* H37Rv. *Tuberculosis* **88**, 553–559 (2008).
294. Chen, J. M., Islam, S. T., Ren, H. & Liu, J. Differential productions of lipid virulence factors among BCG vaccine strains and implications on BCG safety. *Vaccine* **25**, 8114–8122 (2007).
295. Oldenburg, R. & Demangel, C. Pathogenic and immunosuppressive properties of mycobacterial phenolic glycolipids. *Biochimie* **141**, 3–8 (2017).
296. Gonzalo-Asensio, J. *et al.* Evolutionary history of tuberculosis shaped by conserved mutations in the PhoPR virulence regulator. *Proc. Natl. Acad. Sci.* **111**, 11491–11496 (2014).

297. Borgers, K., Vandewalle, K., Festjens, N. & Callewaert, N. A guide to Mycobacterium mutagenesis. *FEBS J.* **286**, 3757–3774 (2019).

298. Maitra, A. *et al.* Cell wall peptidoglycan in Mycobacterium tuberculosis: An Achilles' heel for the TB-causing pathogen. *FEMS Microbiol. Rev.* **43**, 548–575 (2019).

299. Murphy, K. C. *et al.* ORBIT: a New Paradigm for Genetic Engineering of Mycobacterial Chromosomes. *mBio* **9**, e01467-18 (2018).

300. Court, D. L., Sawitzke, J. A. & Thomason, L. C. Genetic Engineering Using Homologous Recombination1. *Annu. Rev. Genet.* **36**, 361–388 (2002).

301. van Kessel, J. C., Marinelli, L. J. & Hatfull, G. F. Recombineering mycobacteria and their phages. *Nat. Rev. Microbiol.* **6**, 851–857 (2008).

302. Armianinova, D. K., Karpov, D. S., Kotliarova, M. S. & Goncharenko, A. V. Genetic Engineering in Mycobacteria. *Mol. Biol.* **56**, 830–841 (2022).

303. Kaiser, K. & Murray, N. E. Physical characterisation of the 'Rac prophage' in E. coli K12. *Mol. Gen. Genet. MGG* **175**, 159–174 (1979).

304. Muyrers, J. P. P., Zhang, Y., Buchholz, F. & Stewart, A. F. RecE/RecT and Redα/Redβ initiate double-stranded break repair by specifically interacting with their respective partners. *Genes Dev.* **14**, 1971–1982 (2000).

305. Van Kessel, J. C. & Hatfull, G. F. Efficient point mutagenesis in mycobacteria using single-stranded DNA recombineering: characterization of antimycobacterial drug targets. *Mol. Microbiol.* **67**, 1094–1107 (2008).

306. Murphy, K. C., Papavinasasundaram, K. & Sassetti, C. M. Mycobacterial Recombineering. in *Mycobacteria Protocols* (eds. Parish, T. & Roberts, D. M.) 177–199 (Springer, New York, NY, 2015). doi:10.1007/978-1-4939-2450-9_10.

307. Pandey, A. K. *et al.* Nitrile-inducible gene expression in mycobacteria. *Tuberc. Edinb. Scotl.* **89**, 12–16 (2009).

308. Ansari, M. Y. *et al.* A novel function of Mycobacterium tuberculosis chaperonin paralog GroEL1 in copper homeostasis. *FEBS Lett.* **594**, 3305–3323 (2020).

309. Keenholtz, R. A., Grindley, N. D. F., Hatfull, G. F. & Marko, J. F. Crossover-site sequence and DNA torsional stress control strand interchanges by the Bxb1 site-specific serine recombinase. *Nucleic Acids Res.* **44**, 8921–8932 (2016).

310. Ghosh, P., Wasil, L. R. & Hatfull, G. F. Control of Phage Bxb1 Excision by a Novel Recombination Directionality Factor. *PLoS Biol.* **4**, e186 (2006).

311. Kim, A. I. *et al.* Mycobacteriophage Bxb1 integrates into the Mycobacterium smegmatis groEL1 gene. *Mol. Microbiol.* **50**, 463–473 (2003).

312. Peña, C. E. A., Lee, M. H., Pedulla, M. L. & Hatfull, G. F. Characterization of the mycobacteriophage L5 attachment site, *attP* 1. *J. Mol. Biol.* **266**, 76–92 (1997).

313. Mediavilla, J. *et al.* Genome organization and characterization of mycobacteriophage Bxb1. *Mol. Microbiol.* **38**, 955–970 (2000).

314. Ghosh, P., Kim, A. I. & Hatfull, G. F. The Orientation of Mycobacteriophage Bxb1 Integration Is Solely Dependent on the Central Dinucleotide of attP and attB. *Mol. Cell* **12**, 1101–1111 (2003).

315. Borgers, K., Vandewalle, K., Festjens, N. & Callewaert, N. A guide to Mycobacterium mutagenesis. *FEBS J.* **286**, 3757–3774 (2019).

316. Dube, D. *et al.* Chapter 2 - Animal models of tuberculosis. in *Animal Biotechnology (Second Edition)* (eds. Verma, A. S. & Singh, A.) 21–41 (Academic Press, Boston, 2020). doi:10.1016/B978-0-12-811710-1.00002-1.

317. Soldevilla, P., Vilaplana, C. & Cardona, P.-J. Mouse Models for Mycobacterium tuberculosis Pathogenesis: Show and Do Not Tell. *Pathogens* **12**, 49 (2022).

318. Orme, I. M. The mouse as a useful model of tuberculosis. *Tuberculosis* **83**, 112–115 (2003).

319. Flynn, J. L. *et al.* An essential role for interferon gamma in resistance to Mycobacterium tuberculosis infection. *J. Exp. Med.* **178**, 2249–2254 (1993).

320. Harper, J. *et al.* Mouse Model of Necrotic Tuberculosis Granulomas Develops Hypoxic Lesions. *J. Infect. Dis.* **205**, 595–602 (2012).

321. Ji, D. X. *et al.* Role of the transcriptional regulator SP140 in resistance to bacterial infections via repression of type I interferons. *eLife* **10**, e67290 (2021).

322. Dharmadhikari, A. S. & Nardell, E. A. What Animal Models Teach Humans about Tuberculosis. *Am. J. Respir. Cell Mol. Biol.* **39**, 503–508 (2008).

323. Medina, E. & North, R. J. Resistance ranking of some common inbred mouse strains to Mycobacterium tuberculosis and relationship to major histocompatibility complex haplotype and Nramp1 genotype. *Immunology* **93**, 270–274 (1998).

324. McMurray, D. N. Disease model: pulmonary tuberculosis. *Trends Mol. Med.* **7**, 135–137 (2001).

325. Flynn, J., Chan, J. & Lin, P. Macrophages and control of granulomatous inflammation in tuberculosis. *Mucosal Immunol.* **4**, 271–278 (2011).

326. Rydell-Törmänen, K. & Johnson, J. R. The Applicability of Mouse Models to the Study of Human Disease. *Mouse Cell Cult.* **1940**, 3–22 (2018).

327. Zhan, L., Tang, J., Sun, M. & Qin, C. Animal Models for Tuberculosis in Translational and Precision Medicine. *Front. Microbiol.* **8**, (2017).

328. Bouté, M. *et al.* The C3HeB/FeJ mouse model recapitulates the hallmark of bovine tuberculosis lung lesions following Mycobacterium bovis aerogenous infection. *Vet. Res.* **48**, 73 (2017).

329. Irwin, S. M. *et al.* Presence of multiple lesion types with vastly different microenvironments in C3HeB/FeJ mice following aerosol infection with Mycobacterium tuberculosis. *Dis. Model. Mech.* **8**, 591–602 (2015).

330. Kramnik, I. Genetic Dissection of Host Resistance to Mycobacterium tuberculosis: The sst1 Locus and the Ipr1 Gene. in *Immunology, Phenotype First: How Mutations Have Established New Principles and Pathways in Immunology* (ed. Beutler, B.) 123–148 (Springer, Berlin, Heidelberg, 2008). doi:10.1007/978-3-540-75203-5_6.

331. Logan, K. E., Gavier-Widen, D., Hewinson, R. G. & Hogarth, P. J. Development of a *Mycobacterium bovis* intranasal challenge model in mice. *Tuberculosis* **88**, 437–443 (2008).

332. Serrano, M. *et al.* Different lesion distribution in calves orally or intratracheally challenged with Mycobacterium bovis: implications for diagnosis. *Vet. Res.* **49**, 74 (2018).

333. Waters, W. R. *et al.* Virulence of Two Strains of *Mycobacterium bovis* in Cattle Following Aerosol Infection. *J. Comp. Pathol.* **151**, 410–419 (2014).

334. Hunter, L., Ruedas-Torres, I., Agulló-Ros, I., Rayner, E. & Salguero, F. J. Comparative pathology of experimental pulmonary tuberculosis in animal models. *Front. Vet. Sci.* **10**, (2023).

335. Duffy, S. C. *et al.* Establishment of persistent enteric mycobacterial infection following streptomycin pre-treatment. *Gut Pathog.* **15**, 46 (2023).

336. Hewinson, R. G., Vordermeier, H. M. & Buddle, B. M. Use of the bovine model of tuberculosis for the development of improved vaccines and diagnostics. *Tuberculosis* **83**, 119–130 (2003).

337. Pollock, J. M., Rodgers, J. D., Welsh, M. D. & McNair, J. Pathogenesis of bovine tuberculosis: The role of experimental models of infection. *Vet. Microbiol.* **112**, 141–150 (2006).

338. Cassidy, J. P. The pathogenesis and pathology of bovine tuberculosis with insights from studies of tuberculosis in humans and laboratory animal models. *Vet. Microbiol.* **112**, 151–161 (2006).

339. Williams, A. & Orme, I. M. Animal Models of Tuberculosis: An Overview. *Microbiol. Spectr.* **4**, 10.1128/microbiolspec.tbtb2-0004–2015 (2016).

340. Gill, C. M., Dolan, L., Piggott, L. M. & McLaughlin, A. M. New developments in tuberculosis diagnosis and treatment. *Breathe* **18**, (2022).

341. Manual for selection of molecular WHO-recommended rapid diagnostic tests for detection of tuberculosis and drug-resistant tuberculosis. https://www.who.int/publications-detail-redirect/9789240042575.

342. Iketleng, T. *et al.* Mycobacterium tuberculosis Next-Generation Whole Genome Sequencing: Opportunities and Challenges. *Tuberc. Res. Treat.* **2018**, 1298542 (2018).

343. Parsons, L. M. *et al.* Laboratory Diagnosis of Tuberculosis in Resource-Poor Countries: Challenges and Opportunities. *Clin. Microbiol. Rev.* **24**, 314–350 (2011).

344. Shrestha, P., Khanal, H., Dahal, P. & Dongol, P. Programmatic Impact of Implementing GeneXpert MTB/ RIF Assay for the Detection of Mycobacterium Tuberculosis in

Respiratory Specimens from Pulmonary Tuberculosis Suspected Patients in Resource Limited Laboratory Settings of Eastern Nepal. *Open Microbiol. J.* **12**, 9–17 (2018).

345. Oxlade, O., Sugarman, J., Alvarez, G. G., Pai, M. & Schwartzman, K. Xpert®MTB/RIF for the Diagnosis of Tuberculosis in a Remote Arctic Setting: Impact on Cost and Time to Treatment Initiation. *PLoS ONE* **11**, e0150119 (2016).
346. Lawn, S. D. *et al.* Rapid microbiological screening for tuberculosis in HIV-positive patients on the first day of acute hospital admission by systematic testing of urine samples using Xpert MTB/RIF: a prospective cohort in South Africa. *BMC Med.* **13**, 192 (2015).
347. Zürcher, K. *et al.* Drug susceptibility testing and mortality in patients treated for tuberculosis in high-burden countries: a multi-centre cohort study. *Lancet Infect. Dis.* **19**, 298–307 (2019).
348. Danchuk, S., Mcintosh, F., Jamieson, F., May, K. & Behr, M. BCG strains with defined resistance mutations: a new tool for TB lab quality control. *Clin. Microbiol. Infect.* **26**, (2019).
349. Rodriguez-Morales, A. J. & Castañeda-Hernández, D. M. Bacteria: *Mycobacterium bovis*. in *Encyclopedia of Food Safety* (ed. Motarjemi, Y.) 468–475 (Academic Press, Waltham, 2014). doi:10.1016/B978-0-12-378612-8.00103-7.
350. Canada, P. H. A. of. Pathogen Safety Data Sheets: Infectious Substances – Mycobacterium spp. https://www.canada.ca/en/public-health/services/laboratory-biosafety-biosecurity/pathogen-safety-data-sheets-risk-assessment/mycobacterium.html (2011).
351. Woods, G. L. *et al. Susceptibility Testing of Mycobacteria, Nocardiae, and Other Aerobic Actinomycetes*. (Clinical and Laboratory Standards Institute, Wayne (PA), 2011).

352. World Health Organization. Technical report on critical concentrations for drug susceptibility testing of isoniazid and the rifamycins (rifampicin, rifabutin and rifapentine).

353. Chakravorty, S. *et al.* The New Xpert MTB/RIF Ultra: Improving Detection of Mycobacterium tuberculosis and Resistance to Rifampin in an Assay Suitable for Point-of-Care Testing. *mBio* **8**, 10.1128/mbio.00812-17 (2017).

354. Blakemore, R. *et al.* Evaluation of the Analytical Performance of the Xpert MTB/RIF Assay. *J. Clin. Microbiol.* **48**, 2495–2501 (2010).

355. Canetti, G. *et al.* Mycobacteria: laboratory methods for testing drug sensitivity and resistance. *Bull. World Health Organ.* **29**, 565–578 (1963).

356. van Kessel, J. C. & Hatfull, G. F. Recombineering in Mycobacterium tuberculosis. *Nat. Methods* **4**, 147–152 (2007).

357. Helb, D. *et al.* Rapid Detection of Mycobacterium tuberculosis and Rifampin Resistance by Use of On-Demand, Near-Patient Technology. *J. Clin. Microbiol.* **48**, 229–237 (2010).

358. Prammananan, T. *et al.* Distribution of rpoB mutations among multidrug-resistant Mycobacterium tuberculosis (MDRTB) strains from Thailand and development of a rapid method for mutation detection. *Clin. Microbiol. Infect.* **14**, 446–453 (2008).

359. WHO. Catalogue of mutations in Mycobacterium tuberculosis complex and their association with drug resistance. (2021).

360. André, E. *et al.* Novel rapid PCR for the detection of Ile491Phe rpoB mutation of Mycobacterium tuberculosis, a rifampicin-resistance-conferring mutation undetected by commercial assays. *Clin. Microbiol. Infect.* **23**, 267.e5-267.e7 (2017).

361. Mon, A. S. *et al.* First Detection of Mycobacterium tuberculosis Clinical Isolates Harboring I491F Borderline Resistance rpoB Mutation in Myanmar. *Antimicrob. Agents Chemother.* **66**, e00925-22.

362. Beckert, P. *et al.* MDR M. tuberculosis outbreak clone in Eswatini missed by Xpert has elevated bedaquiline resistance dated to the pre-treatment era. *Genome Med.* **12**, 104 (2020).

363. Mariner-Llicer, C. *et al.* Monitoring of First-line Drug Resistance Mutations Outside the Scope of Xpert MTB/RIF Ultra is Needed for Successful Control of DR-TB in Southern Mozambique. *Clin. Infect. Dis.* ciad684 (2023) doi:10.1093/cid/ciad684.

364. Scarparo, C., Ricordi, P., Ruggiero, G. & Piccoli, P. Evaluation of the Fully Automated BACTEC MGIT 960 System for Testing Susceptibility of Mycobacterium tuberculosis to Pyrazinamide, Streptomycin, Isoniazid, Rifampin, and Ethambutol and Comparison with the Radiometric BACTEC 460TB Method. *J. Clin. Microbiol.* **42**, 1109–1114 (2004).

365. Nimmo, C. *et al.* Evolution of Mycobacterium tuberculosis drug resistance in the genomic era. *Front. Cell. Infect. Microbiol.* **12**, (2022).

366. Modongo, C. *et al.* Tuberculosis Variant with Rifampin Resistance Undetectable by Xpert MTB/RIF, Botswana - Volume 29, Number 11—November 2023 - Emerging Infectious Diseases journal - CDC. doi:10.3201/eid2911.230987.

367. Sibandze, D. B. *et al.* Rapid molecular diagnostics of tuberculosis resistance by targeted stool sequencing. *Genome Med.* **14**, 52 (2022).

368. Seifert, M. *et al.* A Performance Evaluation of MTBDRplus (version 2) for the Diagnosis of Multidrug-resistant Tuberculosis. *Int. J. Tuberc. Lung Dis. Off. J. Int. Union Tuberc. Lung Dis.* **20**, 631–637 (2016).

369. Jian, J., Yang, X., Yang, J. & Chen, L. Evaluation of the GenoType MTBDRplus and MTBDRsl for the detection of drug-resistant Mycobacterium tuberculosis on isolates from Beijing, China. *Infect. Drug Resist.* **11**, 1627 (2018).

370. Hain Lifesciences. (2015).

371. Rostamian, M. *et al.* Prevalence of *Mycobacterium tuberculosis* mutations associated with isoniazid and rifampicin resistance: A systematic review and *meta*-analysis. *J. Clin. Tuberc. Mycobact. Dis.* **32**, 100379 (2023).

372. Dorman, S. E. *et al.* Genotype MTBDRplus for Direct Detection of Mycobacterium tuberculosis and Drug Resistance in Strains from Gold Miners in South Africa. *J. Clin. Microbiol.* **50**, 1189–1194 (2012).

373. Lee, R. S., Proulx, J.-F., McIntosh, F., Behr, M. A. & Hanage, W. P. Previously undetected super-spreading of Mycobacterium tuberculosis revealed by deep sequencing. *eLife* **9**, e53245 (2020).

374. Qadir, M. *et al.* Phenotype versus genotype discordant rifampicin susceptibility testing in tuberculosis: implications for a diagnostic accuracy. *Microbiol. Spectr.* **12**, e01631-23 (2023).

375. Vanino, E. *et al.* Update of drug-resistant tuberculosis treatment guidelines: A turning point. *Int. J. Infect. Dis.* **130**, S12–S15 (2023).

376. Park, M., Satta, G. & Kon, O. M. An update on multidrug-resistant tuberculosis. *Clin. Med.* **19**, 135–139 (2019).

377. Chien, J.-Y. *et al.* Mutations in gyrA and gyrB among Fluoroquinolone- and Multidrug-Resistant Mycobacterium tuberculosis Isolates. *Antimicrob. Agents Chemother.* **60**, 2090–2096 (2016).

378. Hartkoorn, R. C., Uplekar, S. & Cole, S. T. Cross-Resistance between Clofazimine and Bedaquiline through Upregulation of MmpL5 in Mycobacterium tuberculosis. *Antimicrob. Agents Chemother.* **58**, 2979–2981 (2014).

379. 6. TB research and innovation. https://www.who.int/teams/global-tuberculosis-programme/tb-reports/global-tuberculosis-report-2023/tb-research-and-innovation.

380. Rinder, H., Mieskes, K. T. & Löscher, T. Heteroresistance in Mycobacterium tuberculosis. *Int. J. Tuberc. Lung Dis.* **5**, 339–345 (2001).

381. Folkvardsen, D. B. *et al.* Rifampin heteroresistance in Mycobacterium tuberculosis cultures as detected by phenotypic and genotypic drug susceptibility test methods. *J. Clin. Microbiol.* **51**, 4220–4222 (2013).

382. Hofmann-Thiel, S. *et al.* Mechanisms of heteroresistance to isoniazid and rifampin of Mycobacterium tuberculosis in Tashkent, Uzbekistan. *Eur. Respir. J.* **33**, 368–374 (2009).

383. Ye, M. *et al.* Antibiotic heteroresistance in Mycobacterium tuberculosis isolates: a systematic review and meta-analysis. *Ann. Clin. Microbiol. Antimicrob.* **20**, 73 (2021).

384. Gajic, I. *et al.* Antimicrobial Susceptibility Testing: A Comprehensive Review of Currently Used Methods. *Antibiotics* **11**, 427 (2022).

385. da Silva, M. P. *et al.* More Than a Decade of GeneXpert® Mycobacterium tuberculosis/Rifampicin (Ultra) Testing in South Africa: Laboratory Insights from Twenty-Three Million Tests. *Diagnostics* **13**, 3253 (2023).

386. Getahun, D. A., Layland, L. E., Hoerauf, A. & Wondale, B. Impact of the use of GeneXpert on TB diagnosis and anti-TB treatment outcome at health facilities in Addis Ababa, Ethiopia in the post-millennium development years. *PLOS ONE* **18**, e0289917 (2023).

387. Naidoo, K. & Dookie, N. Can the GeneXpert MTB/XDR deliver on the promise of expanded, near-patient tuberculosis drug-susceptibility testing? *Lancet Infect. Dis.* **22**, e121–e127 (2022).

388. Chakaya, J. M., Harries, A. D. & Marks, G. B. Ending tuberculosis by 2030—Pipe dream or reality? *Int. J. Infect. Dis.* **92**, S51–S54 (2020).

389. Gutacker, M. M. *et al.* Genome-Wide Analysis of Synonymous Single Nucleotide Polymorphisms in Mycobacterium tuberculosis Complex Organisms: Resolution of Genetic Relationships Among Closely Related Microbial Strains. *Genetics* **162**, 1533–1543 (2002).

390. Gallant, J. *et al.* Identification of gene fusion events in Mycobacterium tuberculosis that encode chimeric proteins. *NAR Genomics Bioinforma.* **2**, lqaa033 (2020).

391. Namouchi, A., Didelot, X., Schöck, U., Gicquel, B. & Rocha, E. P. C. After the bottleneck: Genome-wide diversification of the Mycobacterium tuberculosis complex by mutation, recombination, and natural selection. *Genome Res.* **22**, 721–734 (2012).

392. Mendonca, L. E. *et al.* Human alveolar macrophage metabolism is compromised during Mycobacterium tuberculosis infection. *Front. Immunol.* **13**, 1044592 (2023).

393. Liu, Y. *et al.* Immune activation of the host cell induces drug tolerance in Mycobacterium tuberculosis both in vitro and in vivo. *J. Exp. Med.* **213**, 809–825 (2016).

394. Sassetti, C. M. & Rubin, E. J. Genetic requirements for mycobacterial survival during infection. *Proc. Natl. Acad. Sci. U. S. A.* **100**, 12989–12994 (2003).

395. Bosserman, R. E. & Champion, P. A. Esx Systems and the Mycobacterial Cell Envelope: What's the Connection? *J. Bacteriol.* **199**, e00131-17 (2017).

396. Chen, J. M. *et al.* EspD Is Critical for the Virulence-Mediating ESX-1 Secretion System in Mycobacterium tuberculosis. *J. Bacteriol.* **194**, 884–893 (2012).

397. Garces, A. *et al.* EspA Acts as a Critical Mediator of ESX1-Dependent Virulence in Mycobacterium tuberculosis by Affecting Bacterial Cell Wall Integrity. *PLoS Pathog.* **6**, e1000957 (2010).

398. Lou, Y., Rybniker, J., Sala, C. & Cole, S. T. EspC forms a filamentous structure in the cell envelope of Mycobacterium tuberculosis and impacts ESX-1 secretion. *Mol. Microbiol.* **103**, 26–38 (2017).

399. Uplekar, S., Heym, B., Friocourt, V., Rougemont, J. & Cole, S. T. Comparative Genomics of esx Genes from Clinical Isolates of Mycobacterium tuberculosis Provides Evidence for Gene Conversion and Epitope Variation ▿. *Infect. Immun.* **79**, 4042–4049 (2011).

400. Abdallah, A. M. *et al.* The ESX-5 Secretion System of Mycobacterium marinum Modulates the Macrophage Response1. *J. Immunol.* **181**, 7166–7175 (2008).

401. Ates, L. S. *et al.* Essential Role of the ESX-5 Secretion System in Outer Membrane Permeability of Pathogenic Mycobacteria. *PLoS Genet.* **11**, e1005190 (2015).

402. Elliott, S. R., White, D. W. & Tischler, A. D. Mycobacterium tuberculosis Requires Regulation of ESX-5 Secretion for Virulence in Irgm1-Deficient Mice. *Infect. Immun.* **87**, e00660-18 (2019).

403. Gey van Pittius, N. C. *et al.* The ESAT-6 gene cluster of Mycobacterium tuberculosis and other high G+C Gram-positive bacteria. *Genome Biol.* **2**, research0044.1-research0044.18 (2001).

404. Gey van Pittius, N. C. *et al.* Evolution and expansion of the Mycobacterium tuberculosis PE and PPE multigene families and their association with the duplication of the ESAT-6 (esx) gene cluster regions. *BMC Evol. Biol.* **6**, 95 (2006).

405. Brennan, M. J. The Enigmatic PE/PPE Multigene Family of Mycobacteria and Tuberculosis Vaccination. *Infect. Immun.* **85**, e00969-16 (2017).

406. Sridhara, A. A. *et al.* Strong antibody responses to *Mycobacterium bovis* infection in domestic pigs and potential for reliable serodiagnostics. *Vet. Immunol. Immunopathol.* **231**, 110161 (2021).

407. Domingo-Gonzalez, R., Prince, O., Cooper, A. & Khader, S. Cytokines and Chemokines in Mycobacterium tuberculosis infection. *Microbiol. Spectr.* **4**, 10.1128/microbiolspec.TBTB2-0018–2016 (2016).

408. Sumanth, L. J. *et al.* Clinical features of human tuberculosis due to Mycobacterium orygis in Southern India. *J. Clin. Tuberc. Mycobact. Dis.* **32**, 100372 (2023).

409. Harrison, L. B., Kapur, V. & Behr, M. A. An imputed ancestral reference genome for the Mycobacterium tuberculosis complex better captures structural genomic diversity for reference-based alignment workflows. *Microb. Genomics* **10**, 001165 (2024).

410. Clemmensen, H. S. *et al.* Rescuing ESAT-6 Specific CD4 T Cells From Terminal Differentiation Is Critical for Long-Term Control of Murine Mtb Infection. *Front. Immunol.* **11**, 585359 (2020).

411. Clemmensen, H. S. *et al. In Vivo* Antigen Expression Regulates CD4 T Cell Differentiation and Vaccine Efficacy against Mycobacterium tuberculosis Infection. *mBio* **12**, e00226-21 (2021).

412. Complete Genome Sequence of Mycobacterium orygis Strain 51145 | Microbiology Resource Announcements. https://journals.asm.org/doi/10.1128/mra.01279-20.

413. Cavalcante-Silva, L. H. A. *et al.* Mycobacterium tuberculosis in a Trap: The Role of Neutrophil Extracellular Traps in Tuberculosis. *Int. J. Mol. Sci.* **24**, 11385 (2023).

414. Ramos-Kichik, V. *et al.* Neutrophil extracellular traps are induced by *Mycobacterium tuberculosis*. *Tuberculosis* **89**, 29–37 (2009).

415. Lovewell, R. R., Baer, C., Mishra, B. B., Smith, C. M. & Sassetti, C. M. Granulocytes act as a niche for Mycobacterium tuberculosis growth. *Mucosal Immunol.* **14**, 229–241 (2021).

416. Borrell, S. *et al.* Reference set of Mycobacterium tuberculosis clinical strains: A tool for research and product development. *PLoS ONE* **14**, e0214088 (2019).

417. Pym, A. S., Brodin, P., Brosch, R., Huerre, M. & Cole, S. T. Loss of RD1 contributed to the attenuation of the live tuberculosis vaccines Mycobacterium bovis BCG and Mycobacterium microti. *Mol. Microbiol.* **46**, 709–717 (2002).

418. Reed, M. B., Gagneux, S., DeRiemer, K., Small, P. M. & Barry, C. E. The W-Beijing Lineage of Mycobacterium tuberculosis Overproduces Triglycerides and Has the DosR Dormancy Regulon Constitutively Upregulated. *J. Bacteriol.* **189**, 2583–2589 (2007).

419. Napier, G. *et al.* Robust barcoding and identification of Mycobacterium tuberculosis lineages for epidemiological and clinical studies. *Genome Med.* **12**, 114 (2020).

420. Berube, B. J. *et al.* Characterizing in vivo loss of virulence of an HN878 Mycobacterium tuberculosis isolate from a genetic duplication event. *Tuberc. Edinb. Scotl.* **137**, 102272 (2022).

421. Brodin, P. *et al.* Bacterial Artificial Chromosome-Based Comparative Genomic Analysis Identifies Mycobacterium microti as a Natural ESAT-6 Deletion Mutant. *Infect. Immun.* **70**, 5568–5578 (2002).

422. Berthet, F.-X., Rasmussen, P. B., Rosenkrands, I., Andersen, P. & Gicquel, B. A Mycobacterium tuberculosis operon encoding ESAT-6 and a novel low-molecular-mass culture filtrate protein (CFP-10). *Microbiol. Read. Engl.* **144 (Pt 11)**, 3195–3203 (1998).

423. Refai, A. *et al.* Two distinct conformational states of Mycobacterium tuberculosis virulent factor early secreted antigenic target 6 kDa are behind the discrepancy around its biological functions. *FEBS J.* **282**, 4114–4129 (2015).

424. Malone, K. M. *et al.* Comparative ‘omics analyses differentiate Mycobacterium tuberculosis and Mycobacterium bovis and reveal distinct macrophage responses to infection with the human and bovine tubercle bacilli. 220624 Preprint at https://doi.org/10.1101/220624 (2017).

425. Mombaerts, P. *et al.* RAG-1-deficient mice have no mature B and T lymphocytes. *Cell* **68**, 869–877 (1992).

426. Hilda, J. N., Das, S., Tripathy, S. P. & Hanna, L. E. Role of neutrophils in tuberculosis: A bird’s eye view. *Innate Immun.* **26**, 240–247 (2020).

427. von Both, U. *et al.* Mycobacterium tuberculosis Exploits a Molecular Off Switch of the Immune System for Intracellular Survival. *Sci. Rep.* **8**, 661 (2018).

428. Lombardi, A., Villa, S., Castelli, V., Bandera, A. & Gori, A. T-Cell Exhaustion in Mycobacterium tuberculosis and Nontuberculous Mycobacteria Infection: Pathophysiology and Therapeutic Perspectives. *Microorganisms* **9**, 2460 (2021).

429. Emery, J. C. *et al.* Self-clearance of Mycobacterium tuberculosis infection: implications for lifetime risk and population at-risk of tuberculosis disease. *Proc. R. Soc. B Biol. Sci.* **288**, 20201635 (2021).

430. Pollock, J. M. & Neill, S. D. Mycobacterium boviss Infection and Tuberculosis in Cattle. *Vet. J.* **163**, 115–127 (2002).

431. Sassetti, C. M., Boyd, D. H. & Rubin, E. J. Genes required for mycobacterial growth defined by high density mutagenesis. *Mol. Microbiol.* **48**, 77–84 (2003).

432. Ramon-Luing, L. A., Palacios, Y., Ruiz, A., Téllez-Navarrete, N. A. & Chavez-Galan, L. Virulence Factors of Mycobacterium tuberculosis as Modulators of Cell Death Mechanisms. *Pathogens* **12**, 839 (2023).

433. Sabio y García, J. *et al.* Does Mycobacterium bovis persist in cattle in a non-replicative latent state as Mycobacterium tuberculosis in human beings? *Vet. Microbiol.* **247**, 108758 (2020).

434. Yang, H.-J., Wang, D., Wen, X., Weiner, D. M. & Via, L. E. One Size Fits All? Not in In Vivo Modeling of Tuberculosis Chemotherapeutics. *Front. Cell. Infect. Microbiol.* **11**, (2021).

435. Chackerian, A. A. & Behar, S. M. Susceptibility to *Mycobacterium tuberculosis*: lessons from inbred strains of mice. *Tuberculosis* **83**, 279–285 (2003).

436. Carrisoza-Urbina, J., Morales-Salinas, E., Bedolla-Alva, M. A., Hernández-Pando, R. & Gutiérrez-Pabello, J. A. Atypical granuloma formation in Mycobacterium bovis-infected calves. *PLOS ONE* **14**, e0218547 (2019).

437. Wangoo, A. *et al.* Advanced Granulomatous Lesions in Mycobacterium bovis-infected Cattle are Associated with Increased Expression of Type I Procollagen, γδ (WC1+) T Cells and CD 68+ Cells. *J. Comp. Pathol.* **133**, 223–234 (2005).

438. Whipple, D. L., Bolin, C. A. & Miller, J. M. Distribution of Lesions in Cattle Infected with Mycobacterium Bovis. *J. Vet. Diagn. Invest.* **8**, 351–354 (1996).

439. Corner, L. A. Post mortem diagnosis of Mycobacterium bovis infection in cattle. *Vet. Microbiol.* **40**, 53–63 (1994).

440. Fitzgerald, S. D. *et al.* Herd outbreak of bovine tuberculosis illustrates that route of infection correlates with anatomic distribution of lesions in cattle and cats. *J. Vet. Diagn. Invest.* **28**, 129–132 (2016).

441. Liebana, E. *et al.* Pathology of naturally occurring bovine tuberculosis in England and Wales. *Vet. J.* **176**, 354–360 (2008).

442. Chronic Indigestion Syndrome in Ruminants - Digestive System. *Merck Veterinary Manual* https://www.merckvetmanual.com/digestive-system/diseases-of-the-ruminant-forestomach/chronic-indigestion-syndrome-in-ruminants.

443. Karimi, S. *et al.* Histopathological Findings in Immunohistological Staining of the Granulomatous Tissue Reaction Associated with Tuberculosis. *Tuberc. Res. Treat.* **2014**, 858396 (2014).

444. Velayati, A. A. *et al.* Morphological modification by tubercle bacilli: no time for denial. *J. Infect. Dev. Ctries.* **6**, 97–99 (2012).

445. Carrisoza-Urbina, J. *et al.* Mycobacterium bovis naturally infected calves present a higher bacterial load and proinflammatory response than adult cattle. *Front. Vet. Sci.* **10**, 1105716 (2023).

446. Maunsell, F. P. & Donovan, G. A. *Mycoplasma bovis* Infections in Young Calves. *Vet. Clin. North Am. Food Anim. Pract.* **25**, 139–177 (2009).

447. Booker, C. W. *et al.* Microbiological and histopathological findings in cases of fatal bovine respiratory disease of feedlot cattle in western Canada. *Can. Vet. J.* **49**, 473–481 (2008).

448. Domingo, M., Vidal, E. & Marco, A. Pathology of bovine tuberculosis. *Res. Vet. Sci.* **97**, S20–S29 (2014).

449. Neill, S. D., Skuce, R. A. & Pollock, J. M. Tuberculosis – new light from an old window. *J. Appl. Microbiol.* **98**, 1261–1269 (2005).

450. Gormley, E. & Corner, L. A. L. Pathogenesis of Mycobacterium bovis Infection: the Badger Model As a Paradigm for Understanding Tuberculosis in Animals. *Front. Vet. Sci.* **4**, (2018).

451. Remot, A. *et al.* Mycobacterial Infection of Precision-Cut Lung Slices Reveals Type 1 Interferon Pathway Is Locally Induced by Mycobacterium bovis but Not M. tuberculosis in a Cattle Breed. *Front. Vet. Sci.* **8**, (2021).

452. Whelan, A. O. *et al.* Revisiting Host Preference in the Mycobacterium tuberculosis Complex: Experimental Infection Shows M. tuberculosis H37Rv to Be Avirulent in Cattle. *PLOS ONE* **5**, e8527 (2010).

453. Moule, M. G. & Cirillo, J. D. Mycobacterium tuberculosis Dissemination Plays a Critical Role in Pathogenesis. *Front. Cell. Infect. Microbiol.* **10**, 65 (2020).

454. Lombard, J. E. *et al.* Human-to-Cattle Mycobacterium tuberculosis Complex Transmission in the United States. *Front. Vet. Sci.* **8**, (2021).

455. Khalid, H., van Hooij, A., Connelley, T. K., Geluk, A. & Hope, J. C. Protein Levels of Pro-Inflammatory Cytokines and Chemokines as Biomarkers of Mycobacterium bovis Infection and BCG Vaccination in Cattle. *Pathogens* **11**, 738 (2022).

456. Palmer, M. V., Thacker, T. C. & Waters, W. R. Differential Cytokine Gene Expression in Granulomas from Lungs and Lymph Nodes of Cattle Experimentally Infected with Aerosolized Mycobacterium bovis. *PLoS ONE* **11**, e0167471 (2016).

457. Arko-Mensah, J. *et al.* Resistance to mycobacterial infection: A pattern of early immune responses leads to a better control of pulmonary infection in C57BL/6 compared with BALB/c mice. *Vaccine* **27**, 7418–7427 (2009).

458. Widdison, S. *et al.* Cytokine expression profiles of bovine lymph nodes: effects of Mycobacterium bovis infection and bacille Calmette–Guérin vaccination. *Clin. Exp. Immunol.* **144**, 281–289 (2006).

459. Pro- and anti-inflammatory cytokines in tuberculosis: A two-edged sword in TB pathogenesis. *Semin. Immunol.* **26**, 543–551 (2014).

460. Widdison, S., Watson, M., Piercy, J., Howard, C. & Coffey, T. J. Granulocyte chemotactic properties of *M. tuberculosis* versus *M. bovis*-infected bovine alveolar macrophages. *Mol. Immunol.* **45**, 740–749 (2008).

461. Magee, D. A. *et al.* Innate cytokine profiling of bovine alveolar macrophages reveals commonalities and divergence in the response to *Mycobacterium bovis* and *Mycobacterium tuberculosis* infection. *Tuberculosis* **94**, 441–450 (2014).

462. Lartigau, A. J. A Study of the Variation in Virulence of the Bacillus Tuberculosis in Man. *J. Med. Res.* **6**, 156–162 (1901).

463. Palmer, M. V., Wiarda, J., Kanipe, C. & Thacker, T. C. Early Pulmonary Lesions in Cattle Infected via Aerosolized Mycobacterium bovis. *Vet. Pathol.* **56**, 544–554 (2019).

464. Menin, Á. *et al.* Asymptomatic Cattle Naturally Infected with Mycobacterium bovis Present Exacerbated Tissue Pathology and Bacterial Dissemination. *PLoS ONE* **8**, e53884 (2013).

465. Kanipe, C., Boggiatto, P. M., Putz, E. J. & Palmer, M. V. Histopathologic differences in granulomas of Mycobacterium bovis bacille Calmette Guérin (BCG) vaccinated and non-vaccinated cattle with bovine tuberculosis. *Front. Microbiol.* **13**, 1048648 (2022).

466. Palmer, M. V., Waters, W. R. & Thacker, T. C. Lesion Development and Immunohistochemical Changes in Granulomas from Cattle Experimentally Infected with Mycobacterium bovis. *Vet. Pathol.* **44**, 863–874 (2007).

467. Thacker, T. C., Palmer, M. V. & Waters, W. R. Associations between cytokine gene expression and pathology in *Mycobacterium bovis* infected cattle. *Vet. Immunol. Immunopathol.* **119**, 204–213 (2007).

468. Barilar, I. *et al.* Quantitative measurement of antibiotic resistance in Mycobacterium tuberculosis reveals genetic determinants of resistance and susceptibility in a target gene approach. *Nat. Commun.* **15**, 488 (2024).

469. Dijkman, K. *et al.* A protective, single-visit TB vaccination regimen by co-administration of a subunit vaccine with BCG. *NPJ Vaccines* **8**, 66 (2023).

470. van Leeuwen, L. M., van der Sar, A. M. & Bitter, W. Animal Models of Tuberculosis: Zebrafish. *Cold Spring Harb. Perspect. Med.* **5**, a018580 (2015).

471. Prouty, M. G., Correa, N. E., Barker, L. P., Jagadeeswaran, P. & Klose, K. E. Zebrafish-Mycobacterium marinum model for mycobacterial pathogenesis. *FEMS Microbiol. Lett.* **225**, 177–182 (2003).

472. Akram, S. M. & Aboobacker, S. Mycobacterium marinum Infection. in *StatPearls* (StatPearls Publishing, Treasure Island (FL), 2024).

473. Grunwald, D. J. & Eisen, J. S. Headwaters of the zebrafish — emergence of a new model vertebrate. *Nat. Rev. Genet.* **3**, 717–724 (2002).

474. Glasson, Y. *et al.* Single-cell high-dimensional imaging mass cytometry: one step beyond in oncology. *Semin. Immunopathol.* **45**, 17–28 (2023).

475. Lee, S., Clémentine, C. & Kim, H. Exploring the genetic factors behind the discrepancy in resistance to bovine tuberculosis between African zebu cattle and European taurine cattle. *Sci. Rep.* **14**, 2370 (2024).

476. Trinchieri, G. Type I interferon: friend or foe? *J. Exp. Med.* **207**, 2053–2063 (2010).

477. Dorhoi, A. *et al.* Type I IFN signaling triggers immunopathology in tuberculosis-susceptible mice by modulating lung phagocyte dynamics. *Eur. J. Immunol.* **44**, 2380–2393 (2014).

478. Desvignes, L., Wolf, A. J. & Ernst, J. D. Dynamic roles of type I and type II interferons in early infection with Mycobacterium tuberculosis. *J. Immunol. Baltim. Md 1950* **188**, 6205–6215 (2012).

479. Vordermeier, M. *et al.* The influence of cattle breed on susceptibility to bovine tuberculosis in Ethiopia. *Comp. Immunol. Microbiol. Infect. Dis.* **35**, 227–232 (2012).

480. Carmichael, J. Bovine Tuberculosis in the Tropics, with Special Reference to Uganda: Part I. *J. Comp. Pathol. Ther.* **52**, 322–335 (1939).

COPYRIGHT ©

In this dissertation, **Figure 2 (Animal-adapted members of the MTBC subspecies)** was derived from Figure 2 featured in Brites et al., 'A new phylogenetic framework for the animal adapted *Mycobacterium tuberculosis* Complex' (DOI: 10.3389/fmicb.2018.02820)[47]. Figure used with permission under Creative Commons Attribution License (CC BY). **Figure 10 (Overview of oligonucleotide-mediated recombineering followed by Bxb1 integrase targeting (ORBIT))** was derived from Figure 4 featured in Murphy et al., 'ORBIT: a New Paradigm for Genetic Engineering of Mycobacterial Chromosomes' (DOI: 10.1128/mBio.01467-18)[299]. Figure used with permission under Creative Commons CC BY 4.0 license.